NASW-4435

IN-16-CR
73897
P.349

DART

DELTA ADVANCED REUSABLE TRANSPORT

An Alternate Manned Space System Proposal

Department of Aerospace Engineering
University of Maryland, College Park

FINAL REPORT

By the
Delta Design Team

May 13, 1991

(NASA-CR-189978) DART: DELTA ADVANCED REUSABLE TRANSPORT. AN ALTERNATE MANNED SPACE SYSTEM PROPOSAL Final Report (Maryland Univ.) 349 p CSCL 22B

N92-21371

Unclas
G3/16 0073897

Introduction

Currently, the United States space program is moving from the administering of an occasional manned flight towards creating and sustaining a permanent human presence in Earth orbit. The Shuttle Transport System (STS) is presently the only operating system providing the US program with manned capability in this effort. The Shuttle has shown itself to be a valuable and diverse tool, providing unique and diverse manned capabilities, but also has shown itself to possess serious shortcomings. The Shuttle has no tolerance for small man-rated missions not requiring the use of such a large, costly, and sophisticated system. In addition, the permanent access to space required for a permanent presence requires a robust, flexible, reliable and cost-effective launch system. These factors encourage the development of an alternate manned vehicle. In response to this need the Delta Design Team, based at the University of Maryland, is currently completing the Delta Advanced Reusable Transport (DART). The DART craft is being developed to add multiple, rapid and cost-effective space access to the US capability and to further the program's efforts towards a permanent space presence.

The DART craft provides an augmentative and an alternative system to the Shuttle. As a supplement launch vehicle the DART adds low cost and easily accessible transport of crew and cargo to specific space destinations to the US program. This adds significant opportunities for manned rated mission that do not require Shuttle capabilities. In its alternative role the DART can provide emergency space access and satellite repair, the continuation of scientific research, and the furthering of US manned efforts in the event of Shuttle incapabilities. In addition, the DART is being designed for Space Station Freedom compatibility including use as a "lifeboat" emergency reentry craft for Freedom astronauts, as-well-as, the transport of crew and cargo for station resupply. The demand for such a craft was clearly illustrated by the unfortunate fate of STS - 51L, an accident which rendered the United States incapable of manned access to space for a significant period of time.

Perspective missions for the DART program include:

1.) Space Station Freedom Support - 5 man crew and 1000 Kg payload supply.

2.) Satellite repair and servicing (EVA).

3.) Space Station Freedom lifeboat and emergency vehicle.

4.) General manned in-flight experimentation.

5.) Emergency launch and recovery system for STS.

H. Magazu

Descriptions of the outlined missions and expanded mission to alternate launch vehicles, such as Titan IV, are provided in the accompanying report: Chapter 1, Section 1.2: DART Mission Analysis, and Chapter 7, Section 7.1: Expanded Missions to Alternate Launch Vehicles.

The DART system utilizes the McDonnell Douglas Delta II, 7920 existing, expendable commercial booster (figure I.1). The Delta's proven 96 percent reliable launch program gives the DART the needed cost-effective and readily available launch capability the program requires. The Delta II system also provides the DART with existing launch complexes and facilities at Complex 17, Cape Canaveral Air Force Station (CCAFS), Florida. This reduces overall complexity and cost of the integration of DART into the US manned program while providing reliable launch and ground facilities.

The Delta II 7920 maximum payload weight capability of 4600 Kg defines the DART mass and size constraints. See table I.1 for a listing of the DART components and mass breakdown. To maximize the capabilities of DART to achieve the outlined missions while maintaining low cost, accessibility, and reliability the Delta Design Team has expanded and refit with current technology a capsule-based, manned spaceflight system. The DART capsule outlined within utilizes an expendable strap-on, hypergolic propulsion system, an ablative heat protection system, a semi-ballistic parachute low altitude re-entry, and a low lift conical geometry. It maintains Freedom rendezvous and docking capability through the use of the reaction control system and the top docking port. The capsule utilizes the Tracking Data Relay Satellite (TDRS) and Global Positioning Satellite (GPS) systems for communications, tracking, and data relay (figures I.2, I.3, I.4, I.5, I.6, I.7, I.8).

Through the incorporation of current technology the DART capsule is being developed with a high degree of reuse, maintaining a refurbishment fraction of 0.07. Specifications of reusability and refurbishment are presented in Chapter 7, Sections 7.2: Reuse and Refurbishment, and 7.3: Costing and Reliability. The Delta design Team is currently re-evaluating the degree and requirements for DART reuse and refurbishment. These studies are focused primarily on the propulsion and thermal protective systems.

The following report presents the DART alternate manned system for design review and consideration.

H. Magazu

Introduction

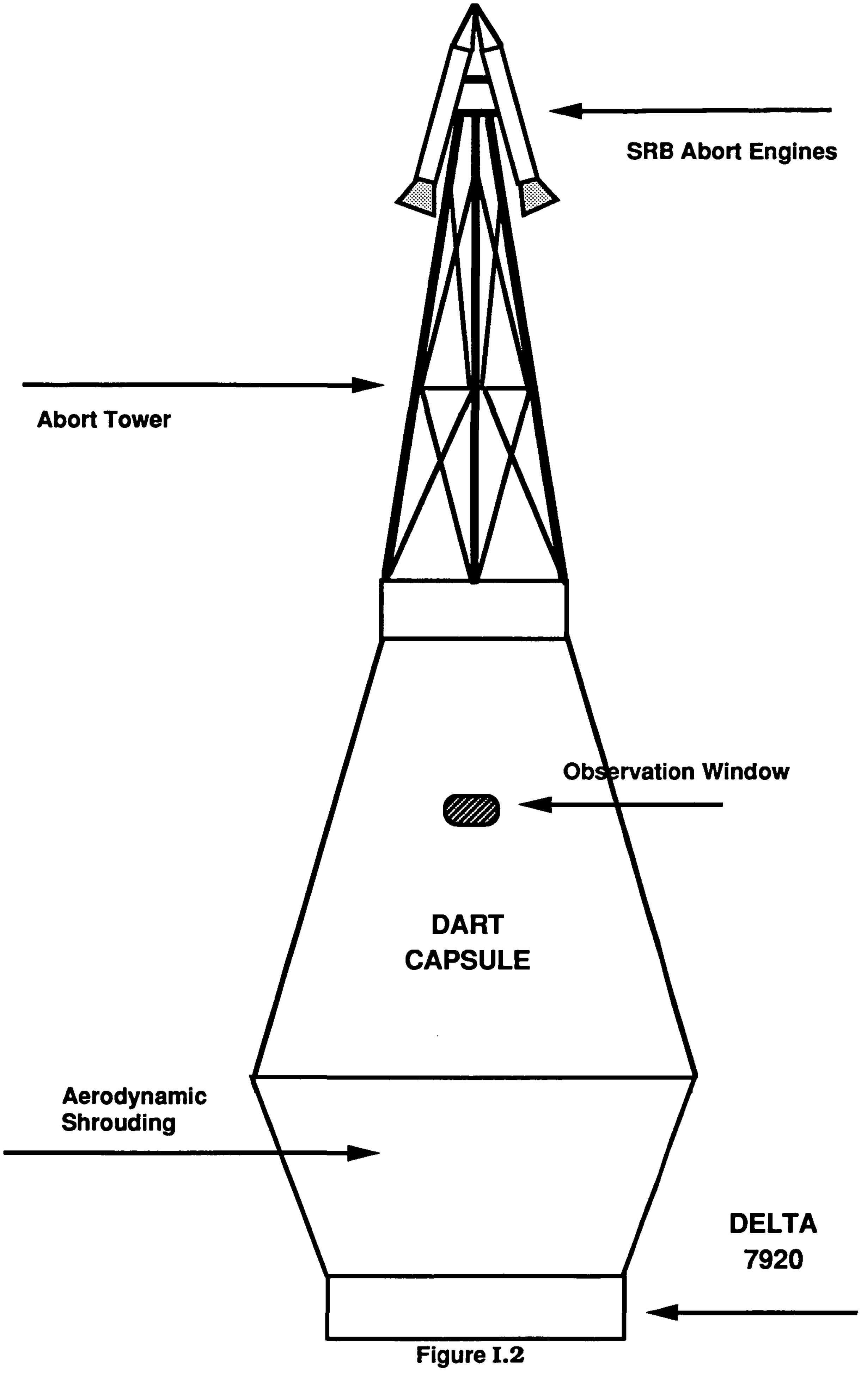

Figure I.2

H. Magazu

Mass Breakdown

System	Subsystem	Mass(kg)
Avionics		
	Data processing	96
	Altitude sensors	10
	Sensors	150
	Radar	75
	Guidance and navigation	29
	Communication	82
	Power generation	131
Human factors		
	ECLSS	634
	Food & water	574
	5 Astronauts	400
Systems Integration		
	Interface	0
	Propulsion	3
Structures		
	Main structure	237
	Docking module	28
	TPS	318
	Abort tower/motors	-22
	Impact attenuation system	129
	Chutes	200
Propulsion		
	Main engines	136
	Main propellant tanks&plumbing	80
	RCS	491
	Fuel	767
Total		**4548**

Table I.1

-C.White

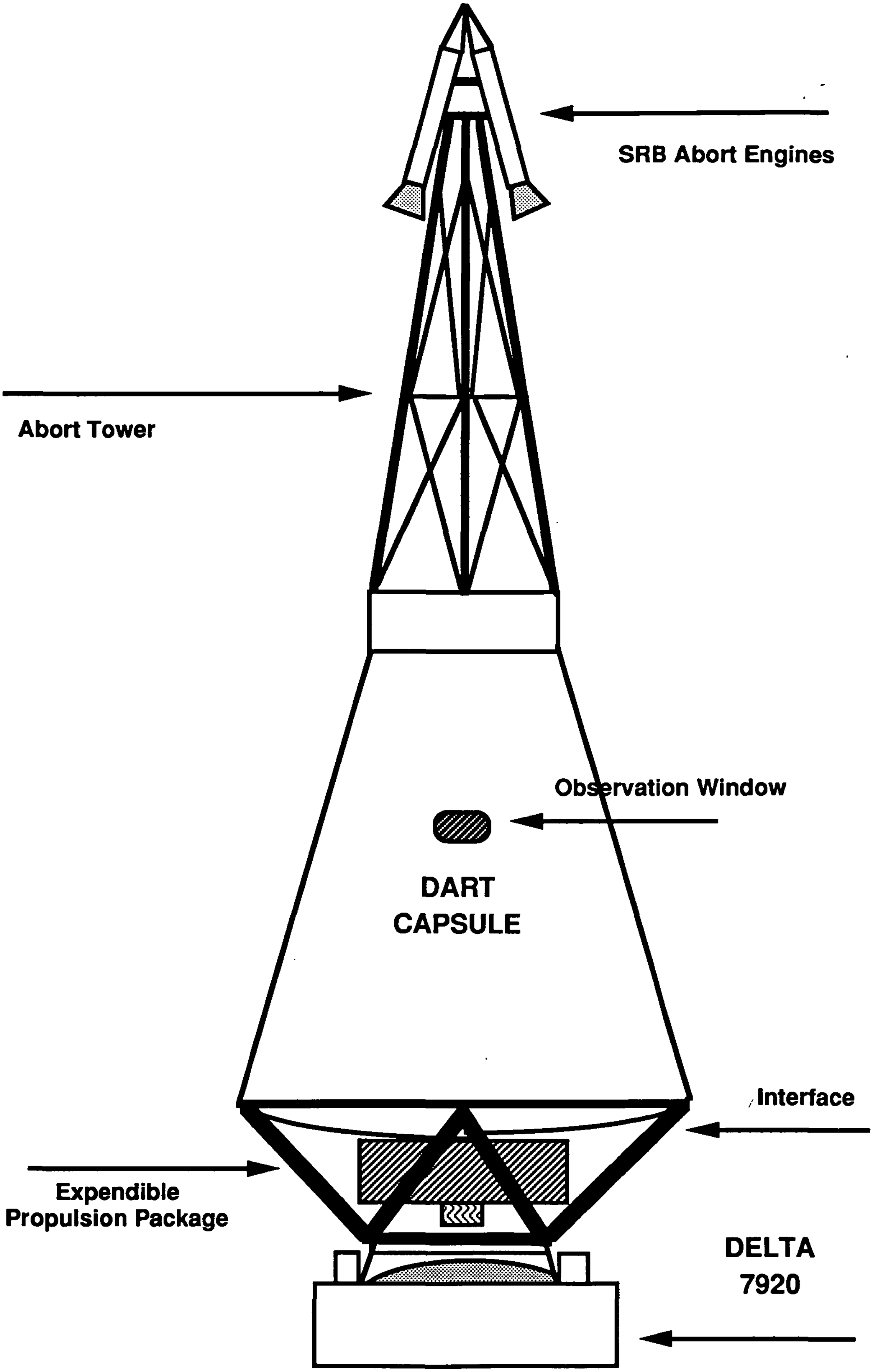

Figure I.3

H. Magazu

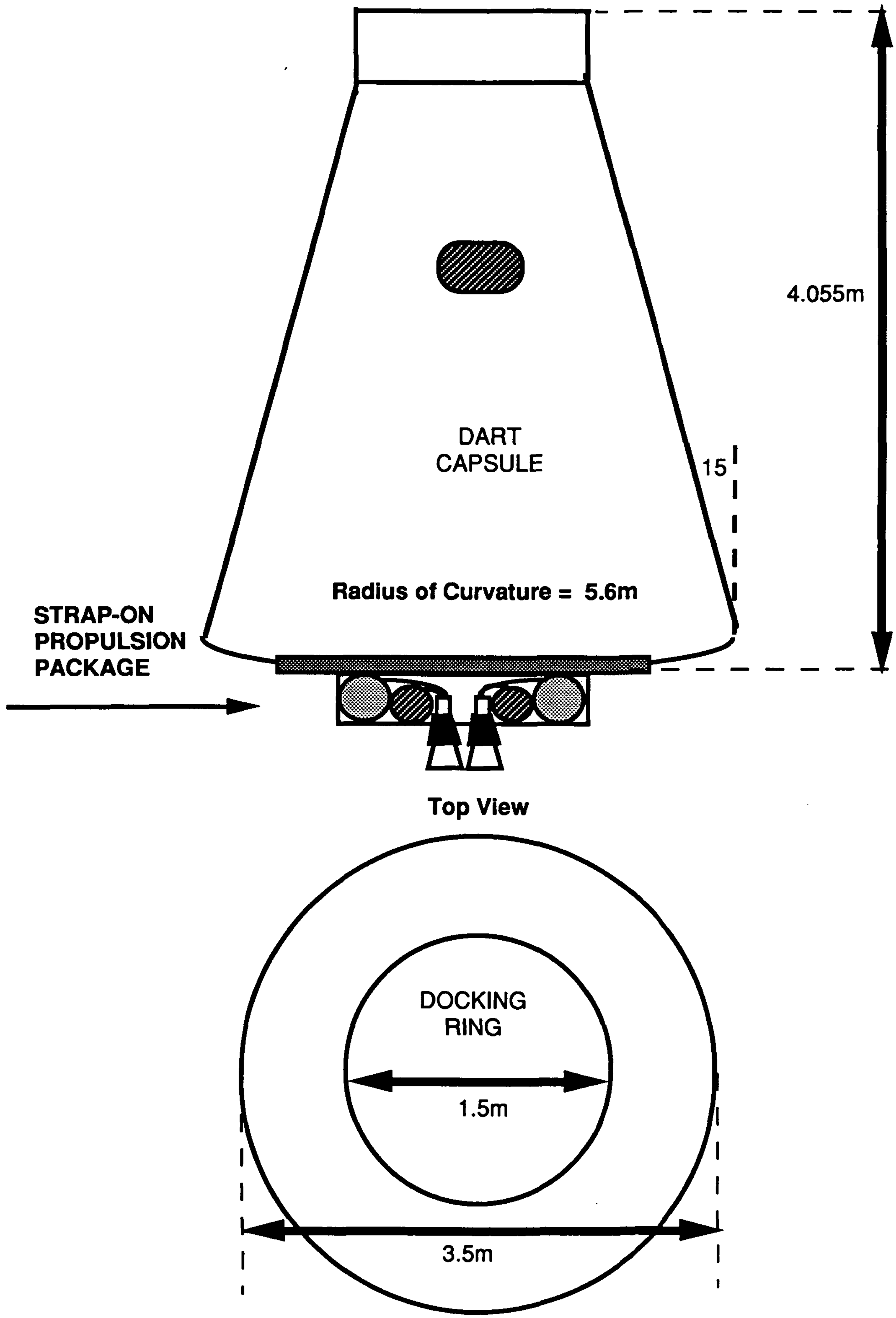

Figure I.4

H. Magazu

Interior Layout (Side View)

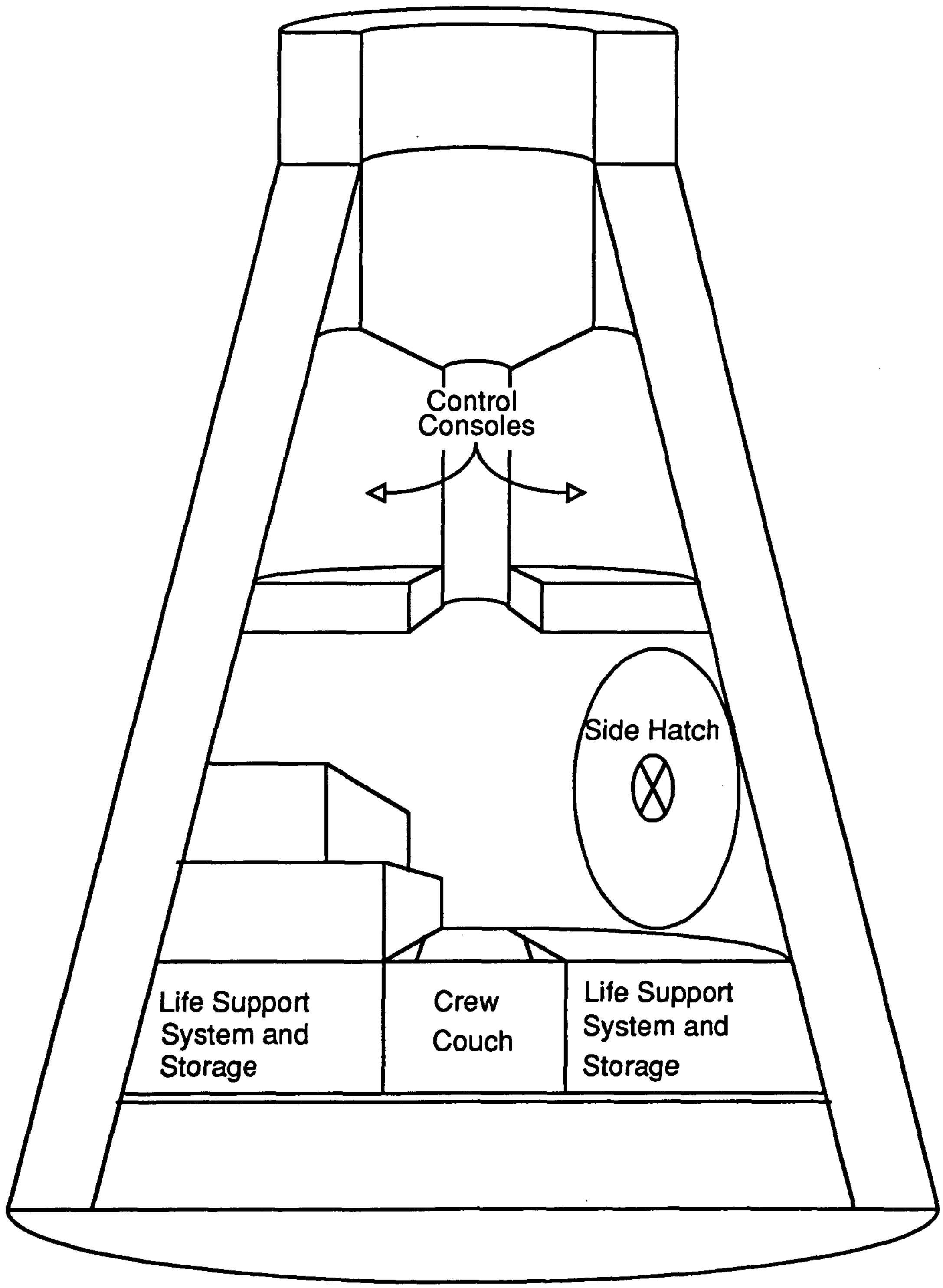

Figure I.5

R. Cunningham

Internal Layout of Capsule

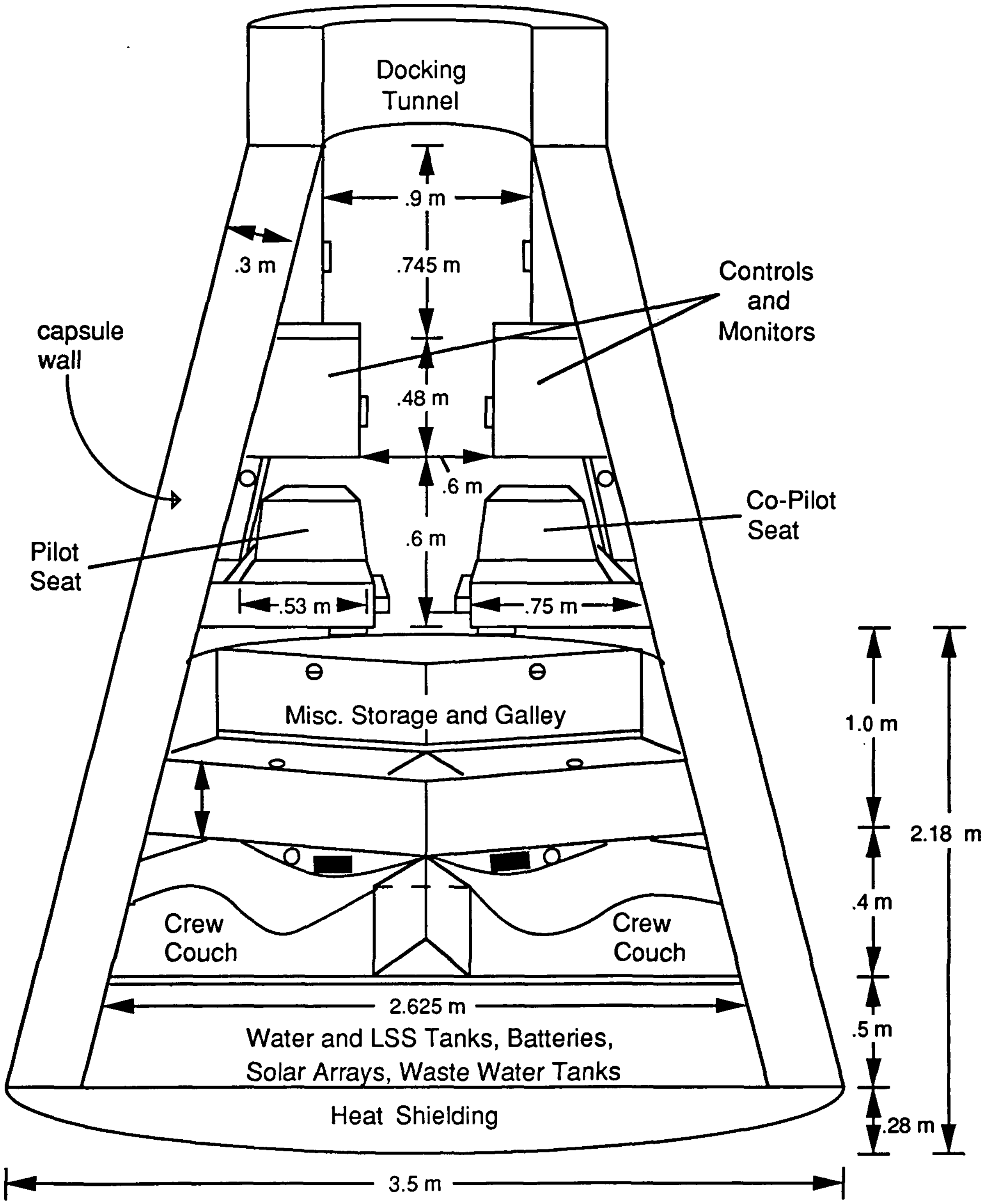

Figure I.6

R. Cunningham

View From Bottom

Front View

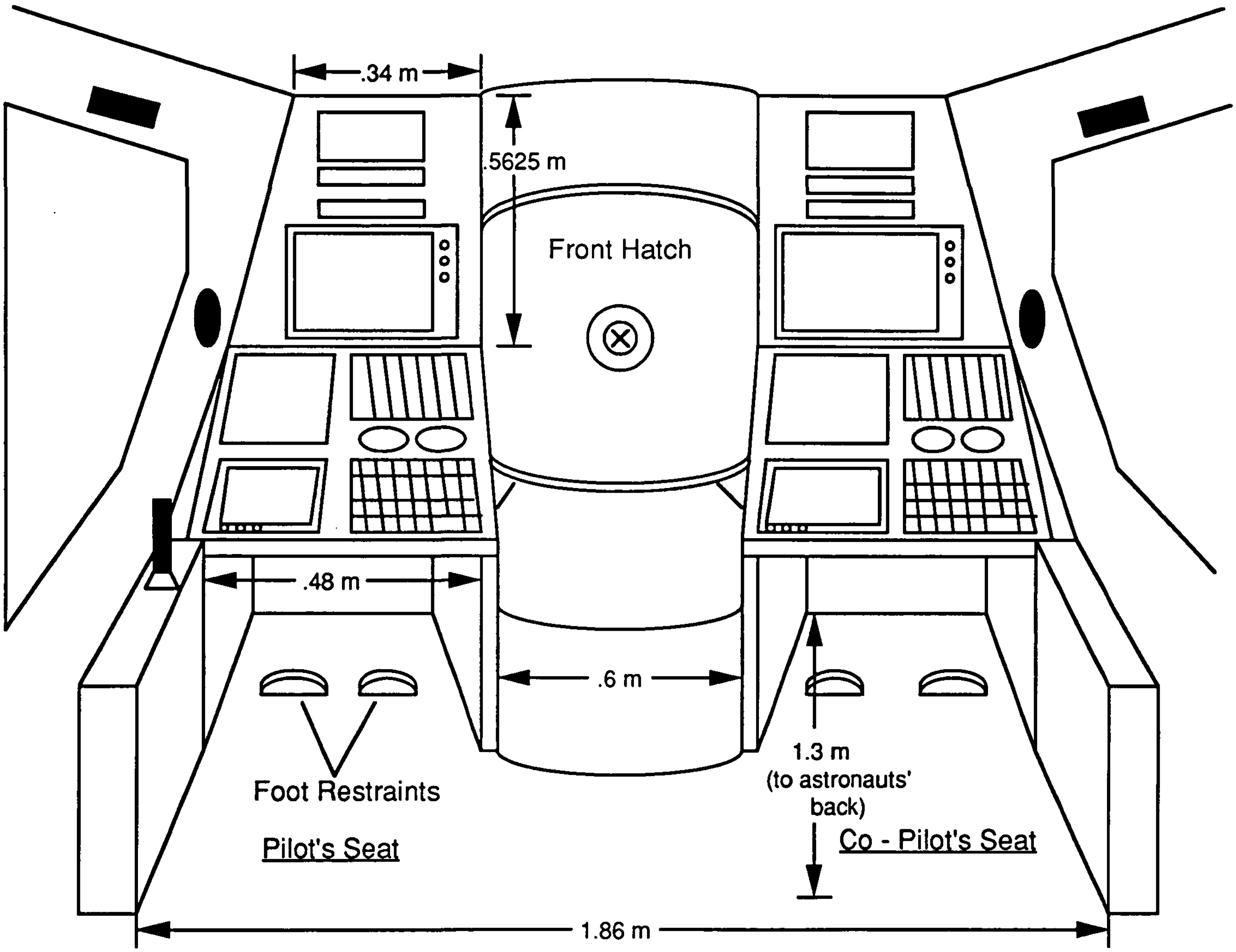

Figure I.7

R. Cunningham

View From Top

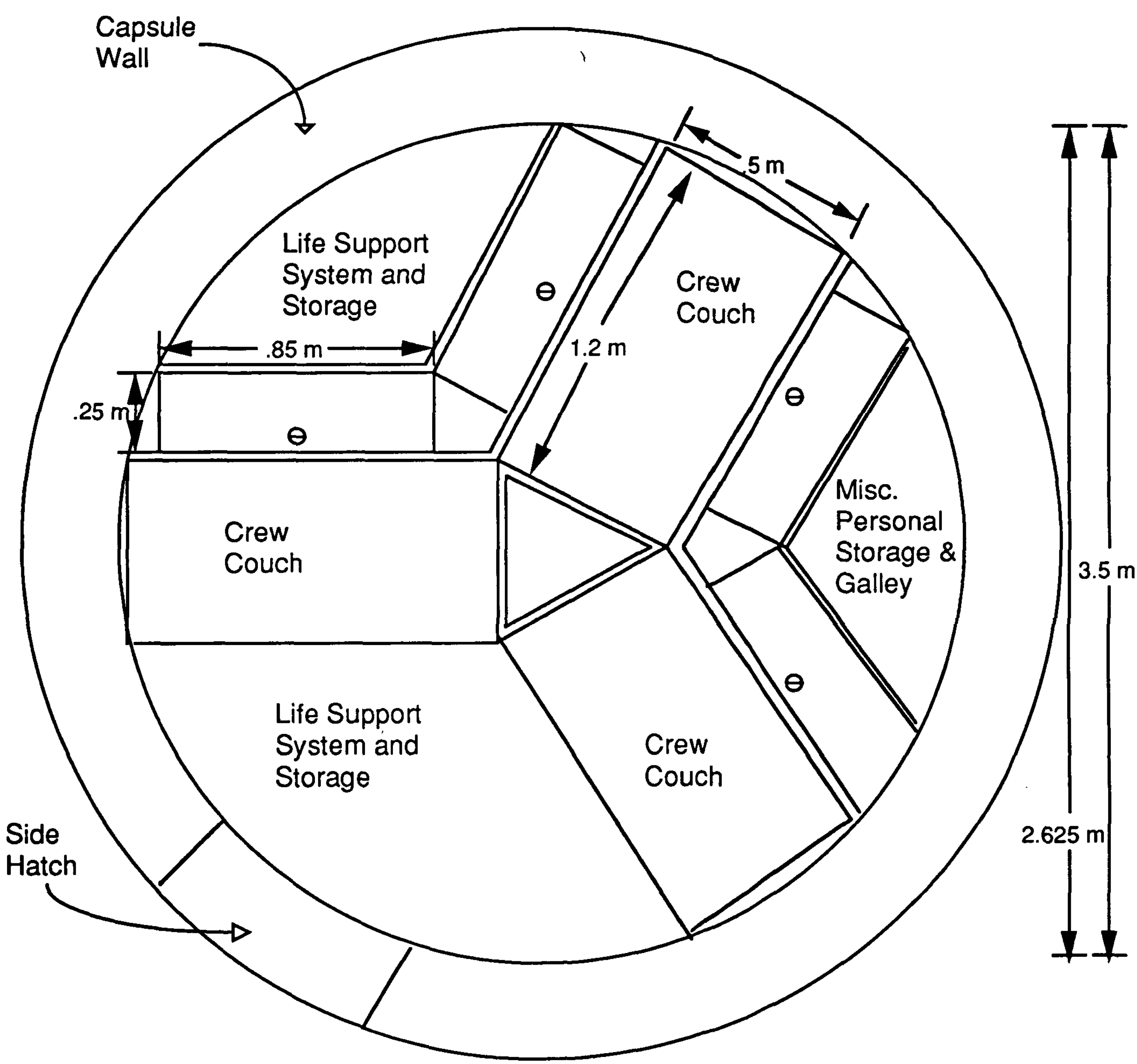

Figure I.8

R. Cunningham

Table of Content

Chapter 1

DART Mission Analysis

Section 1.1: Ground Processing

Prelaunch Activities (ref. 1)

The existing accommodations at the Kennedy Space Center will be utilized for the Delta Advanced Reusable Transport (DART) spacecraft, and the existing Delta II facilities at Cape Canaveral Air Force Station, will be employed for the launch vehicle.

Prelaunch verifications will begin at the time the DART arrives at the launch site and terminate with the initiation of the final countdown.

Prelaunch verifications shall be performed to verify that the DART systems are in readiness for the mission. All planned flight equipment/test/checkout activities shall be minimized, shall be at the systems level, and shall be oriented toward verifying the continued integrity of the hardware.

This effort includes post-flight evaluation and checkout of the DART. Hardware failing to meet post-flight acceptance criteria shall be identified for refurbishment. Upon completion of the refurbishment cycle, the DART shall be subject to prelaunch verification.

Prelaunch verification shall include but not be limited to the following verification activities:

a. Inspection for damage during shipment including review of the shipping environmental data.

b. Space vehicle combined system test including practice count (dry run) extending through spacecraft separation.

c. Interface and electrical tests, and

d. Any special tests necessary to verify adequacy of installation or operations performed at the site.

Douglas P. Vine

Launch Windows

For all space missions there are time constraints placed on the launch of space vehicles. The time span in which it is acceptable to launch is called a launch window (ref. 4). When the launch site, in the case of the DART vehicle, the Kennedy Space Center, coincides with the target objects's ground track, the spacecraft will be launched directly into the plane of the target. This launch window will be timed to occur during the early daylight hours of our launch site so that our spacecraft will have maximum daylight during its initial trajectory to orbit in case abort scenarios must be implemented. Thus recovery operations can occur in an area of maximum lighted ocean.

Launch Vehicle

The Delta Advanced Reusable Transport has been designed to be integrated with the Delta II model 7920 launch vehicle manufactured by the McDonnell Douglas Astronautics Company. The 7920 is a two stage launch vehicle which incorporates nine solid rocket motors to augment thrust during the first stage. The two-stage circular orbit capability from the Kennedy Space Center is shown in Figure 1.1a.

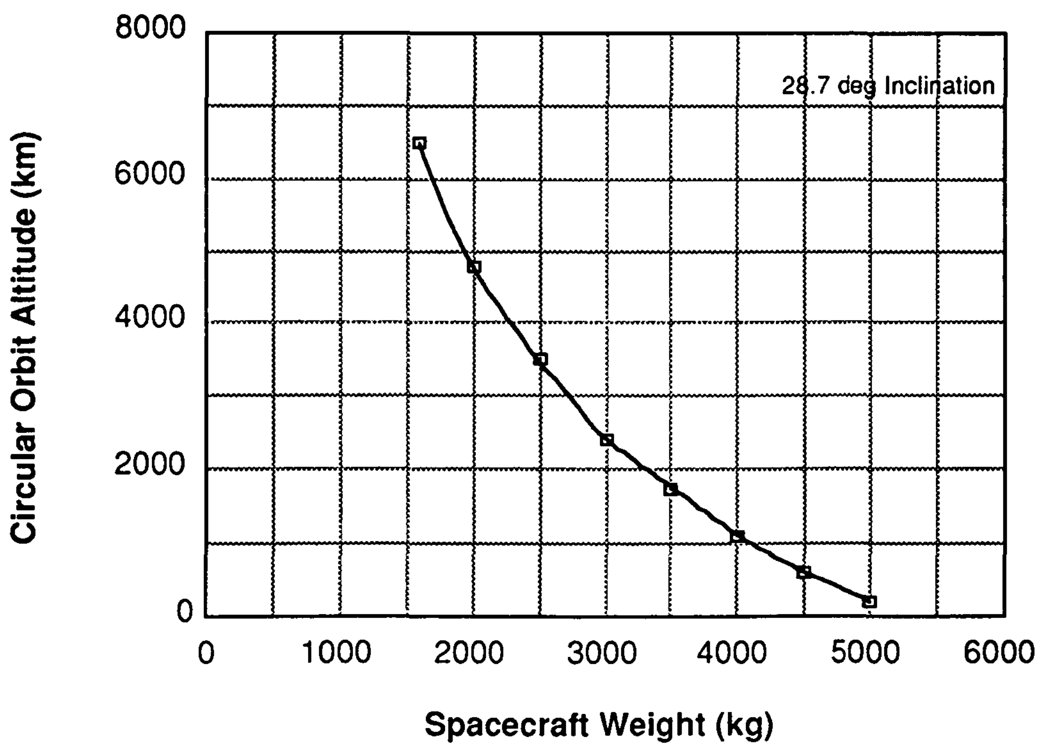

Figure 1.1a (ref 5)

Douglas P. Vine

Thus it can be seen that the maximum spacecraft weight to a 500km circular orbit altitude is approximately 4600kg.

For the mission involving launch to higher inclination orbits from the Western Space and Missile Center (Figure 1.1b), it can be seen that the maximum allowable spacecraft weight is reduced to around 3500kg to reach the 400-500km circular orbit altitude.

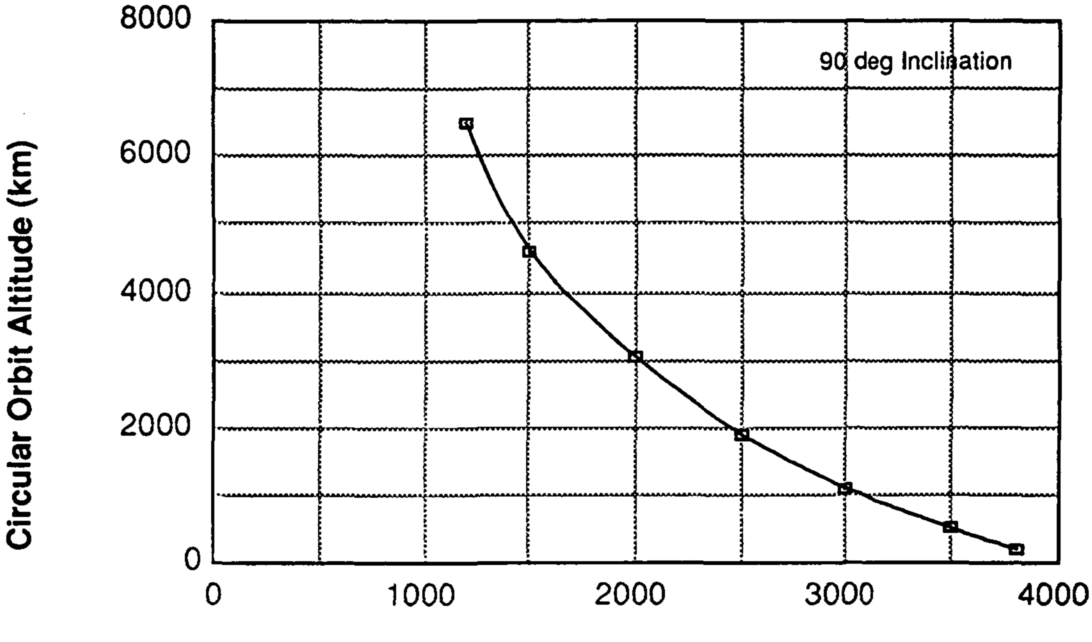

Figure 1.1b (ref 5)

Douglas P. Vine

Section 1.2: Proposed Missions

Baseline Mission

There are four basic missions which are proposed for the Delta Advanced Reusable Transport (DART) spacecraft, although each mission most likely has several spinoffs. Due to the uncertainty of the actual operation and/or construction of the Space Station Freedom, and a proposed launch date of 1995 for the DART spacecraft, it became important to design a useful mission which did not involve the Space Station.

Thus, the baseline mission proposed for the Delta Advanced Reusable Transport (DART) is a low earth orbit (LEO) satellite servicing operation. Three astronauts will be launched from the Kennedy Space Center to a rendezvous orbit which contains the particular satellite which requires servicing. While orbiting the earth for three days to become acclimated to the microgravity environment, microgravity experiments will be performed. When the astronauts have become acclimated to the microgravity environment, extravehicular activities or EVA's can be performed. The mission would be completed with a precisely timed firing of the retrorockets and a splashdown in the Atlantic Ocean (see reentry section). Recovery operations would involve a Navy ship and a compatible helicopter to hoist the DART by means of a hook to the ship's deck. Compatibility requirements for the helicopter include being able to operate from the particular Navy ship, and being able to lift and support the approximately 4000kg spacecraft. The duration of this mission is four to five days.

Microgravity experimentation on board the DART will provide a productive enhancement to the overall DART baseline mission. Available storage, contingent on weight, and volume constraints, will be the limiting factor on the numbers of experiments which can be performed. Power limitations during the mission will also limit the number and types of experiments which can be performed. The United States, Europeans, Soviets and Japanese have all conducted microgravity research in areas as diverse as: metals, alloys, and composites, fluid dynamics and transport phenomena, biotechnology, gases, ceramics, and combustion science (ref. 6). Another area of interest is the study of how to perform these experiments in space. The design of these experimental technologies, facilities, and their instrumentation is of primary concern to successful experimentation aboard the DART. Storage facilities for experimentation is provided near the base of the astronaut pressure vessel in the form of a series of drawers or storage bins (see human factors section). An initial ideal series of microgravity experiments could include the NASA Get Away Specials or GAS can experiments. These experiments are compact, generally light weight, and are designed with their own power generation (ref. 6).

Douglas P. Vine

The next phase of the baseline mission involves a satellite EVA. An EVA would most likely include routine maintenance on a satellite. Routine maintenance is a general class of situations in which components of a system are scheduled for maintenance as determined by lifetime (ref. 1). A satellite may also need to be tended to if there is an expected failure of a component.

Besides the general life support equipment i.e. food, oxygen, other gases, there are special requirements and instruments for this type of mission. One requirement is that the astronauts must be in a microgravity environment for at least three days before an EVA can be performed. Another requirement is that a minimum of two EVA crew shall engage in EVA activities so that a "buddy system" can be used (ref. 2). Other procedures involving cabin pressurization, prebreathing, etc., are discussed in the human factors section of this report.

Special tools are also required for performing the EVA. Considerations must be made for the masses of the tools used, for the masses of the replacement components, and for the mass of any recoverable components. Considerations must also be provided for the proper storage and placement of the aforementioned items. One possible area for the stowing of the aforementioned equipment would be in the compartments designed for microgravity experiments. This area could easily be shared or converted depending upon the particular mission needs.

Other mission concerns include space radiation. The danger from radiation in LEO is relatively small. One area of concern however is a region known as the South Atlantic anomaly, where the radiation levels are significantly higher. Astronauts would have to come back into the spacecraft if the EVA were occurring in this region to be adequately protected from this radiation hazard. We are mainly limited to low earth orbit operations due to the dangerous radiation levels at higher altitudes.

An extension of the baseline mission could include a second day of EVA. Since vital gases like nitrogen and oxygen are relatively light, we have the potential to pressurize and depressurize the pressure vessel of DART at least two times. There is however a question of whether or not the same astronaut can perform EVAs on consecutive days. Another possibility and a potentially shorter mission to maintain or repair satellites would involve the use of a robotic arm. The special considerations in this mission include advanced software to aid in the control of the robotic arm. Only two astronauts would be required for this mission. Therefore the weight of the robotic related equipment should be designed to be about equal to the weight of the replaced astronaut. It should be pointed out that the EVA to be performed would have to be relatively simple since robot manipulation of sensitive components is quite a difficult task (ref. 3).

The more expensive geosynchronous earth orbital (GEO) satellites might be serviceable with this DART/robotic arm configuration. This would be a very desirable mission. It would require an orbital transfer from LEO, since due to weight constraints,

Douglas P. Vine

our launch vehicle can only deliver the DART spacecraft to an approximately 500km circular orbit (see launch vehicle). Important considerations for this mission are: fuel consumption during LEO to GEO transfer, weight problems due to possible additional radiation shielding required, and problems with the present capabilities of existing robotic technology. The DART could reach significantly higher orbits if a Titan booster were implemented (see advanced missions). Such an integration would significantly reduce the LEO to GEO transfer fuel consumption, and reduce the time to transfer through dangerous radiation. More weight in the form of additional shielding could also be applied to the spacecraft with higher orbit altitudes still achievable. These engineering difficulties do not seem insurmountable, and we are confident that such a mission could be realized before the end of the decade.

Space Station "Taxi"

One proposed mission is utilizing the DART spacecraft as a space "taxi". The "taxi" concept entails the delivery of new astronauts to the space station, and returning the current station personnel to earth. The latest United States proposal for a space station would have a permanently manned station with four existing personnel on board at any given time. Crew rotation is scheduled to occur approximately every ninety days.

The mission involves launching four astronauts from the Kennedy Space Center to an approximately 460km, 28.5 degree inclination orbit. This orbit is in the same plane as the space station and only about 40km lower in altitude. The reasons for the selection of launch to this particular orbit reflect a plus or minus 18.5km possible altitude error in our launch vehicle selection, and a 16.1km distance rule for the firing of our thrusters too near to the space station due to the exhaust fuel's potentially corrosive effects to Freedom (see rendezvous section). After the DART spacecraft successfully rendezvous and docks with the space station, there will be a complete crew rotation of DART and station personnel. The spacecraft will then separate from Freedom, drift away until DART can safely fire its retrorockets without deleterious effects to Freedom for reentry, reenter the atmosphere, and splashdown in the Atlantic Ocean. Recovery operations would utilize Navy ships and compatible aircraft. The length of the mission would be anywhere from one to three days.

The mission will take one day if there is a successful rendezvous and docking. The mission may have a second chance for docking in which case the duration of the mission could extend to three days. If too much fuel is expended either in orbital plane change corrections or rendezvous attempts, docking will not be able to occur and the mission will not be successful.

Douglas P. Vine

Special requirements for a docking mission include a spacecraft window and/or a special camera to observe the docking procedure. Space radiation is not a concern during this mission.

The spacecraft interior will have to be reconfigured from the baseline mission, since the space "taxi" concept will require a couch for the fourth or additional astronaut. A lesser amount of supplies will be necessary than on the aforementioned EVA baseline mission. Thus, the needed space for our additional passenger could easily be taken from a removed storage compartment in the capsule.

It is clear that the space shuttle can easily perform this mission, however, the costing section of this report shows that a DART mission is a significantly less "expensive" undertaking than a shuttle mission. The DART spacecraft is designed to augment the shuttle program, and in the unfortunate event of another shuttle accident or in the time period of the eventual phasing out of the shuttle program, the DART will continue the United States' manned space capabilities.

Space Station "Tug"

Another station dependent mission proposed, is utilizing the DART spacecraft as a space "tug". The "tug" concept involves the delivery of necessary vital items to the space station.

Similar to a space station "taxi", this mission entails launching two astronauts from the Kennedy Space Center to an approximately 460km, 28.5 degree inclination orbit. This orbit is in the same plane as the space station and only about 40km lower in altitude. The reasons for the selection of launch to this particular orbit reflect a plus or minus 18.5km possible altitude error in our launch vehicle selection, and a 16.1km distance rule for the firing of our thrusters too near to the space station due to the exhaust fuel's potentially corrosive effects to Freedom (see rendezvous section). After the DART spacecraft successfully rendezvous and docks with the space station, the payload will be delivered to Freedom through the docking tunnel. It is also possible to exchange one or both of the DART astronauts with station personnel should the need arise. The spacecraft will then separate from Freedom, drift away until DART can safely fire its retrorockets for reentry, reenter the atmosphere, and splashdown in the Atlantic Ocean. Recovery operations would utilize Navy ships and aircraft. The length of the mission would be anywhere from one to three days.

The mission will take one day if there is a successful rendezvous and docking. The mission may have a second chance for docking in which case the duration of the mission could extend to three days. If too much fuel is expended either in orbital plane

Douglas P. Vine

change corrections or rendezvous attempts, docking will not be able to occur and the mission will not be successful.

Special requirements for a docking mission include a spacecraft window and/or a special camera to observe the docking procedure. Space radiation is not a concern during this mission.

The two astronaut crew for this mission will mean that the payload capacity of DART can be greatly augmented from the payload capacity for the baseline mission. It is clear that the space shuttle could deliver larger payloads to the station. The goal, however, is to be able to deliver vital items quickly and cheaply to the station (see costing section). Also, it will become necessary to have a vehicle that can deliver the necessary vital items to the space station should the shuttle program be interrupted by another accident.

Emergency Space Station Escape

Should an emergency arise on board the Space Station Freedom it may become necessary to evacuate the station personnel. Through the production of several DART spacecraft, one could be configured and ready to perform as an emergency space station escape vehicle at all times. On this mission, one astronaut would be launched from the Kennedy Space Center, rendezvous and dock with the space station, evacuate the up to four station crew, and reenter the atmosphere with up to five astronauts. The DART may, depending upon the final station configuration, be able to be used as a permanent lifeboat attached to the actual station structure.

Other Missions

Of the four proposed missions, it is evident that there are numerous spinoff capabilities such as: extended periods aboard the space station or partial crew exchanges during the "taxi" or "tug" missions. Other proposed missions could include launches to higher inclination orbits from the Western Space and Missile Center (see launch vehicle). The foreseeable problems include higher radiation levels, and more stringent spacecraft weight allowances. A higher inclination orbital mission could include the servicing of higher inclination satellites including the polar mission to planet earth platforms (see advanced missions).

Douglas P. Vine

Section 1.3 Rendezvous Analysis

Introduction

The rendezvous of a chase vehicle with a target spacecraft is a complex problem. Any movement in a gravitational field is followed by perturbations caused by the field.

The vis-viva equation relates the velocity in an orbit to the distance from the center of the gravitating body[7]:

$$v^2 = \mu\left(\frac{2}{r} - \frac{1}{a}\right)$$

The velocity is inversely proportional to the square root of the radius. Therefore, to increase velocity, decrease the orbital radius. The vis-viva equation was used to calculate necessary velocity changes for Hohmann transfers in the rendezvous sequence.

The following set of equations are Hill's Equations[8] which describe the motion of satellites in neighboring orbits.

$$\ddot{x} - 2ny - 3n^2x = f_x$$
$$\ddot{y} + 2nx = f_y$$
$$\ddot{z} + n^2z = f_z$$

where $n = \sqrt{\frac{\mu}{a^3}}$ $\quad a$ = semi-major axis

The force-free, in-plane solutions to Hill's Equations are the Clohessey-Wilshire Equations[8], given below. These equations were solved for the final approach to the target vehicle. The space station Freedom was chosen as the baseline for the rendezvous analysis, though the equations can be applied to many other scenarios.

$$\dot{y}_o = \frac{[6x_o(nt - \sin nt) - y_o]n \sin nt - 2nx_o(4 - 3\cos nt)(1 - \cos nt)}{(4\sin nt - 3nt)\sin nt + 4(1 - \cos nt)^2}$$

$$\dot{x}_o = -\frac{nx_o(4 - 3\cos nt) + 2(1 - \cos nt)\dot{y}_o}{\sin nt}$$

M. Gates

The two-dimensional coordinate system used consisted of the radial line from the Earth (x-axis) and the tangential along the orbit (y-axis), as shown below.

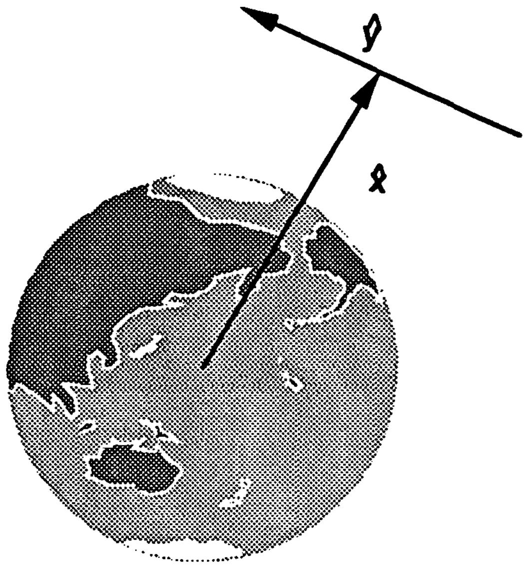

Figure 1.3a: Coordinate system

Rendezvous Considerations

There are many factors to consider in planning a rendezvous sequence[9]. Some are outlined below:

1) Achieving an appropriate phase angle between the target and chase vehicle restricts the launch window and forces a phasing maneuver to be used.

2) The launch window and direction of launch must be chosen so that the chase vehicle is in the orbit plane of the target. Out-of-plane maneuvers are very fuel expensive. Corrections for slight deviation must be allowed for in orbit.

3) The final maneuvers are performed visually, so the vehicles must both be in lighted conditions during this time, they cannot be in the Earth's shadow.

4) The rendezvous sequence must be flexible to correct for errors in navigation, guidance, and flight control systems.

5) The rendezvous sequence must not violate any mission rules - launch window must allow for correct lighting conditions at launch, enough RCS (reaction control system) fuel must remain onboard to accomplish mission and return if OMS (orbital maneuvering system) fails.

6) Resulting launch window must be of reasonable duration.

Initial Analysis

In the first-cut analysis, the launch and in-flight deviations were not considered. The rendezvous consisted of one maneuver that would bring the DART to the target vehicle. Many cases were done for various distance vectors. Since only in-plane approach maneuvers were considered, no z components were used. Figure 1.3b shows some results of the preliminary analysis. It was found that the smaller the distance, the smaller the impulse needed, as was expected. A trajectory with only one component, x or y, seemed the most efficient.

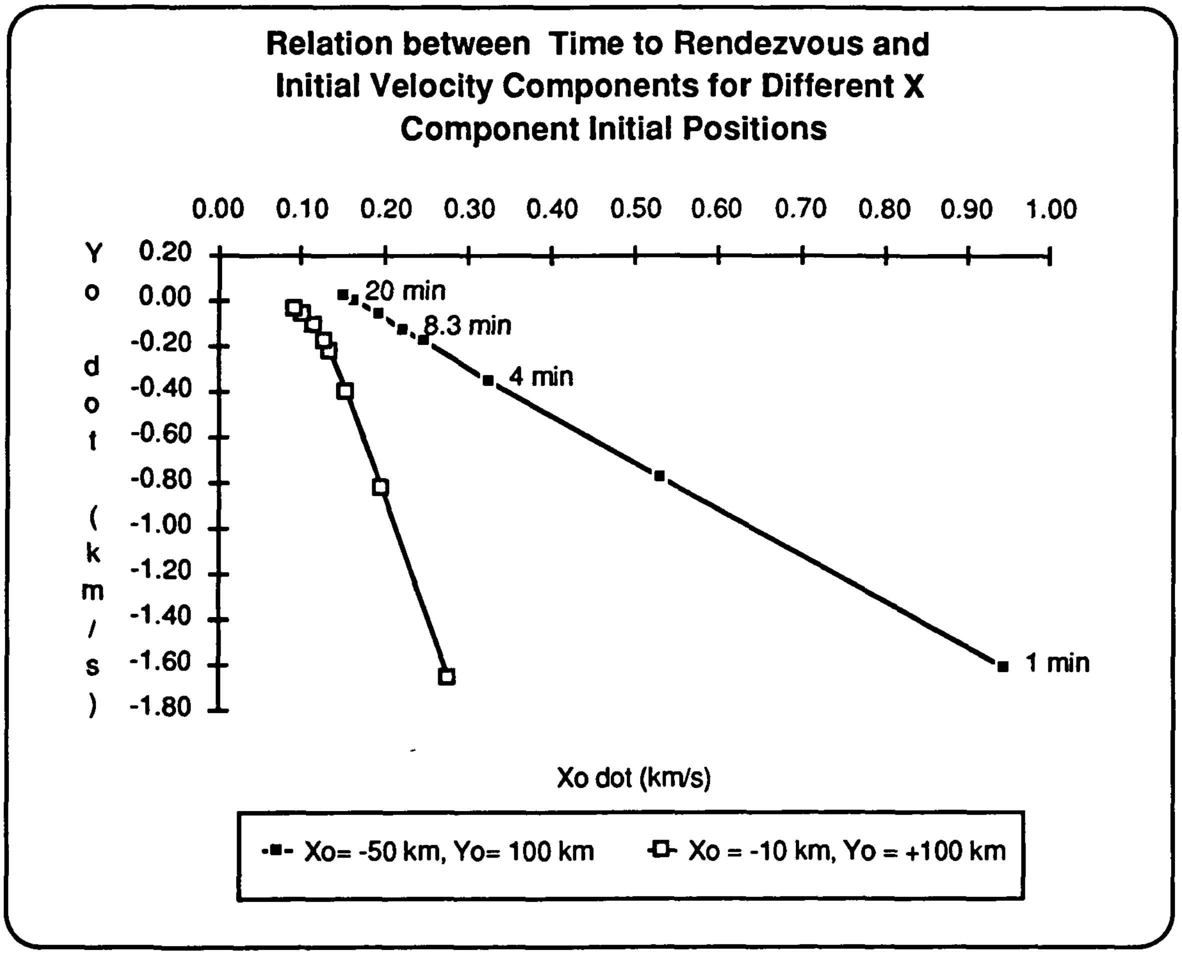

Figure 1.3b: Velocity Components corresponding to generic approaches.

M. Gates

Secondary Analysis

Following the initial analysis, which showed the trend toward lower velocities for smallest distances, several analyses were then done for a maneuver with no y component, which is called a r-bar maneuver. The Clohessey-Wilshire Equations were again solved for many cases with radial distances from 10 km to 100 km. A chart summarizing several analyses is shown below in Figure 1.3c, demonstrating the relationship between velocity components and time to rendezvous for three generic approach distances.

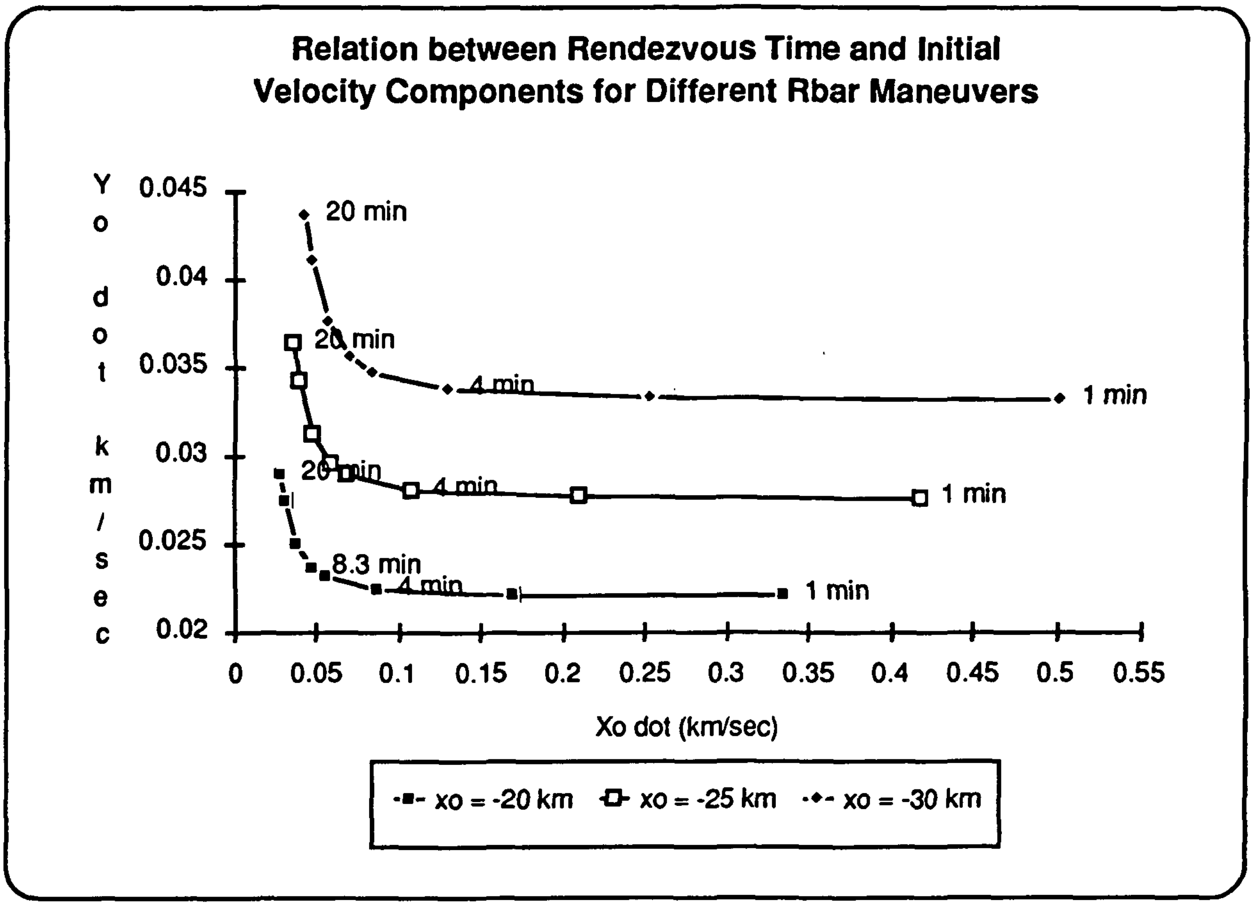

Figure 1.3c: Relationships between impulse velocity components, time to rendezvous, and initial radial distance.

The velocity components clearly drop off for small radial distances. Note that there are still x and y components of velocity needed. This is due to the coupling of the motion from orbital mechanics.

Figure 1.3d shows the time to contact vs. magnitude of impulse velocity for a 40 km r-bar trajectory.

M. Gates

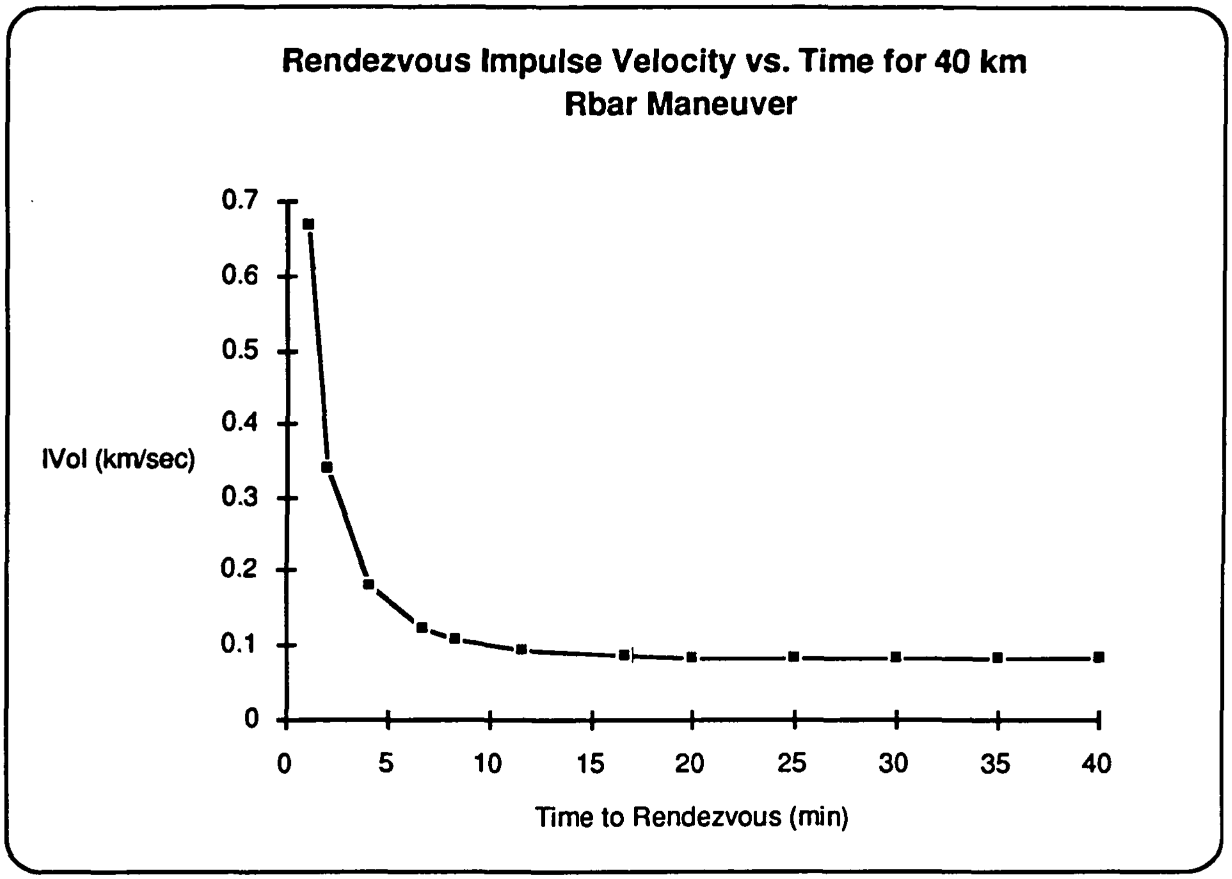

Figure 1.3d: Time to rendezvous vs. Impulse Velocity Magnitude

In viewing this curve, it is evident that the curve levels off for times larger than about 4 - 5 minutes. Since we are concerned with minimizing time as well as fuel consumption, a 4 minute rendezvous was decided upon as a baseline rendezvous time. Obviously, a 4 minute rendezvous time for a 40 km distance is unreasonable since the ΔV would be 167 m/sec. However, the shape of this curve is representative of typical ΔV vs. time graphs, so the 4 minute time was chosen for smaller distances.

The analysis up to this point did not take into account in-flight deviations and errors due to navigation instrumentation, human error, or the Delta craft. To account for these errors, a rendezvous sequence was set up to allow for specific points were corrective maneuvers would be made, and a much slower (and safer) approach could be done.

Rendezvous Sequence

The rendezvous sequence consists of the collection of maneuvers from the final stage Delta separation to the arrival at the final point of interest; docking, inspection sight, etc.

Rendezvous sequences were researched[9] and pertinent points were applied in the rendezvous sequence below (Figure 1.3e). The sequence given is for the space station, though similar sequences would be used for other missions.

Rendezvous Sequence for Space Station Scenario

- ΔV to circularize at 460 km, 28.5° (difference in altitudes leaves room for corrective maneuvers)
- Stay at 460 km to achieve correct phase (this allows for larger launch window)
- Corrective combination (NCC1) - burn to achieve an elliptic orbit with apogee at 499 km
- Second Coelliptic Maneuver (NSR2) - burn from apogee to circularize at 499 km, also include plane change maneuver up to 0.5° if necessary
- Terminal Phase Initiation (TPI) - when on Freedom's radial line, null relative rates

Figure 1.3e: Rendezvous Sequence

This sequence allows for corrective maneuvers to be made in-flight using sensor and visual input. Plane change maneuvers of up to and including 0.5° will be permitted, though not above, unless there are some extenuating circumstances. This is because a 0.5° plane change maneuver made at 499 km requires 65 m/s velocity change, as calculated using the law of cosines. The vis-viva equation was used for the Hohmann transfer calculation. For the present, it has been assumed that the Delta will leave the DART at an angle of about 0°, making the circularization maneuver very small. In addition, using the vis-viva equation, the difference in orbital velocity at 500 km and 400 km orbits was found to be only 0.5 m/s. It has therefore been assumed that nulling the relative rates will be a fairly small maneuver. The ΔV's required for the majority of the sequence are given below in Figure 1.3f.

ΔV's for Rendezvous Sequence
NCC1 => ΔV = 12.18 m/sec
NSR2 => ΔV = 3.4 m/sec
Plane correction => ΔV = 65 m/sec

Figure 1.3f: Major ΔV's

At the end of the TPI, the relative rates of the two spacecraft are nulled, they are on the same radial line, and are ready for the final approach after checking all sensors and readying the crew.

Proximity Operations - The Final Approach

In choosing a final maneuver, three basic types were considered[9]. Maneuvers with components in x and y are called direct approach, those with the distance vector in x (radial) are termed R-bar maneuvers, and maneuvers with the distance vector in y (tangential) are called V-bar maneuvers. All are outlined below in Figure 1.3g.

Final Approach Manuevers - Proximity Operations Options

Direct Approach

- from below and ahead of target, enhanced lighting conditions
- reduce ΔV with braking thrusters
- sufficient closing velocity must be maintained to insure intercept
- null significant ΔV near target => plume impingement

V-Bar Approach

- establish initial closing rate toward target, usually from ahead of target
- combination retrograde and radially outward burns until very close
- burn to dock
- close burns produce plume impingement

R-Bar Approach

- initiated with orbiter on target's radial line with relative rates nulled
- initial closing rate established
- orbital mechanics provides braking force
- combination retrograde and radial downward burn moves chase up radial line
- minimizes plume impingement

Figure 1.3g: Proximity Operations Options

An r-bar maneuver was chosen to minimize exhaust plume impingement upon the target vehicle and so orbital mechanics would provide the braking, decreasing fuel consumption.

To insure that the final approach is made slowly, a rule has been implemented that no burns will be made that are over 1% of the distance of the vehicle to the target. Consequentially, many short burns must be made, each with decreasing strength as the DART approaches. At the onset of the final maneuver, proximity operations, the DART is 1000 meters from its target. A sequence has been developed and is listed below in Figure 1.3h.

Proximity Operations
1) 1000 m => 500 m
2) 500 m => 100 m
3) 100 m => 50 m
4) 50 m => 25 m
5) 25 m => 10 m
6) 10 m => 5 m
7) 5 m => 0.5 m

Figure 1.3h: Rendezvous Burn Sequence

The Clohessey-Wilshire equations were again used to solve for impulse velocity components and the time to complete each maneuver. The impulse velocity components corresponding to each of these r-bar maneuvers are shown in the following figures.

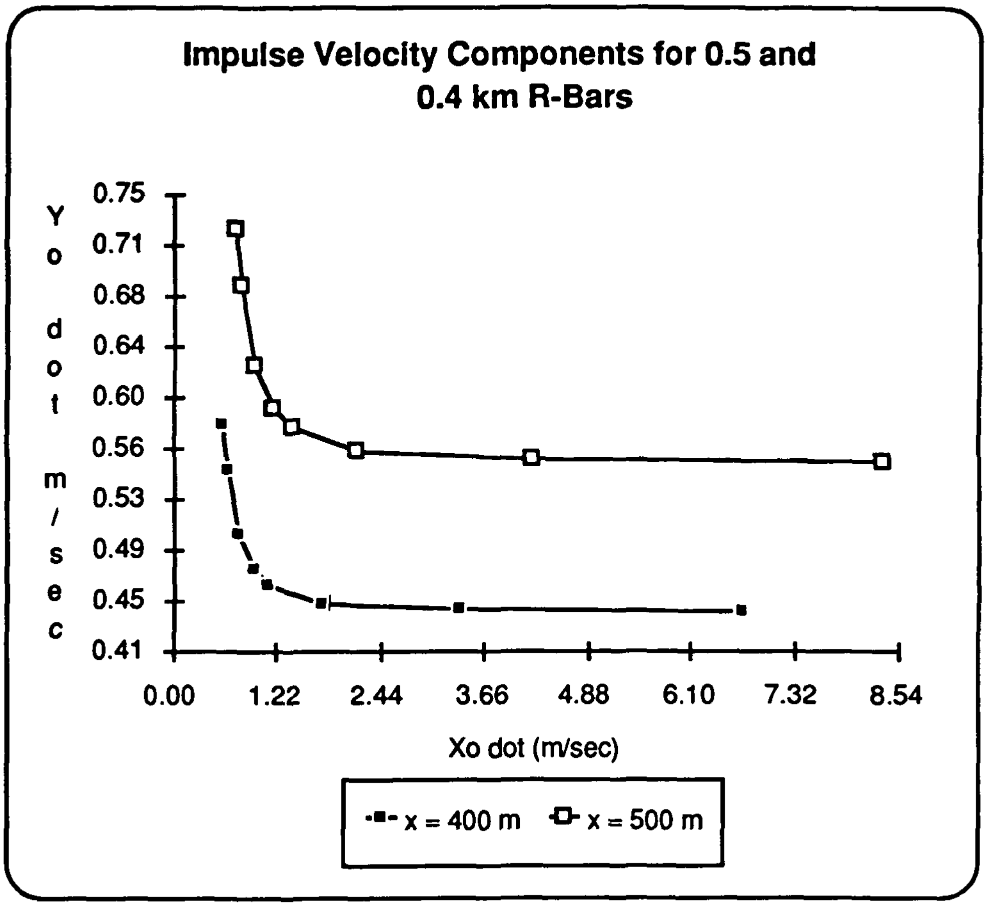

Figure 1.3i: Impulse velocity components for first two burns.

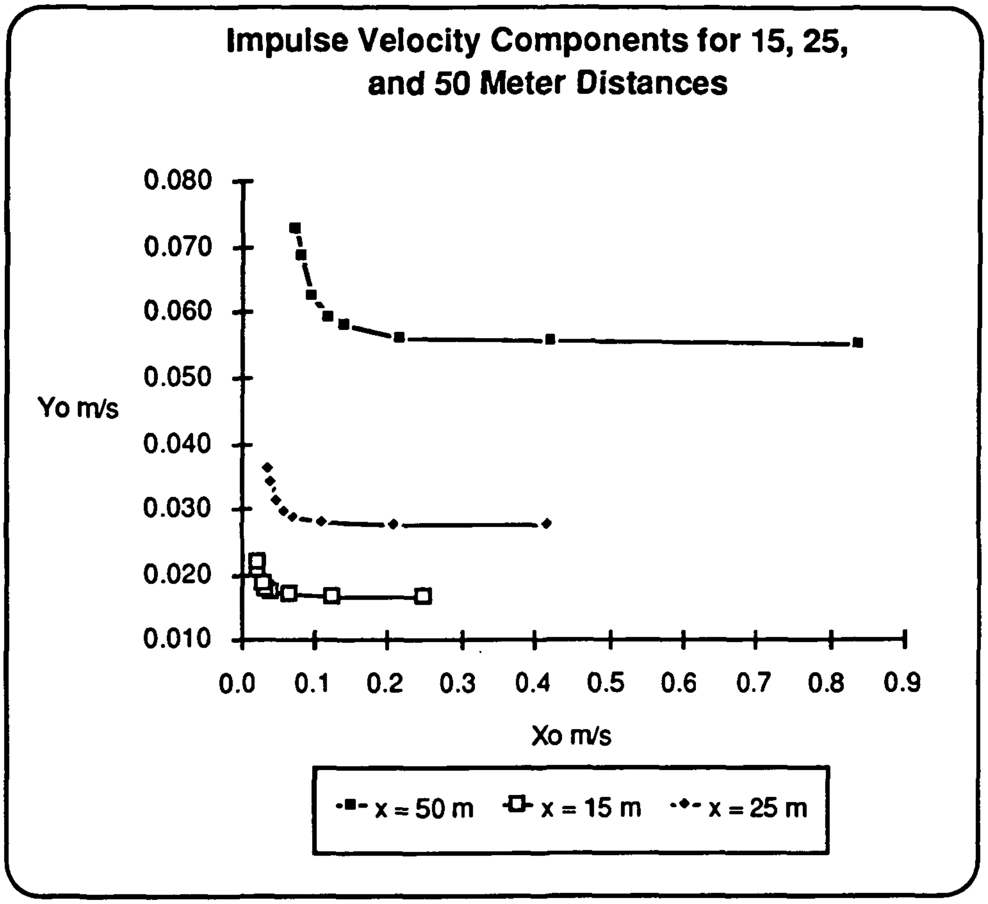

Figure 1.3j: Impulse Velocity Components for 15, 25, and 50 Meter R-Bars

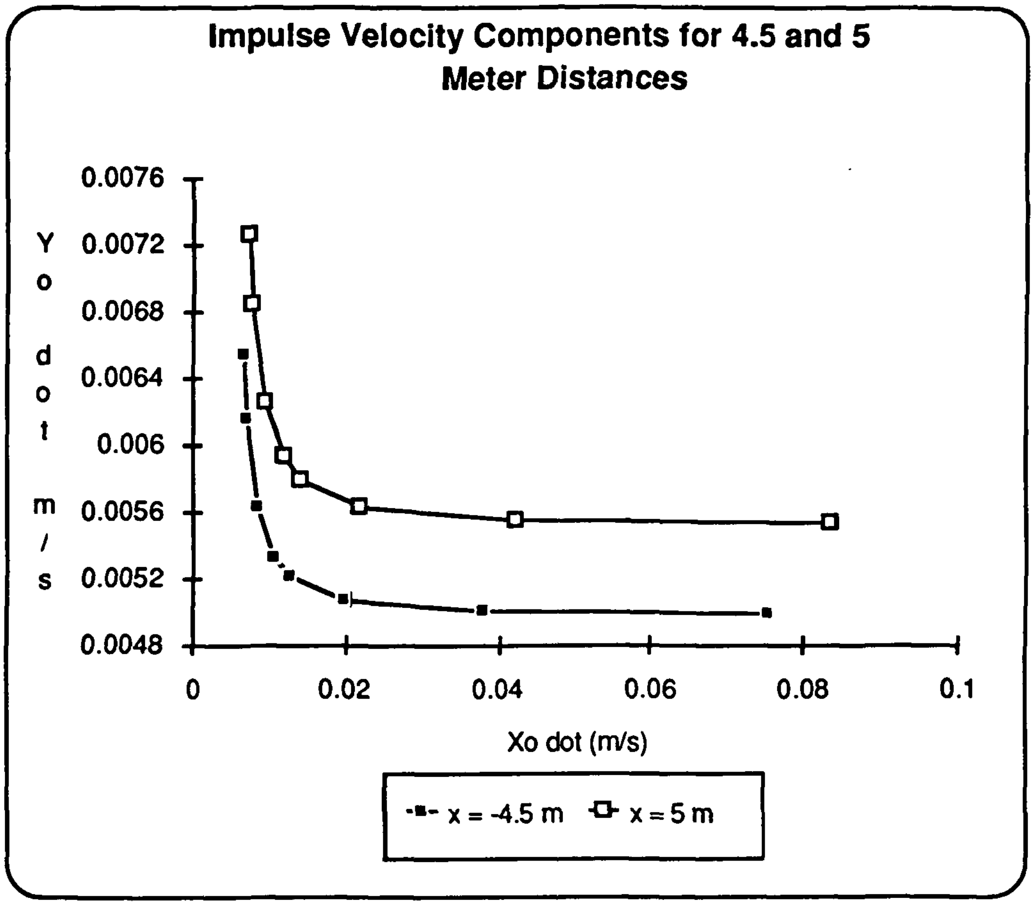

Figure 1.3k: Impulse Velocity Components for 5 and 4.5 Meter R-Bars

To minimize both the velocity and time to complete each maneuver, the time to contact vs. total velocity for each case was again graphed. These results are given in the following figures.

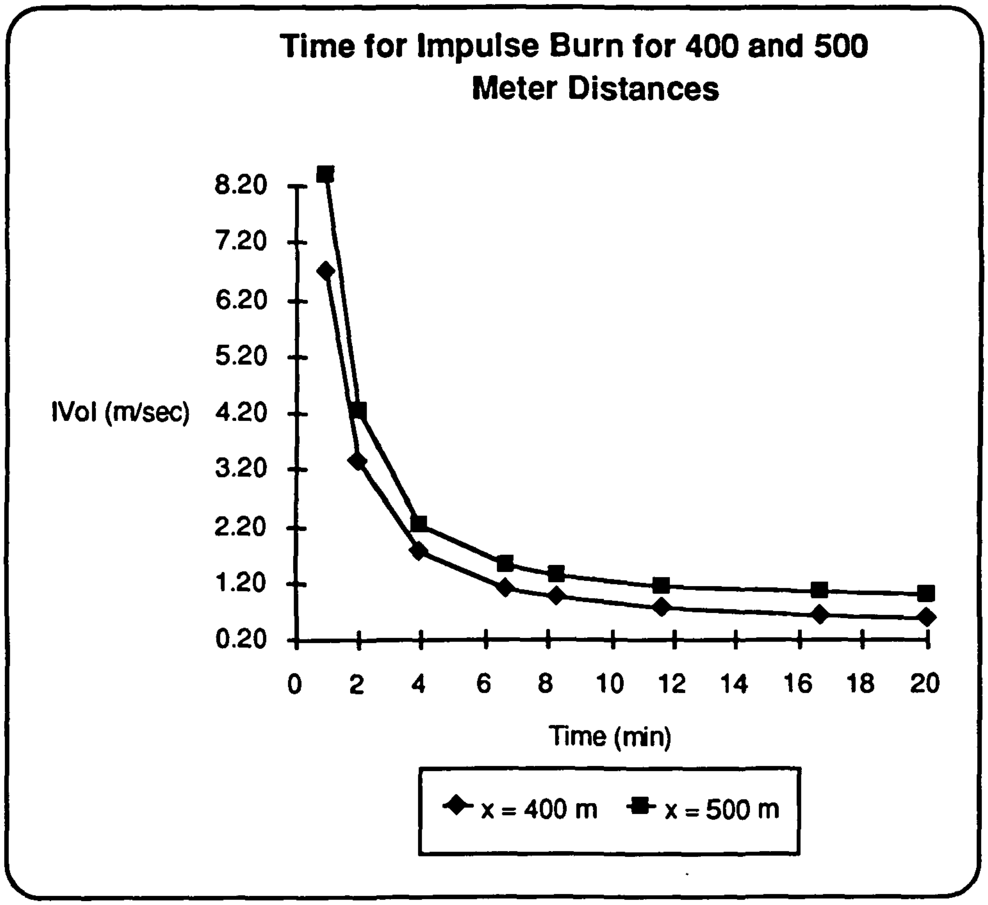

Figure 1.3l: Time for 400 and 500 Meter R-Bars

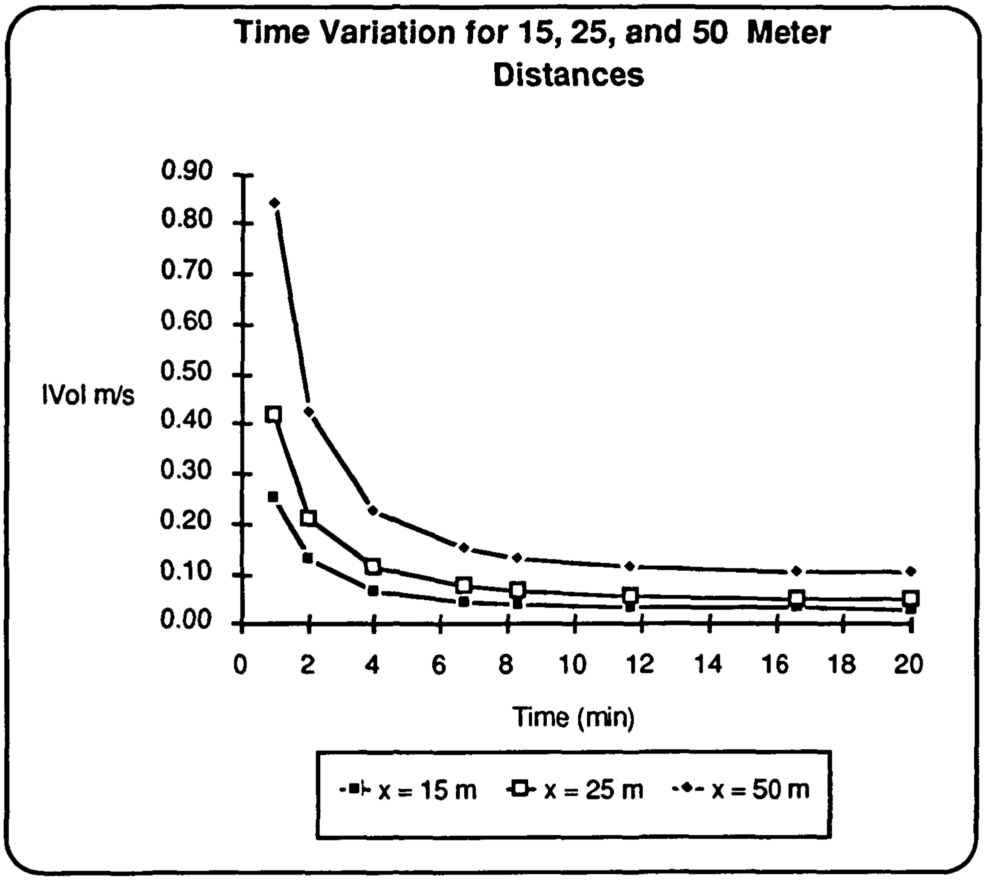

Figure 1.3m: Time for 15, 20, and 50 Meter R-Bars

M. Gates

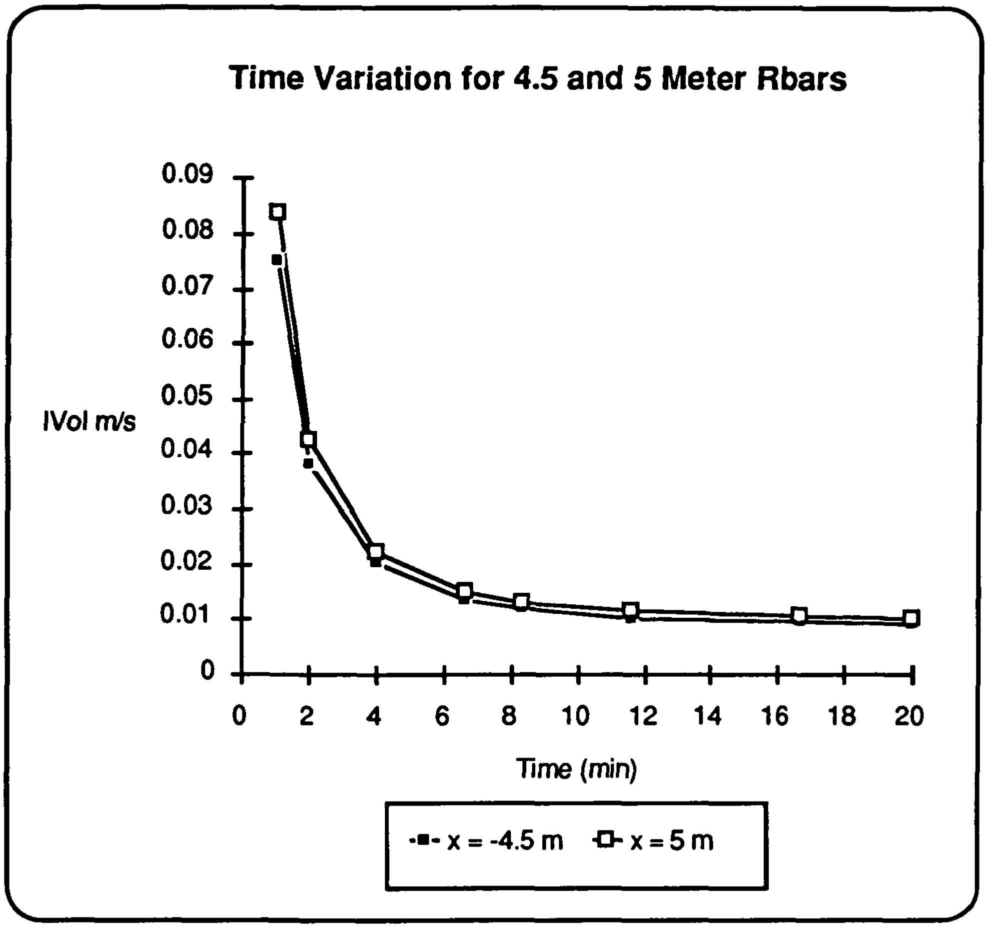

Figure 1.3n: Time for 4.5 and 5 Meter R-Bars

Note that these curves behave exactly as those shown previously. The four minute transfer has been chosen for each of the maneuvers, making the total final approach a 28 minute maneuver. The choice of the four minute maneuvers allows a slow approach, since for each maneuver the magnitude of the impulse velocity is 0.45% of the magnitude of the distance, which is well within the 1% criterion. The ΔV's for the proximity operations have been calculated given the time of 4 minutes per maneuver, and are shown in Figure 1.3o.

Proximity Operations ΔV

$\Delta V1$ = 2.2510 m/s
$\Delta V2$ = 1.8008 m/s
$\Delta V3$ = 0.2251 m/s
$\Delta V4$ = 0.1125 m/s
$\Delta V5$ = 0.1125 m/s
$\Delta V6$ = 0.0251 m/s
$\Delta V7$ = 0.0234 m/s

Total operation = 4.5 m/s

Figure 1.3o: ΔV for Proximity Operations

This is a much smaller ΔV than originally anticipated. To do a sanity check, the vis-viva equation was solved for the 499 and 500 km orbits to find orbital velocities at each. When subtracted, the ΔV was 0.51 m/s. Since this is a low bound, it looks like the ΔV is in the correct range.

Complete Operation

Summing the ΔV's for the rendezvous and proximity operations, the total ΔV is approximately 20 m/s without a plane change maneuver, and 85 m/s with a 0.5° plane change correction. Allowing for in-flight deviations, a ΔV of 100 m/s was stated for the OMS (orbital maneuvering system) engines, which will perform the rendezvous sequence; and a ΔV of 6 m/s was stated for the RCS (reaction control system) engines, which will perform the final approach.

The proximity operations approach allows for in-flight deviations by providing for many burns so that the guidance equipment can recalculate relative distances to rendezvous and provide for corrections. In additions, larger corrective maneuvers are included in the corrective combination of the rendezvous sequence.

M. Gates

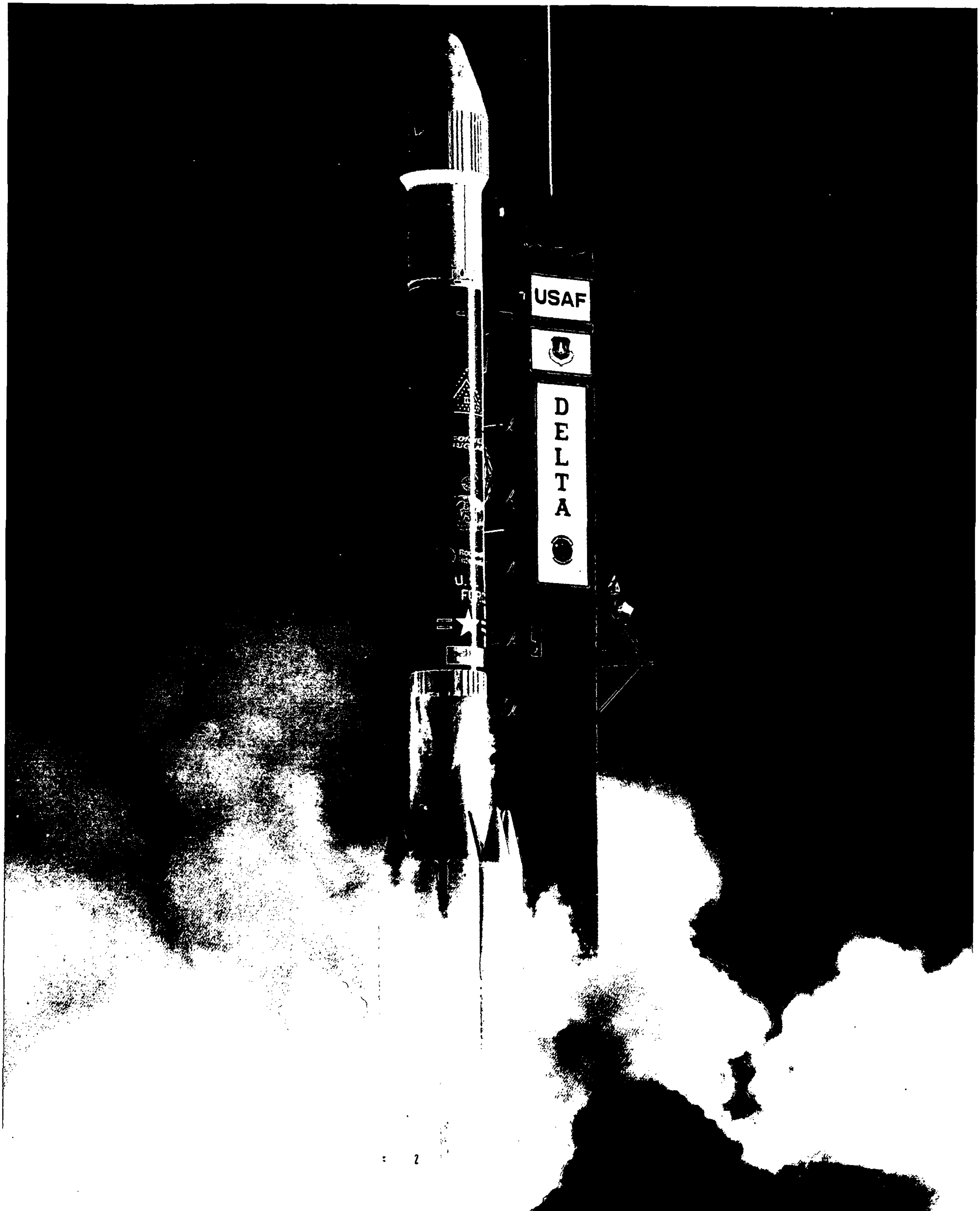

FIGURE I.1 : De

Section 1.4 Abort Analysis

One of the major distinctions between a man-rated spacecraft and a spacecraft not designed to carry humans is the requirement for a reliable escape system to protect the crew in the event of an accident. This is the topic of this section. The factors that go into determining an abort trajectory will be discussed. Then an estimated abort trajectory using approximate values for some of the variables will be determined.

In general the objective of an abort is to eject the crew from the launch vehicle in such a way and to such a distance that neither the astronauts nor their escape vessel (the entire capsule in our case) incur any injuries or damage respectively. The primary threat to an escaping spacecraft is from the over pressure that would result from an explosion of the launch vehicle. The spacecraft has particular pressure limits beyond which structural damage will occur. The overall pressure being exerted on a spacecraft (including the over pressure) is given by (see reference 4)

$$P_{net}=(C_p q-(\pm P_C))+\Delta P \quad (\psi)$$ where

P_{net}= net pressure on spacecraft

q= dynamic pressure

P_c= pressure difference between ambient and the pressure in the crew compartment

ΔP= blast over pressure

It can be seen that P_{net} is a function of mach number ,dynamic pressure, and angle of attack as well as the thrust of the escape rocket. Also, empirical data has shown that the blast over pressure resulting from an explosion of a mixture of LOX/RP-1 is roughly equivalent to that of 10% of the fuels weight in dynamite (see reference 4).The objective then is to insure that the spacecraft is accelerated to a velocity and distance, given, sufficient warning time, so that the over pressure are kept within the region between curves D and B in figure 1.4a (see reference 4). Note that the assumption was made that only the first stage exploded. This is a reasonable assumption in that it is generally felt that the first stage is the most likely to fail due to its complexity.

In order to determine the warning time required one would have to do a detailed analysis of eq. 1 for various angles of attack.

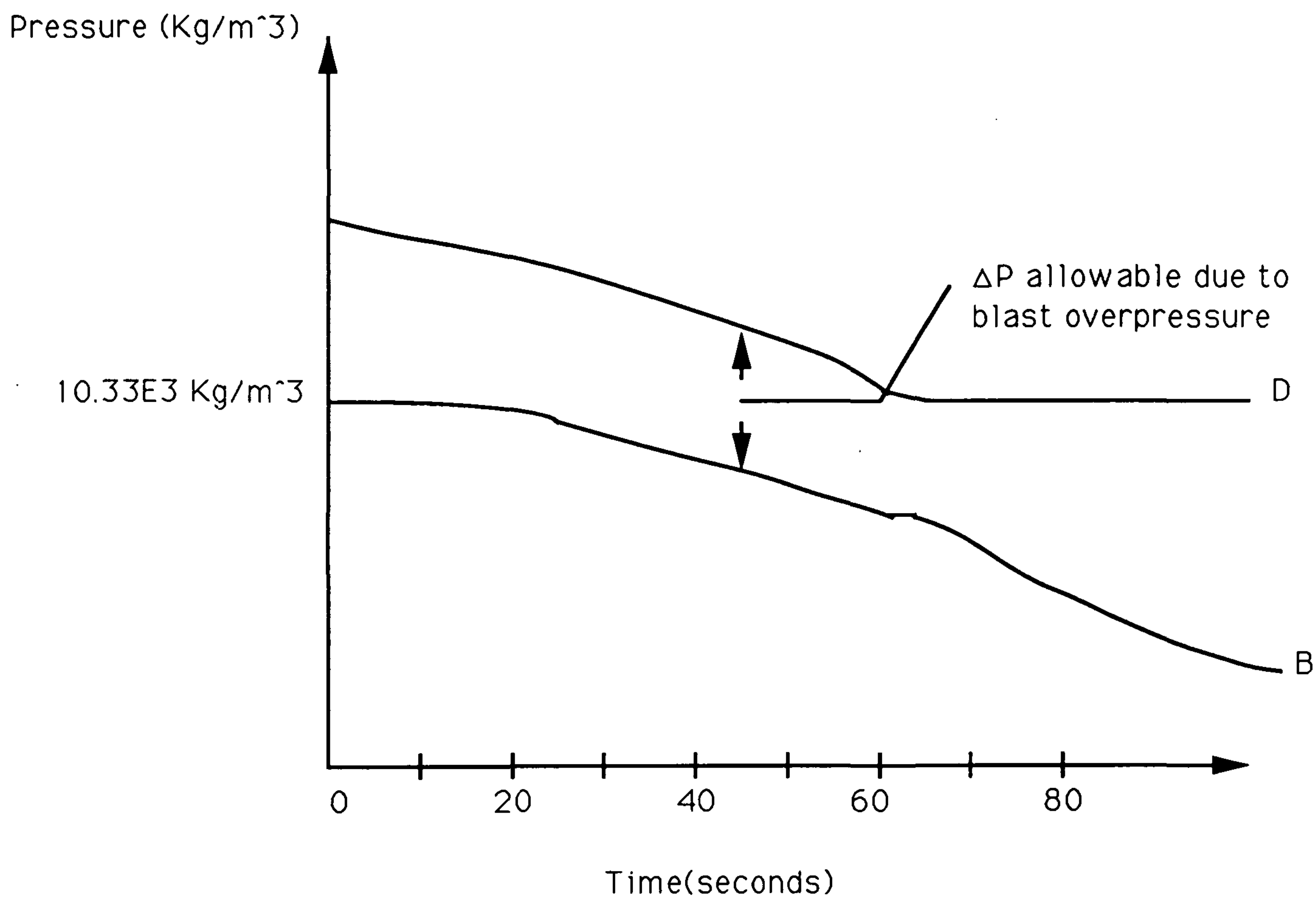

Figure 1.4a Time history of pressures on spacecraft

Z. KHAN

This would require wind tunnel test data. However for the present case we can use data from figure 1.4b(see reference 4) to get fairly representative data. This is because the warning time required at a particular altitude is relatively insensitive to change. Note that the maximum warning time required is between 2.5 to 3 seconds which would be required at an altitude of between 25,000 and 30,000 ft. This is because q is at its greatest hence a small over pressure may result in exceeding the structural limits of the spacecraft. Also the drag is much higher and so the separation distance is not as large as it would be otherwise. If we take the above warning times and multiply by a safety factor of 1.5 we get a required warning time of 4.5 seconds.

Now having sufficient warning time and knowing to keep the overall pressure on the spacecraft between curves B and D (figure 1.4a) and using the rule of thumb obtained from Akin that you want to accelerate to a distance of .5 miles in 5 seconds from the separation plane , a vertical acceleration of 7.53 g's provided by the escape rockets is sufficient to accomplish this with the 5 second burn time.

$$D = .5 * at^2 = .5 * 7.53 * 9.81 * (25)$$
$$= 923.37\text{m} > .5 \text{ mile}$$

where D=distance
a=acceleration
t=burn time

In this vertical abort mode the acceleration on the crew would of course be 7.53g's.This is within human tolerance levels (see reference 4) but could be reduced further by pitching the thrust line of the escape motor by some angle.

As stated earlier there are three regimes in which an abort may take place. They are:

1.)low altitude abort (pad-7,620m)
2.)medium altitude abort(7,620m-36,576m)
3.)high altitude abort (36,576m-above)

In a low altitude abort, the escape system would be jettisoned immediately after the fuel has been expended. This is followed by deploying the main chutes to stabilize the craft. In a medium altitude abort scenario, the escape tower and rocket are retained and aerodynamic surfaces(canards) are used to orient the spacecraft into a heat-shield-forward configuration so as to distribute the aerodynamic loads over a larger area and provide increased aerobreaking. In the event of a high altitude abort these canards would not be useful in the low density atmosphere, hence the escape

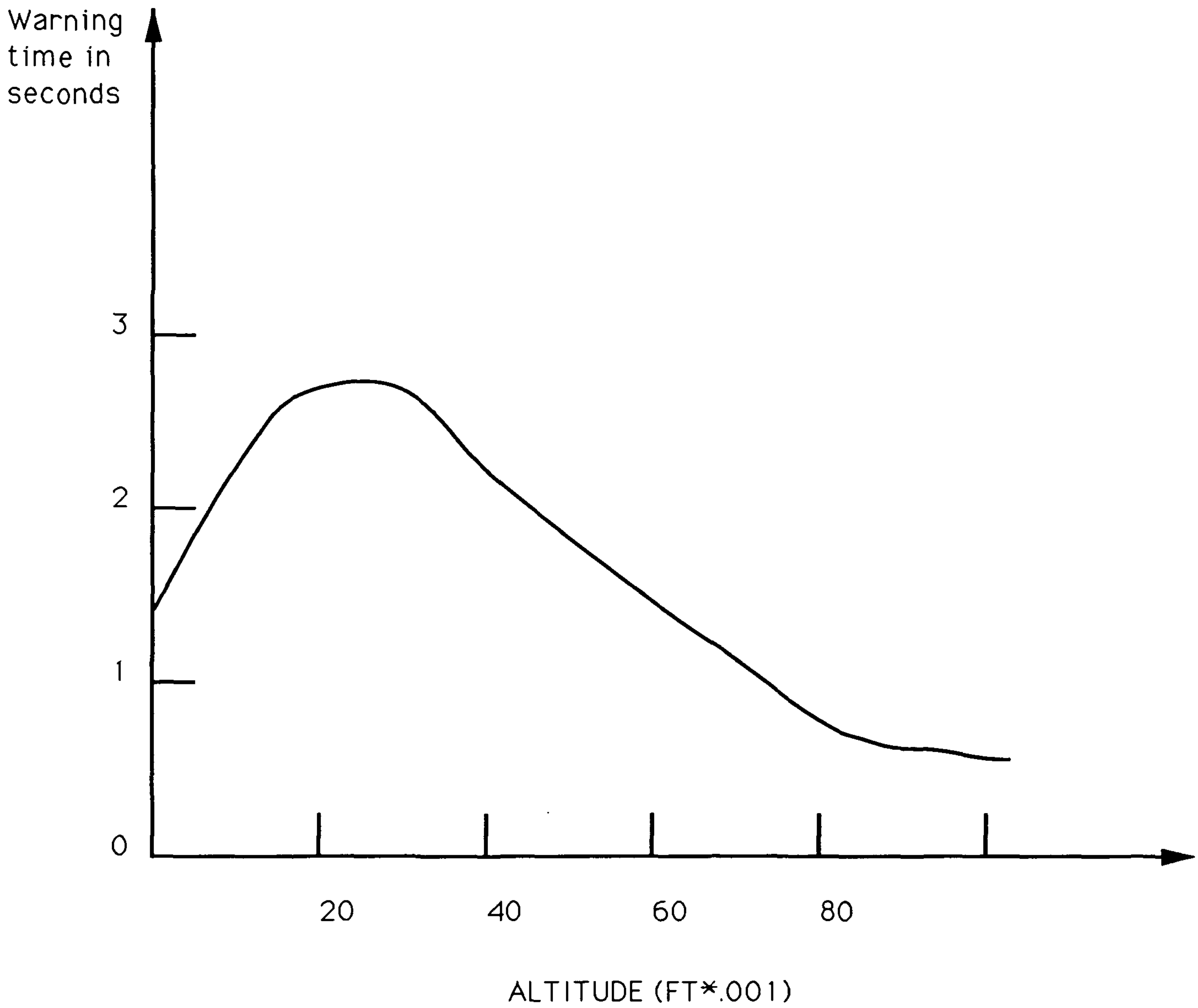

Figure 1.4b Warning time required by escaping
spacecraft

system is immediately discarded after the fuel is expended. Attitude control is achieved via the attitude control thrusters. In the event of an abort from a low orbit, the orbital maneuvering engines would be used to slow the craft to a reentry and the attitude control thrusters would orient the craft to the desired reentry angle. Note that in all cases canopy type parachutes are deployed to slow the vehicle to a terminal descent rate and eventual landing.

References

1. N89-20339 "OTV Mission Requirements", NASA paper, 1989.

2. N89-18516 "Advanced EVA Requirements", NASA paper, 1989.

3. N89-24795 "The Human Role in Space (THURIS)", NASA paper, 1989.

4. Puret, Faget, Smith; *Manned Spacecraft: Engineering, Design & Operation,* 1964.

5. *Delta II Commercial Spacecraft Users Manual,* McDonnell Douglas Astronautics Company, 1989.

6. N88-17435 "Microgravity Experiments in Space..." NASA paper, 1989.

7. Bate, Roger; Mueller, Donald; and White, Jerry; *Fundamentals of Astrodynamics.* New York: Dover Publications, 1971.

8. Kaplan, Marshall, *Spacecraft Dynamics and Control.* John Wiley and Sons, 1976.

9. *Rendezvous. Proximity Operations Workbook*, Training Division Flight Training Branch, NASA RNDZ 2102, Lyndon B. Johnson Space Center, March 1, 1983.

Douglas P. Vine

Chapter 2

Human Factors

Section 2.1 Radiation Shielding

The radiation environment to which the DART spacecraft will be exposed in the presently envisaged mission is not a particularly formidable one. In general however, there are orbital inclinations and regions in space where radiation can pose a health risk for humans and problems for the spacecraft. The objective of this section is to examine human tolerance to radiation and how best to protect the occupants of the DART spacecraft from this radiation environment (450 km at 28.5 deg). First however, a background into the radiation environment in a low Earth orbit would provide a basis for the continued discussion of radiation related problems for this mission.

In general there are three sources of radiation in space(see reference 4):

1.) Solar particle radiation
2.) Galactic cosmic radiation
3.) Earths trapped radiation belts

The degree to which each source of radiation contributes to the overall radiation exposure is influenced by several factors. Among the more significant are the altitude, inclination of the orbit, shielding and duration of mission. In a low Earth orbit at an inclination of 28.5 deg. the predominate source of radiation are the protons from Earths radiation belts (The Van Allen belt) with a very small contribution from galactic cosmic radiation. However Earths magnetic field provides a natural shield against even unusually high levels of radiation due to solar particle events such as occurred in August 1972 (see reference 4), hence this source does not present a great threat.

What is of concern now that the radiation environment has been identified is how much exposure to radiation is an astronaut going to be subjected to in this environment. Calculations performed by the National Council on Radiation Protection and Measurements (NCRP) in cooperation with Johnson Space Center show that over a 90 day period in a LEO at an inclination of 28.5 deg the blood forming organs would be subjected to 110 mSv which is equivalent to an average daily dose of 122 mrem based on 1gm/cm^2 of aluminum shielding (see reference 4). Current guidelines recommend an annual exposure limit of no more than 50 rem(see reference 1). Given a thickness of aluminum shielding of .659 g/cm^2 (based on an aluminum thickness of .238 cm obtained from the structures group) the daily exposure to the crew would be about 185 mrem. At this daily dosage level, it would take 270 days out of a year to reach the NASA limit.

In conclusion, it would appear the shielding provided by the thickness of the aluminum shell and pressure vessel determined strictly from a structural consideration is sufficient to provide the required protection for the astronauts from radiation exposure. That is to say radiation is not significant enough at 28.5 deg inclination and 450 km altitude to warrant additional shielding beyond that which would have been provided anyway. However,in the event that an unusually large amount of radiation is detected there are certain options available to the crew. These are:

1.)Abort mission
2.)Face heavily shielded portion towards incoming particles.
3.)Spot shielding-use any movable material present to provide additional shielding.

It is unlikely that any of the above procedures would be required for the present mission(450 km at 28.5 deg). However if the spacecraft were required to perform a mission at 450 km and 90 deg. inclination (polar orbit) where the Earths magnetic field does not provide sufficient protection against solar particle events, additional shielding may be required.

CHAPTER 2.2 HUMAN FACTORS

LIFE SUPPORT

Water and Food Requirements

In order to allow the survival of the crew of the Delta DART capsule, sufficient food and water must be available to supply between 2500 cal. to 3200 cal. for a male crew member, and 2200 cal. to 2900 cal. for a female crew member. Since the meals will be eaten in a microgravity environment, certain limitations are forced on the packaging and preparation of adequate meals. Fortunately, NASA has already developed food packages that already meet the requirements of the crew.

The two types of food rations chosen to go onto the Delta DART are the Standard Shuttle ration and the Meal Ready to Eat (MRE) ration. As its name suggests, the Standard Shuttle ration is currently being used on the space shuttle. This ration contains over 23 menus, ranging from steak to pasta. This will allow an extended meal rotation, especially considerating that the expected standard mission duration will be 7 days at the most. All meals are thermostabilized (already cooked) and dehydrated. If any heating of the food is required for palatable reasons, a chemical heat packet is included in the packaging. Each Standard Shuttle ration packs 2750 cal. in it, with a dry weight of 1.5 kg.. To this 1.9 kg. of preparatory water must be added. Each meal takes up a volume of 0.004 cubic meters, increasing to 0.005 cubic meters when the preparatory water is added (see Tables 1 and 2). The Standard Shuttle ration will be used for all planned meals during the length of the mission, with the MRE ration relegated for the one day emergency reserve.

The MRE ration was originally developed for the U.S. special forces field use. As such, it is a very compact ration, needing no preparation to eat, being thermostabilized also. The MRE packs 2600 cal. per meal, has 12 different menus currently available, and weights only 3.1 kg. compared to the 3.4 kg. total weight of the Standard Shuttle ration. The MRE fits into a volume of 0.004 cubic meters, compared to the 0.005 cubic meters of the Standard Shuttle ration. Despite the weight and volume savings, the MRE is not as palatable as the more appetizing shuttle rations. However, for extended mission durations and/or for the maximum crew of 5, the MRE could easily be substituted for the Standard Shuttle ration.

The potable water requirements for each crew member are approximately 1.3

kg. per person-day. This will have to be carried in full, because the mass and volume requirements of a water recycling system will be to great for the short duration of the expected Delta DART mission. In addition, their is no water recycling system that delivers potable water available given the 1990 technology cutoff date.

Cabin Atmosphere

The interior of the Delta DART capsule will be held at standard atmospheric conditions. Metabolic oxygen requirements are an average of 1.0 kg. per person-day (30 lit. per hour), while waste metabolic carbon dioxide given off will be approximately 1.0 kg. per person-day (22 lit. per hour). The carbon dioxide will be removed from the atmosphere using solid amine, which has been developed from the liquid amine currently being used on the navy's nuclear submarines. It consists of small micro porous beads whose surface is covered by amine. The beads themselves are composed of a polymeric acrylic ester. Solid amine was chosen over lithium hydroxide because of its ease of use and regenerable capabilities. Since solid amine absorbs carbon dioxide at room temperature, and desorbes it at a higher temperature , with little degradation of performance, it is easy to use and economical. The cabin air will be passed thru a inlet filter to remove any trace elements or particles, then into a chamber where one of three amine canisters will be. When the amine canister becomes saturated with carbon dioxide, the inlet flow will be switched to an other canister, while the saturated canisters heated and the desorbed carbon dioxide sent thru a compressor and stored. The three amine canisters are used as absorbing, desorbing, and precooling, and by the combination of canister cooling and heating, continuous carbon dioxide separation can be accomplished.

The total system will provide a 3600 liter per hour flow rate, have a total mass of just over 50 kg., require 300 W of power for the compressor, pumps, and heaters in a volume of under 0.4 cubic meters.

Humidity control will consist of a heat exchanger, a wicking material in the heat exchanger passages between fins. The air is cooled below its dewpoint around the wicking material, with the condensed water being trapped in the wick. The water is then forced thru the wicking material by a low pressure head to a collecting tank. The water then can be used as non-potable wash water.

Trace contamination of the cabins atmosphere are basically of three types; particles, gases, and oils. Particles include: dust, skin flakes, hair, bacteria, clothe fibers; gases include leaks from equipment, and vapors from materials; while oils come mainly from human skin. Most inspection and cleaning can be done visually and manually, although none of these contaminates is expected to pose any problem to the crew or equipment for a mission duration of up to two weeks, which is the outside limit of the capsule.

Minute cabin leakage estimated at around 1.1E -4 cubic meters (for a cabin volume of 40 cubic meters), will be corrected by releasing more oxygen or nitrogen, as needed. This will also keep the cabin pressurized to nominal pressure of 1 atmosphere.

Waste

Waste solids and liquids require special handling in a microgravity environment. Each crew member will, on average, produce 4.0 kg. of waste per person-day. This waste includes exhaled carbon dioxide, urine, fecal solids, perspiration, food packaging, and other trash solids.

The disposal of the carbon dioxide was dealt with in the preceding section. Human defecation will be done using baggies to eliminate the need of a toilet in the space starved cabin. These baggies will be stored for disposal after landing.

Hygiene washing will not be needed for mission durations of less than 4 days, and for the longer duration missions, washing can be accomplished using a sponge in a water tight cocoon. This cocoon can be folded up when not in use, with the excess water evacuated by a pump. A shower using the cocoon will use approximately 2.0 kg. of water.

Fire Protection and Prevention

In the Delta DART capsule, the confined space, limited atmosphere, lack of any viable rescue option, and the poorly understood effects of the microgravity environment on combustion make the hazard of fire extremely dangerous.

The necessary elements for fire are the presence of fuel, ignition, and oxygen. The NASA Handbook NHB 8060.1B gives the criteria that for unrestricted use in spacecraft, materials must burn for less than 15 cm upwards with a burning time not to exceed 10 minutes. This standard cannot be met in all circumstances, for several reasons, including: the poorly understood behavior of fire in microgravity, the fire resistance of most materials in space in unknown, and breakdowns, or waivers of non-approved materials, and any fire elements that have to be accepted in order to allow certain necessary and useful activities. Irrespective of all this, the main fire prevention techniques will be to minimize the chance of all three elements necessary for a fire to be at the same place and time. This mainly will be accomplished thru the actual design of the capsule to limit risk. Since this still leaves some chance of fire due to chance of necessary risk, ionization smoke detectors will be placed where trouble spots are expected (ie oxygen tanks, electronics, etc.). However, due to the small size of the DART capsule, human detection will remain the main way to detect the existence of a fire.

Fire extinguishment will be accomplished using Halon 1301. Flooding the area of a fire with an inert gas was considered, but two main problems exist. The first is that the oxygen concentration in the atmosphere must be reduced to below 9 percent for the fire to be extinguished. Since only the crew module contains an atmosphere, the effects on the crew and the difficulty in lowering the oxygen concentration preclude its use. The second is the fact of the increased cost, mass, and volume required would offset any benefits received.

Halon 1301 is currently being used on the space shuttle, and is a chemical extinguishant that inhibits the combustion reaction. It is very effective on surface fires, but has less effect on smoldering fires. While unreacted halon 1301 is harmless to humans for short exposures, when the halon is used on a fire some of the resultant chemicals are Hydrogen Fluoride and Hydrogen Bromide, both of which are toxic in a enclosed atmosphere. This requires that the DART capsule be returned to Earth as quickly as possible.

Heat Rejection

Waste metabolic heat is approximately 100 W per person. Originally, this heat will have been rejected using a 2 phase fluid loop system with freon as its working fluid. Heat exchange involves a change of phase (evaporation or condensation) to a space radiator. 10 kW of heat transport can be accomplished using 10 W of power and a radiator area of 0.3 square meters, and a mass of 15.0 kg. The system contains a mixing valve, heat rejection panel, supply resavoir, 2 pumps, power supply and waste heat exchanger, and an instrument panel.

Overall thermal efficiency is unknown, and since the waste metabolic heat is much lower than originally estimated, this system might be able to be replaced by heat pumps.

Heat pumps involve no moving parts, thus are basically 100% reliable and cheaper to make. A heat pump will contain evaporators (or condensers, as needed) that contain a fine pore sized wick. Liquid residing in the wick is evaporated at the surface, where a 'slug' is formed. Pressure exerted by the flow of the vapor on the liquid column ahead of it drives the liquid back to the evaporator. Some drawbacks are that the heat pipes can only transport heat one way from an evaporation zone to the remainder of the loop.

Unfortunately, work still must be done to get data on heat pipes, although heat transfers of 1440 W per 10 kg. of piping have been achieved on Earth.

Total Mass and Power

The total mass breakdown, exclusive of consumable food and water, is given in table 4. From table 5, the estimated total power required for the life support systems is shown. The difference in the power requirements for the air circulation arise from the inclusion of the amine heaters and pumps, which were forgotten in the CDR.
The value for the lighting assumes 4 circular phosphorescent bulbs at 12 W each.

David Matthews

TABLE 1

VOLUME OF CONSUMABLES PER PERSON-DAY IN M3

CREW		DAYS IN ORBIT				
		3	4	5	6	7
CREW	2	0.09	0.12	0.15	0.18	0.21
	3	0.14	0.18	0.23	0.27	0.32
	4	0.18	0.24	0.30	0.36	0.42
	5	0.23	0.30	0.38	0.45	0.52

TABLE 2

MASS OF CONSUMABLES IN KG. PER PERSON-DAY

CREW		DAYS IN ORBIT				
		3	4	5	6	7
CREW	2	98.0	131.1	164.4	200.3	230.7
	3	152.0	200.0	246.0	296.5	344.3
	4	196.0	262.8	328.1	394.0	460.5
	5	246.7	328.0	410.2	492.2	574.0

TABLE 3

EXPECTED LIFE SUPPORT LOADS

PARAMETER	KG. PER PERSON-DAY
METABOLIC OXYGEN	1.0
METABOLIC CO_2	1.0
POTABLE WATER	1.2
HYGIENE WATER	4.0
PERS./RESP. WATER	1.8
FECAL WATER	2.0
TRASH SOLIDS	0.05
TRASH LIQUIDS	0.12
FECAL SOLIDS	0.09
METABOLIC HEAT	100 W

TABLE 4

MASS BUDGET BREAKDOWN

ITEM	MASS (KG.)	NUMBER	TOTAL (KG.)
COUCH	20.0	5 (max.)	100.0
PORTABLE O_2	2.0	4	8.0
SURVIVAL KIT	15.0	1	15.0
FIRST AID	8.0	1	8.0
SUITS	9.0	5 (max.)	9.0
TOOLS	10.0	1	10.0
MANUALS	4.0	1 set	4.0
FIRE EXT.	2.5	2	5.0
TRASH CONT.	0.5	2	1.0
WATER TANKS	4.5	3	13.5
SOLID AMINE SYS.	50.0	1	50.0
PERSONAL	5.0	5 (max.)	25.0
CREW	70.0	5 (max.)	350.0

TOTALS:	3 PERSON CREW	426.5
	5 PERSON CREW	634.5

TABLE 5

POWER REQUIREMENTS

AIR CIRCULATION	300 W
LIGHTS	48 W
HEAT REJECTION	pending evaluation of heat rejection system

Section 2.3: Interior Layout and Design

Introduction

Section 2.3 of the Human Factors Chapter will cover the Internal Layout of the DART capsule. This includes the dimensions of the habitation environment as well as controls and monitors needed during the mission. Also in this Section is a discussion of the Factors that Affect Crew Productivity. This will describe factors that affect the astronauts while in orbit. This includes architectural factors, living space and personal hygiene. Lastly is a discussion of the Space Suits to be worn during the mission. It will describe the EMU (Extra Mobility Unit), what its functions are and how to prepare it for EVA (Extra Vehicular Activity).

Interior Layout Of The DART Capsule

The most effective way to describe the interior of the DART capsule is to start at the top and work down to the base.

At the top is the front hatch (figure 2.3 a). It's diameter is .9 meters (m). This is wide enough to fit an astronaut in a space suit through and into the Space Station. This front hatch has a video camera on the outside front of it. This is to enable the Pilot of DART to maneuver the capsule to rendezvous with the Space Station or any other craft that is adaptable. The docking mechanisms are detailed by Ola Bello in Section 3.2.

Moving into the capsule through the tunnel, the walls continue straight for .745 m. Behind these walls are the avionic systems including sensors, communications, data management, navigation and guidance systems. Using the .3 m depth of the outer ring of the capsule, in addition to the room behind the control panels, there is ample room for all the avionics and control packages. Exact contents of these packages are detailed in Chapter 5 by the Avionics team. Also included on the outer portions of this .3 m depth is the heat shielding, radiation shielding, skin of the capsule, plus room for Orbital Maneuvering Systems (OMS) thrusters and fuel tanks. These components are detailed in later chapters.

At the end of the tunnel is the Pilot and Co-Pilot areas. This passage narrows to .6 m, but is passable for an astronaut in a space suit. There are handles here, and throughout the capsule to assist movement in zero- and near-zero gravity. These

R. Cunningham

handles all measure .15 m X .05 m. This area is enlarged on figure 2.3 b. This view shows the front of the Pilots and Co-Pilot's seats and controls. This area has a width of 1.86 m. This includes .6 m in between each control console for astronaut maneuverability. Since the DART capsule is being launched in the upright position, the astronauts will be on their backs during the many hours before launch. To keep their legs from coming up into their chests, there are foot restraints under each console (as shown). These are to be used during launch and re-entry when there are gravitational forces acting on the astronaut causing the legs to move with force against the astronaut. These foot restraints are also useful while sleeping in zero-g. Sleeping will be covered in a later part of this section.

The seat allows the astronauts .6 m of knee room vertically and 1.3 m horizontally from the back of the seat (figure 2.3 c and 2.3 e). The back of the seat is .63 m from the front of the front control panel. The armrests are movable to allow access to the chair. Seat belt harnesses are attached to the top and sides of the chair. The DART astronauts will be using a three-point safety harness. This will allow the greatest mobility while effectively securing the astronauts safely to their seats. Both sides have a small window allowing the astronauts limited outer visibility. A window was found to be needed, even if small, to give the astronauts better sense of attitude and direction during the mission. It also enables some sightseeing for the astronauts.

Above either side control panel are air intakes and Passive Radiation Dosimeters (PRDs). The PRDs are data collectors that measure the amount of radiation that is experienced in the capsule. The PRDs have chips that collect radiation samples. The chips are then removed on Earth and the data is read to determine the dosage of radiation the astronauts were subjected to. The effects of this radiation was discussed by Zahid Khan in Section 2.1. Also on either side are air returns and Life Support System (LSS) Hook-ins. This is where the EMU suits are connected to the capsule's LSS.

All the above features are on both the Pilot and Co-Pilot sides of the capsule. The Pilot's controls differ from that of the Co-Pilot's, as seen on figures 2.3 c and 2.3 d, the side and front views of the Pilot's controls. On the left arm rest is the control stick for the Orbital Maneuvering System (OMS). This is used to control the capsule once the DART is in Earth orbit. Pushing the stick forward will cause the capsule to pitch downward, back for pitching upwards. Right and left movements roll the capsule respectively. This system is controlled by the Engine Controls section on the Pilot's front control panel (figure 2.3 d).

The panel on the wall (figure 2.3 c) has controls for Cabin Atmosphere, Auto Pilot and Communications. The Cabin Atmosphere Controls have a dial for adjustable cool to warm air. These are individual for each side of the capsule as the Pilot and Co-Pilot may want different temperatures at different times. Switches to turn on / off the cabin vents; oxygen and nitrogen supply; boiler control and leak checks.

R. Cunningham

Communications has volume controls, capsule intercom on / off and band switches. Also are controls for communications with Earth and Data Flight Instrument Recorders.

On the ceiling, over the astronauts heads, there are circuit breakers to cut power to functions when not needed or in emergencies. There are sensor resets and circuit tests for all systems here also. Switches for engine shut down as well as cutoffs for heaters, hydraulics, oxygen and nitrogen are included. These cut the power at the source and don't leave any doubt if they are off or on.

The front control panel (figure 2.3 d) has a base width of .48 m. The base slopes up at an angle of 45 degrees and has a height of .5 m. The panel has a length of .618 m. The vertical panel has a height of .5625 m and goes to the ceiling which is sloping down with the wall of the capsule. It is also .48 m wide at the bottom and .34 m at the top. The upper front control panel is slanted back at a 20 degree angle from the vertical towards the astronaut for easier visibility and access to upper controls.

On the bottom panel there is a luminous flat panel data display. It is .2 m square and has brightness, horizontal and vertical adjustments. Next to it is a keypad similar to the one on the Space Shuttle. This one is .15 m by .2 m. It has numerical, alphabetical, plus and minus buttons. The extra keys are for automatic enabling of systems such as roll and docking maneuvers preparations.

Moving up the panel there are engine controls and capsule monitors. The engine controls include on / off for the main engines; pressure displays and controls for the OMS and main engines; emergency fuel dump switches and full backups for all. There are also switches for the hydraulic circulation pumps and pressures. Next to the engine controls are the displays for acceleration (m / s^2), velocity (m / s), hydraulic pressure (Pa) and quantity (%), altitude (m), degree of inclination (deg), and equivalent airspeed (km / hr.). The round dials are for attitude indication and heading.

On the vertical panel is a .2 m X .2 m display for visual monitoring of docking maneuvers and contact with Earth. It has knobs for volume, tone, brightness, horizontal and vertical. Above the display are controls for the video camera on the front hatch as mentioned previously. There are controls for adjusting the picture of the camera. This includes an aperture control that allows the camera to operate even if it is pointed directly at the oncoming Sun. On top of that is a digital clock for actual Eastern Standard Time (EST).

Above the clock is a full compliment of warning lights. These warn of troubles or potential troubles with various systems in the capsule. They include: oxygen pressure, hydrogen pressure, fuel cell temperature, solar array, antennae, cabin atmosphere, oxygen heater temp., AC voltage, AC overload, water loop, OMS, APU temp. and auto pilot. These warning lights are put well above the eye level of the astronauts so as not to distract the astronauts, but bright enough to alarm them in time of emergency.

R. Cunningham

Scattered around the control panels are fire holes. If a fire occurs behind the panels, smoke and flames can escape through these holes to warn the astronauts. Fire protection was covered by David Matthews in Section 2.2.

Opposite the Pilot's controls are the Co-Pilot's controls (figures 2.3 e and 2.3 f). The controls are of the same dimensions as before, but there are some differences in the controls. Notice there is not a control stick on this side. Controlling the capsule is the Pilot's job. The Co-Pilot has the Abort System controls on this side. These controls include a light for warning of need for mission abort, controls to start and work the system as well as backups to insure safety.

The Co-Pilot's front control panel (figure 2.3 f) has the same dimensions as the other side's panel. The data display is the same as are the keypad, dials, and displays. These are needed for the Co-Pilot because the mission may call for the Co-Pilot to monitor the displays while the Pilot is occupied with something else in his seat. The Co-Pilot also has the Primary and Secondary Power Unit Controls. They consist of fuel tank and valve enables, Power Unit on / off, voltage, temperature adjust / on / off and displays for Pressure (Pa) and Quantity (%) of power.

The visual display on the upper panel is the same. The digital clock here is for Elapsed Mission Time (EMT). Above the clock here are controls for the deployable solar arrays and various antennae on the capsule. These controls include in / out for all, selection of antennae and solar array and a directional dial (360 degrees) for the antennae in case they need to be turned manually.

Moving through the .5 m passageway between the seats to the back of the capsule, more handles help in zero-gravity. Looking back towards the front of the capsule (figure 2.3 g), the walls dividing the Pilot / Co-Pilot area from the Crew Compartment are 1.5 m high and .75 m wide.

There are three couches for passengers (figure 2.3 h). This area goes to a width of 2.625 m. The distance from the pilot's seats to the bottom of the couches is 1.4 m. There is a .9 m wide side hatch to one side and storage against the other two triangular walls. The couches (figure 2.3 i) are 1.2 m long, .4 m high and .5 m wide. They have handles on either side, oxygen hose hook-up holes on one side and a control panel for the individual Life Support System (LSS) on the other. The astronaut's legs will be positioned up in the air in a sitting-like position. While the legs will be supported by the couch during launch. There are also three point harness systems for the couches to keep the astronauts securely in place.

The total volume of the eight storage compartments around the couches is 2.44 m^3. This is the maximum volume attainable of the three Crew Compartment designs

R. Cunningham

considered. The other designs (figures 2.3 j and 2.3 k) are included here to show alternatives to the design chosen. In figure 2.3 j, the maximum storage attainable is not near the amount obtained with the design chosen (figure 2.3 h). The design in figure 2.3 k, while attaining close to the maximum amount of storage volume, lacks the center of gravity advantages the design chosen has. By putting all the astronauts on one side of the capsule to obtain a large storage volume, it makes for a side-heavy capsule that is not favorable for launching and controlling in orbit.

With the design chosen for crew seating, an effective center of gravity is obtained as well as the maximum amount of storage volume attainable. During the mission, when not being used, plates can be put over the couches to add to the storage area. This area can be used when it comes to storage of the EMUs, which will be detailed later in this Section.

Another added feature of the couch design is the ability of the couches to be removed. Therefore, a mission can be flown with 2, 3, 4 or 5 crew members. According to the mission needs, as many as three couches can be taken out either on the ground or at the Space Station to allow for more storage or room for experiments. Figure 2.3 l shows what the cabin will look like when all couches are removed and a full compliment of experiments and storage is added. The volume attainable with three couches removed is 3.16 m^3. This is a considerable jump in volume that could be needed to transport great amounts of supplies or experiments to or from orbit.

Within the storage compartments is the galley, sink and hot / cold water dispensers (figure 2.3 a). The sink works by shooting water across the astronauts hands and into a collection device before gravity (or lack of it) can act on it. It is a sealed apparatus that requires the hands to be put inside through sealed holes. The water is then put in holding tanks before ejection into space with the rest of the waste water. This system was briefly discussed by David Matthews in Section 2.2. The water dispensers are used to prepare food stored here also.

Figure 2.3 m shows a view of the crew seating and storage from outside the capsule looking in through the side hatch. It shows the three crew couches as well as the eight storage bins. Looking up into the capsule is the passageway into the Pilot / Co-Pilot area.

Below this level are the OMS tanks, water storage, waste water tanks and batteries. The solar arrays are stored here as well. There is a vertical height of .5 m for this area. This is enough room to fit all the items necessary to store below the capsule.

R. Cunningham

Factors That Affect Crew Productivity

When in Earth orbit, the quarters tend to get a little cramped. If a capsule is not designed well enough to keep the astronauts out of each other's way, serious complications and altercations may result. This will definitely reduce the effectiveness of the astronauts and alter their mission. The following is what was done to insure that the astronauts' brief stay in space will be a comfortable and productive one. They include: the living and moving space, storage, architectural design factors, hygiene and sleeping.

One fact that has to be addressed is the fact that once the Space Station Freedom is built and habitable, the DART capsule will be just a taxi of sorts, and the crew will stay aboard the more spacious Freedom where living conditions will be better for the longer duration missions.

When faced with the task of determining the number of astronauts that are able to fly on the DART capsule, a couple of factors came into view. The main factor, obviously, is room. There just is not enough raw volume in the pressure vessel of the capsule to fit as great a number of astronauts as in the space shuttle. But the object of the DART is to supplement the shuttle program, and therefore it does not have to fit as many crew.

The maximum number of astronauts to fly in the DART capsule is five. There is a Pilot, Co-Pilot and three passengers. These pilots as well as the passengers can be ferried to the space station to replace the crew there, and that crew can fly the DART back to Earth. Another possibility is that any number can be exchanged. The facilities on board are adaptable to any crew of five or less.

Specifications of the seating facilities (figures 2.3 a, c, h and i) dictate that the maximum height of the astronauts should be 1.8 m. This will insure comfort and safety. Due to mass specifications, the maximum weight of an astronaut should be 80 kg. There is no age or sex limitation.

By comparison, the habitable volume of the Gemini capsule was 1.56 m^3. That is .78 m^3 per astronaut as there was a crew of two. The habitable volume of the DART capsule is just under 4.0 m^3. So with a crew of five, the volume per person is about .8 m^3. Because of this room restriction, the crew of five will not spend a lot of time in the capsule if not necessary. A crew of three is better for workable room and a crew of two is the optimal amount as there is about 2.0 m^3 of volume per person. When there is limited volume, movement and exercise, there is a loss in efficiency, possible physiological damage and the crew gets in each other's way. This could lead to lack of effectiveness.

R. Cunningham

The movement space, as mentioned before on figure 2.3 a, into the docking tunnel is .745 m wide and .6 m wide further into the capsule. The seats have about .3 m of headroom and 1.3 m of legroom. The distance between the Pilot and Co-Pilot seats is .5 m. The two hatches are both .9 m in diameter and will allow easy and quick access in case of emergency.

The storage bins in the crew compartment will hold such items as work related tools and schedules, clothing and personal items. Of course the most important items that have to be accessed quickly will be stored in the front storage bins for convenience. The EMU suit upper torsos will be stored in these bins if there is room. Otherwise they will be tied down using bungee cords with hooks. They will hook into fasteners located on the sides of the bins as well as in the docking tunnel. This forward storage area will be used when the capsule is not docked with anything. Also stored in these compartments are the food and waste from the food. They will be put in sealable bins to contain odors.

Some architectural factors to help increase productivity of the astronauts are windows as described before; partitions, a solid floor, and sleeping facilities. The partitions are put up between the Pilot and Co-Pilot seats. This allows for privacy when personal needs are being cared for in the crew compartment. This is especially designed for when females travel into orbit. A solid floor is used instead of a grated floor to reduce the amount of sound coming from the engines during launch. The sleeping requirements are not much of a hassle for astronauts in a weightless environment. Astronauts can sleep virtually anywhere in the capsule. They can sleep strapped to a seat or couch, floating freely, or in the front docking tunnel. They can have their heads and feet strapped to their body, a pillow or dangling freely. There isn't too far to go in a 4 m long capsule, so no one will float away. There is also little danger of a floating sleeper accidentally hitting controls. All of the controls have features to lock them in position when not in use. So there is no way a floating sleeper can effect the control of the capsule.

Hygiene will be taken care of in the best manner possible in a limited room, weightless environment. The sink as described previously is provided to clean the astronauts' hands and face as well as for oral hygiene. Bathing is a careful and sometimes messy procedure. Using a washcloth and the water dispenser, a sponge bath will take the place of showering. It has been shown that a sponge bath once a day can take the place of a full shower for up to three days. Over three days, and the astronaut starts to lack the refreshing and esthetically pleasing feeling of a full shower. The Space Station Freedom should have full shower facilities on board to satisfy the astronauts.

Waste management with either the full EMU suit on or regular clothes will be the same while living in the DART capsule. Of course, once inside the Space Station, full

R. Cunningham

facilities will be provided. In the DART capsule, a sort of diaper made of rubberized nylon will be worn to collect urine. It will then be transferred, by hose, to the waste management control system on the storage area. It is stored in tanks and ejected into space with the other waste waters. In space it freezes and dissipates. Feces are stored in what are called "blue bags". These blue bags were used on early missions when space did not allow for a full toilet. These bags are actually two bags in one. The outer one contains a germicide and a skin-cleaning towel. The inner bag contains a rim coated with a sticky cement-like substance protected by a plastic strip. To use, the astronaut first peels back the strip exposing the sticky surface. He (/she) pastes the inner bag onto the buttocks and performs his duty. When done, the germicide is inserted into the inner bag and the outer bag is sealed over it. The bag is then flattened out and stored in a specially sealed waste storage compartment. It is transported back to Earth and disposed. Approximate waste weights are (per crew member per day): Feces, .113 kg water and .049 kg solids; urine, 1.9 kg water; growth, .045 kg.

Food preparation will be done in the makeshift galley (figure 2.3 a). Food is easily prepared by heating or adding water to dehydrated meals. David Matthews covered this topic in Section 2.2. They can be eaten anywhere in the capsule.

There are some routine procedures the astronauts must perform to keep the capsule running perfectly and safely. There are air intakes and returns that need to be cleared of debris. Floating pens, paper and the such can block the flow of air and fog a window or create problems in the circulation system. Air cooled electronic equipment can overheat due to lack of circulation. This can be unwanted trouble. Another routine is the collection of trash and other waste, putting it together and strapping it down or storing it. The astronauts also have to perform routine water dumps. Fuel cells produce excess water that has to be dumped into space.

Spacesuits Worn In Capsule

When the DART astronauts suit up at the Kennedy Space Center, they will be donning virtually the same suits worn by the space shuttle astronauts. This suit was found to be ideal for our mission because of its small size, ideal weight and flexibility. The one difference our suit will have is that it will not have a self-sustaining Life Support System (LSS) permanently attached to its back. It will, however, have places to attach a LSS if the future need ever occurs. This suit will be totally dependent on the capsule's LSS during launch, re-entry and depressurization.

To put on the suit, the astronaut must first strip down to his / her underwear. Medical monitors are then attached to the body. First to go on is a liquid-cooled undergarment (figure 2.3 n). This is like a pair of long johns of tight fitting (but very

R. Cunningham

comfortable) loosely knit, elastic mesh fabric interwoven with plastic tubing. This tubing circulates cool air and water from the LSS to cool the body. The temperature of the water is regulated automatically as the astronaut may not be able to judge his own thermal state. This is controlled by temperature controls on the side of the crew couch.

The heat transfer rate between the skin and the Liquid Cooling Garment (LCG) is as follows:

Heat Rate (watts)

H_{LCG}= total to LCG
H_{STL}= skin to LCG
H_{ATL}= air to LCG

Thermal Exchange Coefficients (watts/ degrees C.)

EX_{STL}= skin to LCG (total)
EX_{ATL}= ventilating air to LCG

Temperatures (degrees C.)

T_S= skin
T_{LAVE}= average water temp. in LCG
T_{AAVE}= average air temp. in outer garment

$$H_{LCG}= H_{STL} + H_{ATL}$$

In exchange coefficient and corresponding temp. differentials:

$$H_{LCG}= EX_{STL}(T_S-T_{AVE}) + EX_{ATL}\,(T_{AAVE}-T_{LAVE})$$

Where EX_{ATL}= 3.78 W/ degrees C. (See Reference 7).

This equation shows the total rate of heat exchanged to the Liquid Cooling Garment in the terms given. It is basically the sum of the heat transfer to the LCG from the skin and the heat transfer to the LCG by the air. It is then expanded using average water temperatures and Thermal Exchange Coefficients. When values are substituted, the heat exchanged is computed. This is useful to determine the average water temperature needed in the LCG.

Over this goes the anti-gravity suit (figure 2.3 n). This helps to counteract the flight dynamic or "g" forces. During these positive g-forces, blood is pulled from the brain causing blackout or unconsciousness. By pressurizing the legs (and abdomen) sufficiently, blood is forced to remain above the diaphragm. Enough blood stays in the chest to feed the heart needed to maintain consciousness, and keep blood pumping to the brain. It looks like a pair of trousers, but has bladders, with heat sealed seams to prevent leaks, that inflate as g-forces increase. This part also has the urine collection device described earlier.

Next goes on the pants and boots. These are made of a light-reflecting, white Ortho fabric underneath which are 5 layers of flexible metallic mylar for heat reflection. This fabric is pleated for bending of the limbs.

A hard-shelled torso is put on from underneath (figure 2.3 n). It is hard to keep the upper body in an upright and erect position. This is because in zero or near zero gravity, the body naturally tends to curl at the waist with the arms dangling in front of the body. This torso piece is connected to the pants by a snap on metal ring. This allows for limited turning of the waist. On the leg of the suit is a Passive Radiation Dosimeter (PRD) as described in the Internal Layout section of this chapter.

For EVA, a helmet and gloves are worn. The helmet is molded plastic with a darkened face shield that blocks UV rays and allows 150 degree visibility. The gloves are made of molded rubber and come in three sizes.

A wireless microphone system is worn at all times. This headset can be either a full head covering cap and microphone, or just a headset with earpiece and microphone. It is connected to the torso.

The whole suit takes about 15 minutes to put on. Old NASA standards were that astronauts were to pre-breath pure oxygen for three and one-half hours prior to EVA. This is to "wash out" the nitrogen from the blood stream. If nitrogen is in the blood, the g-forces could create air pockets in the blood that could cause neurological damage or death. New standards dictate that the cabin pressure be dropped from 100 kPa to 70.3 kPa the night before EVA. The astronauts then only have to pre-breath for one hour. Before EVA, the pressure is brought to 20 kPa to check for leaks.

During the mission, when the astronauts are living in the DART capsule and/ or the Space Station, a shirt sleeve environment will be available. This will enable them to wear regular cotton pants, shirts and jackets if needed. This is also similar to the Space Shuttle as they have a controlled environment also. This is an important advantage because the EMUs are too bulky to wear for an extended amount of time. This was shown during the Apollo missions when bulky suits were worn throughout the mission that lasted over 10 days. The suits will be stored as noted earlier.

In an October 8, 1990 article in Aviation Week and Space Technology (pg. 67), the MIT chairman of overseeing EVA, who was not named, said that development of a new, hard space suit, which would cut astronaut pre-breathing time is needed. But NASA doesn't like the the $352 million for 21 suits and seven backpacks the producer wants.

R. Cunningham

Summary

This concludes the Section on the Interior Design, Factors Affecting Crew Productivity and Space Suits to be used in the DART capsule. It is also the end of the Human Factors Section. With the effective designs presented here and the addition of all the other components following, the DART capsule will fit in with the future plans of NASA, the proposed Space Station Freedom, and any other missions that the capsule will qualify for.

R. Cunningham

Internal Layout of Capsule

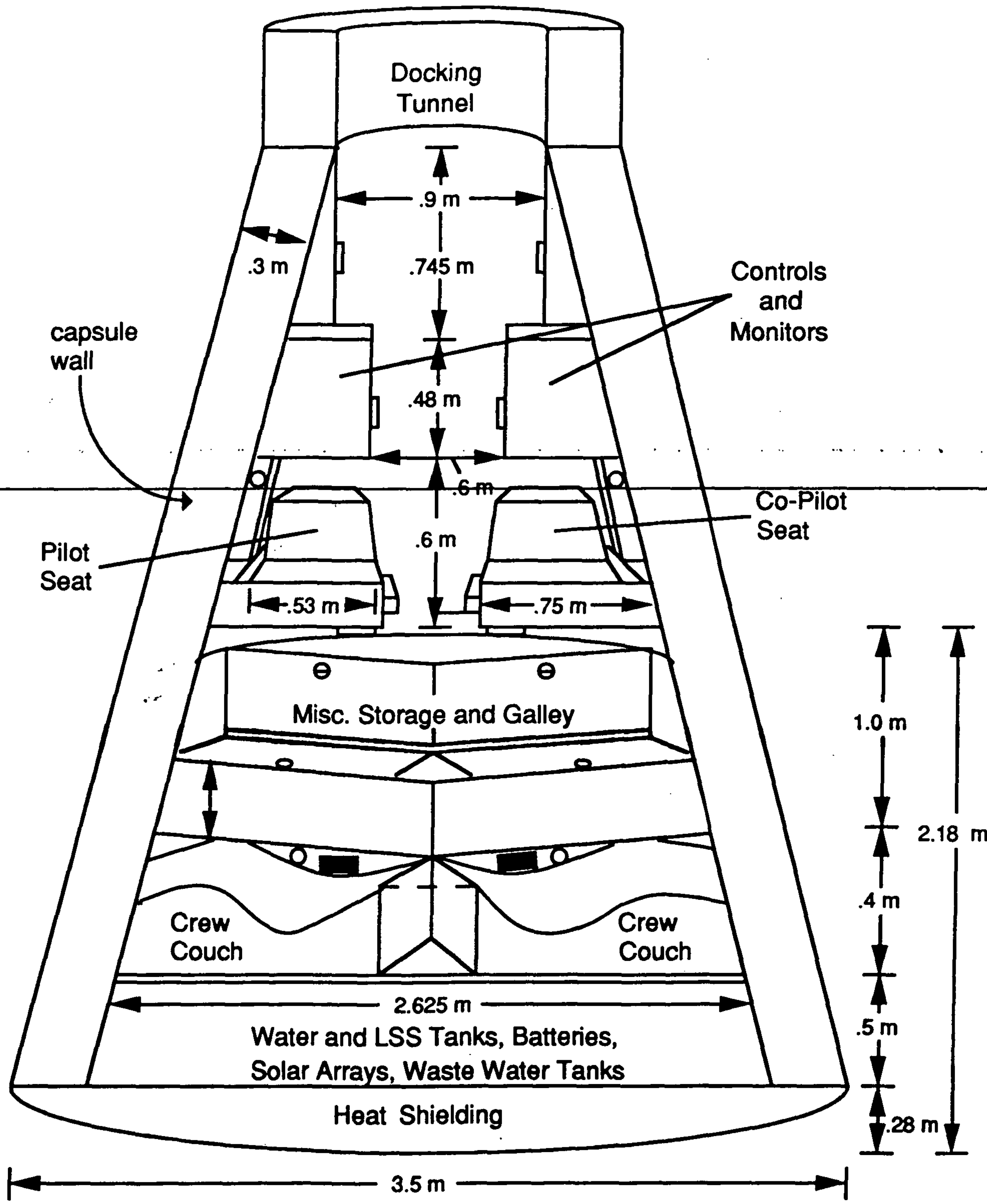

Figure 2.3 a

R. Cunningham

Capsule Controls and Monitors

Front View

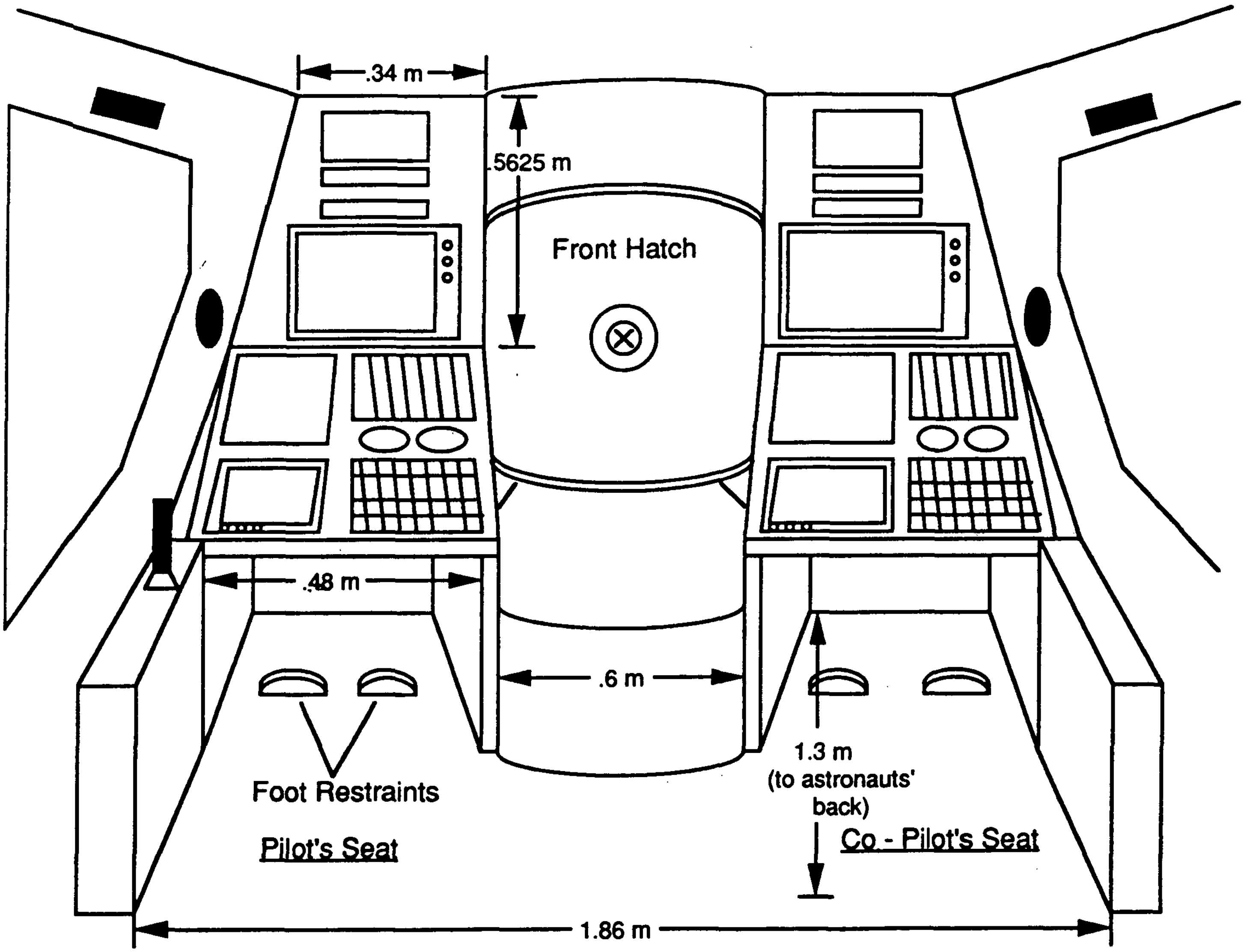

Figure 2.3 b

R. Cunningham

Capsule Controls and Monitors -- Pilot Side

Side View

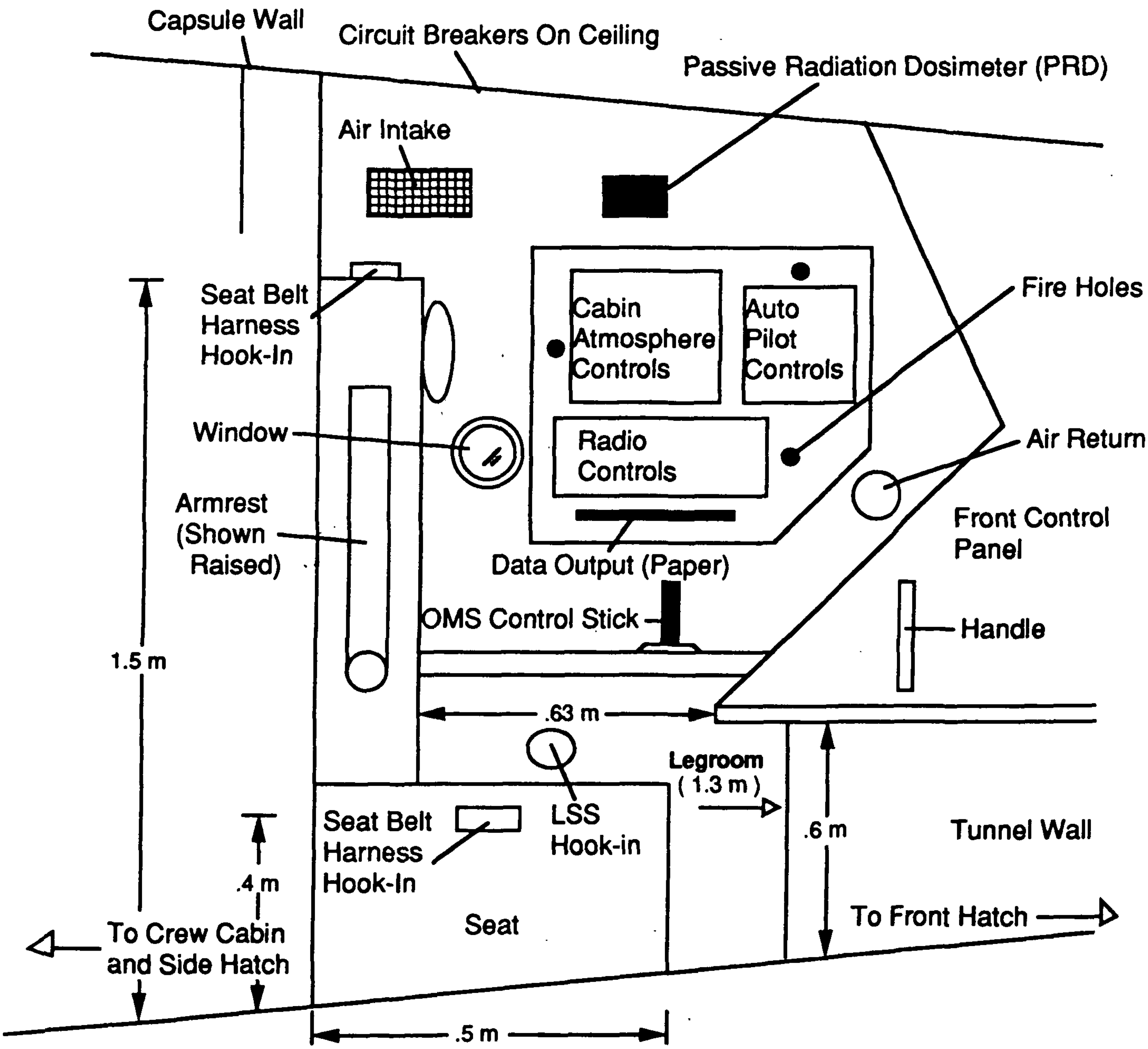

figure 2.3 c

R. Cunningham

Capsule Controls -- Pilot Side

Front View

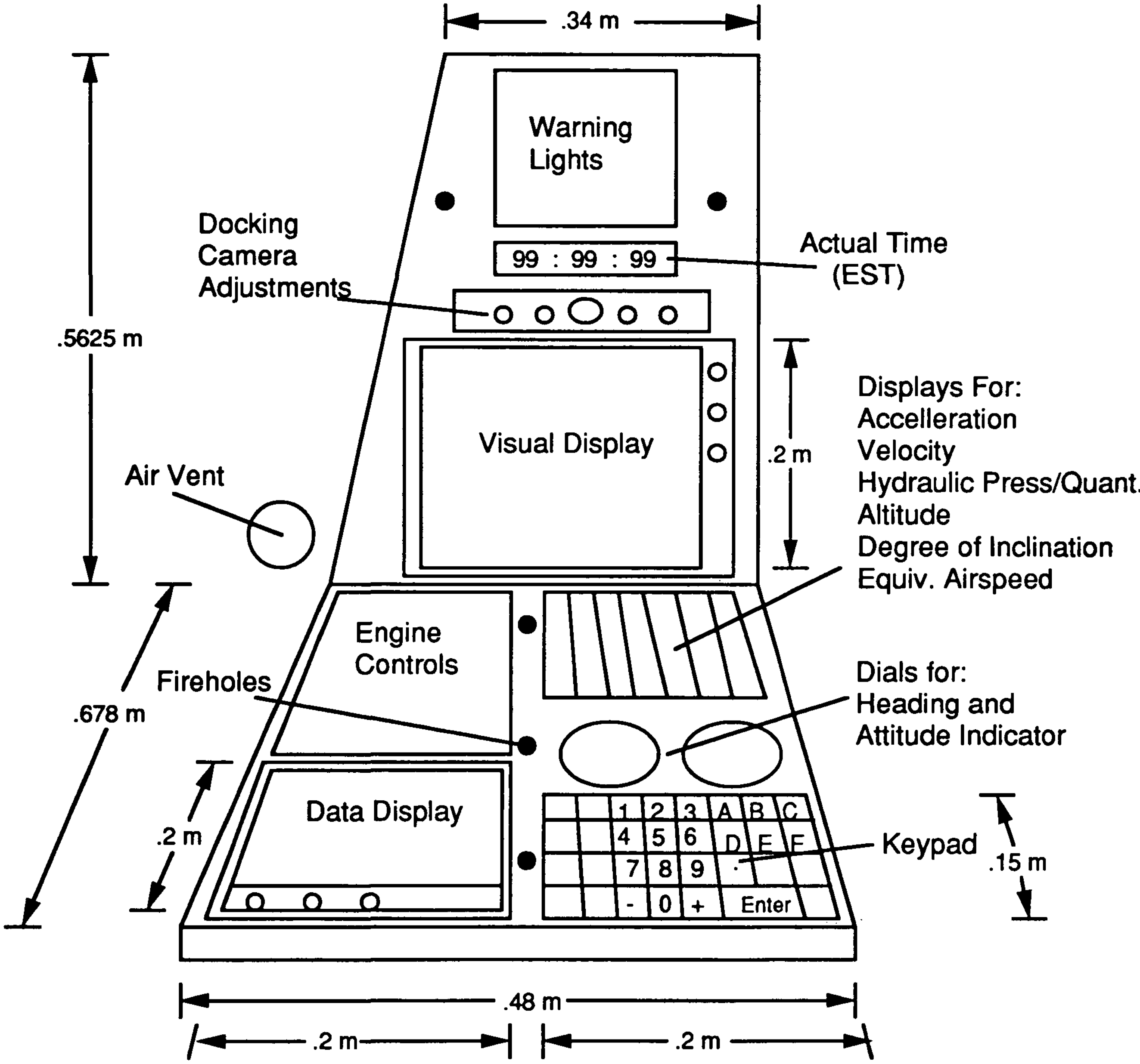

Figure 2.3 d

R. Cunningham

Capsule Controls and Monitors -- Co-Pilot Side

Side View

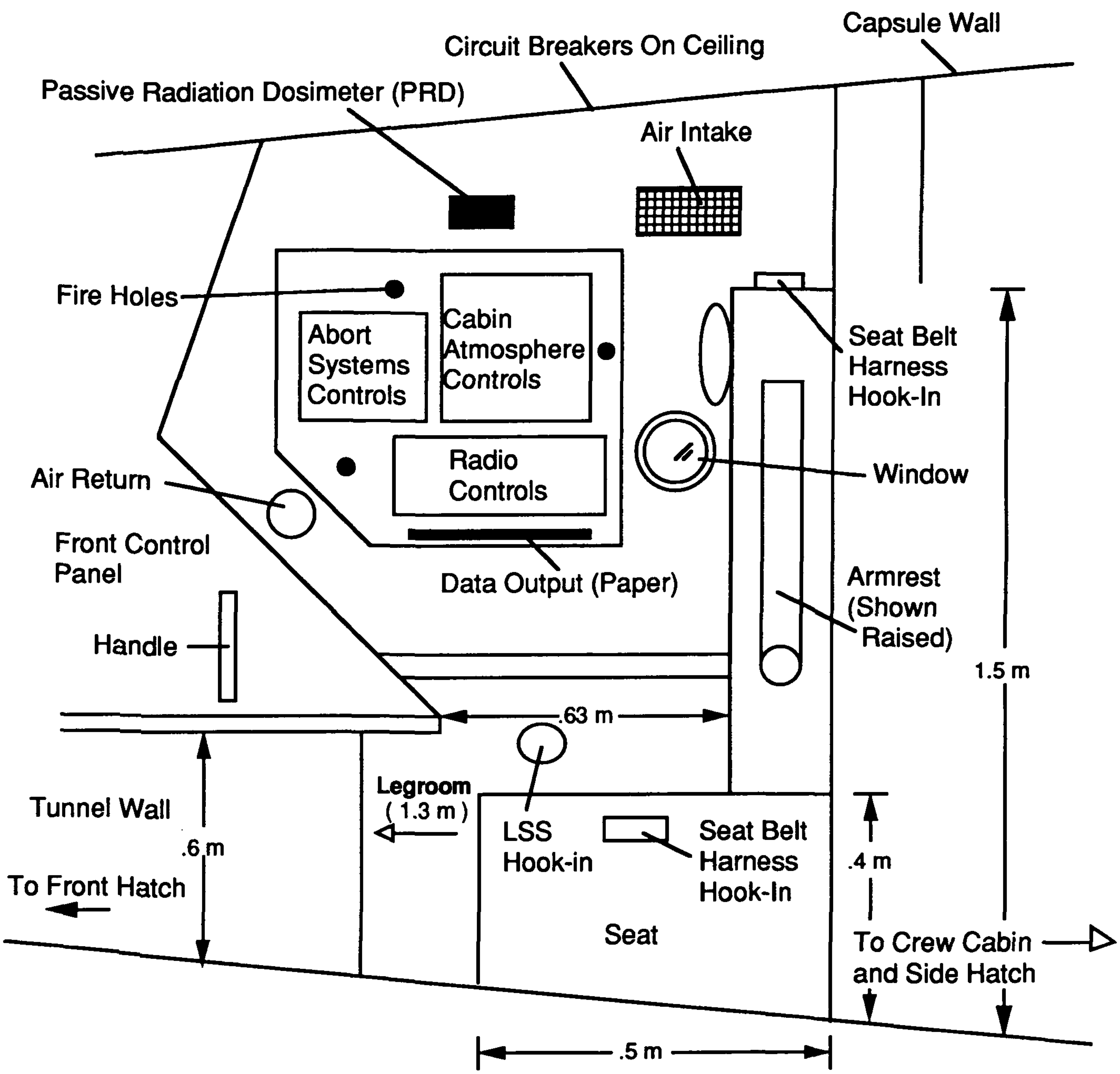

figure 2.3 e

R. Cunningham

Capsule Controls -- Co-Pilot Side

Front View

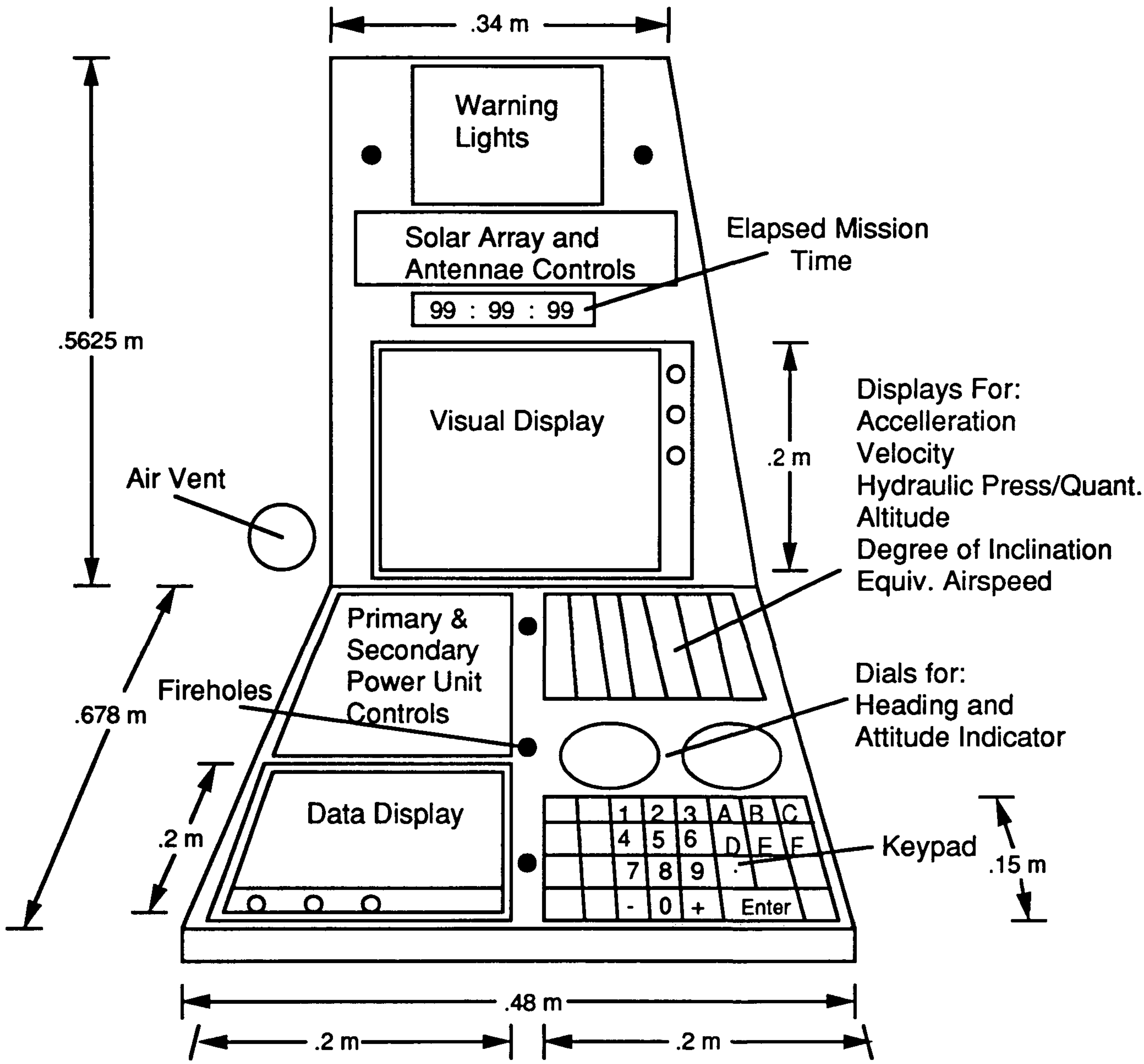

Figure 2.3 f

R. Cunningham

View From Bottom of Capsule

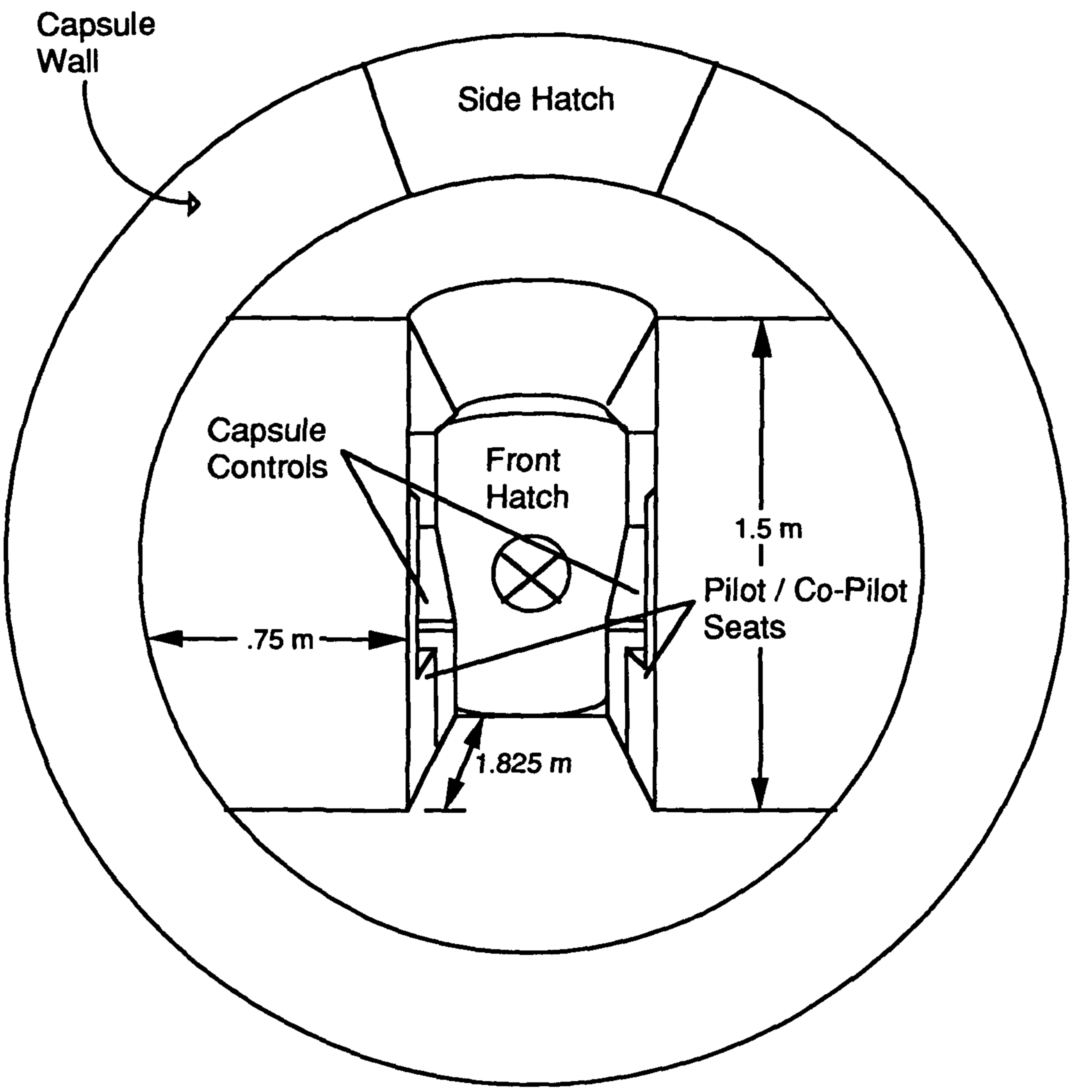

figure 2.3 g

R. Cunningham

Crew Seating

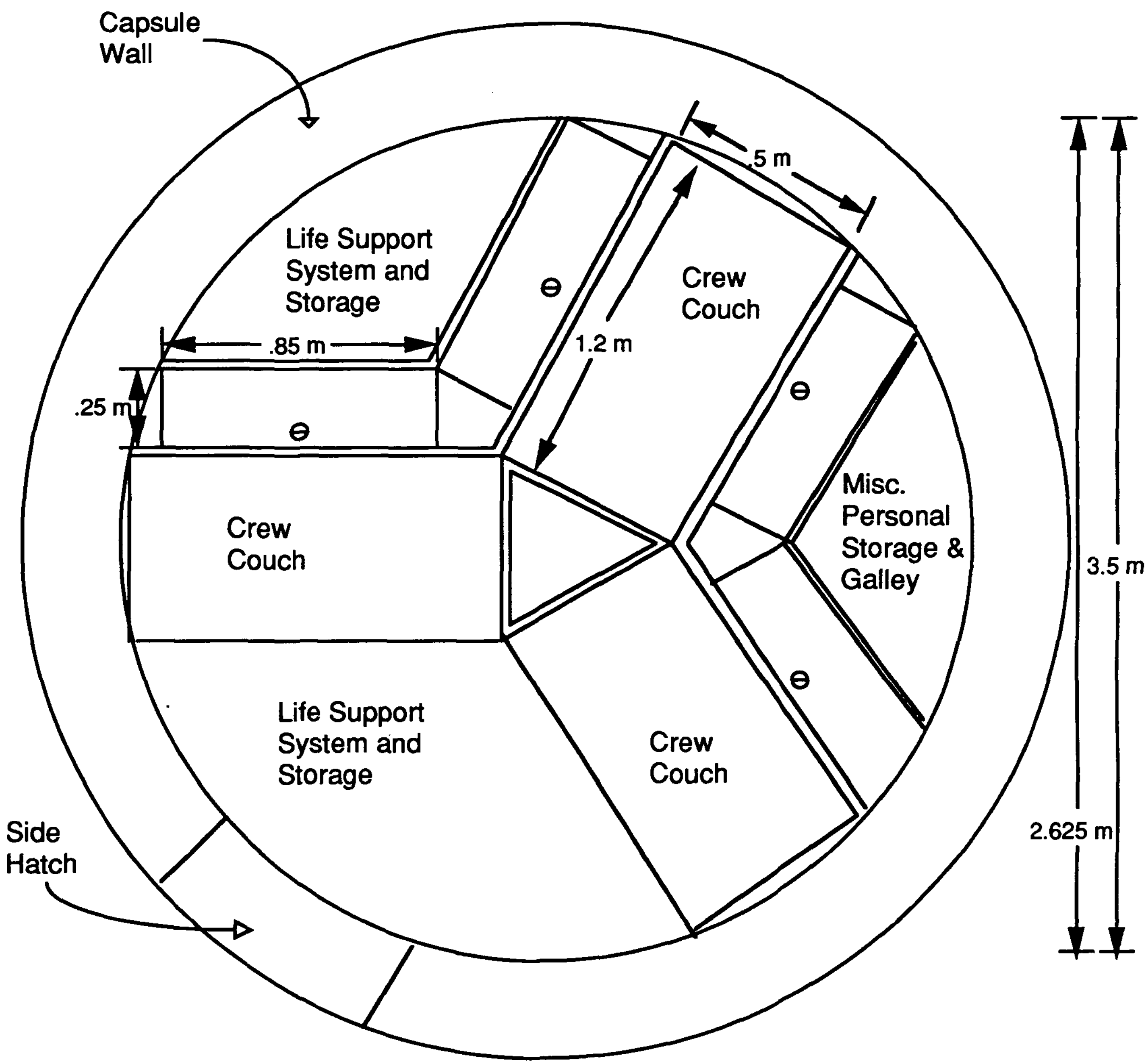

Figure 2.3 h

R. Cunningham

Crew Couch Design

Left Side

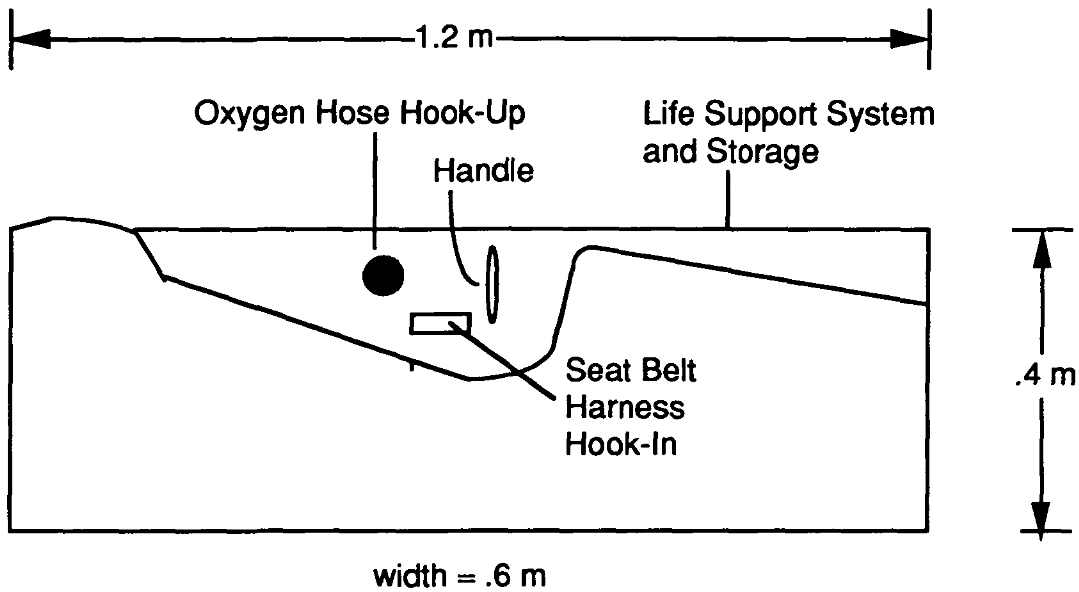

Right Side

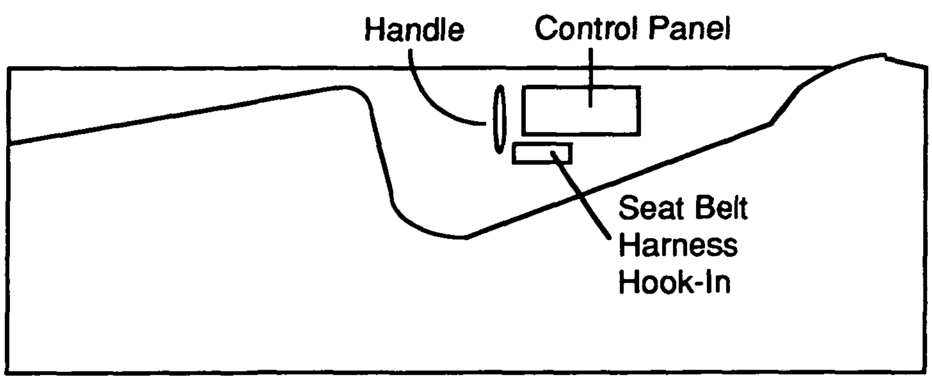

figure 2.3 i

R. Cunningham

Optional Crew Seating Design

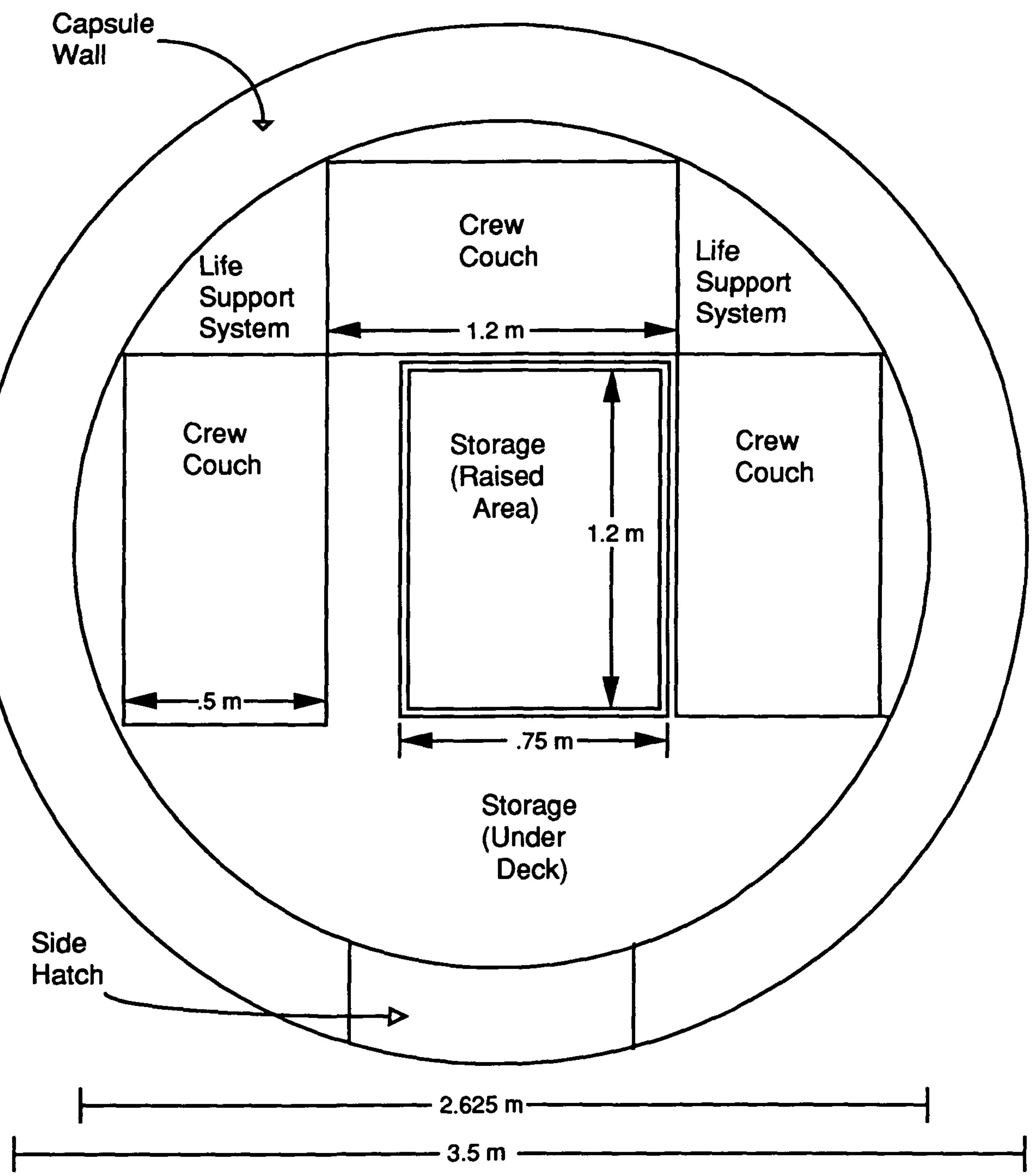

Figure 2.3 j

R. Cunningham

Optional Crew Seating Design

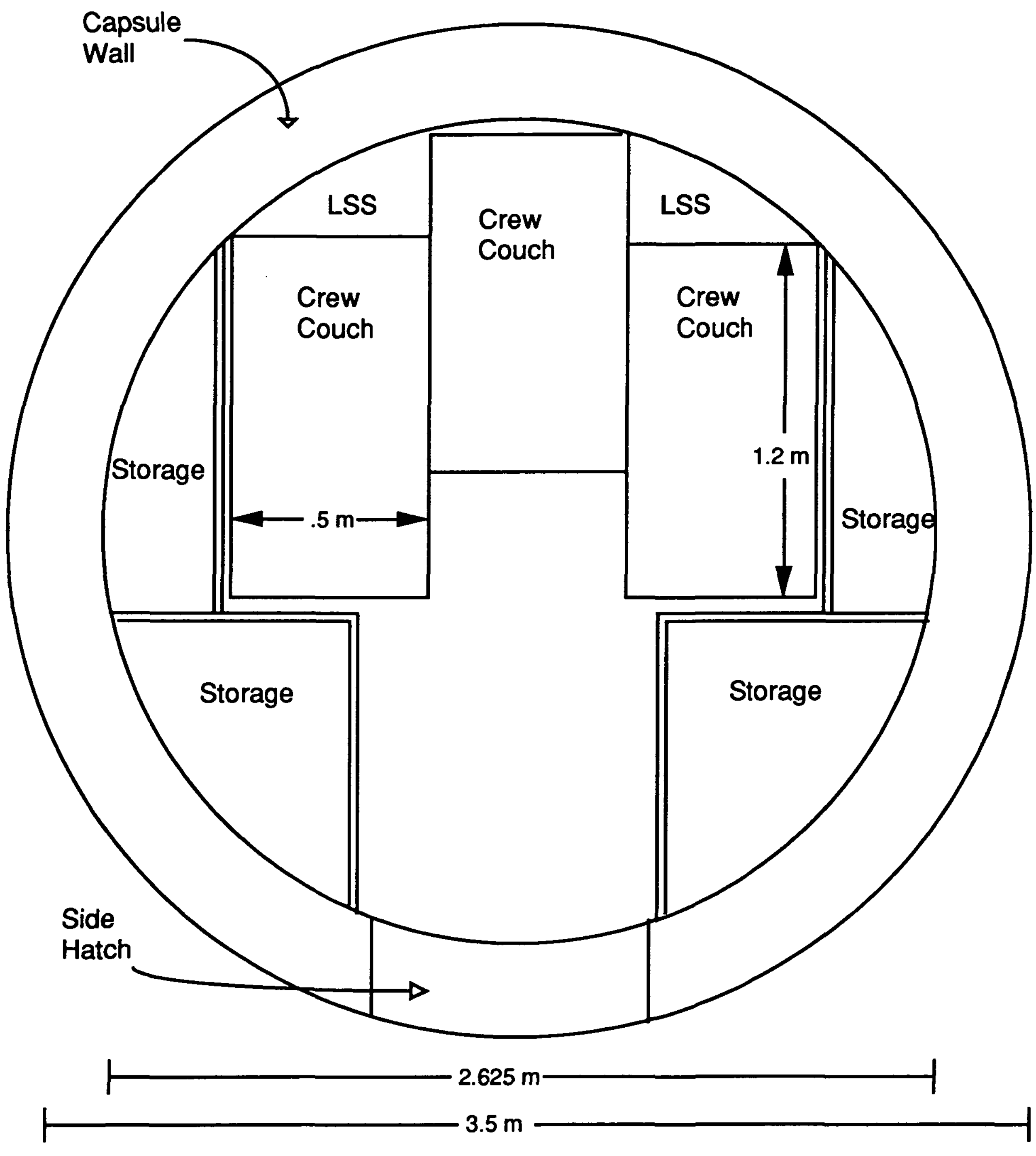

Figure 2.3 k

R. Cunningham

Optional Layout With Maximum Storage

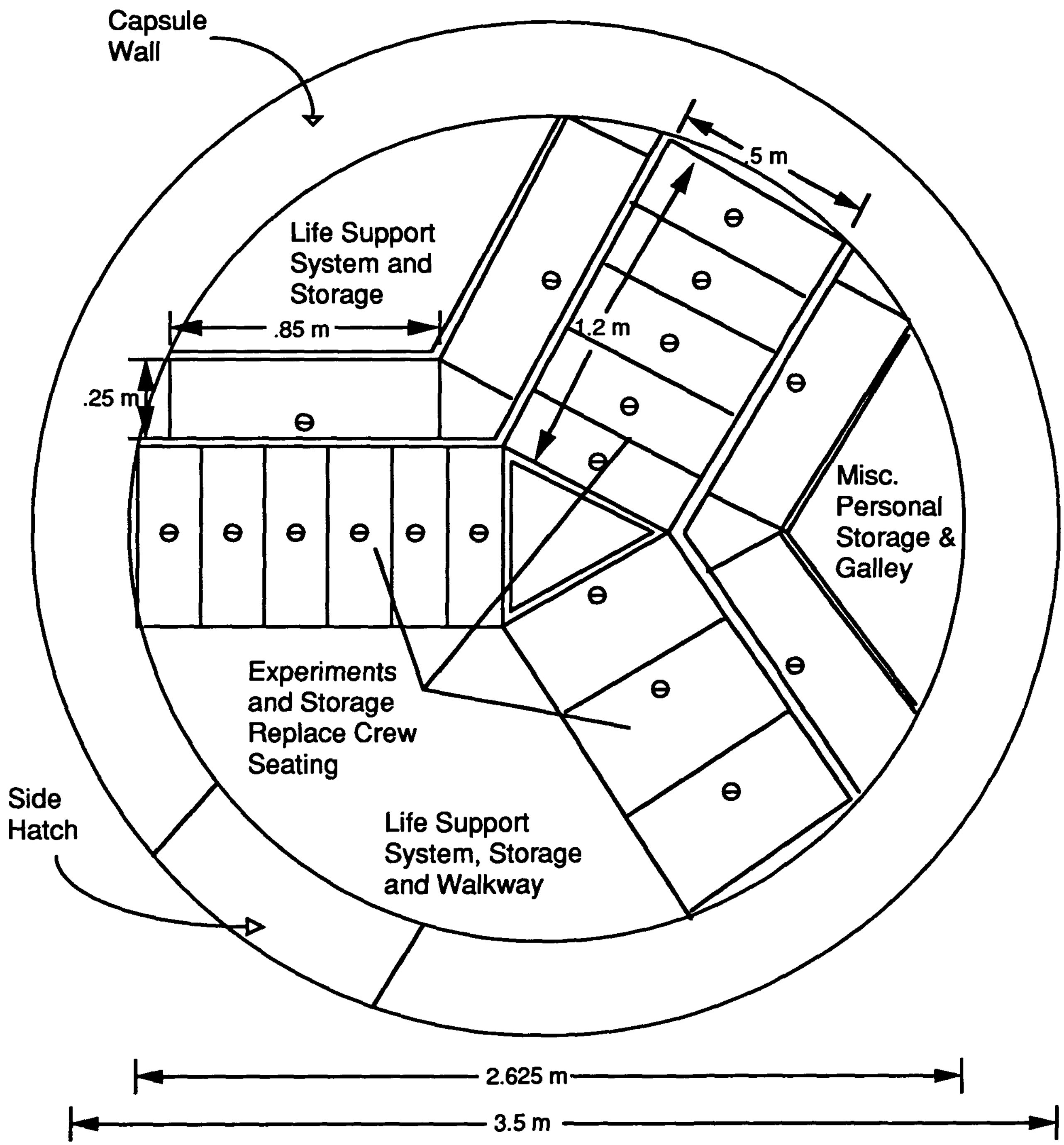

Figure 2.3 I

R. Cunningham

View From Outside Hatch

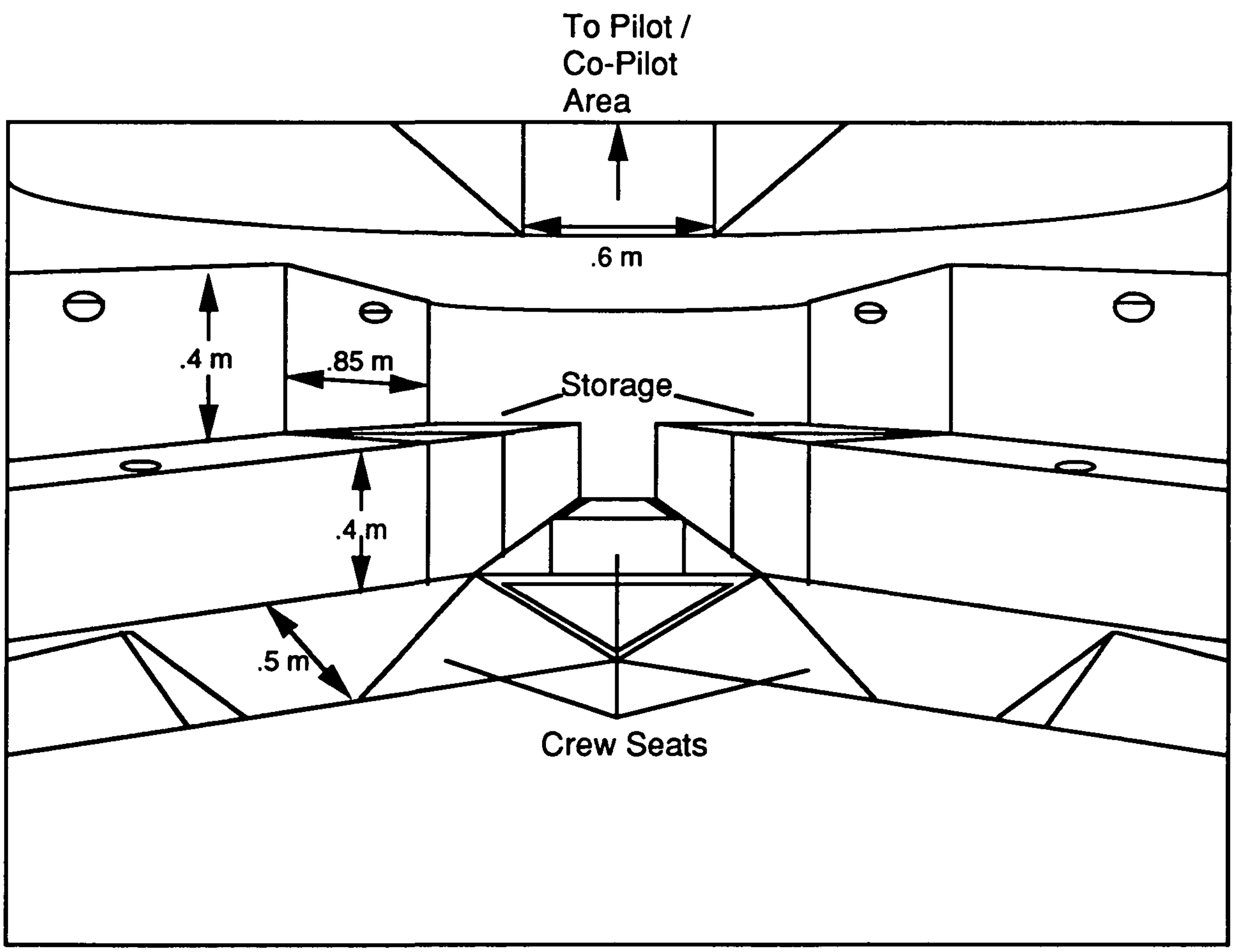

Figure 2.3 m

R. Cunningham

Space Suit Components

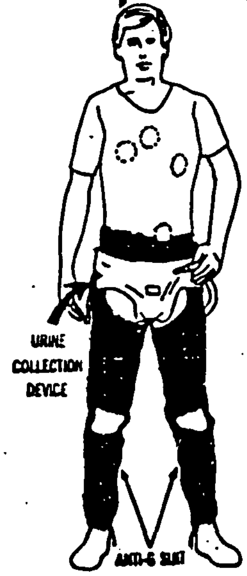

Anti-G Suit

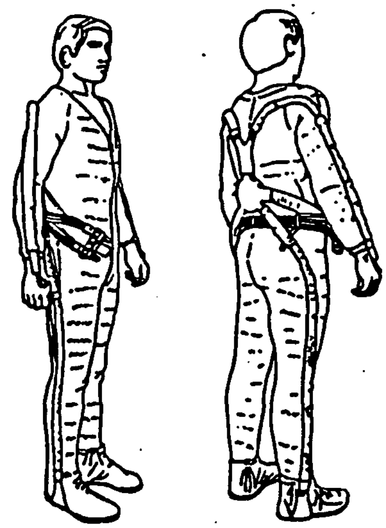

Liquid Cooled Undergarment

Putting On The Torso

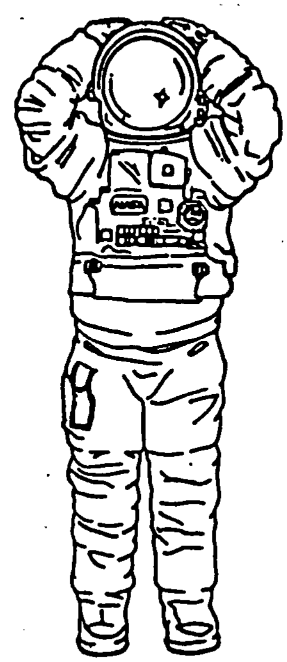

The Extra Mobility Unit
(EMU)

-- The Space Shuttle Operator's Manual, Joels and Kennedy, pg. 68.

figure 2.3 n

R. Cunningham

References

1) Aviation Week and Space Technology, January 22, 1990.

2) Aviation Week and Space Technology, September 24, 1990.

3) Aviation Week and Space Technology, October 8, 1990.

4) Aviation Week and Space Technology, November 12, 1990.

5) Bekey, Ivan and Daniel Herman, Space Stations and Space Platforms, 1985.

6) Chambers, Alan B., A Study of the Thermoregulatory Charateristics of Liquid Cooled Garment With Automatic Temperature Control Based on Sweat Rate: Experimental Investigation and Biothermal Man-Model Development, NASA, Washington D.C., June 1973.

7) Hall, Stephen B., The Human Role In Space, Marshall Space Flight Center, Alabama,1985.

8) Heath, Gloria W. (Ed.), Space Safety and Rescue 1984-85, 1986.

9) Joels, Kerry Mark and Gregory P. Kennedy, The Space Shuttle Operator's Manual, 1982.

10) Kaplan, Marshall H., Space Shuttle: America's Wings into the Future, 1978.

11) Lupton, T., Human Factors - Man, Machine and New Technology, 1986.

12) Mang, Carl K., Spacecraft Contamination Environment, Washington, 1983.

13) Mullen, Lloyd, Suiting Up For Space, New York, 1971.

14) NCRP (1989) National Council On Radiation Protection and Measurments, Guidance On Radiation Received In Space Activities, 1989.

15) Oberg, Alcestis R., Space Farers of the 80's and 90's - The Next Thousand People In Space, 1985.

R. Cunningham

Chapter 3

Structures

Section 3.1 Structure Design

Introduction

The primary goal of the structure group is to develop a lightweight structure that will allow the vehicle to accomplish its missions. This involve iterations and often computer analysis, but simple loading conditions are assumed and symmetrical bending analysis are used to obtain the stresses. Issues such as manufacturing and material selection; weight and cost constraints; and static and dynamic considerations are address during the design process; thus, optimizing the components and creating a fail-safe vehicle.

Material Selection

Since the proposed DART (DELTA ADVANCE REUSABLE TRANSPORT) is to be a reusable earth-to-orbit vehicle, it is only reasonable to select materials which will produce:

1. minimum structural weight
2. materials which have high strength to weight ratio
3. and materials which have gone extensive laboratory and flight testing.

Table 3.1.a list the major materials considered and Table 3.1.b summarizes the potential areas of the structural applications.

Titanium

To address the subject of reusability, titanium alloys are being considered as a primary load carrying stiffeners. Titanium alloys have been successfully used in past and has similar properties of steel. Titanium alloy has higher strength to weight ratio and properties that range to 315°C. Its cost is relatively low at $66.14 per kilogram (kg.). From Table 3.1.a, titanium is the heaviest material being considered, with a density of 4.484 g/cm^3; therefore, its use will be limited to certain areas.

The titanium alloy being considered is the Ti-5Al-2.5Sn. This is an alpha titanium alloy which is prepared by adding elements such as aluminum or tin to stabilize the high temperature hcp phase to temperature higher than 822.2°.C. The alpha alloy has a higher strength than pure titanium and can be used to temperature ranging to 315.5°C. Historically, it has been used in gas turbine area, airframe, and missile structures.

Other types of titanium alloys that can be used are the near-alpha, alpha-beta, and the metastable beta composition alloys. However, since the properties of these types of alloys ranges above that.ofthe.expected temperature (the properties of these alloys ranges up to 537°C), the use of

Table 3.1a - Material selection and Properties

Materials	Density (g/cm^3)	Tensile Strength (MPa)	Young's Modulus (GPa)	Coefficient of Thermal Expansion 10e-6 cm/cm C
Aluminum				
2024-T4	2.768	427.48	72.4	23.2
5086-H32	2.657	275.79	72.33	23.75
6061-T6	2.712	289.58	68.26	23.6
Titanium				
Ti-5Al-2.5 Sn	4.484	792.9	106.87	
Composites				
Boron-epoxy	2.63	3102.67	413.69	
Graphite epoxy	1.43	1241.06	172.37	1
Boron-aluminun	2.66	1103.17	220.63	
Carbon-carbon	1.5	103	41.4	0.5

Table 3.1b - Potential Material application

Skin	Pressure cabin	Struts (ring frames, longerons, stringers and fittings)	Beams of Baseplates
Aluminun	Aluminum	Titanium	Same as struts
Boron-epoxy		Boron-aluminum	
Boron -aluminun		Graphite-epoxy	
Graphite-epoxy		Boron-epoxy	
Carbon-carbon			

alpha titanium alloy is sufficient (Society of Aerospace Material and Process Engineers 1971).

Aluminum

The DART structural components will mainly consist of aluminum, since aluminum alloys have been extensively used in the aerospace industry. Aluminum, costing at $7.72 per kg., is the cheapest material being considered. The types of Aluminum alloys being considered are:

1. 2024-T4 Aluminum alloys
2. 5086-H4 Aluminum alloys
3. 6061-T6 Aluminum alloys

As seen from Table 3.1a, the tensile strength of aluminum 2024-T4 is much greater than the others being considered, making aluminum 2024-T4 the primary material to be used.

Aluminum will be used as a model to calculate the stress loading. If the stresses are low enough, then aluminum will be used due to its low material cost and low structural weight. If the stresses are much greater than expected then other materials will be considered. Aluminum will primarily be used as the outer skin of the spacecraft .

Composites

Composites, on the other hand, will be used as one of major load carrying member or as a reinforced material, where the composites are bonded to the structural member. The use of composites offers a solution to the weight analysis, but it must show sound cost effective judgement. The main composites that the design team are considering are boron-epoxy, graphite-epoxy, boron-aluminum, and carbon-carbon.

Boron-epoxy exhibits high tensile strength, as well as high strength to weight ratio, but the epoxy matrices shows strength degradation at elevated temperature.

Graphite-epoxy shows similar properties as boron-epoxy and also exhibits strength degradation at elevated temperature. Since boron-epoxy is more expensive to manufacture than graphite-epoxy, graphite-epoxy will be more likely be used.

Boron-aluminum, of the other hand, may be used in elevated temperatures and competes fairly well with titanium and aluminum. It shows high tension, compression, shear strength, as well as high fatigue strength and rupture. Some past usage of boron-aluminum were horizontal stabilizer on the F-14 fighter aircraft, the space shuttle, Apollo, and Pioneer 10. Unfortunately, boron-aluminum is very expensive, but a solution to reducing the cost is to manufacture boron-aluminum from semi-finished product. This process has an average cost of $75 to $120 per kilogram.

Carbon-carbon composites are highly considered due to its excellent high temperature performance. Applications vary from heat shielding, rocket engine nozzles, and disc-brakes. The use of carbon-carbon will most likely be use in the design of the bottom of the spacecraft due high heating from re-entry.

In conclusion, the Delta structural team have only looked at the material properties when selecting the appropriate types of materials. Manufacturing and fabrication of materials were not considered in depth, but simply touched upon; thus this subject needs more research, especially for different ways of manufacturing composites, since most of cost evaluations will deal with manufacturing and fabrication. Also, most of the materials being considered will not be used in the final design. Only the materials that will satisfy the given stress loading and the minimum weight requirements will be considered

Static and Dynamic Analysis

The design analysis of a spacecraft vehicle will be based on assumed simple loading conditions. The model utilizes symmetry, simple bending theory, and discrete critical loading conditions such as the skin carries only shear stresses and the stringer carries only flexure stresses. Though in reality, the loads changes under different flight conditions.

All loads are assumed to be acting at the center of gravity. Point loadings such as engines, heat shielding, and fuel tanks are not considered in the design of the structures due to their small loadings compared to the maximum loading. The suggested maximum design loading imposed by the Delta rocket booster is 5.86 g's in the axial direction which occurs at first stage separation and maximum of .7 g's in the lateral direction. Although the suggested design loading is imposed by McDonnell Douglas, DART is designed to withstand a maximum axial force of 10 g's due to the abort system and a maximum .7 g's due to the first stage separation (re-entry, and impact landing will not exert a force greater than 10 g's). Vibrational loadings are taken into account by considering the maximum vibrational loading and assuming it to be a quasi-static load. As of yet the vibrational loadings are not determined and are not taken into account in the design.

The main equation that are used to calculate the stringer stresses are as follows:

Symmetrical Bending Formula: (1)

$$\sigma(y,z) = \frac{P}{A^{*}} + \frac{M_z \times I_y - M_y \times I_{yz}}{I_y \times I_z - I_{yz}^2} \times Y + \frac{M_y \times I_z - M_z \times I_{yz}}{I_y \times I_z - I_{yz}^2} \times Y$$

$\sigma(y,z)$ =stress loading
M_z=moment about the z- axis

A^*= total cross-sectional area of the stringer
P= axial loading
I_y=centroidal moment of inertia about the y-axis
I_z=centroidal moment of inertia about the z-axis

Shape of Stringer support being considered

When determining which types of flanges, stringers, and struts to use, the structures group considered whether the designed flanges or struts will be easily manufactured. The types of stringers being considered for the spacecraft are as follows (see Figure 3.1a):

1. hat sections
2. z-stringers
3. I-beams for baseplates
4. channel section

Hat-section

Hat-sections are chosen due high torsional stiffness since it is allowed to form a closed section with the outer skin. Hat section also has a larger surface area contact with the skin which allows more riveting contact.

There are minor problems with using the hat sections. One is that if moisture get in the closed area corrosion can occur which is hard to check for. Also there is a need to use more riveting materials because of larger surface contact on the skin.

Z-stringers and Channel sections

Z-stringers and channel sections offers torsional stiffness, but not as high as the hat section. they are relatively easier to check for corrosion since they are open sections.

I-beams

I-beams will be mainly used in the baseplate due large bending moments occur there. The I-beams will support most of the internal structures seats and on board computers. It must also be able to support external equipment such as the weight of the heat shield, main propulsion, and fuel tanks

.

Again not all the stringer configurations will be used, only the appropriate shape that will be able to carry the maximum loadings will be considered.

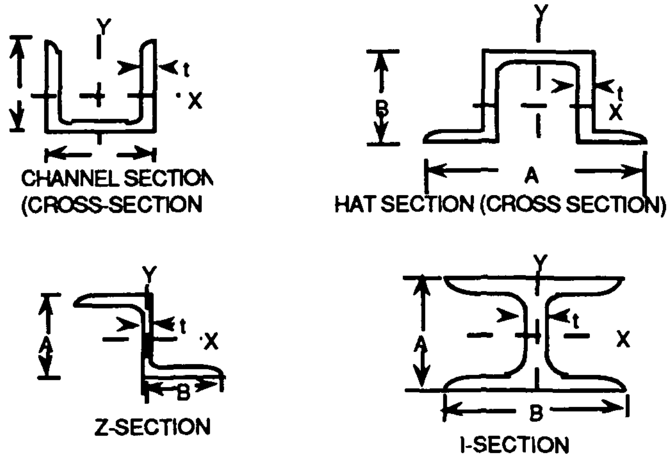

Figure 3.1a: Types of Stringers

Calculated Center of Gravity

Integrating all the equipment, except for the main structures and the maneuvering engines, the calculated center of gravity is (-.244i + 2.08j) m from the bottom of the spacecraft. The center of gravity is extremely high due to the abort engine palcement. For detailed calculations refer to Appendix 3.1.2

Optimum flange and strut design and material fabrication

Using equation 1 and maximum load of P= 4.51e5 N and Mz=My=9.79e5 Nm, the cross-sectional area of the stringers can be calculated. As stated above, several iterations was done to determine the number of hat-stringers to use. First, the number of stringer was assumed, and the cross-sectional area were calculated. As the number of stringer increased, the wall carried less shear loads, until the skin were thin enough that a sandwich panel design could be incorporated. Figure 3.1b shows the cross-section of the spacecraft at any diameter D. With the given loads applied, the cross-sectional area of the stringers are:

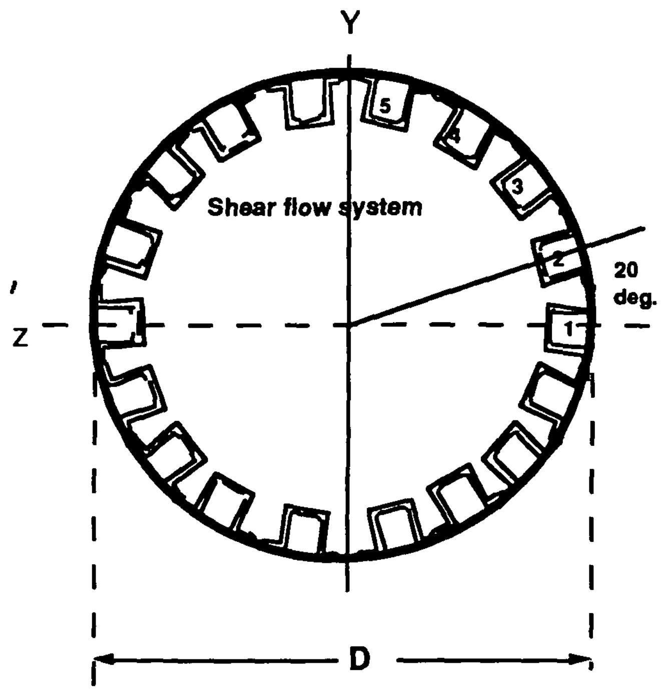

SUPPORT ATTACHMENT

Cross Sectional Areas

Area #1 =2.09 cm^2
Area #2 =3.72 cm^2
Area #3 & #4 =4.90 cm^2
Area #5 =5.49 cm^2

Figure 3.1b- Spacecraft cross-section at any given diameter

For simplicity the cross- section was designed for symmetry and the stringers are 20 degrees apart.

Also to check for failure at any other point, stress evaluation at four other diameter and the result are given in Appendix 3.1.3. From the analysis, the margin of safety were appropriately low, indicating that the optimum design for the cross-sectional area.

The material that was used in this design was graphite epoxy, due to the high concentrated stress. One reason for the high may be accounted for the use of conservatism. Since the application of the load were not specifically determined, one superimposed the forces; thus creating a large stress distribution.

The design for the dimensions of the of the hat stringers was a little more complicated. A length dimension was assumed and thickness was the variable that one had to determine. Again, once the thickness was obtained equation 1 was used to determine if failure would occur. From Table 3.1c, again the margin of safety is quite low which states that the optimum design is reached

Design of outer skin thickness and type of fabrication

The outer skin will be made of aluminum honeycomb. The shear flow for was determined through the process of evaluating the stringer cross-sectional area. Appendix 3.1.3 and Figure 3.1c gives the breakdown of the shear flow along the spacecraft's length. Superimposing the shear flow will obtain a conservative calculation for the skin thickness. With the given shear flow of 1.02e6 N/m, and assuming that the honeycomb panel is supported with all four edge restraint , the facing thickness is calculated to be .119 cm. Using a HIGRID 5052 alloy DURA-CORE honeycomb, the appropriate core density was found to be 354 kg/m^3. This was chosen because it is low weight, and was able to take a maximum compressive stress of 37.3 MPa (see Appendix The total weight of the honeycomb skin is 192.73 kg.

The only problem which faces the design of such panels is the bonding technique. The bonding between the honeycomb and the aluminum was not looked at until the question was asked during the CDR. Further analysis on this subject must done to bring the structures together.

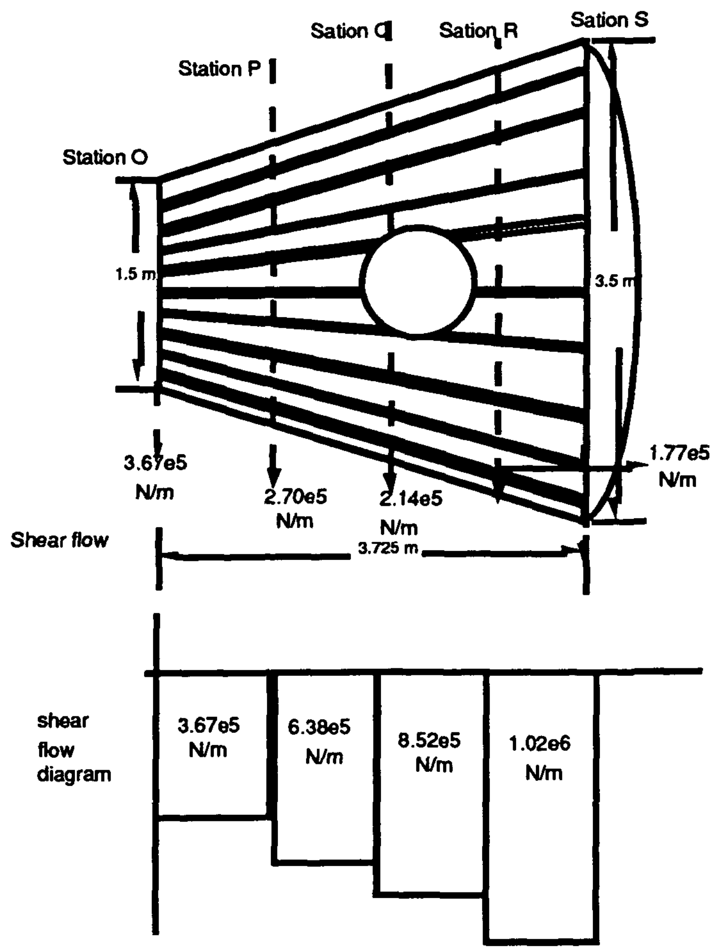

Figure 3.1c: Shear Flow Diagram

Optimum Design of Pressure Vessel

The design of the pressure vessel will remain relatively the same. For ideal situation the necessary internal pressure is assumed to be 15 psi or .1034 MPa greater than outside pressure. Assuming a factor of safety of 1.5 and using the Pressure Vessel Handbook , the thickness of the conic pressure vessel wall is .614 mm. (See Appendix 3.1.1). The materials used for this wall is aluminum due to low stress created by the internal pressure. The joining together of the pressure vessel and the honeycomb will be done by a process of welding or the use of chemical compound. Bolts will not be considered due *to the low allowable compressive stress the honeycomb can withstand*

Conclusion

In conclusion the DART structural components have been determine. The stringer cross-sectional area are 2.09 cm^2, 3.72 cm^2, 4.90 cm^2, and 5.49 cm^2. The total stringer weight is 45. kg. Also the outer honeycomb is designed and will be bonded to the pressure vessel skin. The thickness of the pressure vessel skin will remain the same and the face thickness of the honeycomb skin is.119 cm. The total weight of the entire structures add up approximately to 237.74 kg.

Thought stress analysis have been performed, the areas still need further studies are the manufacturing and fabrications, types of adhesive that will bond the aluminum to the aluminum honeycomb, and vibrational analysis.

Section 3.2 : Delta Docking Mechanism Structure.

Introduction

This Chapter section, starts with the requirements for the docking of Delta Advanced Reusable Transport(DART) with the Space Station Freedom (SSF), describe two methods of docking with SSF and then conclude by choosing one of the systems. Comparative trade study will be provided, then it will become obvious why the system was chosen.

Specific Requirements

The DART is required to perform rendezvous, Extra Vehicular Activities (EVA), inspect and repair satellites. According to National Aerospace Administrations'(NASA) policy, Astronauts have to spend at least three days in orbit before he or she can perform EVA. This time frame is necessary to allow the crew to adjust to the weightlessness environment.

However, the DART capsules' interior layout is limited in adequate accommodation, due to the weight constrain of the delta rocket. Therefore the astronauts will be best accommodated inside the space station. To facilitate this functions docking is required.

Compatibility of the first system with space station freedom

The capture mechanism design for the docking tunnel of SSF is not compatible with DART space craft. Hence, An adapter, with a rendezvous drone will be carried, on board the space shuttle into orbit and fitted with the docking tunnel of freedom during a short EVA by the shuttle crew before de-orbit.

DART Docking Procedure

The spacecraft will maneuver to within three meters of the docking tunnel. The drone, is manually guided to the adapter ring on the SSF docking tunnel, by signal traveling through the cable, until it is sufficiently close for magnetic attraction of the drone to the ring. The drone by magnetic attraction is automatically aligned with the ring and is coupled thereto. By means of the cable interconnecting the DART to the drone coupled ring, the vehicle is slowly drawn together. As the two vehicle near each other, mechanical alignment and connecting means are extended therefrom to complete the final closing operation.

Docking and hermetic sealing of the two vehicle is accomplished by tightly drawing the two vehicle together mechanically and sealing two resilient seal rings by compression thereof. Fig 1 below is a side view of this procedure.

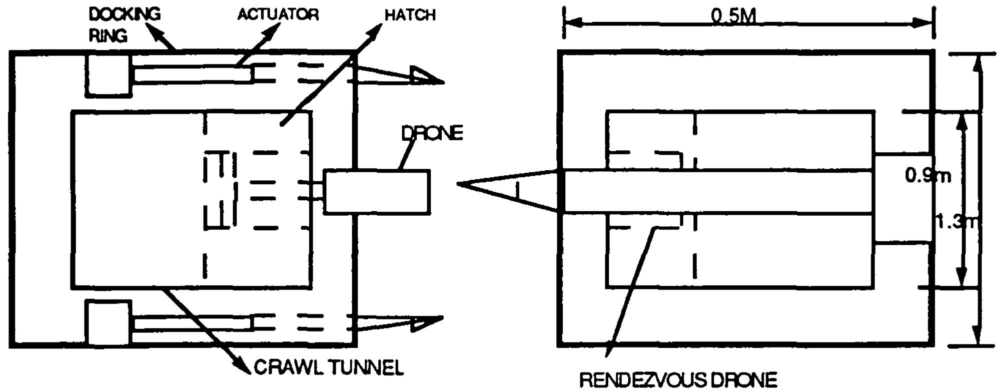

Fig. 1. Docking Mechanism and Adapter

Capture System (Drone)

The drone is equipped with a powerful electromagnet 1, fig. 2, a compressed gas propellant container 2, and control nozzles 3, mounted inside a small cylindrical housing 5, and steel cable or wire 4. By using the compressed gas propellant, a crew member of the DART launches the drone, optically guides it to the adapter, using a manual "fly-by-wire" control system, until the drone is within a few centimeter of making actual physical contact with the adapter.

At this point, the crew member energizes the electromagnet which automatically aligns itself and drone with the adapter, so that the drone attaches itself to the rendezvous drone of the adapter ring. Attachment steel wire, which was fed out from an electric motor driven mechanical winch housed in the hatch door of DART, physically interconnects the DART to the SSF.

The cable winch motor is energized to reel in the cable, slowly drawing the vehicle together. Fig 2, is a cut away view of the drone.

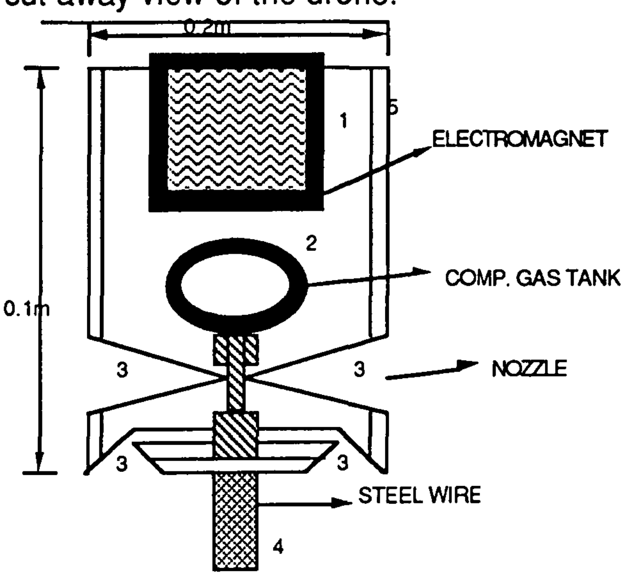

Figure 2: Drone

Compatibility of the second system with SSF.

This system was designed to be compatible with the available design of the SSF, capture mechanism. It is an electro-mechanical actuator, with shock absorber system, for damping the impact force when the two mechanisms make initial contact.

Docking Procedure

DART will maneuver to within a few meter of the docking tunnel. The electro-mechanical actuator is activated, after it has fully extended and is perpendicular to the SSF capture mechanism, the capture latch of SSF is activated and connect to DART.

One crew member will then activate the actuator to retract, and slowly close the gap between the docking ring of the two vehicles. Docking and hermetic sealing of the two vehicle is accomplished by tightly drawing the two vehicle together and sealing two resilient ring by compression thereof. Fig. 3 is a side view of the capsule and capture latch with SSF. tunnel and receptor arm.

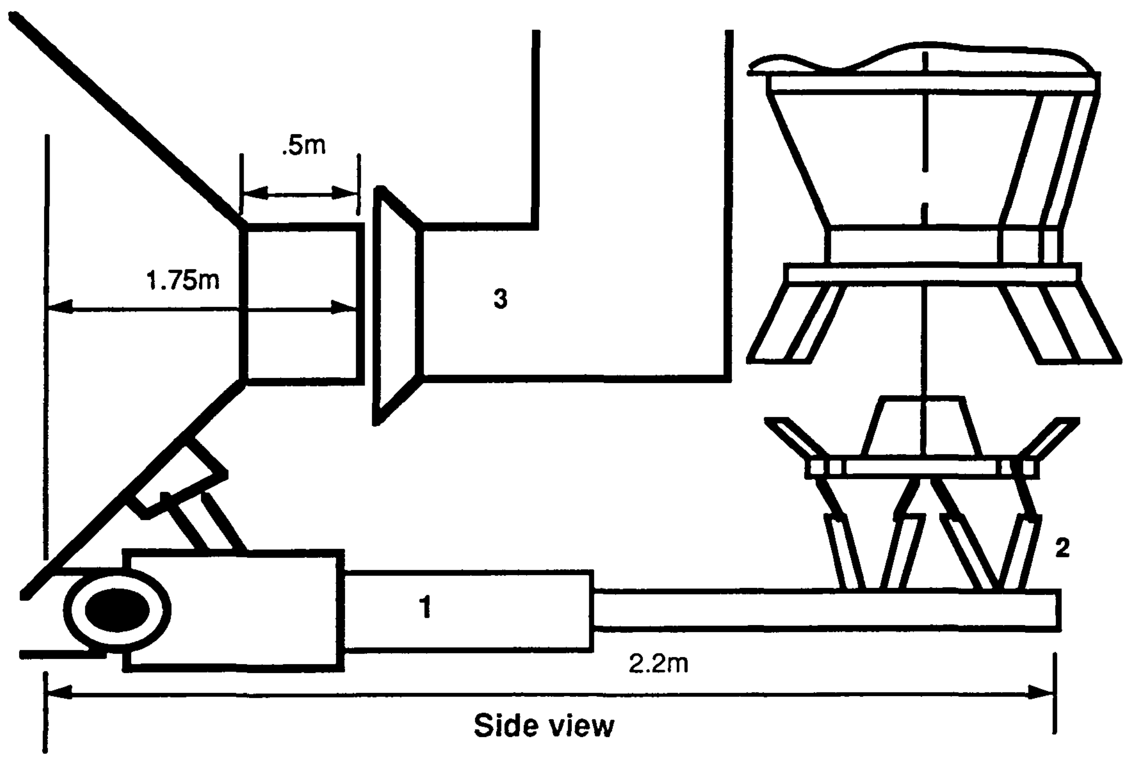

Figure 3: Capture Latch

Capture System.

The electro-mechanical actuator 1 fig. 3, connected to the capture mechanism 2, is bolted to the outside of the DART space-craft. Its primary function is to provide a receptor to the SSF capture latch, which will facilitate the proper alignment of the DART docking ring with the docking tunnel of freedom.

Its other function includes retraction to provide a pressurized seal between the two vehicles, and allow the transfer of personnel and cargo through the tunnel.

The support actuator 4, will provide a folding mechanism for the main actuator, when not in use, and retain it in place during re-entry.

Conclusion

The second system satisfy the minimum weight required for this mission. Since mass translate into dollar saved. But, more importantly the need for an adapter is not required.

Section 3.3: Structural and Propulsion System Interfacing

Structural Interface

Summary

The structural interface is a ring truss made of 6016-T6 Aluminum alloy designed to support the maximum lateral and trust axis forces of the Delta II launch profile, shown in Figure 3.3a. It weighs 29Kg, has a upper diameter of 3.5m, a height of 0.95m, and a lower diameter of 1.58m. The DART capsule connects to the truss using four steel cables loaded in pure tensions, which can hold the craft steady under 22KN of tension; the interface attaches to the Delta second stage with 58 bolts. The main truss members can withstand a maximum compression or tensile stress of 242MPa, see Figure 3.3b. The system also carries a factor of safety of 1.2 throughout the loading and analysis.

Design Constraints

The DART system requires special interfacing considerations due to its mass, geometry, and propulsion system requirements. The capsule configuration maintains a center of gravity 1.4m from the bottom of the capsule, which is held 3.03m above the Delta II, 7920 interfacing plane. This, combined with the DART's 4600Kg maximum launch weight and its base dimension of 3.5m, made the predesigned Delta Payload Attachment System (PAF) and the 6019 Interfacing Ring Attachment obsolete for this system. Further, the 7920 booster requires all payloads launched using the two-staged model to interface with a 1.58m diameter ring using 58 bolts. The Delta II, 7920 also requires payload interfaces to hold the center of gravity no higher than 3.1m above the Spacecraft Separation Plane, that between the Delta second stage and the plane of separation.. Dart's expendable propulsion system, which must hang in the central void of the interface structure, provides the final geometric constraint to the interface design.

The final structure must hold the 4600Kg spacecraft statically stable under the maximum loadings of the Delta II launch profile. Vibrational side loading will create a maximum of 0.7g acceleration along the lateral axis; and, the longitudinal thrust axis will experience no more than 5.86g during launch. This loading system and a factor of safety of 1.2 complete the constraints placed upon interface proposals.

Design

The interface mechanism is a ring truss with top diameter of 3.5m, to match the DART bottom surface, and a bottom diameter of 1.58m, to bolt onto the mechanical interface of the Delta booster, connected together by eight equilateral triangle support members. Height was the varied dimension. As stated, the interior volume must allow for the propulsion system. The height of the interface unit controlled the volume as-well-as the forces in the members by reducing the angle of the incline. This dimension could not exceed 0.95m to insure center of gravity interfacing below 3.1m above the Spacecraft Separation Plane.

The final height was dictated by the length of the engine nozzles and the radii and lengths of the propulsion fuel tanks. Studying the gain in mass created by increasing the length of each truss member versus the increase caused by decreasing the side angle, thus increasing the stresses, it was found that the taller structure had greater mass efficiency. The height was than calculated from the max remaining height adding to 3.03m, 0.95m. This defines the side angle by:

$$O = (\text{DART Diameter} - \text{Second Stage Diameter})/2 = 0.5585$$
$$A = \text{Height of the Structure} = 0.95\text{m}$$
$$\text{Side Angle} = \text{Arctan}\,(O/A) = 52^\circ$$

$$\text{Height Study of C.G.:} \quad H = 0.95 + .2805 + 1.7995$$

The cross sectional area, $7 * 10^{-4} m^2$ was then backed out of the stress equation using the maximum stresses the system will experience.

The shape of the cross section was first assumed to be an "L" shaped beam to allow for riveting faces. Upon studying the current welding procedures it was discovered that heat treated welds of 2025, 6016-T6, and 7075-T6 Aluminum will maintain fastening integrity for the expected loading. This allows the use of a multi-axial symmetric cross section, which provide better pure tension compression members. Figure 3.3a shows the interface dimensions and two possible cross sectional area: the "L" shaped, and a circular shaft.

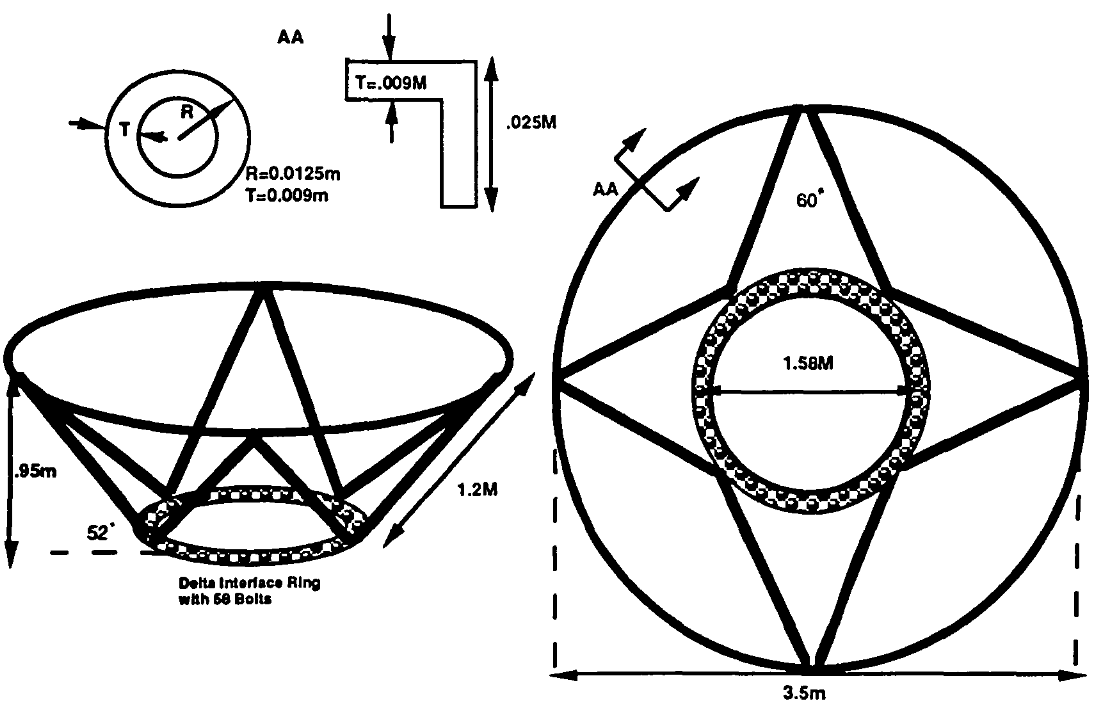

Figure 3.3a: Interface Dimensions

Loading and Analysis

The interface truss was designed around the maximum loadings of the launch environment. The DART capsule is secured using a "strap-on" system of cables in tension. Four cables will be loaded in pure tension, one down each planer axis to the bottom of the craft. As stated earlier the maximum axial loadings for the 7920 booster are:

$$\text{Max Long.} = 4600\text{kg} * 5.86 * g * 1.2$$
$$\text{Max Lat.} = 4600\text{Kg} * 0.70 * g * 1.2$$

These loads were applied at the center of gravity and the stress in the members were then calculated. Summing the moments about the potential pivot point (A) for the maximum lateral forces the ultimate force (Tmax) for the steal cables was found to be 22KN.

Using the method of sections and joints and the definition of static stability the forces in each member were isolated as a statically determinant system. The weight of the craft was distributed evenly over each of the four nodes on the upper ring of the truss. The critical members were those on the 52° side angle; they bear a maximum force of 169.1KN, which generates a stress maximum of 242MPa. The maximum value of stress was allowed to equal the ultimate tensile strength of 6016-T6 Aluminum (200MPa) multiplied by a safety factor of 1.2. Using the resultant value, the cross sectional area of $7.0*10^{-4}m^2$ was backed out of the stress equation.

From the final dimensions and the minimum cross sectional area, the volume of each member was calculated and summed over the entire structure. The total volume of the interface is $0.0107m^3$ which produces a mass of 29Kg of 6016-T6 Aluminum. Figure 3.3b shows the loading method and the dimensions needed for the analysis.

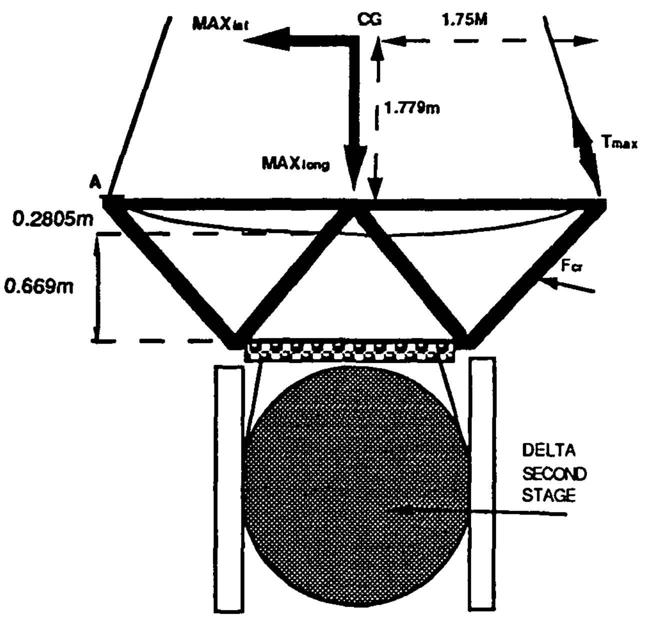

T_{max}	=	22 KN
F_{cr}	=	169.1 KN
MAX_{lat}	=	WC*0.7*g*1.2
MAX_{long}	=	WC*5.8*g*1.2
Area AA	=	7.0E-4m
Max St.	=	242mPa
	=	Ult * 1.2
Mass	=	29 Kg
Material	=	6016-T6 Alum

Figure 3.3b: Loading Method and Analysis Results

Strap-on Propulsion Package

Summary

The propulsion system holds 17.8KN force of the engines steady using a box truss and ring fitting of 6016-T6 Aluminum. It weighs 2.89Kg and uses conical engine cuffs holding the engines in line with a 5cm zone for vibrations. The entire system is connected to the DART with steal cables and is designed for a 1.2 factor of safety.

Design Constraints

The overiding constraints for the propulsion interface are those dictated by the missions of the vehicle: fuel mass, engine power and the dimensions needed to carry and create these loadings. In addition, the Delta II interfacing constraints add a degree of complication. The maximum height of 0.95m allotted for the interfacing truss created a side angle of 52°. This side inclination constricts the shape of the fuel and oxidizer tanks, shown in figure 3.3d. The impingement of the sides and that of the Delta second stage must be cleared by 5cm to allow for structural vibration during the violent launch phase of the missions.

Additionally, the structure must carry the needed volume of fuel and oxidizer, and with-stand the maximum force of 17.8KN created by the engines. This force is then projected directly into the DART heat shield, which must remain intact to secure safe re-entry.

Design

The DART strap-on propulsion package is basically a box truss connected to a ring "force footprint" of 2.26m diameter. The box forms a structural basket to hold the fuel and oxidizer tanks as-well-as the necessary plumbing and regulators. The force "footprint" diffuses the engine force over an area of 0.178m^2 as opposed to direct force loads. These conditions are acceptable to maintain the heat shield and structural integrity. Figure 3.3c shows the basic three-view dimensional drawing of the system.

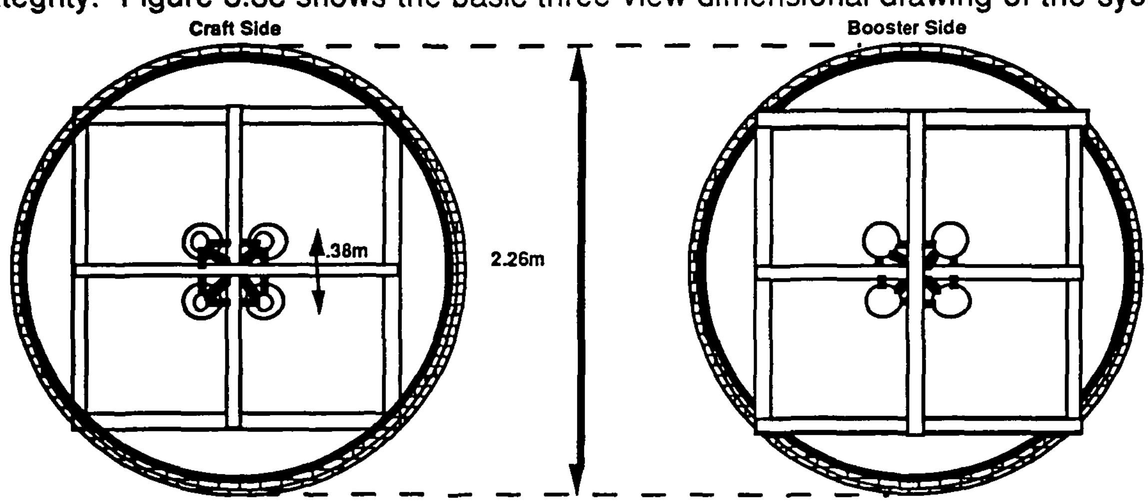

Figure 3.3c: DART Strap-on Propulsion Package

H. Magazu

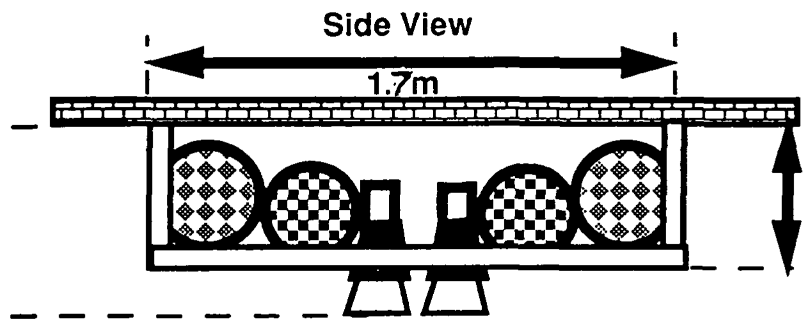

Figure 3.3c Continued: DART Strap-on Package

Each engine is connected to the cross members of the box truss using a conical cuff. These cuffs are fit around the heat sink material used to cool the nozzle, and are secured with three arms bolted to the box truss. The nozzle area is built up with a carbon material to diffuse the forces, create a heat sink, and allow for the conical cuff design to hold the engines down as they fire (figure 3.3d). These cuffs are held together with 10 steel, side bolts. They hold the engine nozzles 5cm apart to avoid nozzle impingement .

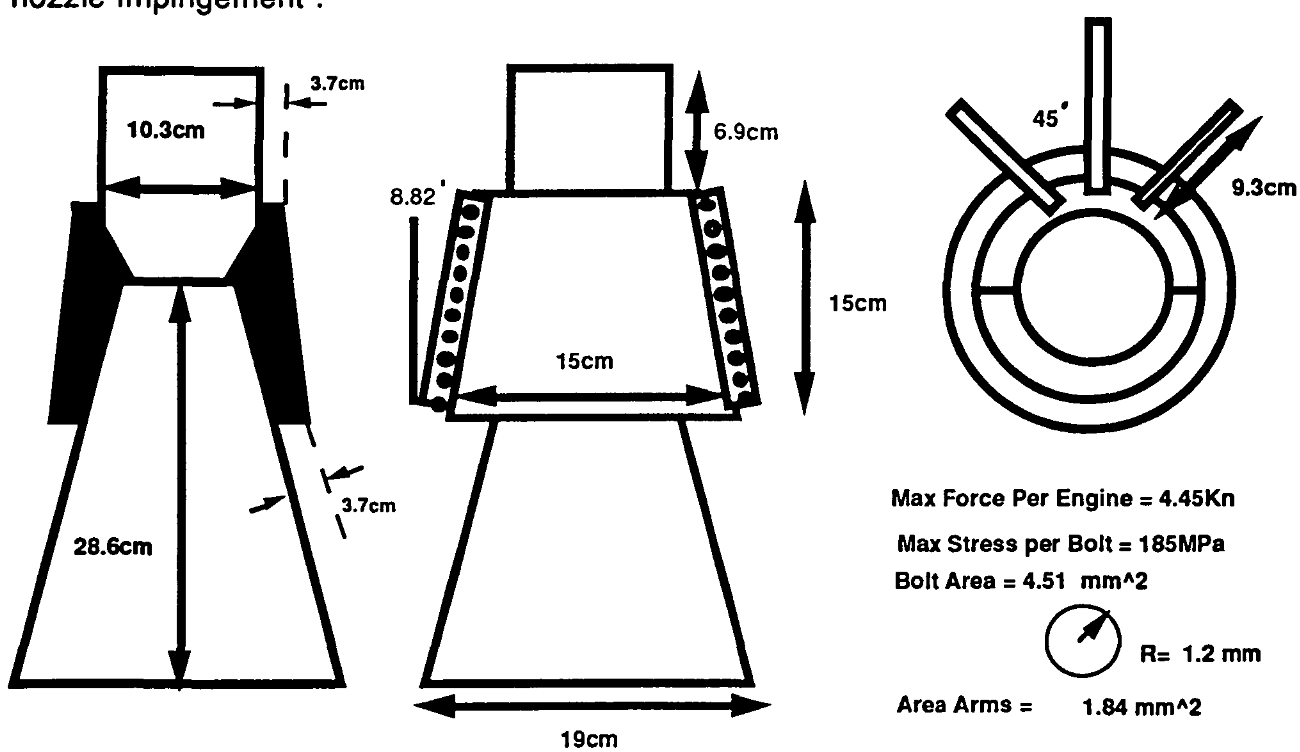

Figure 3.3d: Engine Build-up and Cuffs

Loading and Analysis

When the DART astronauts fire the main engines for re-entry the propulsion package will experience its maximum loading of 17.8KN. During this phase the exact alignment and stability of the engines is a paramount concern. Each member of the truss system has been design to withstand this maximum loading in sheer and tension with a safety factor of 1.2. Once again the maximum stresses were allowed to reach the ultimate stress of 6016-T6 Aluminum multiplied by a 1.2 safety factor, 242MPa. The new cross sectional area was calculated using the same method outlined above. The new area is $1.84mm^2$, using an "I" beam shape with a greater moment of inertia used to counter the pure moment created by the engines as they push to gimbal upwards.

The engine cuffs were assumed to have a primary failure mode laterally, bolt seam failure. From the inner pressure and shear created from the engine forces a study of the bolts and the side of the conic section was conducted. As shown in Figure 3.3d, the bolt stress was found to be 185MPa demanding a cross sectional area of $4.51mm^2$.

Size and volumetric constraints, as discussed, presented the main problems with the design. All the sides of the propulsion package, including the engine nozzles, clear the interface structure and Delta by 5cm limiting the stacking ability, and thus the geometry, of the systems. Figure 3.3e shows the dimensions and launch configuration of the two systems

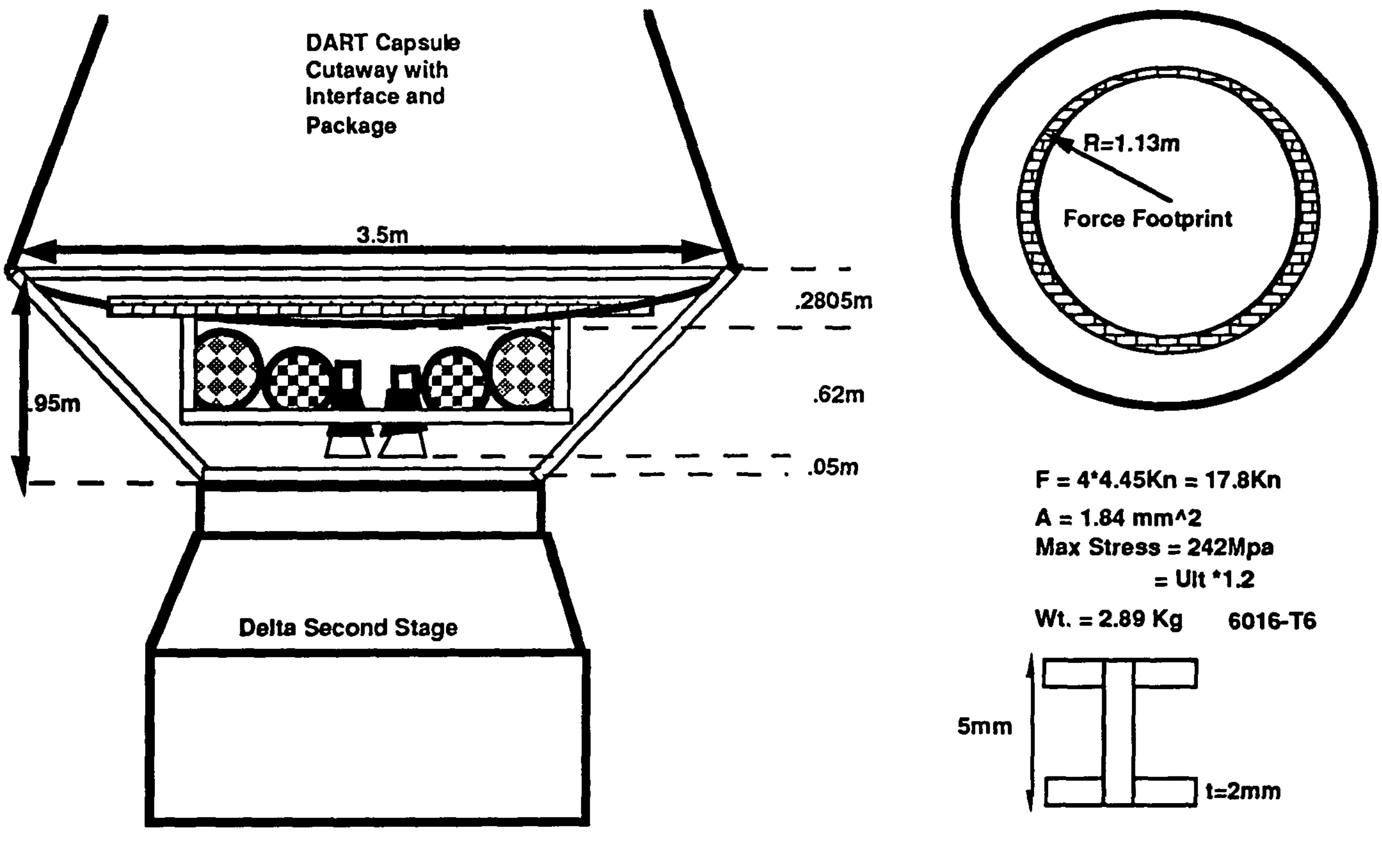

Figure 3.3e: Propulsion and Structural Interface Launch Configurations

Chapter 3 Bibliography

American Cyanamid Company/Aerospace Products, *HIGRID Aluminum Honeycomb*

American Society of Metals, *Fabrication of Composite Materials Source Book, Award of Outstanding* Art. from Technical Literature, American Society of Metals, Metal Park , Ohio, 1985.

ASM International, *Metals Handbook Vol. 2, Properties and Selected Non-Ferrous alloys and Special Purpose Materials*, ASM, 1990.

Bruhn, E. F. *Analysis and Design of Aircraft Structures Vol. 1*, Cincinnati, Ohio, 1958.

Megyesy, Eugene F., *Pressure Vessel Handbook Eight Edition,* Pressure Vessel Handbook, 1973.

Niu, M. C. Y. *Airframe Structural Design*, Commilit Press Ltd., Hong Kong, 1988.

Osgood, Carl. *Spacecraft Structures*, Prentice-Hall Inc, Englewood Cliffs, N.J., 1966.

Watt, W., B.V. Perov, *Book of Composites " Strong Fibres" Vol. 1*, North Holland, Amsterdam, 1985.

Chapter 4

Propulsion and Power

Section 4.1 Main Engine System

Main Engines

Objectives

The objectives for the main engine system of the DART capsule was to design a propulsion system that was reliable, small, light weight and capable of the thrust required for the system's intended use.

Reliability was the primary concern for the main engine system. If the engines were not reliable the mission would be worthless. Since the survivability of the crew had to be 99.9%, the main engine system had to be one that was well tested. This caused the propulsion system to be one that relied on current technology. Coupled with the maximum duration of the DART capsule in orbit, less than a week, the propulsion system called for a high thrust chemical engine system. This type of engine system would then meet the well tested, reliable objective desired for the DART.

Size and weight were also of concern before designing the propulsion system. For the chosen orbit of the DART capsule, 500 km, the Delta booster 7920 could only take 4600 kg. This meant that the propulsion system had to be as light and efficient as possible to keep the weight within reason. Not only does the engine itself need to be light, but it must be efficient to keep the propellant mass low. Also in designing the interface between the DART and the Delta booster the size and shape of the engine was important. The propulsion system had to be constrained within the interface or kept around the craft. This necessitated the need for a low mass, efficient and compact propulsion system.

The third objective for the propulsion system was that it be able to perform all of the missions that it is required. The missions that the main engines must perform are orbital maneuvers, which includes rendezvous, and de-orbit. The most demanding of the missions on the propulsion system was the de-orbit maneuver. The main engine system had to be capable of bringing the capsule back to Earth.

Requirements

The requirements for the DART propulsion system was that it have the thrust required for re-entry. The thrust required was then determined by using the delta V that was required for re-entry and the time that the maneuver needed to be performed. The delta V was found to be 240 m/sec by the mission analysis team and the time for the maneuver was approximated as 1 minute. This approximation was made so that there would be less than 1° of rotation about the Earth for the duration of the re-entry burn. This would then be an impulsive maneuver. With the delta V and the burn time, the thrust required could be determined by finding the deceleration, 4 m/s^2, and then multiplying by the re-entry mass. The thrust required for the re-entry maneuver was found to be 18 kN.

Propellant Selection

The first decision in the propellant selection was to decide which type of chemical engine system to use for DART's main engine system. The choices were either liquid or solid propellants. The choice of liquid propellants was made so that the engine system could have several restarts, which would be very difficult with solid propellants.

The second decision that was made in the choice of propellants was the ignition system. The two choices for ignition were either using an ignition system or using hypergolic propellants, propellants that ignite on contact. The advantage for the ignition system is that a more varied selection for fuel choices can be made. These fuel choices also usually have a higher Isp which provides a greater efficiency. The disadvantage with the ignition system is that there is always a greater chance for error and simply that the system weighs more. With hypergolic propellants, there is almost no chance of failure. The main disadvantage with the hypergolic propellants is that the injection system must be well designed to ensure proper mixing of the propellants. The choice of ignition for this capsule was to use a hypergolic propellant combination because of simplicity of design and its lower weight.

Once the propellants were narrowed down to liquid and hypergolic, the selection was based on which propellant combination would be most compatible and provided the best efficiency for the DART. This was done by examining the properties and characteristics of several propellant combinations which are listed in Table 4.1a. Upon reviewing the properties and characteristics of the propellants, hydrazine and nitrogen tetroxide were chosen to be the propellants for the DART main engine system. The combination was chosen because the ease in storing and the better characteristics made it the best combination for this system.

Propellant Feed Systems

The propellant feed system choice was made by examining the two types of feed systems. The two types of feed systems for liquid propellants are pressure fed and turbopump fed. The turbopump system is a complicated system which provides high pressures for the chamber, in excess of 6 MPa. The high pressures increase the thrust to weight ratios but the DART capsule does not need to have very high thrust. On the other hand, the pressure fed system delivers a lower pressure to the chamber, usually less than 5 MPa. The system also has a minimal amount of moving parts which makes it lighter and less expensive. From the objectives of wanting a reliable and light weight system and the requirements of thrust , the pressure fed system was chosen. A schematic of a pressure fed system is shown in figure 4.1a.

PHYSICAL PROPERTIES OF SOME HYPERGOLIC LIQUID PROPELLANTS

(Shifting Equilibrium)

FUEL	OXIDIZER	MOL. WT.	COMB. TEMP.(K)
Hydrazine	Nitrogen Tetroxide	19	2857
50/50	Nitrogen Tetroxide	23	3194
Hydrazine	Fluorine	19.4	4603
Hydrogen	Fluorine	11.8	3833

FUEL	OXIDIZER	Isp (sec)	c* (m/sec)
Hydrazine	Nitrogen Tetroxide	292	1781
50/50	Nitrogen Tetroxide	288	1745
Hydrazine	Fluorine	363	2208
Hydrogen	Fluorine	410	2550

FUEL	BOILING PT. (K)	OXIDIZER	BOILING PT. (K)
Hydrazine	386.4	Nitrogen Tetroxide	294.3
50/50	360.7	Nitrogen Tetroxide	294.3
Hydrazine	386.4	Fluorine	84.8
Hydrogen	20.4	Fluorine	84.8

FUEL	STORABILITY	OXIDIZER	STORABILITY
Hydrazine	Good	Nitrogen Tetroxide	Good
50/50	Good	Nitrogen Tetroxide	Good
Hydrazine	Good	Fluorine	Fair-Poor
Hydrogen	Fair-Poor	Fluorine	Fair-Poor

Table 4.1a : Propellant Properties

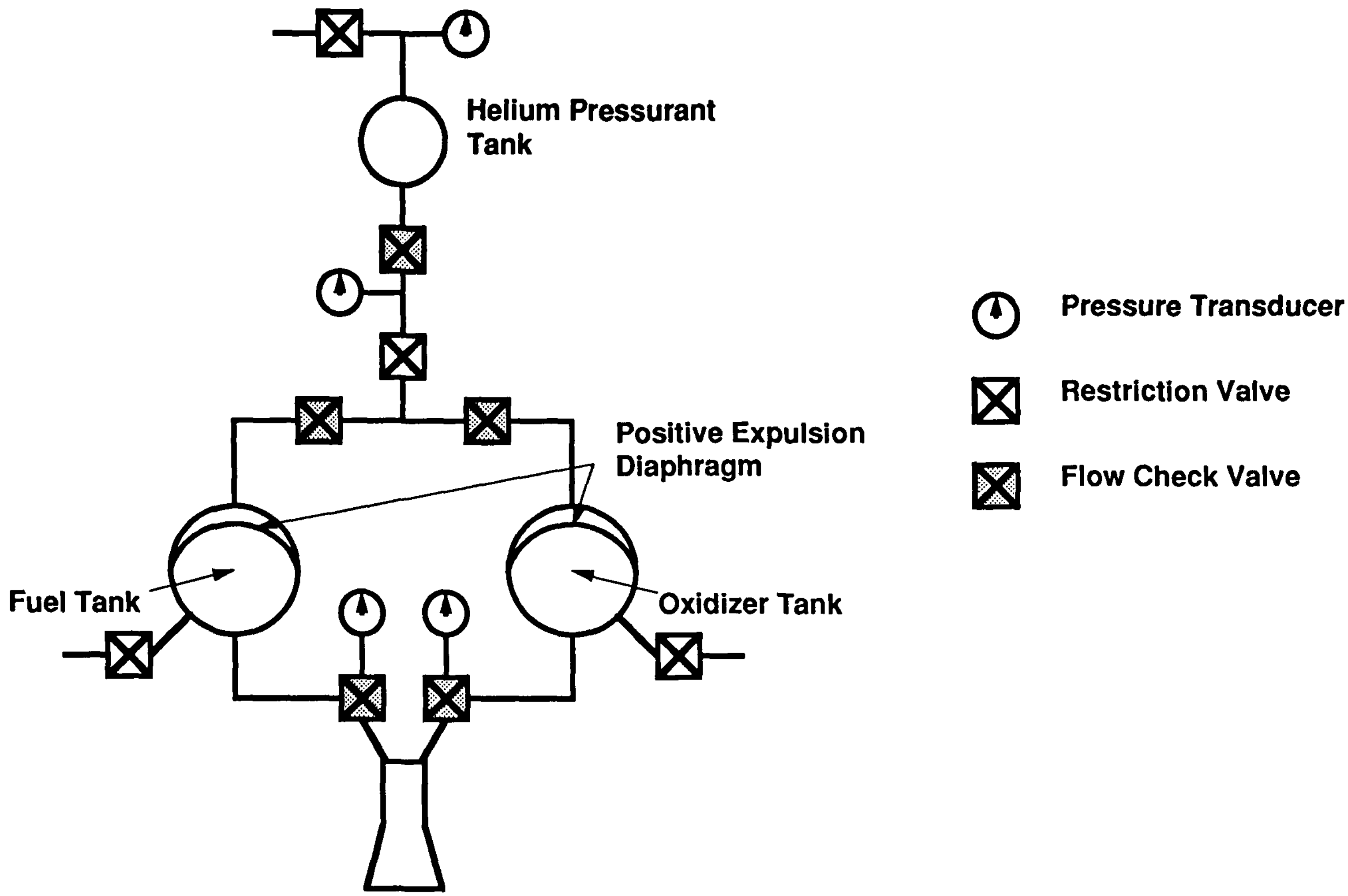

Figure 4.1a : Pressure Feed System

Engine Configurations

The design configuration of the propulsion system for DART has been a teetering point since the beginning. Because of the volume constraints set by the interface, the choice of using four main engines was made instead of using one engine. With four smaller engines, each using one quarter of the total thrust required, the volume that the propulsion system has could more easily be maximized. The four engines also provide a redundancy which would be an increase in reliability over a single engine.

The four engines then will form two individual systems, each pair of engines being fed off of their own separate umbilicals. These individual systems than provide another redundancy. If one system were to fail than the other could be used for an emergency de-orbit.

There have been two configuration of the engines with respect to the DART capsule since the mid-point. The first configuration which is known as the "bolt-on" engine system was eliminated (appendix 4.1.1). The second engine system, known as the "strap-on" engine system, was the system that was chosen for the DART. The "strap-on" package consists of the tanks, propellant and engines and it is stored beneath the DART. The entire system is on the exterior of the DART capsule. This will make the entire propulsion system expendable. The details of the structure of the "strap-on" package have already been discussed. A schematic of the "strap-on" engine system is shown in figure 4.1b.

Chamber Pressure Determination

The chamber pressure is the first step in the physical design of the main engines. The chamber pressure is a function of the geometry of the nozzle as well as a function of the chemistry of the propellants. The chamber pressure can be determined with known values of thrust, ratio of specific heats of the propellants, exit area and exit pressure (appendix 4.1.2). With the ratio of specific heats of the propellants known and the exit pressure set at 6.89 kPa, a close limit to a vacuum, the exit diameter (area) and thrust can be varied to determine the optimum chamber pressure for the DART main engines (figure 4.1c).

The optimum chamber pressure was determined to be 2.41 MPa. This was determined by taking the minimum thrust required and locating the smallest exit diameter. The smallest exit diameter which still provides the minimum thrust was found to be 19 cm. The thrust that was used was 4.45 kN.

Engine Design

The engine design was the combination of all of the material so far. It took the objectives, requirements and choices and combined them to get a working tool. The engine design was done using isentropic flow relations and

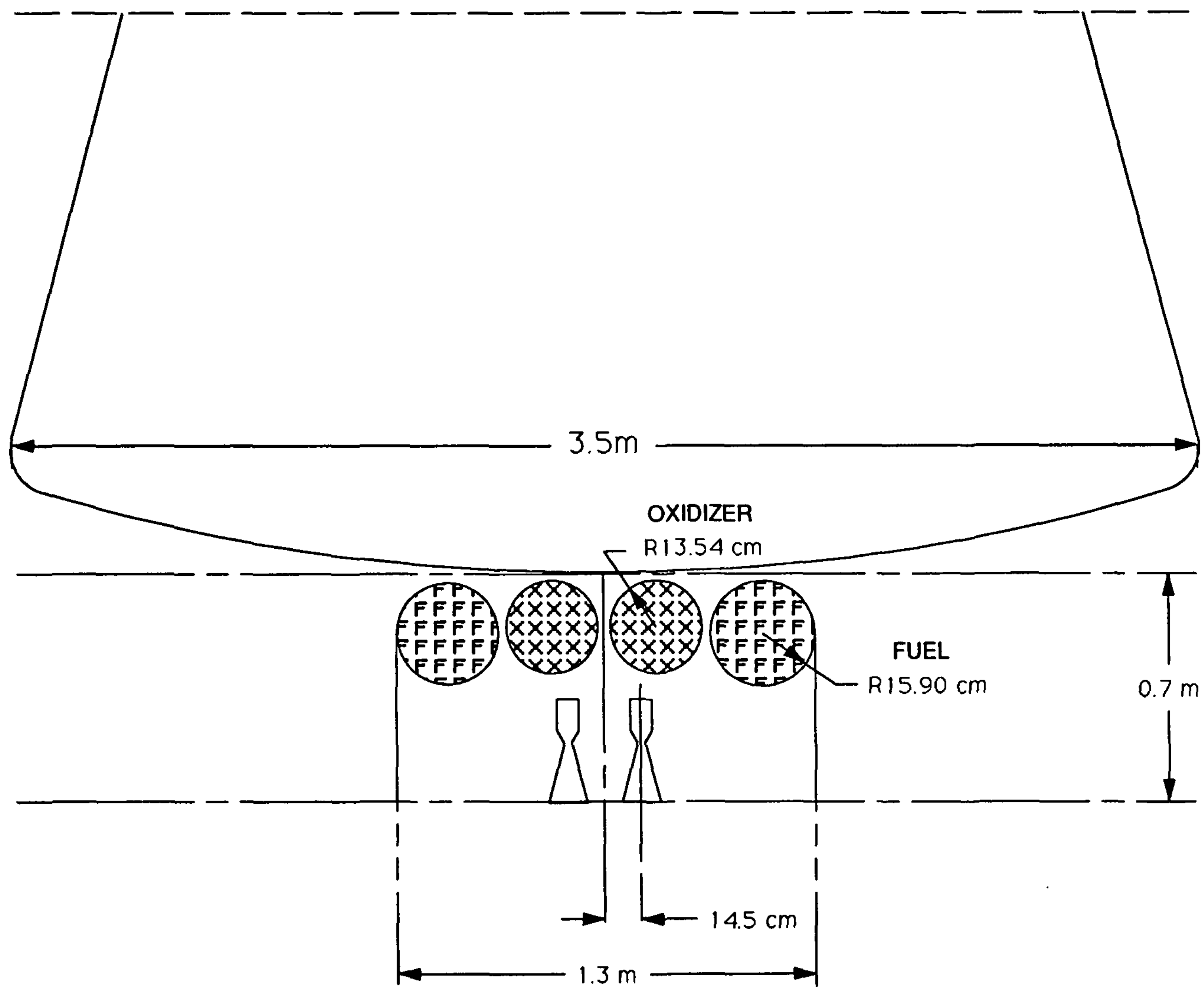

Figure 4.1b : "Strap-on" Engine System

assuming one-dimensional flow. The engine specifications were determined using the code in appendix 4.1.3. The specifications are shown on figure 4.1d.

Part of the engine is the injector. This part is of crucial design because if the propellants do not mix properly the engines might not fire correctly. The injector specifications were performed by using incompressible flow equations for flow through a hydraulic system. The injector specifications are also shown on figure 4.1d.

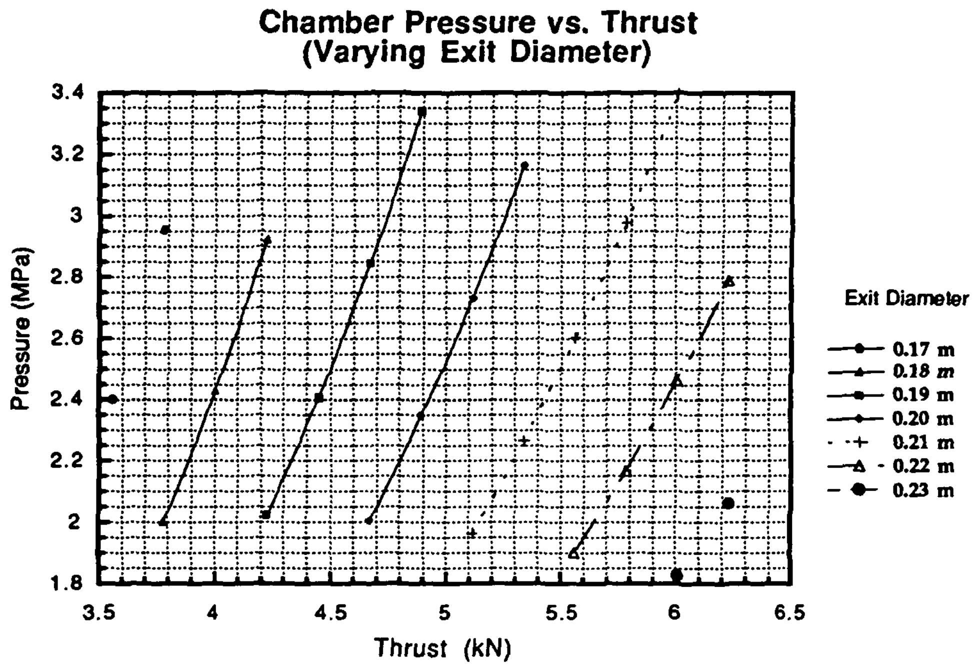

Figure 4.1c : Chamber Pressure Study

Nozzle Design

The design of the nozzle was a decision made between two choices. The choices were either using a bell nozzle or using a conical nozzle. The choice was made by looking at the length, cost and losses that are involved with the nozzles. The length of the conical nozzle found from simple geometry was determined to be 28.6 cm while the length of the bell nozzle was determined to be 43.8 cm. The length of the bell nozzle was found using a method of characteristics program with the same input as the conical nozzle. The cost of the nozzles is also important since the engines are not going to be reusable. The cost of constructing a conical nozzle is much less than the cost of manufacturing a bell nozzle. The main disadvantage of the conical nozzles is that there are more losses than in a bell nozzle. For a conical nozzle with a half- angle of 15°, the radial losses are 1.7% (reference 1). The losses, though, are small, and when the cost and length are compared between the bell and conical nozzles, the conical nozzle was the best choice for the DART propulsion system.

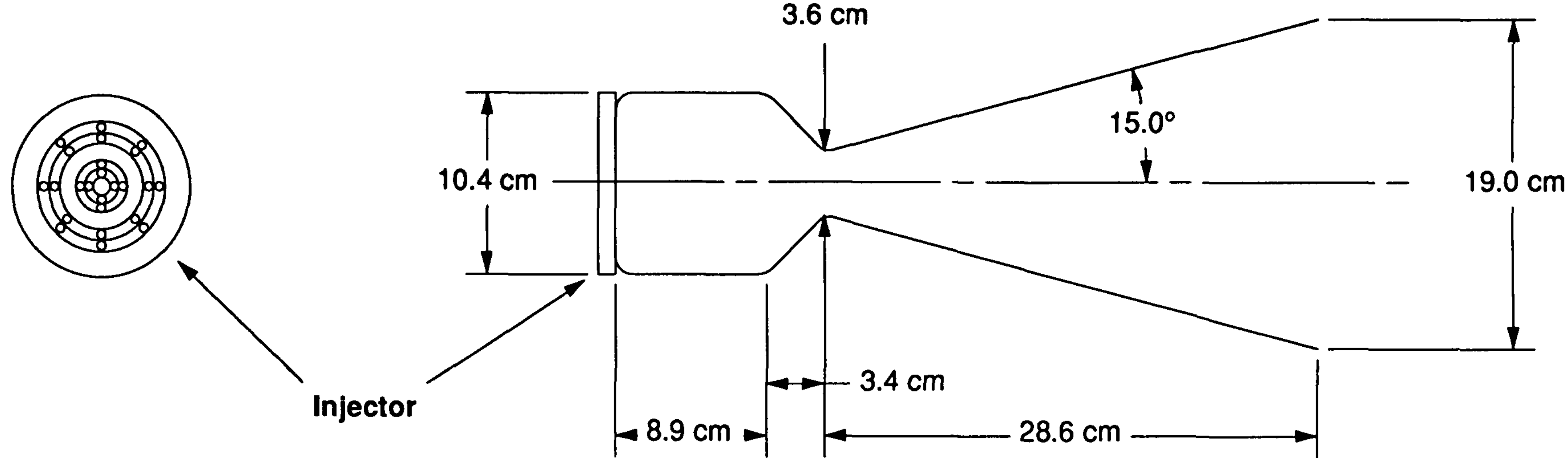

Injector Specifications

Δp = 482.6 kPa
m_{ox} = 0.77 kg/s
m_f = 0.71 kg/s
Q_{ox} = 532.6 cm^3/s
Q_f = 707.8 cm^3/s
u_{ox} = 18.1 m/s
u_f = 22.0 m/s
Θ_{ox} = 46.4°
Θ_f = 40.0°

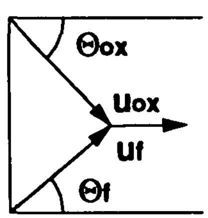

P_1 = 2.41 MPa
T_1 = 2857 K
u_1 = 91.0 m/s

P_t = 1.36 MPa
T_t = 2597.3 K
u_t = 1167.8 m/s

P_e = 6.89 kPa
T_e = 1076.3 K
u_e = 2865.4 m/s

Main Engine Information

Fuel - Hydrazine
Oxidizer - Nitrogen Tetroxide
Average Molecular Wt.-19 kg/mole
C_p/C_v - 1.26

Thrust/Engine - 4.45 kN
Isp - 305.6 sec
Flow Rate - 1.48 kg/s
Nozzle Mass - 28.6 kg
Chamber Mass - 2.3 kg

Figure 4.1d : Main Engine Specifications

Engine Thickness

When the engines are operated, they generate great amounts of heat. If the engine walls are not designed properly they will begin to melt and send particulates into the flow. The proper thickness of the walls were designed by using the equations for heat conduction (reference 2). The assumptions that were made in the heat conduction equations is that the time is equal to the longest burn time of the engines, 83.3 sec, and that the adiabatic wall temperature decreases as the flow exits the nozzle. With those assumptions the thickness of the wall was determined to be 3.7 cm tapering to 1.0 cm at the nozzle exit (appendix 4.1.4). The wall thickness is shown in figure 4.1e.

The material that was used to make the walls into a heat sink was a high grade nickel alloy. With the density known the mass of the nozzle and chamber could be determined (appendix 4.1.5). The mass of the nozzle was found to be 28.6 kg and the mass of the chamber was found to be 2.3 kg (figure4.1d).

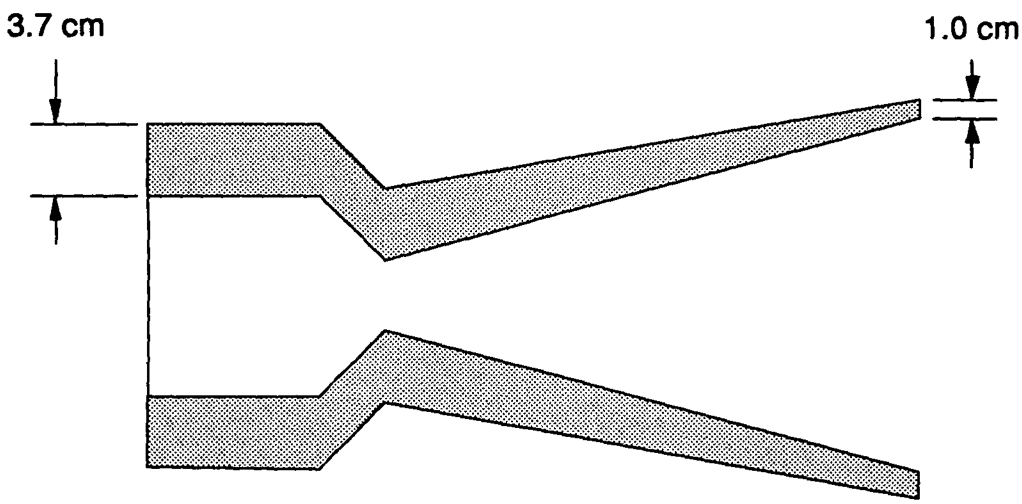

Figure 4.1e : Wall Thickness

Engine Performance

The engine performance of the DART capsule was mainly determined by the specific impulse, Isp of the engine system. The Isp of the of the engine system using hydrazine and nitrogen tetroxide was determined to be 305.6 sec. The Isp was found using the code in appendix A4.1.3 and equations from reference 1. The fuel necessary for the mission were then determined using the rocket equation which simply relates mass and Isp to delta V.

$$\Delta V = g * Isp * \ln(R)$$

where g is Earth's gravity and R is the mass fraction, mass initial per mass final. This equation can simply be manipulated to find the propellant mass required for a known delta V.

$$m_p = m_i * (1 - e^{-(\Delta V/(g*Isp))})$$

A delta V of 340 m/s was determined by the mission analysis team for the main engines. With this information the propellant mass could be determined. The total propellant mass was determined to be 493.3 kg. A code was written to calculate the mass of the propellant for different delta V (appendix A4.1.6).

With the mass of the total propellant, the mass of the fuel and oxidizer could be found. This was calculated using the mass ratio of oxidizer to fuel required for shifting equilibrium of hydrazine and nitrogen tetroxide which is 1.08. The individual propellant masses were determined in the code in appendix A4.1.6. The mass of hydrazine required for a delta V of 340 m/s is 237.2 kg and the mass of the oxidizer is 256.1 kg.

Abort Engines

Abort Hardware Design

The design of the engines has been done by James Clegern of the Taurus L.M.S. design team (appendix A4.1.7). He has modified the abort engines for the Taurus L.M.S. to meet the requirements of the DART. His work has been done using solid rocket motors to provide 8 g's of acceleration to pull the DART capsule away from the Delta booster. The specifications for the abort system are shown in figure 4.1f.

Abort Tower Design

With the design of the abort engines, a code was written to optimize the abort tower height with the angle of the solid rocket motors. The design was to have the flow impinge on the bottom of the capsule. The place where the flow would hit the bottom of the capsule would be protected by the thermal protection system enough to provide a safe means of abort. The tower mass was assumed to be 5 kg/m as specified by the structures team. As the motor angle increased so did the motor mass. An optimum angle of 8° was determined to provide the lowest mass of tower and motor. The total mass was determined to be 779.1 kg and the total height to be 7.7 m. The effective mass seen by the DART and Delta booster is -22.0 kg. This mass is negative to account for the extra mass that was gained when the standard Delta fairing was eliminated. The abort tower is shown in figure 4.1f.

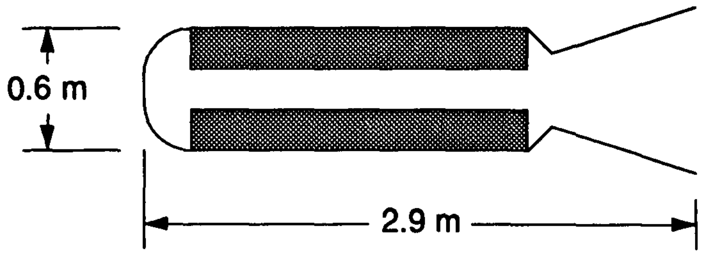

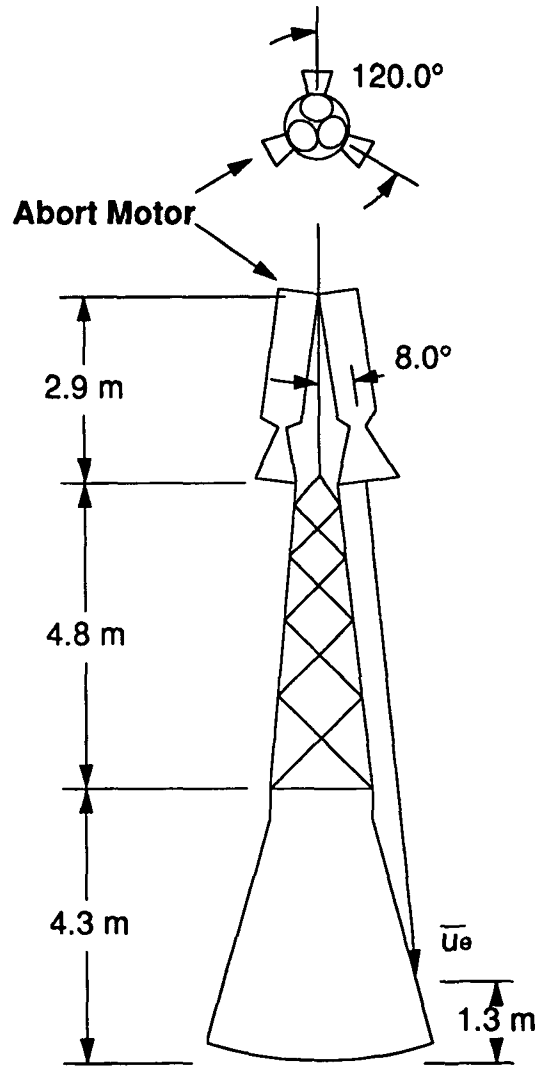

Abort Motor Information

DB/AP-HMX/Al
Process Type - Double Base
Fuel - Aluminum Powder
Oxidizer - Ammonium Perchlorate
- Cyclotetramethylene Tetranitramine
Thrust/Motor - 113.8 kN
Isp - 270 sec
Chamber Pressure - 12.8 MPa
Flame Temperature - 4000 K
Burn Rate - 2.2 cm/s
C_p/C_v - 1.24
Motor Mass - 247.0 kg

(Material Compiled by James Clegern)

Abort Motor Assumptions

Escape Distance - 805 m
Abort time - 5 sec
Atmospheric Pressure

Abort Motor Results

Average Thrust - 341.4 kN
Acceleration - 7.56 gee

Abort Tower

Mass - 38.5 kg

Total Abort System

Mass - 779.1 kg
Effective Mass - (-22.0 kg)

Figure 4.1f : Abort Motor/Tower Specifications

Section 4.2 Propellant Tanks

Introduction

First of all in designing the propellant tanks for the DART vehicle, it was necessary to look at the design constraints of the capsule. Originally it was planned for the propellant tanks to be reusable and on board the vessel with the engines outside.[see Appendix A.4.2.1] This was not feasible due to the lack of room on board. It was then determined to put the tanks and engines in a "strap on" module underneath the bottom of the vessel on the outside.

Figure 4.2.1 shows the bottom of the DART capsule with a generic "strap on" module containing the engines. The propellant tanks to be designed will also be contained the module inside with the engines.

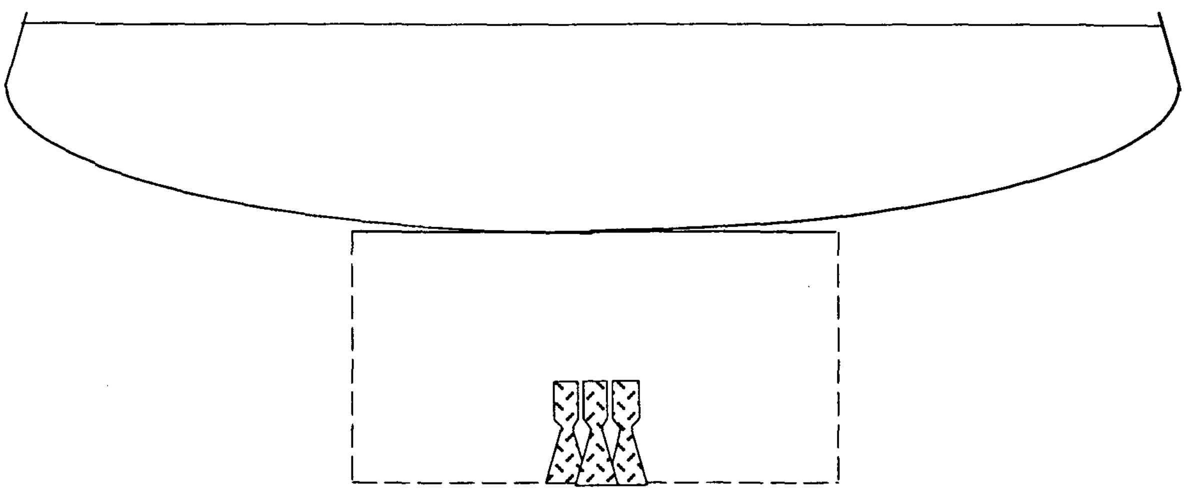

Fig. 4.2.1

Propellant Tank Contents

By looking at the mission requirements, the mission analysis group came up with a ΔV =340 m/s. In turn the propulsion group was able to calculate a required amount of fuel using this and an I_{sp}=305 sec. The required amount of fuel was determined to be 237.2 Kg. The type of fuel to be used on the DART vehicle is Hydrazine. The oxidizer to compliment the fuel is to be Nitrogen Tetroxide. These two propellants combine together in an oxidizer to fuel ratio of 1.08. Thus requiring 256.1 kg. of Nitrogen Tetroxide.

T. Foor

The propellant system is going to be pressure fed, which means the liquid propellants are fed into the combustion chambers of the rocket engines by pressure from stored gases. The fuel and oxidizer tanks must remain a constant 450 psi or 3.10 MPa. The highly pressurized gas to feed the system will be Helium at 4000 psi or 27.58 MPa.

To calculate the amount of 27.58 MPa Helium we will need, it is necessary to assume an isentropic process. This is not a bad assumption considering that charging and emptying the tanks on the mission will be a relatively fast process. Using the isentropic relation

$$\left(\frac{V_1}{V_2}\right)^{\gamma}=\left(\frac{P_2}{P_1}\right) \text{ where g=1.66 for He.}$$

the volume of Helium needed is <u>0.08643 m^3</u>. Since the density of He is r=147 Kg/m^3, the total mass of Helium to drive the system is <u>12.7 Kg</u>.

Number of Propellant Tanks

There are four main booster engines on the DART vehicle. In determining the number of propellant tanks, there is no real in depth analytical method. However, three scenarios will be covered.

The first scenario is where the system will have one set of propellant tanks for all four engines. (A set meaning one fuel, oxidizer, and Helium tank) This is probably not a very good idea due to the fact that the vehicle would experience total loss of booster power if any part of this one system were to fail. Also the tanks would have to be large and therefore heavy.

The second scenario would be a separate set of tanks for each engine. This again is not very conducive because it would mean having 12 tanks on the module along with alot of extra plumbing and this would make the weight somewhat excessive. Also with the increased number of tanks, comes the increased risk of something going wrong. Simplicity seems to work better.

The third and last scenario is having two sets of tanks for all four engines. Six tanks (2 fuel, 2 oxidant, and 2 Helium) would be connected across from one another in parallel, so that in the case of a failure of one set, the other set along with the reaction control motors could safely stabilize the vessel. This seems to be the best way to reduce tank weights and sizes along with having a safe and reliable system.

T. Foor

Propellant Tank Shapes

Propellant tanks are pressure vessels. Both vehicle configuration and tank pressure level will determine the shape of the propellant tanks. For vehicles of relatively large length-to-diameter ratios and of limited space envelopes, cylindrically shaped tanks are used. The ends of cylindrical tanks can have either spherical or ellipsoidal ends. The basic cylindrical tank with spherical ends is lighter than one with ellipsoidal ends.

For relatively high tank pressures and less stringent space conditions, spherical tanks may be employed to best advantage. The lightest pressure vessel for a given volume is a spherical shell, since it has the smallest surface to volume ratio. It also has the smallest shell stress for a given internal pressure.[see ref. 3]

Figure 4.2.2 shows the basic two configurations for each type of tank. These tanks shown are drawn to scale to represent their planform areas accurately. It is also evident to see how the tanks can fit together in the usage of available space.

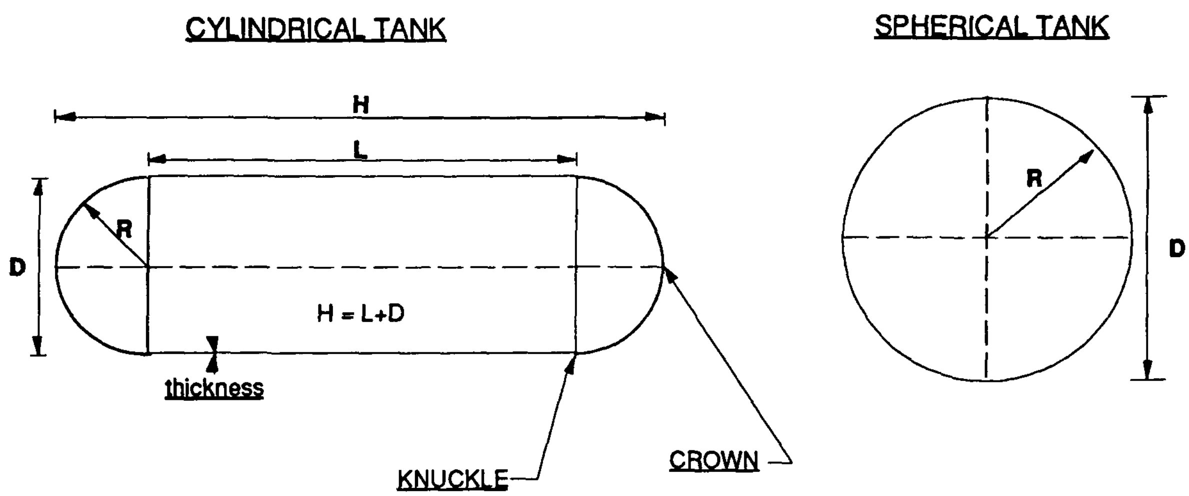

Fig. 4.2.2

For the DART vehicle, the module containing the propellant tanks has a relatively large length-to-diameter, so cylindrical tanks with spherical ends will be used for the fuel and oxidizer tanks. Due to the very high pressure of the Helium tanks, spherical tanks will be used. This is also possible because the Helium tanks will be smaller than the other tanks and pose much less stringent size restrictions on where they are placed.

T. Foor

Material Considerations in Propellant Tank Design

The most important factor in selection of construction materials for propellant tanks is based on on their strength-to-density ratio. For a given working pressure, the lightest tank structure will be the one made of the material with the highest ratio of ultimate strength to density (F_u/ρ). Most common used construction materials for propellant tanks are:

(1) Aluminum alloys, such as 6061-T6, 6066-T6, and 2014-T6. Room temperature properties:

ρ= 0.1 lb/in^3 or 2768 Kg/m^3
F_y= up to 60000 psi or 413.7 MPa
F_u/ρ= 70 x 10^4

(2) Stainless steels, such as AISI 347 (for low pressure tanks only), 17-7 PH, and PH 15-7 Mo .
Room temperature properties:

ρ= 0.285 lb/in^3 or 7889 Kg/m^3
F_y= up to 220,000 psi or 1517 MPa
F_u/ρ= 77.2 x 10^4

(3) Fiber glass, filament wound with an aluminum-alloy liner. Room temperature properties:

ρ= 0.08 lb/in^3 or 2214.4 Kg/m^3
F_y= 120,000 psi or 827.4 MPa
F_u/ρ= 150 x 10^4

It is obvious that the best (F_u/ρ) ratio is for a Fiber glass filament wound tank with an Aluminum-alloy liner. In addition to the ultimate strength to density ratio, consideration must be given to the compatibility of the tank contents to the tankage material. The contents of the tanks, Hydrazine, Nitrogen Tetroxide, and Helium are all compatible with Aluminum-alloy 6061-T6 (see reference 4). Since the material of choice is filament wound fiber glass with Aluminum-alloy liner, the liner should be made of 6061-T6 to avoid conflicts with compatibility. This liner will also be used to separate the fiber glass from the contents, providing a positive sealing barrier. Figure 4.2.3 shows a typical aluminum-lined, fiber-glass filament wound liquid propellant tank.

T. Foor

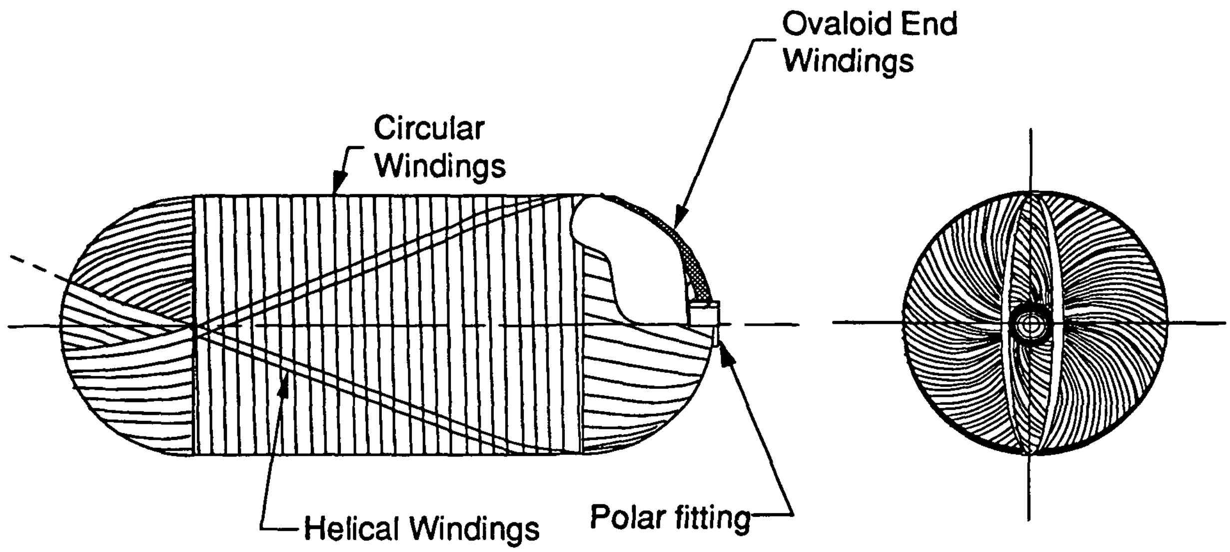

Figure 4.2.3

Good reliability and close dimensional control of filament-wound pressure vessels is assured through the use of calibrated winding machines which orient the reinforcing fibers precisely. Design and fabrication of fiber-glass filament wound tanks with a thin aluminum liner is basically simple. However, a key problem arises from the fact that the modulus of elasticity of fiber-glass resin-bonded materials is about $5x10^6$ psi, while that of aluminum is about $10x10^6$ psi, and that the strength of the aluminum is usually no more than a third of that of the fiber-glass. Since the geometry of the tanks usually imposes equal strain on aluminum liner and fiber glass as the tank is pressurized, the aluminum becomes loaded to its elastic limit long before the fiber glass reaches the level of its high strength capability. Consequently, with a plain liner configuration, the aluminum is stretched far beyond its elastic limit and forced back to its original shape each time the tank is pressure cycled. Thus, the liner may experience fatigue failure after a small number of pressure cycles. The pressure cycle life of a plain liner depends on amount of stretch beyond the elastic limit, type of aluminum, bonding between the lines and fiber glass, weld joints, and variation in thickness and contours, etc. A well designed, plain type tank liner should have a life of about 10 to 20 cycles.

One design approach to extend cycle life is to use a corrugated liner. The corrugations have an effect equivalent to reducing the modulus of elasticity of the aluminum liner to a value less than that of the fiber glass. For instance, if the fiber glass is stressed to 100000 psi and has a modulus of elasticity of $5x10^6$, its extension will be 2 percent. The corrugations of the liner then should be designed to permit the 2 percent extension so that the aluminum will not be stressed beyond its elastic limit.

T. Foor

Propellant Tank Specifications

As already mentioned, the tanks will be cylindrical for the two fuel and two oxidizer tanks, and spherical for the two helium tanks. The following will be an analysis on calculating the sizes of these tanks. Instead of having one correct way to make these calculations, there are many ways. It is possible however to take into account simplicity and overall configuration when making decisions. It is probably a good idea to start with the helium tanks because spheres are more simple than cylinders.

Helium Tanks

The total amount of helium needed is 12.7 Kg. There will be two tanks so that is 6.35 Kg per tank. Using the equation:

ρ=147 Kg/m^3

$$m\rho = \frac{4}{3}\pi r^3$$

The radius r= 0.2177 m

P=max working pressure
r=tank radius
S_w=max. allowable working stress
F_y=yield stress
F_u=ultimate stress (same as F_y for fiber glass)
t= thickness
N_s=safety factors (see ref. 5)

$S_w=F_y / N_s$= 120000 psi / 1.10 = 109091 psi
$S_w=F_u / N_s$= 120000 psi / 1.40 = 85714.4 psi (will use the smaller one)

Thickness

$$t = \frac{Pr}{2S_w}$$ t= 0.0051 m = 5.1 mm

Fiber glass density ρ=2214.4 Kg/m^3
Mass= $M = 4\pi r^2 t\rho$= M = 6.35 Kg. (x2 tanks)= M_{total} = 12.7 Kg.

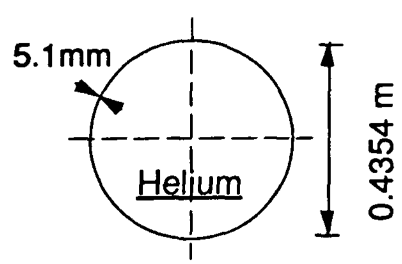

Fig.4.2.4

T.Foor

Fuel Tanks

The total mass of the fuel needed is 237.2 Kg. Which is 118.6 Kg per tank. Using the equation:

$$v = \frac{4}{3}\pi r^3 + \pi r^2 l = m\rho \qquad \rho = 1008.5 \text{ Kg/m}^3$$

For the fuel tank there is a 5:1 ratio on length to diameter. Therefore solving for radius r we find $r = 0.159$ m giving overall parameters of

L = 1.589 m   D = 0.318 m

Calculate the thickness of the fuel tanks. The thickness calculated for the tank pressure is small compared to the thickness needed due to external loads on the tank. Therefore in calculating the thickness it is necessary to use a critical pressure put on the tanks due to the external loading.
P_{crit}=2500 psi

Thickness $t = (P_{crit})\,(r) / S_w$

$t = 0.0046$ m = 4.6 mm

Mass $M = 2\pi r L t \rho$ = M = 16.3 Kg (x2 tanks) = M_{total}= 32.6 Kg.

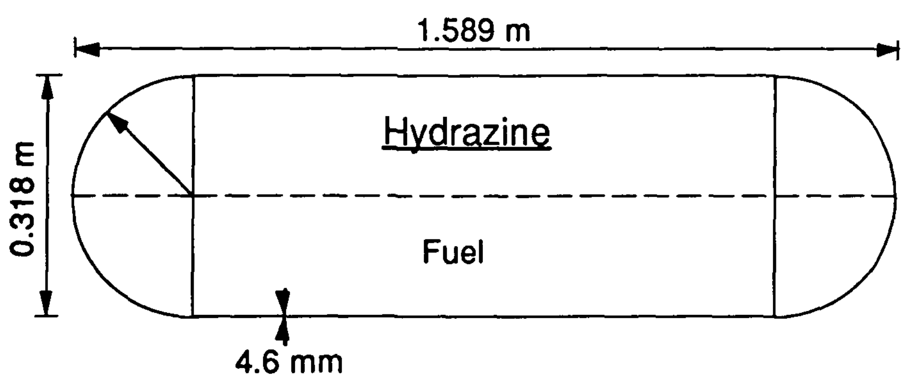

Figure 4.2.5

Oxidizer Tanks

The analysis of the oxidizer tanks is essentially the same for that of the fuel tanks. We use a mass of m=128.05 Kg in each oxidizer tank.
Nitrogen Tetroxide ρ= 1450 Kg/m^3
Results in a tank volume of V=0.0883 m^3

T. Foor

For the oxidizer tank there is a 6:1 ratio on length to diameter

Therefore the radius for this volume is $\underline{r=0.1354\ m}$

Giving overall parameters of:

$\underline{L = 1.624\ m}$ $\underline{D = 0.2707\ m}$

Thickness: (again using Pcrit = 2500 psi)

$\underline{t = 0.00395\ m}$

Mass $M=2\pi rLt\rho=$ $\underline{M = 12.08\ Kg}$.....(x2 tanks) $\underline{M_{total}= 24.16\ Kg}$

Figure 4.2.6 shows an oxidizer tank.

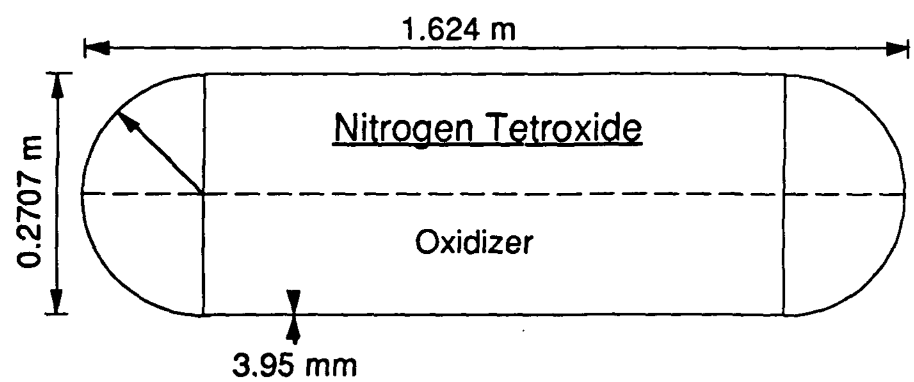

Figure 4.2.6

Layout and Configuration of Tanks

The modules' only design constraints was that it be symmetrical with a low c.g. It was decided to use a square box configuration for optimal support of the interface. Inside the box, the engines are in the center occupying a space of 0.38m x 0.38m By knowing this, the proper ratios were selected (see figure 4.2.7) for the tanks to give the best square symmetrical shape to the module.

T. Foor

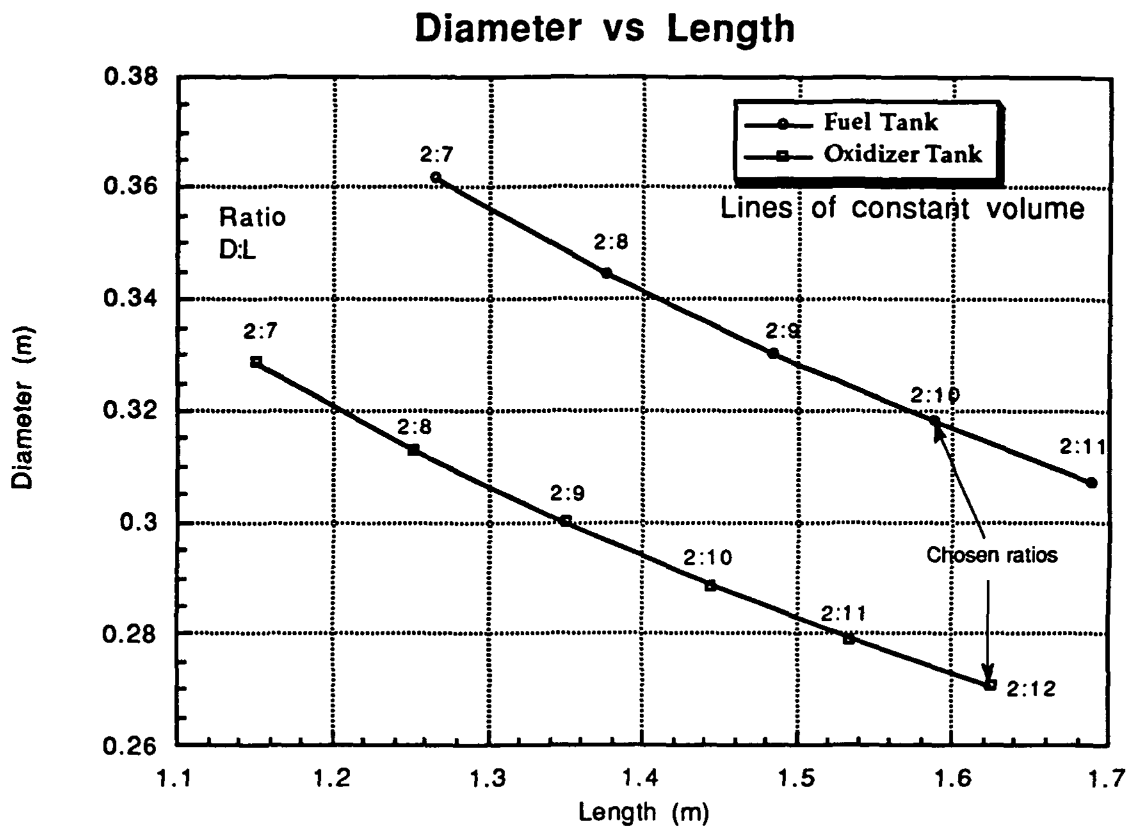

Figure 4.2.7

This resulted in a 1.7m x 1.7m x 0.5m module box containing the engines and propellant tanks. This is somewhat larger than necessary to accommodate adequate plumbing and insulation along with slight expansion of materials in weightlessness. Figure 4.2.8 shows a view of the configured module.

T. Foor

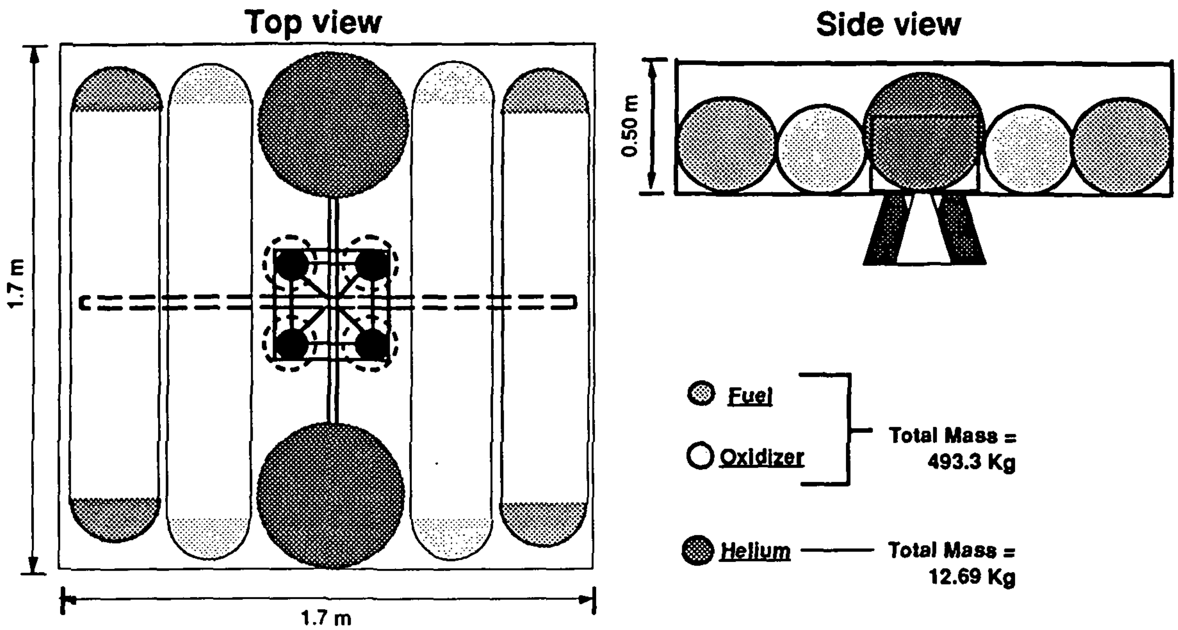

Figure 4.2.8

T. Foor

Section 4.3 Reaction Control System (RCS)

INTRODUCTION

During the spacecraft mission, the DART will experience a variety of forces which will cause it to rotate and/or translate. The purpose a Reaction Control System (RCS) of a spacecraft vehicle is to measure, correct, and counteract the adverse motion (yaw, roll and pitch). Besides responding to forces and moments, the RCS of a spacecraft will maneuver the vehicle in the following activities: altitude control, position keeping, and re-entry.

Forces that will cause the spacecraft to rotate or translate can be categorized as short-term or long-term. The daily or orbital period oscillating forces are called *diurnal* and the long periods are called *secular.* For a medium altitude mission profile (500 to 3500 km), the vehicle will experience perturbations due to the earth oblateness. Since the earth bulges in the vicinity of the equator, the cross section through the pole is not circular. Depending on the inclination of the orbit plane to the equator and the altitude of the orbit, the spacecraft will experience two kinds of perturbation. The are as follows: the regression of the nodes (Figure 1) and shifting of the apsides line (major axis, Figure 2). Regression of the nodes is an effect which cause the vehicle to change its angle plane of orbit. The plane of the orbit can change as much as 9 degrees per day . However, regression theoretically does not occur in equatorial orbits and therefore is dependent on the orbit. Figure 1 show an exaggerated shift of the apsidal line with the center of the earth remaining the focus point (Sutton,1986.). This perturbation may be visualized as the movement of the predetermined elliptical orbit. The change in apogee and perigee position is a function of the vehicle altitude and plane of inclination.

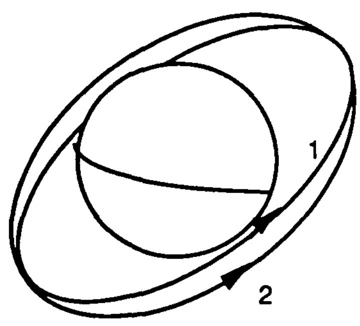

Figure 1. Regression

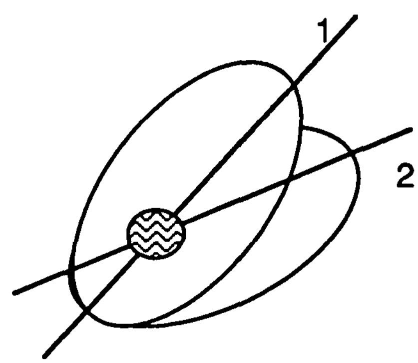

Figure 2. Apsidal Shifting

Khanh Q. Le

There are other forces that the spacecraft will experience throughout its mission. The principal forces are as follows: solar radiation, aerodynamic drag, and internal acceleration. Solar radiation is not significant factor at altitude less than 800 km and will not be considered. Aerodynamic drag is only significant for orbits below 500 km, and internal acceleration will occur in deployment of solar array panels, the shifting of propellant , movement of the astronauts or other mass within the spacecraft.

Other needs for a RCS on a spacecraft are for attitude control, stationkeeping, repositioning, and re-entry.

With the above requirements in mind, the RCS will be analyzed by the following criteria. It must meet the vehicle operational requirements in weight and size, thrust level and duration, space available, and reliability.

THRUSTER SYSTEM

The simplest and most common means of pressurizing the propellant is to force them out of their respective tanks by displacing them with high-pressure gas. This gas is fed into the propellant tanks at a controlled pressure, thereby giving a controlled propellant discharge.

For low thrust and/or short duration, such as for space vehicle attitude control, a feed system of this type is preferred. Although the propellant tanks in a gas-pressure feed systems have to be heavy to withstand the high internal pressure, the overall system weight is lower than that of a turbo pump system (Sutton, 1986). Because of their relative simplicity, the rocket engines with pressured feed systems can be reliable. A typical pressured-fed liquid propellant rocket engine is schematically shown in Figure 3.

It consists high-pressure gas tanks, gas shutoff and starting valves, pressure regulators, propellant tanks, propellant valves, and feed lines. Additional components, such as filling and draining provisions, check valves, filters, flexible elastic bladders for separating the liquid from the pressurizing gas, and pressure sensors or gages. For more details refer to Section 4.2 of this report.

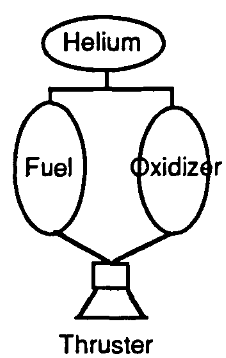

Figure 3. Propulsion System

By using $C^* = PoA^* / \dot{M}$, $Ct = T / PoA^*$, and data given by "a past to build on", by Rockwell International, thrust, weight, chamber pressure and Ae/A^* for each thruster were determined. Refer to Table 1 for thruster data.

Table 1. Thruster Data

Section	Thrust (N)	Mass (kg)	Po (MPa)	Ae/A*	Dimension (cm)
A-A Vernier	100.0	1.090	0.917	20:1	21.7 long/6.4 wide
B-B	351.0	2.260	0.945	40:1	58.3 long/8.2 wide
B-B Vernier	42.0	0.634	0.937	20:1	18.0 long/7.4 wide

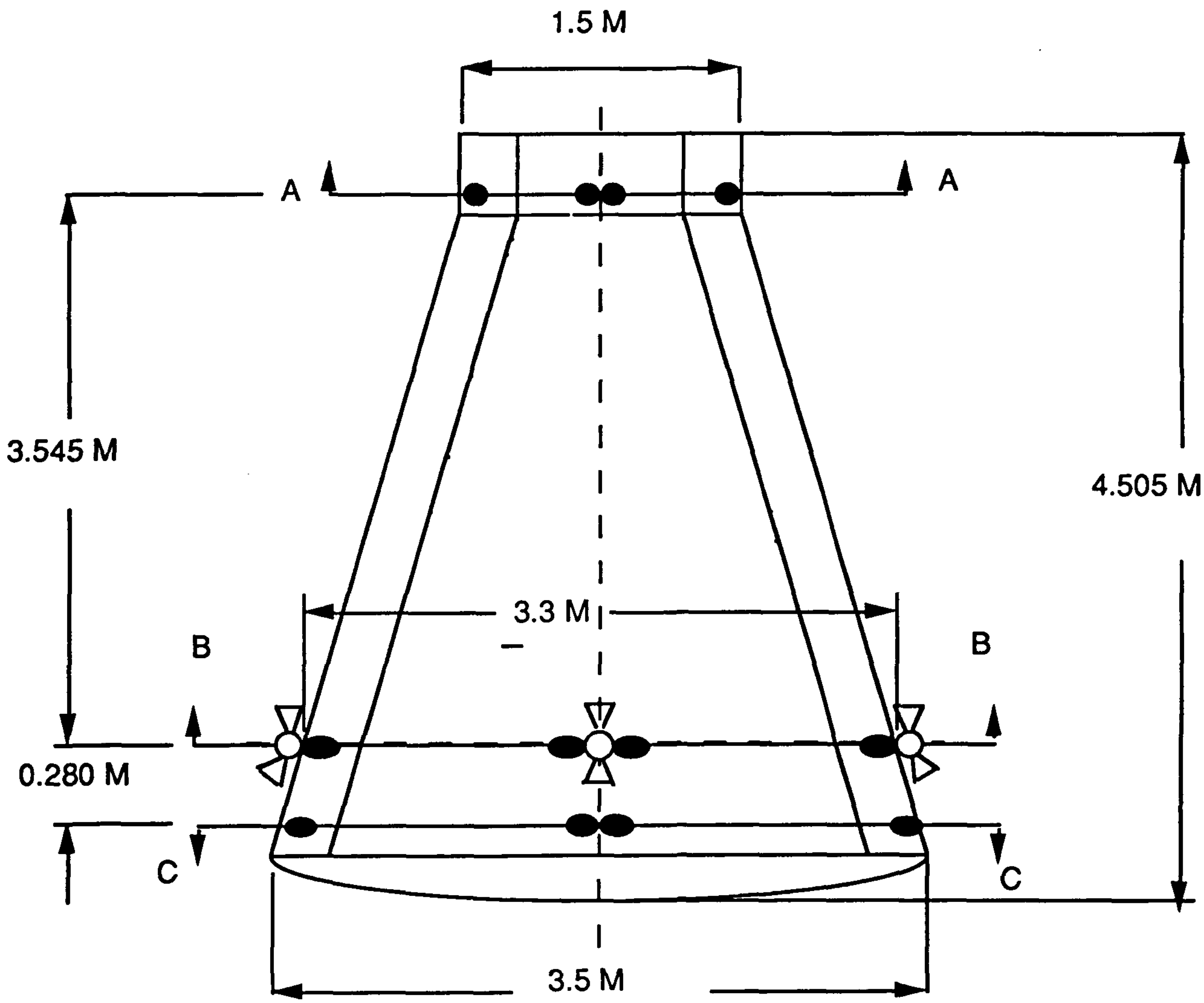

Figure 4. Thruster Location

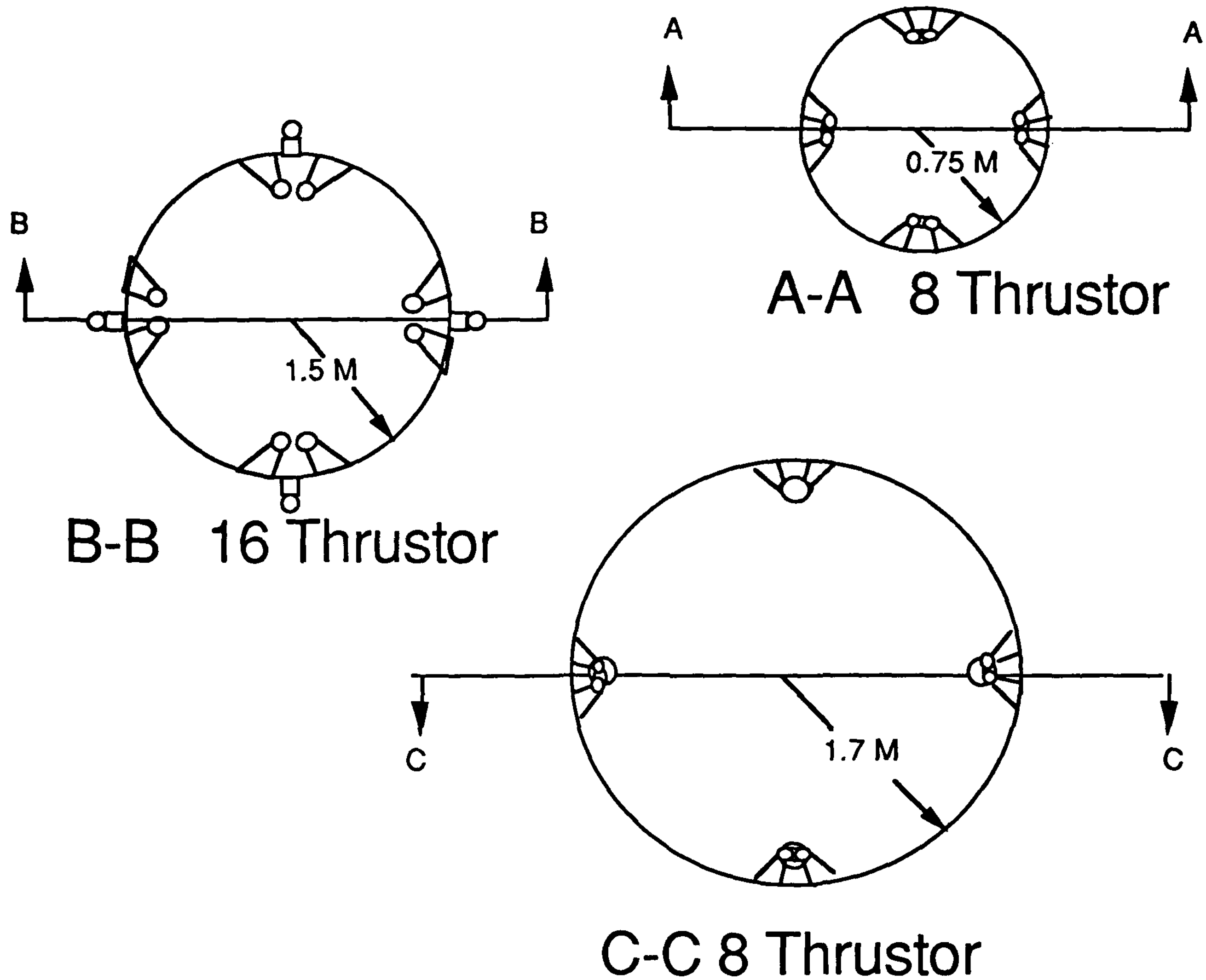

Figure 5. Thruster Cross Section

SPACECRAFT DYNAMICS

The moment of inertia was determined to calculate the maximum rotational angular velocity. From this a RCS thrust was calculated to adequately counteract the angular moments about all major axis.

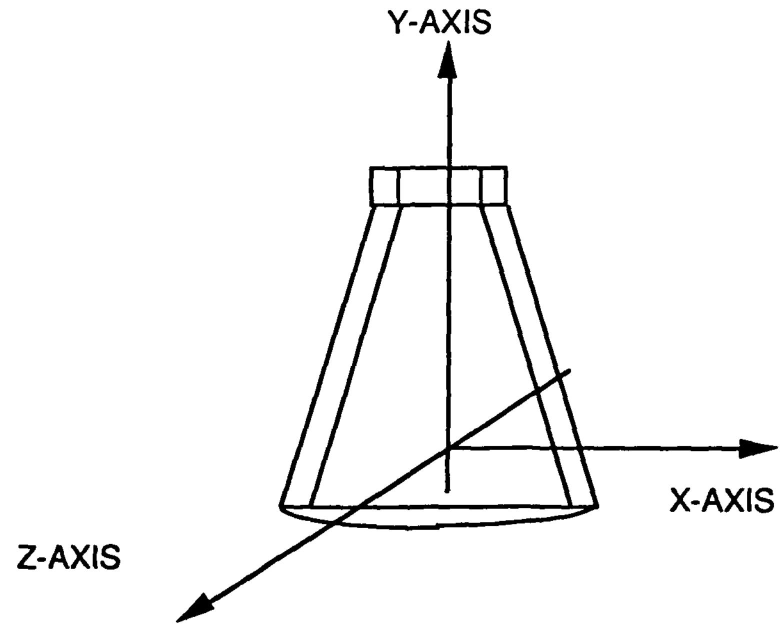

$I_{YY} = Ixx = 1687.4$ KgM^2
$Izz = 687.1$ KgM^2

If the forces which causes rotation are external, the moment of the spacecraft can be calculated by taking the angular momentum and dividing it by a time derivative. The equation used was:

$$M=[h / dt] + W \times h$$

where: $h = (IxxWx-IxyWy-IxzWz)i+ (IyyWy-IyzWz-IxyWx)j+(IzzWz-IxyWx-IyzWy)k$

Angular Velocity

The angular velocity of a spacecraft is dependent upon the total impulse $I(total)= \int Fdt = M(u_2-u_1)$. Assuming that the initial velocity is zero, the final velocity is $u2 = \int Fdt / M$. This is true if the mass expelled out of the thruster nozzle is assumed to be negligible . For each axis, a pair of thrusters are coupled to produce the angular velocity $W = u / r$ where u is the final velocity and r is the location of the thruster. The external moments are related to the the angular velocity by Torque = W*I, where I is the moment of inertia about a given axis.

PROPELLANT SELECTION

In choosing a propellant, criteria such as economics, performance, hazards, and physical properties have to be meet. The economics of a good fuel are in the availability and costs. If the production process is simple and the raw materials required are easily obtain, then the fuel is economical. Listed below are studies on performances, hazards, and physical properties of propellants.

Table 1. Performance

Oxidizer	Fuel	Specific Impulse(Isp) sec
Oxygen	Hydrazine	301
	Hydrogen	388
	UDMH	295
Fluorine	Hydrazine	334
	Hydrogen	398
Nitrogen Tetroxide	Hydrazine 50% UDMH-50% Hydrazine	278

Table 2. Hazards

Characteristics	Fuel	Oxidizer
Explosive	Nitromethane	Hydrogen Peroxide
	Hydrogen	
Fire		Nitric Acid
		Nitrogen Tetroxide
		Hydrogen Peroxide
Toxicity	Hydrazine*	Fluorine
		Nitric Acid
Corrosive	Hydrazine*	Fluorine
		Nitric Acid

* Includes all forms of hydrazine.

Table 3. Physical Properties

	Monomethylhydrazine	Nitrogen Tetroxide
Molecular Mass	46.08	92.016
Melting Point	220.7 K	261.5 K
Specific Gravity	0.8788 g/cm^3	1.447 g/cm^3
Vapor Pressure	0.0069 Pa	0.00689 Pa
	Fluorine	**Oxygen**
Molecular Mass	38.0	32.0
Melting Point	53.7 K	54.4 K
Specific Gravity	1.66 g/cm^3	1.26 g/cm^3
Vapor Pressure	0.158 Pa	0.0052 Pa

Table 4. Overall Benefits

	Fuel	Oxidizer
Stability	Hydrazine*	Oxygen
		Nitrogen Tetroxide
Specific Density	Hydrazine*	Nitrogen Tetroxide
Freezing point	fluorine	Nitrogen Tetroxide
Boiling point	Hydrazine	Nitrogen Tetroxide

From the equation Ue=sqrt((2*ψR / (ψ-1)M))To[1-(Pe/Po)$^{(\psi-1)/\psi}$], high performance thruster should have high energy context of chemical energy per unit of propellant mixture is desirable because it permits a high chamber temperature . A low molecular mass of the product gases of the propellant combination is also desirable.

Overall, hydrazine is the best fuel and nitrogen tetroxide is the best oxidizer. The combustion of hydrazine and nitrogen tetroxide produces a chamber temperature of 2857° K. Both hydrazine and nitrogen tetroxide were chosen for the reaction control system because they are storable at a room temperature of 288 ° K. Hydrazine and nitrogen tetroxide are relatively dense and therefore reduce propellant tank mass. Refer to section 4.2 of this report for further details.

Propellant Mass

The propellant mass was determine by the mission profile of 24 hours. Therefore a worse case scenario of 3 hours continuous impulse was determined to be 10,800.0 sec. But the thrusters will be fire at 24 second interval with pulse time of one second. Since two thrusters will be burning at any one time, the total impulse is reduced to 225.0 seconds for each thruster cluster. From the equation thrust = mass flow * Ue, the mass of propellant required for this mission is 274.058 kg. The total impulse of the RCS is 754,240.0 N-Sec. This value is reasonable when compare to the Gemini Program (Figure 6).

REACTION CONTROL SYSTEM TOTAL IMPULSE

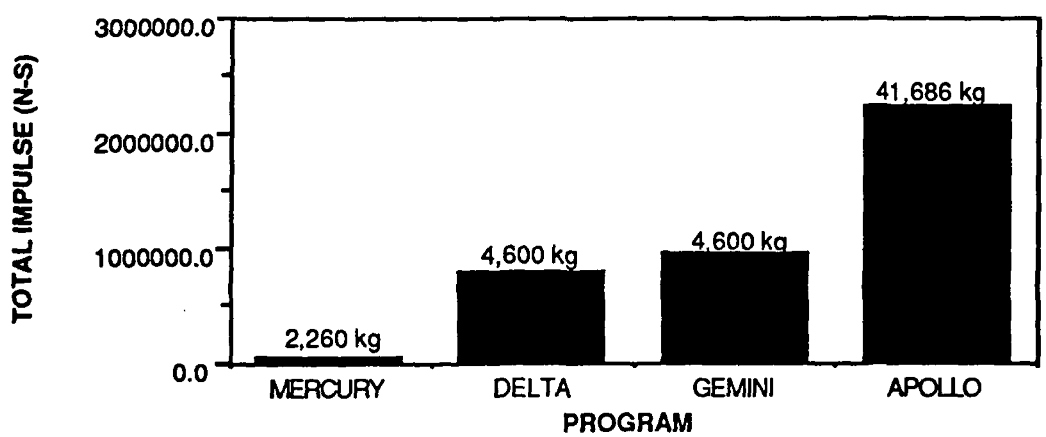

Figure 6. Total Impulse

The mass of fuel is divided into two subsystems. They are as follows: the Orbit Attitude Manuevering System (OAMS) and the Re-entry Control System (ReCS). The OAMS is used for attitude control, stationkeeping, docking, and EVA while the ReCS is for re-entry and attitude control.

Since the mission profile calls for three docking attempts at Δv=6.0 m/sec, the propellant mass required for this maneuver is 45.0 kg. The regress from docking at Δv=6.0 m/sec requires 15.0 kg of propellant. To guarantee a safe re-entry, 15.16 kg of propellant with a burn time off 400 seconds is kept in reserve for that purpose. This leaves 198.89 kg for reaction control, EVA and other mission that will be determined at the beginning of each launch.

Hydrazine Mass	92.980 kg
Nitrogen Tetroxide Mass	150.468 kg
Helium Mass	30.620 kg

Tank Shape

Propellant tanks are pressure vessels. Disregarding other factors, the lightest pressure vessel for a given volume is a spherical shell, since it has the smallest surface to volume ratio.

Tanks Working Loads

Designing the tanks required the knowledge of the working loads. The working loads are as follows:

1. Internal pressure loads and their dynamic effects
2. Bending moments due to vehicle transverse acceleration
3. Aerodynamic forces
4. Vibration loads
5. Loads produced by mounting arrangement
6. Loads caused by thermal transients and gradients
7. Loads produced during ground handling

Safety Factors for Propellant Tank Designs

This data is taken from NASA standard (Huzel,1971). Therefore when calculating allowable working stresses from tank internal pressure, the following correlations are recommended for various situations:

1. No hazard to personnel or vital equipment:

   Sw=Fy

   or

   Sw=Fu/1.25

2. Special safety devices are provided for personnel

   Sw=Fy/1.1

   or

   Sw=Fu/1.35

Tank Pressure

It has been demonstrated that the thrust / weight of the thrusters increases with increasing chamber pressure, refer to section 4.1. But by increasing the chamber pressure, the mass of the tanks and thrust chambers will also increase. Therefore an optimal thruster chamber pressures of 0.917 to 0.945 megapascal were determined using data from section 4.1 of this report and from Sutton's Rocket Propulsion Elements textbook. These chamber pressures correspond to the many existing attitude control thrusters. By using the chamber pressures as a driving factor, the pressures of the tanks were determined. The fuel and oxidizer tanks were chosen to be 1.034 megapascal. This was chosen because the pressure lost between the propellant tanks and the thruster chambers were ranges from 15-30 % (Huzel, 1971). The pressure lost are due to the viscous effects along the plumbing and the pressure drops along the control valves and regulators. The oxidizer and fuel tanks are kept at these pressures by using pressurized helium gas tanks. The helium gas tanks are most efficient at pressures between 10.342 to 34.474 megapascals (Huzel, 1971), but for pressures between 10.342 to 34.474 megapascals, the tank exceed the weight criteria. A pressure of 10.0 megapascal was chosen for the helium tanks because the reduction in tank volumes.

Tank Mass

The tank mass is dependent upon materials used and on the tank pressures. Several materials were examined to determined the best overall characteristics for use as propellant tanks. The materials examined are aluminum 6066-T6, composite fiber line with aluminum, and Ti-6Al-4V ELI. The results are listed below in Table 4 to Table 5.

Table 4. Tank Mass ReCS

	Al 6066-T6 Mass	**Composite-line Al Mass**	**Ti-6 Al-4V ELI Mass**
Oxidizer	4.102 kg	1.612 kg	2.897 kg
Fuel	7.343 kg	2.885 kg	5.187 kg
Helium	15.519 kg	6.740 kg	12.037 kg

Table 5. Tank Mass OAMS

	Al 6066-T6 Mass	**Composite-line Al Mass**	**Ti-6 Al-4V ELI Mass**
Oxidizer	62.660 kg	25.945 kg	43.450 kg
Fuel	109.510 kg	31.392 kg	60.392 kg
Helium	206.911 kg	107.658 kg	192.720 kg

Since Nitrogen tetroxide is very corrosive and explosive, the tank material chosen is Ti-6 Al-4V ELI. The helium and fuel tanks will be made of composites-line Al. Figure 7 and Figure 8 shows were the tank are located.

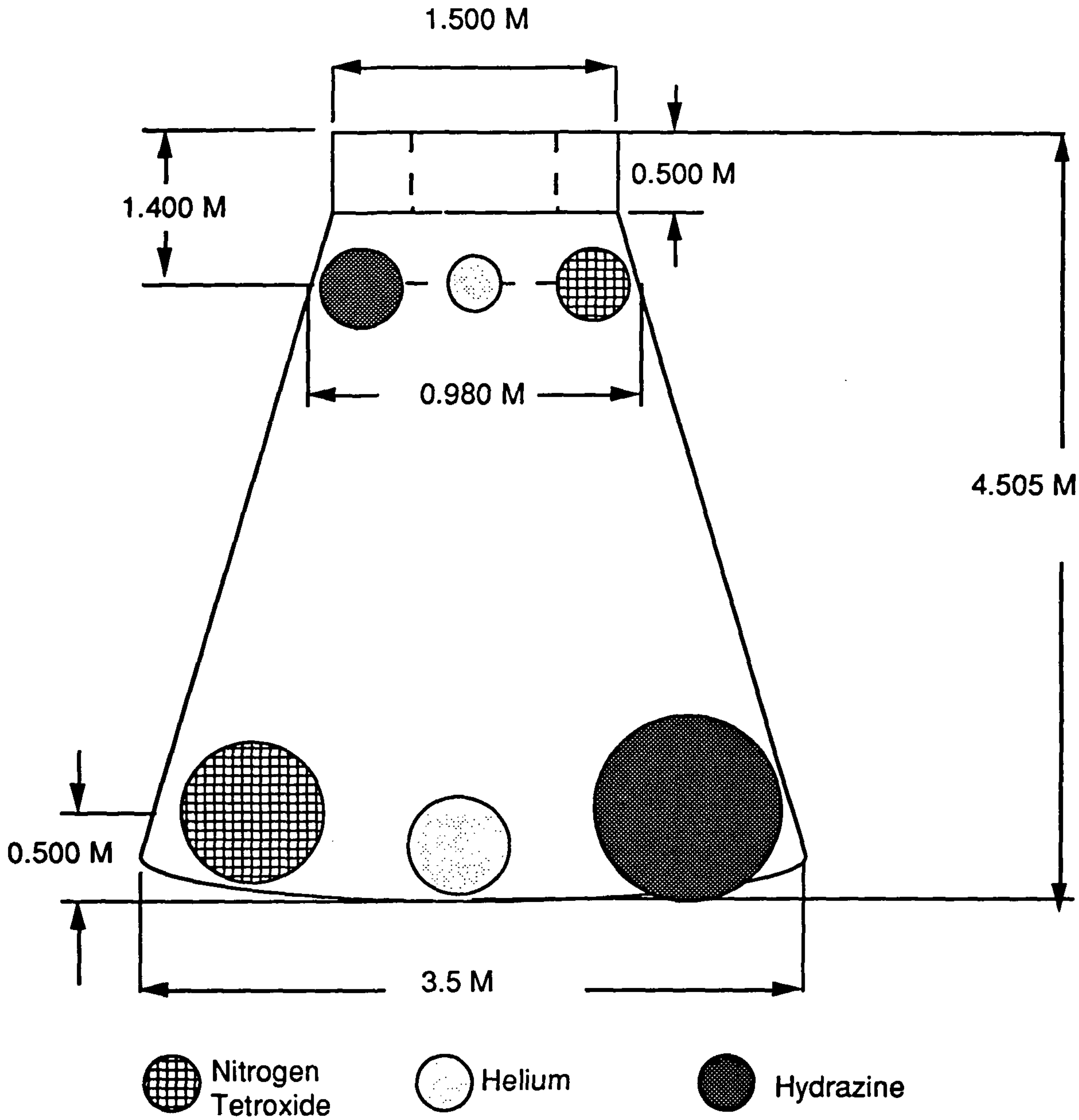

Figure 7. Tanks Location

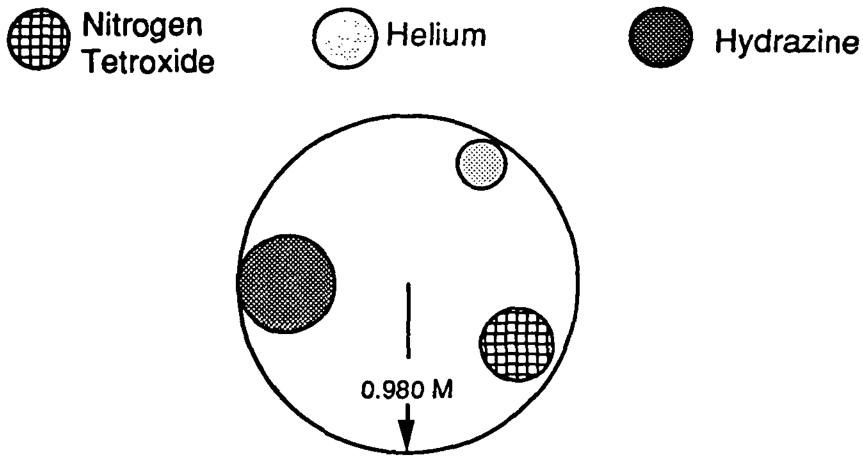

ReCS	Thickness	Radius	Mass
Hydrazine	0.048 CM	0.383 M	2.885 Kg
Nitrogen Tetroxide	0.040 CM	0.383 M	1.612 Kg
Helium	0.290 CM	0.289 M	6.740 Kg

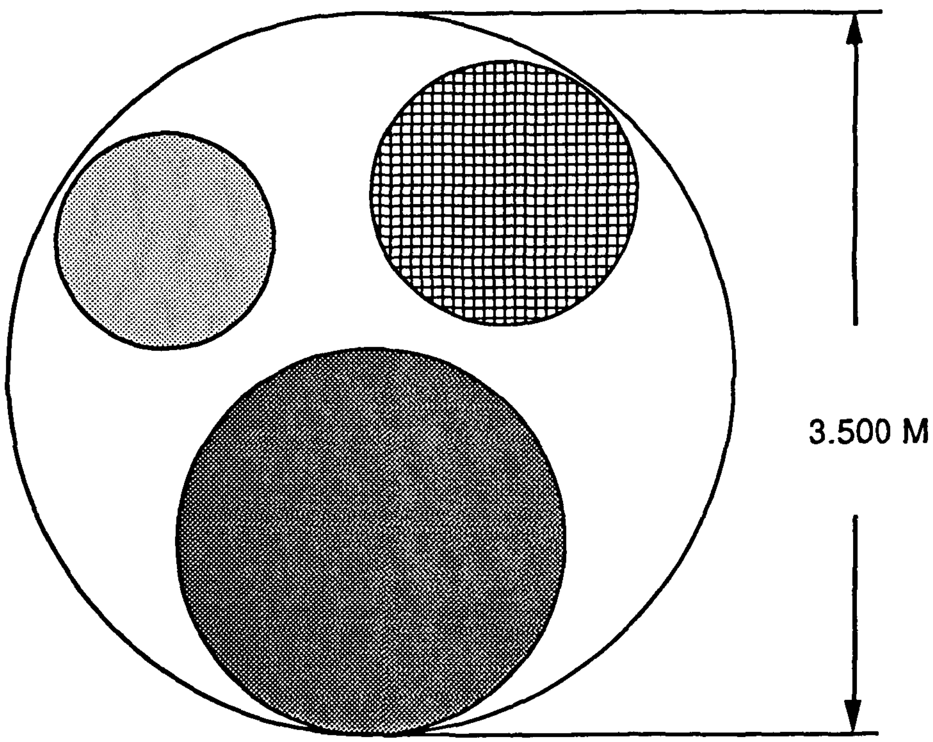

ReCS	Thickness	Radius	Mass
Hydrazine	0.121 CM	1.170 M	31.392 Kg
Nitrogen Tetroxide	0.100 CM	0.967 M	25.945 Kg
Helium	0.700 CM	0.728 M	107.658 Kg

Figure 8. Tank Cross Sectional View

SUMMARY

Studies which will need more attention are as follows: the tank radius and the plumbing system. The radius of these tanks are to large, but if the radius is decreased, two trade-offs can be made. First, the temperature of the tanks can be decreased, but this will require installation of the tanks and will increase tank volume. The second is increasing tank pressure, but if tank pressure is increased, the mass of the tanks will exceed the mass of the fuel. The plumbing system was considered in section 4.2.

Section 4.4: Power Generation Systems

Introduction:

The power generation system is the most important system in a spacecraft. It is responsible for providing the electrical power necessary to keep the spacecraft working smoothly. Without this system the spacecraft wouldn't be able to get off the ground; for this reason the electrical power system must be very reliable. The electrical power system is composed of two subsystems: Primary power supply and secondary power supply.

The mission requirements and the configuration of the spacecraft are the main elements to be considered when designing an electrical power system. There are many sources that can provide electrical power to a spacecraft. Some of these sources are nuclear, chemical, and solar. The following table shows the advantages and disadvantages of these sources.

Source	Type	Pros	Cons
Nuclear	Reactors	Reliable	Shielding is needed
Solar	Solar Cells	Usefull in long missions	Low efficiencies
Chemical	Batteries Fuel Cells	Reliable Compact	Additional power supply needed Radiators needed

Table 4.4.a: Energy Sources

Solar Energy

The sun is the most reliable source of energy available, its radiation can be used to generate the power needed to maintain a spacecraft working. The sun produces 1.35 Kw / m^2 of power in space. This power is collected and converted to electricity by solar cells. Solar cells are made of different materials but the most common are silicon, gallium, and cadium cells. Inside the cells a photovoltaic effect takes place, converting the solar radiation into useful electrical power. These cells are approximately 0.02 X 0.02 m and produce 75 to 84 mW of power. These cells have low efficiencies, approximately, 10 to 15 %. To achieve high power demands, large arrays of solar cells are needed.

Edison W. Villacís.

Chemical Energy

Rechargeable batteries are the most common source of electrical power. Electricity is generated as result of a chemical reaction. There is a wide variety of rechargeable batteries, each with its own application in space. Batteries are characterized by their energy density, weight, and life expectancy. The most used and reliable batteries in a spacecraft are: Nickel-Cadium (Ni-Cd), Nickel-Hydrogen (Ni-H2), Lithium-Hydried (Li-H), ands Silver-Zinc (Ag-Zn). Nickel-Hydrogen batteries are very efficient and posses a long cycle-life of approximately 12,500 cycles. Their energy density is relatively low, close to 40 Wh / Kg. Nickel-Cadium batteries are very similar to the Nickel-Hydrogen batteries, they also have a relative long life, close to 10,000 cycles. These batteries have even lower energy densities, around 22 to 26 Wh / Kg. Lithium - Hydried batteries have very high energy densities (600 Wh / Kg), but as a result of their chemical reactions, great amounts of heat are released. Finally, Silver-Zinc batteries also have high energy densities, but very low life-cycles. They produce around 152 Wh/Kg, and they sustain a life of 20 to 200 cycles. These batteries are used in short missions where weight is a primary concern.

Fuel cells were also considered, they were a very competitive option because of their weight and energy ratios. Although fuel cells are very efficient ways to produce power, they create very high heat loads which are difficult to control and dissipate. Because of the size of the spacecraft, heat dissipation is a difficult problem. Almost every single instrument placed in the spacecraft produces heat which is accumulated inside the cabin. Additional heat loads from the fuel cells would had been almost impossible to manage. Also, a weight restriction would had come when using fuel cells and larger radiators to dissipate the heat.

Nuclear Energy

Radioisotopes have been succesfully used as a thermal source for space power supply. Compact nuclear reactors can be designed to supply the required electricity and propulsion for the spacecraft. These reactors are reliable, rugged, insensitive to space environment, and they have large specific thermal power. Because of dangerous radiation, nuclear reactors require large amount of shielding. It will be impossible for a nuclear reactor to supply power to a small spacecraft where weight is very important.

Requirements For The Delta Spacecraft

There are three major requirements for the electrical power system. First, it must be able to produce the amount of power required by the avionics, electronics, and all other systems that need some form of electrical power. For the Delta spacecraft, it has been set at 1500 Watts of continuous electrical power, most of the power goes to the avionics and human factors systems. Second, the system must be composed of a primary and a secondary power supply, this will add redundancy and safety to the system. Besides these two primary requirements, the electrical power system must also meet the weight and size limitations imposed by the spacecraft. For a five day mission with a power demand of 1500 Watts, the primary and secondary sources of power were obtained. The solar array was chosen as the primary or main power supply because of its reliability and because no fuel is taken with the spacecraft, all the fuel comes from the sun. Also, for a proposed mission where docking with the space station is necessary, the spacecraft will be able to consume its own electrical power, and won't depend on the space station's electricity. This array will be backed up by a secondary system consisting of Siver-Zinc rechargeable batteries which will be turned on automatically when the power demand increases. Silver-Zinc batteries were chosen because of their relatively high energy density and reliability. They have been used in spacecrafts for the past 20 years without any damages or problems.

Primary Power Supply

The DART spacecraft will require 1.1 KW of electrical power for the avionics and other instruments. An array of solar cells was chosen to supply all the electrical power necessary to keep the spacecraft working properly. Since the secondary power supply will come from a system of rechargeable batteries, an extra power output will be needed to recharge the batteries. There must be 400 Watts of extra power to recharge these batteries, bringing the total power demand to 1500 KW. The spacecraft will be in a low earth orbit with a period of 94 minutes. Depending on the solar angle of incidence, as shown in the following picture, the time of direct sunlight will be around 60.4 %.

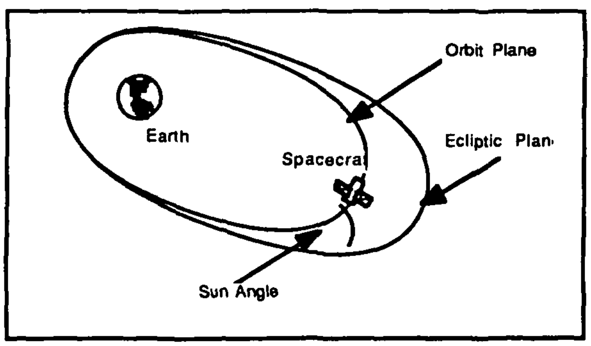

Figure 4.3d: Determination of the sun's angle with respect to spacecraft.

Edison W. Villacís.

For a mission of five days, which is the longest mission that the DELTA will carry, and with an average illumination period of 60.4%, the total energy produced by the 1.5 KW will be:

(5 day)*(24 hour/day)*(0.604 illumination)*(1.5 KW) = **108.72W-h.**

The size of the solar array to be used is determined using the solar power in space, 1.35 KW / m^2, and the efficiency of the solar cells = 12.5%. So that the cells capture 168.75 W / m^2. For the 1.5 KW of power, the area needed will be:

$$\frac{1500\ \mathrm{W}}{168.75\ \mathrm{W/m^2}} = \mathbf{8.888\ m^2}$$

The 8.888 m^2 area will be divided into two wings, each measuring 1.5m X 2.95m. These wings when fully deployed will look like the following picture:

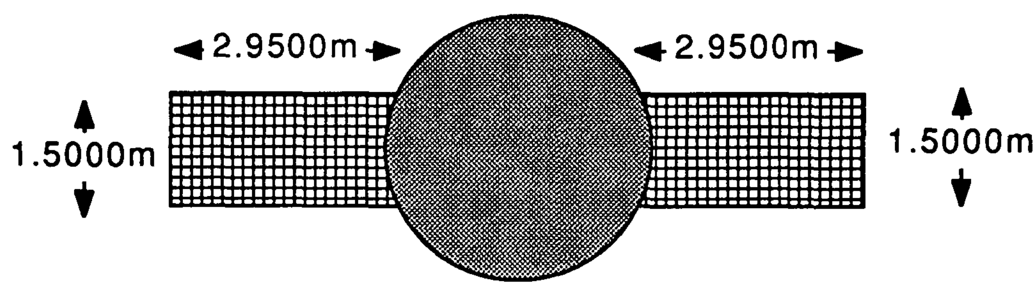

Figure 4.4.b: Solar Array in Deplyed Position

The average weight of a solar cell is 0.1 g /cm^2 so that for the entire area of 88,888 cm^2, the weight will be: (0.1gm/cm^2)*(88,888 cm^2) = **8.8 Kg** The average weight of other materials used such as cell covers, adhesive, solder, insulators, and thermal paint is 400 gm./m^2. For the entire solar array, this weight will be:

(400 gm/m^2)*(8.888m^2) = **3.556 Kg.**

The total weight of the assembled solar cells will be: **12.44 Kg.**

The weight of the flexible Roll-up blanket which will be used to deploy the solar array is 25.05 Kg. This brings the weight of the primary power supply to **46.37 Kg**. This blanket and the deployment mechanism has been used before in missions such as the Agena spacecraft, and it has proven to be very reliable and functional. The solar cells will lay on this flexible blanket which will be rolled up into a cylinder 0.25 m in diameter. This cylinder will be stowed inside the spacecraft until the it is safely delivered to its orbit. At this point a small motor will begin to unroll the blanket and will keep it stretch throughout the entire mission. A picture showing this deployment mechanism can be seen next.

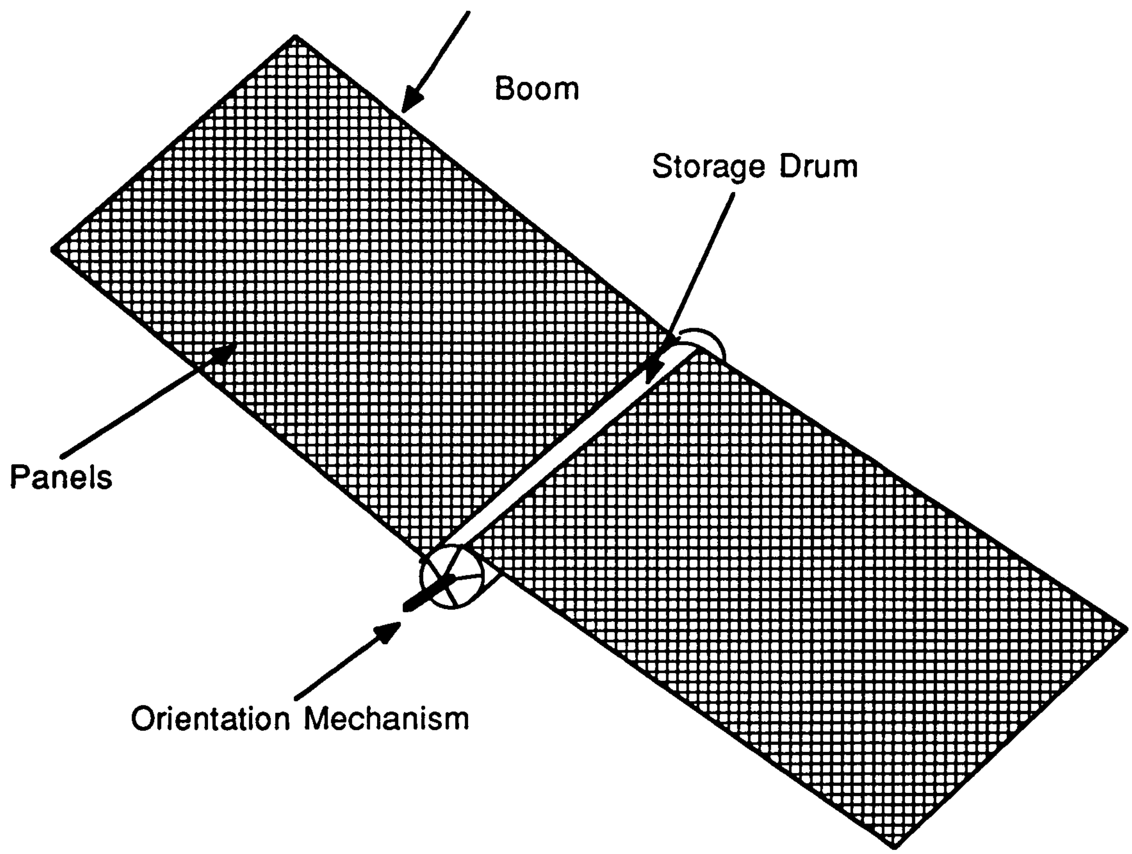

Figure 4.4.c: Deployment Mechanism

Secondary Power Supply

The spacecraft will need electrical power long before the solar array can be deployed; electricity is needed to keep the monitoring systems functioning during launch, and to activate the motor that will deploy the solar array. As stated before, Silver-Zinc (Ag-Zn) batteries were selected because of their high energy density, 152 Wh / Kg. These batteries will be used to aid the solar array during solar eclipses and/or when more power is needed.

In the Low Earth Orbit which the spacecraft will maintain, the period 94 minutes; and the solar eclipse period will vary between 28 to 36 minutes depending on the angle of the sun's ecliptic orbit plane and the orbit plane of the spacecraft. This angle is illustrated in figure 4.3.1. The 36 minutes means that the spacecraft will be in the shadow (the sun's rays will not reach the solar panels) 39.6 % of the time. This is a very crucial time and will determine the final design of batteries. So that during the entire five day mission, the period of solar eclipses will be 39.6% X 120 hours = **47.52 hours**.

The batteries will supply the same amount of power as the solar array, 1.5 KW. This amount of power was kept to provide additional redundancy to the secondary power supply. The total energy produced by the required 1500 W during the 47.52 hours is:

(47.52 hours) X (1500 W) = **71.28 KWhr**.

Since the energy density of Ag-Zn batteries is 152 Whr/ Kg, to produce this energy we will need:

(71.28 KWhr) ÷ (152 Whr / Kg) = **468.95 Kg**.

This would be the weight of the batteries if they were to continuously discharge their energy in one cycle. But since Ag-Zn batteries have a cycle life of 20 to 200 cycles, they can be constantly recharged using the solar cells electrical output. At a discharge rate of 10 hours, the batteries will be recharged five times during the entire mission. This will bring down the total weight of the batteries to **93.75 Kg**. We must keep the charge-recharge cycles as low as possible to prevent any leakage and because as the recharging cycles increase, the efficiencies of the batteries decrease very fast. The batteries are composed of 45 to 50 cells or plates which are connected together and stored inside a sealed box to prevent leakage and to protect them against the space environment. A selection of four batteries was made to add redundancy and reduce the risks of malfunction. Three batteries will be charged and discharged to supply the power needed, the other battery will stay as an emergency battery with power for three hours. In this way if one battery fails the other two will take over without any noticeable losses, and if everything fails, there will be one battery that will be used to abort the mission. For a system of batteries with a total weight of 93.75Kg, each battery will weight 23.434 Kg. The total volume of the battery system will be 0.0216 m^3. These batteries can be stocked or piled up one over the other, or one next to the other.

They are placed in the rear of the pressurized cabin to save space inside. When the mission is completed and the spacecraft is ready for reentry, the batteries will be discharged to the lowest power output needed by the avionics and control systems during this time. This will be done to avoid fires and short circuits due to the extreme conditions during reentry.

Power Distribution System

The functions of the power distribution system are to control the output of the solar arrays and of the batteries. Since there are many instruments that work with different voltages and frequencies, regulators and inverters must be used to deliver the correct voltage to the instruments. The Electric Power System (EPS) is designed to meet the requirements imposed by the spacecraft, this requirements are: load profile, orbit mission, and system configuration. The EPS basically takes the electrical power from a source, and distributes it to the equipment.

Due to solar eclipses, the voltage output from the solar arrays is maximum when the arrays are coming out of the shade. The temperature of the solar cells drops drastically; thus, producing less resistance and giving a higher voltage. To control this variability in voltage, both partial shunt regulation and full shunt regulation were considered. The full shunt regulator was chosen because it gives a more constant current from the array. These shunt regulators and the battery discharge controller form part of the power control unit, which is inside of the primary and secondary buses. Most aerospace instruments work at 28 V dc (direct current is preferred because of vehicle size and weight restrictions) so that the voltage output must be designed for this desired voltage. Alternate current will also be needed for separate systems, so that an inverter will be used in order to change dc to ac. Since the design is for 28 V dc, a maximum voltage produced when the spacecraft is coming out of the shade will be around 59 V dc (due to the lower resistance at those times). This means that the regulators used must provide the required voltage and must protect the sensitive electronics from power surges. The same problem arises during battery recharging, high charge currents go into the battery and overheat it; thus, reducing the battery life expectancy. The solar array will be connected to the full shunt regulator that will automatically operate when the solar array current exceeds the spacecraft load and the battery current. The full shunt also produces maximum efficiency.

Two bus-voltage systems will be used to provide equal battery discharge rate and to protect against single point faults. The main bus will be connected directly to the power source, the solar arrays and the batteries, and to the main electronics. The main electronics are used 100% of the time and essential for the mission. The inverter providing alternate current to the Environmental Control System (ECS) is also connected to the main bus. The secondary bus is connected in series to the primary bus. The non-essential avionics and other instruments are connected to the secondary bus. Another inverter providing alternate current to the Stabilization Control System (SCS) is also connected

here. The ECS and the SCS are partially connected insuring a redundancy that keeps the possibilities of failure down. The battery charge/discharge controller regulates battery voltage to the bus at the original 28 V dc. It also controls and modifies the rate of charge and discharge to suit the mission requirements.
Some of the avionics and control units and their respective power demands that the DELTA spacecraft will be using are tabulated here:

CPU	40 W
Bus Controllers	50 W
Attitude Sensors	15 W
Communications	70 W
Guidance & Navigation	150 W
Tracking Devices	50 W
Human Factors	135 W
Total	510 W

Table 4.4.b: Power Requirements of Instruments Used

Note that the instruments recorded in the table are not all the instruments used by the DELTA spacecraft, all the instruments used are listed in the avionics chapter.
Protection devices must be added to prevent short circuits and other failures. Circuit breakers and fuses are excellent choices. Figure 4.3.4 is a schematic of the spacecraft electrical system. This figure shows the main connections among the power generators and the instrumentation.

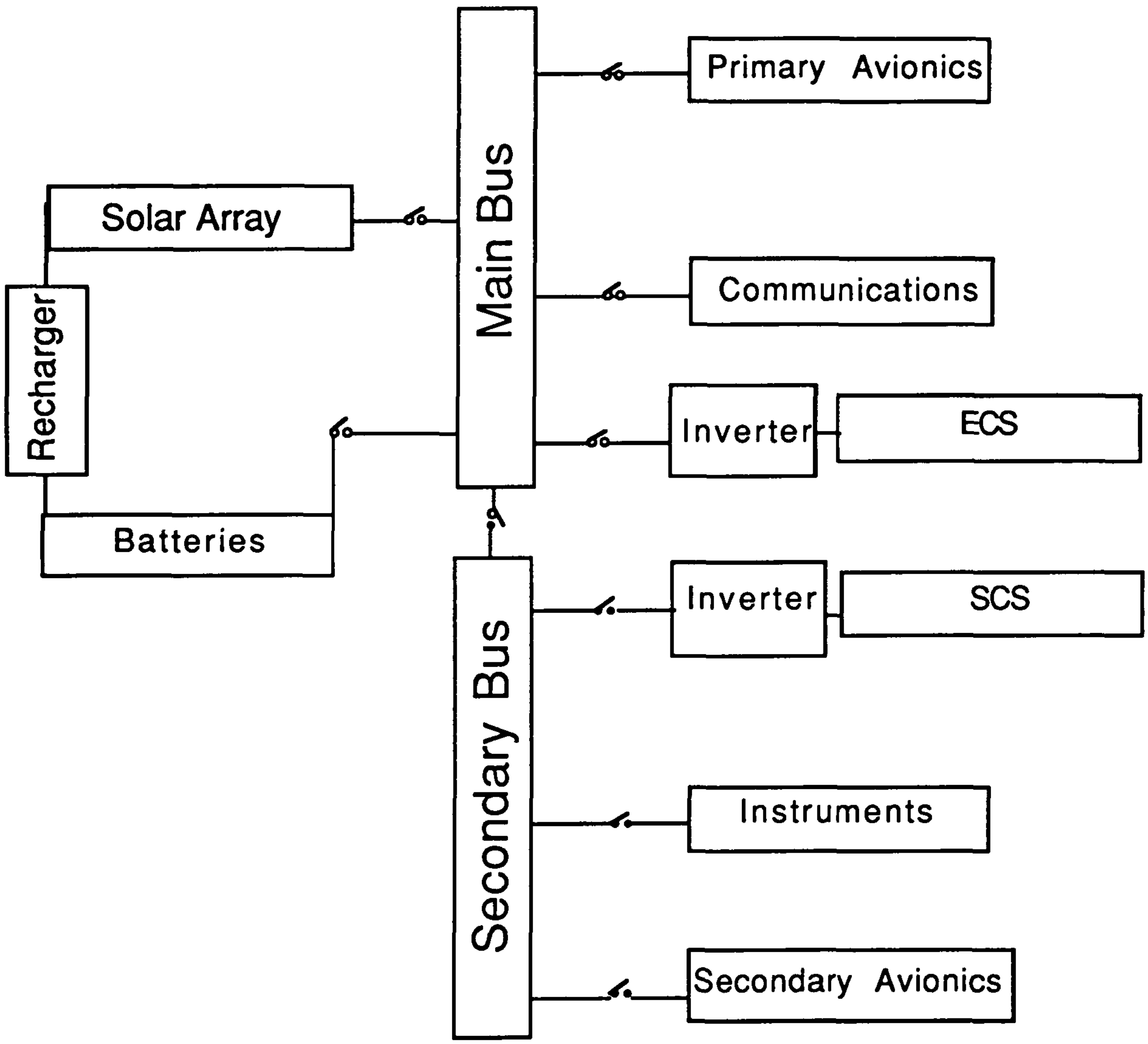

Figure 4.3.4: Schematic of Power Control System

Chapter 4 References

1. Sutton, George P., and Donald M. Ross, *Rocket Propulsion Elements.* New York: John Wiley & Sons, 1976

2. Hill, Philip G., and Carl R. Peterson, *Mechanics and Thermodynamics of Propulsion.* Reading, Mass: Addison-Wesley Publishing Company, 1970

3. Huzel, Dieter K., and David H. Huang, *Design of Liquid Propellant Rocket Engines,* NASA report SP-125. National Aeronautics and Space Administration, Washington, D.C., 1971

4. Kit, B., and D. Evered, *Rocket Propellant Handbook.* New York: The Macmillan Company, 1960

5. *Structural Strength Program Requirements.* MSFC-HDBK-505 Rev. A Jan. 1981

6. Chuse, Robert, *Pressure Vessels.* New York: McGraw-Hill Book Company, 1977

Chapter 4 Bibliography

Agrawal, B. N., *Design of Geosynchronous Spacecraft.* New York: John Wiley & Sons, 1985

Ball, K. J., and G. F. Osborne, *Space Vehicle Dynamics.* Oxford, Great Britain: Oxford University Press, 1967

Chuse, Robert, *Pressure Vessels.* New York: McGraw-Hill Book Company, 1977

Collins, W. B., and D. R. Newell, "Power Conditioning Requirements and Tradeoff Considerations for the Space Shuttle." *IEEE 1971 Power Conditioning Specialists Conference*

Empell, C. M., "Multirole Capsule An Introduction." Journal of the British Interplanetary Society, Vol. 2, 1989

Fleischer, A., "Silver-Zinc Batteries." *Symposium on Silver-Zinc Batteries.* New York: John Wiley & Sons, 1968

Gross, S., *Battery Design and Optimization.* Princeton, NJ: Electrical Society, 1979

Hill, Philip G., and Carl R. Peterson, *Mechanics and Thermodynamics of Propulsion.* Reading, Mass: Addison-Wesley Publishing Company, 1970

Huzel, Dieter K., and David H. Huang, *Design of Liquid Propellant Rocket Engines,* NASA report SP-125. National Aeronautics and Space Administration, Washington, D.C., 1971

Jasinski, R., *High Energy Batteries.* New York: Plenum Press, 1987

Kit, B., and D. Evered, *Rocket Propellant Handbook.* New York: The Macmillan Company, 1960

Langton, N. H. (editor), *Space Research and Technology: Volume 2 - Rocket Propulsion.* New York: American Elsevier Publishing Company, Inc., 1970

Manzo, M., and N. R. Schulze, "NASA Aerospace Battery System Program Update." *1989 24th Intersociety Energy Conversion Engineering Conference*

Morgan, N. E., and W. D. Morath, "Development of a Hydrogen-Oxygen Internal Combustion Engine Space Power System."

Pytel, A., and F. L. Singer, *Strength of Materials - Fourth Edition.* New York: Harper & Row, Publishers Inc., 1987

Rausenbach, H. S., *Solar Cell Array Design Handbook.* New York: Van Nostram Peinhold Co., 1980

Sandor, B. I., *Strength of Materials.* New Jersey: Prentice-Hall, Inc., 1978

Structural Strength Program Requirements. MSFC-HDBK-505 Rev. A Jan. 1981

Sutton, George P., and Donald M. Ross, *Rocket Propulsion Elements.* New York: John Wiley & Sons, 1976 and 1986

Thompson, T. William, *Introduction to Space Dynamics.* New York: Dover Publishing, 1985

Chapter 5

Avionics

Section 5.1 Navigation and Guidance

Positioning, Tracking, and Time Keeping

To navigate a spacecraft, you need the spacecraft's position, how to track it, and and a way to keep accurate time between the spacecraft and the navigational system. While in orbit, periodic fixes will be measured by the on board and satellite based navigational systems. Many periodic fixes are not necessary because once in orbit, the trajectory is predictable to within hundreds of meters for several revolutions of low orbit.

The Inertial Navigation System (INS) on board the DART spacecraft will give instantaneous data to the astronauts. The LTN-90 ring laser gyro inertial reference system (built by the Litton Company) serves as the primary attitude source and as the sensor for position, velocity, spacecraft rotation rates, and accelerations (see figure 5.1a).Because the LTN-90 is built for and used in aircraft, perhaps some adjustments to the INS would have to be made, but probably not very much.

The LTN-90 is composed of an inertial sensor display unit, a mode selector, and an inertial reference unit. In the inertial reference unit are the ring laser gyros (RLG) that measure rotation accelerations and rates about the three spacecraft axes, and three single axis accelerometers that measure accelerations and rates. The system uses a square path configuration as opposed to the triangular path because for the same scale factor, a square is smaller than a triangular gyro. Also, the square gyro produces less backscatter.

Other systems were looked at but they either required more weight or power for better accuracy. It's true the DART could manage more mass or power or both, but the DART wishes to minimize its mass, cost, and power. The excess mass can be used for payload or other areas of operation.

Dynamic Stability and Control

Because the LTN-90 has been used and proven to be reliable, test for gyroscopic motion have already been performed. Most likely, Lagrange's equations were used for formulating the differential equations for rotational motion about principal axes and free motion. If the DART had built its own INS, these equations would have been implemented to give the necessary equations of motion.

Updating the INS

Because the positional error of the LTN-90 increases every hour, it will have to be updated by another navigation system (see figure 5.1b).The primary satellite navigational system considered for updates is the Global Positioning System (GPS). GPS is a satellite based navigational system which will give continuous worldwide coverage by the year 1992, when there are 21 operational satellites in orbit. The satellites orbit once every 12 hours and transmit two L-band signals, L1 at

LTN-90 Inertial Navigation System

Inertial reference unit
Weight: 19.9kg
Dimensions: 194 X 322 X 318mm
Power: 110W
MTBR: 2500h

Inertial sensor display unit
Weight: 2.27kg
Dimensions: 114 X 146 X 152mm
Power: 15W
MTBR: 15,000h

Mode selector unit
Weight: 0.45kg
Dimensions: 38 X 146 X 51mm
Power: negligible
MTBR: 50,000h

Total Weight = 22.62kg
Total Volume = .0227 cubic meters
Total Power = < 130W

Performance: 95%
Heading: 0.4 degrees
Pitch: 0.1 degrees
Roll: 0.1 degrees
Position: 3.704km/h
Ground speed: 4.12m/s
Flight path angle: 0.4 degrees
Body rates: 0.1 degrees
Body accelerations: 0.01g
Reaction time: 10 minutes

Figure 5.1a. The LTN-90 (Ref.1)

1575.42MHz and L2 at 1227.60MHz. This system of orbits ensures at least four satellites will be in view at all time. GPS will provide an accuracy of better than 30m using the public available coarse acquisition code (C/A code called "standard positioning."). This type of accuracy will be sufficient when the spacecraft is in orbit and only periodic fixes are taken.

There are also times when more precise accuracies will be required by GPS, for example, rendezvous and change of orbit. Using the P code (military code), GPS will be able to give an accuracy of 1 to 10m, depending on the position of the satellites. When a change of orbit is desired, fixes will be measured by accelerometers to guide an orbit change maneuver. On board computers will calculate the instantaneous orbit while the spacecraft is thrusting, using the integrated accelerometer outputs.

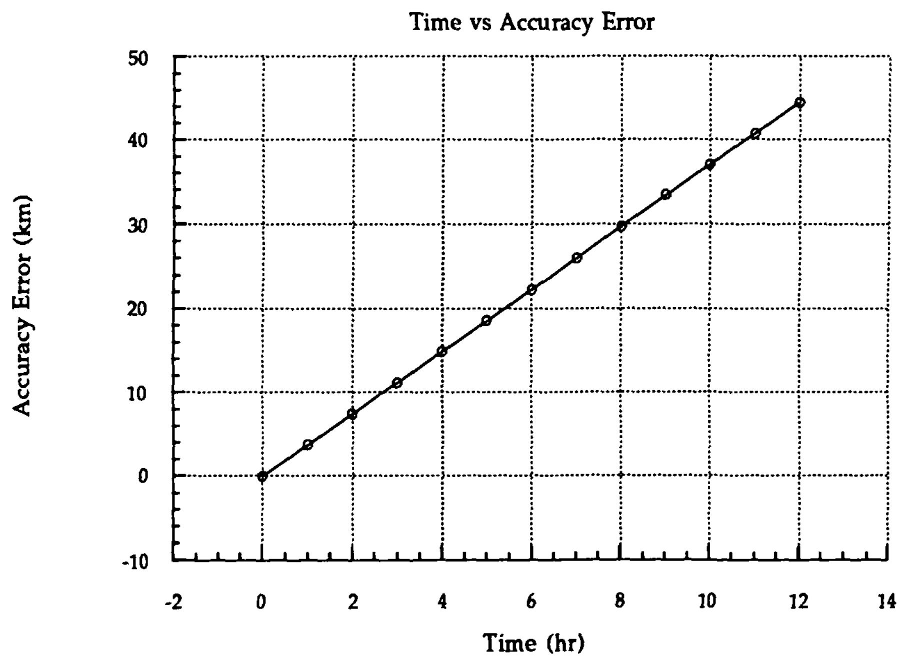

Figure 5.1b. INS Error increases with time.

The position of each satellite will be known at all times with a high degree of accuracy and each satellite is equipped with four atomic clocks called hydrogen masers for redundancy. Accurate satellite position data and accurate clocks are essential for accurate, three-dimensional position determination. Three satellites will determine the latitude, longitude, and altitude of the spacecraft.

Because the clock on the craft is not atomic, a time bias occurs. To correct it, a fourth satellite is used to provide a fourth line of position (LOP), which eliminates the time bias and reduces the area fix to a point in space. Thus, the fourth satellite acts as the spacecraft's atomic clock.

To navigate and guide, a C/A code sent at 1,023,000 bits/s is repeated every millisecond and is deciphered fairly quickly. A P code can be sent also at 10,230,000 bits/s and takes a week to repeat itself. A GPS receiver has the same program for generating the C/A and P codes as the satellites. By matching the two patterns, the satellite and receiver can be synchronized, all in a matter of seconds. Once synchronized, the satellite can measure the elapsed time since transmission by comparing the phase shift, or remaining difference between the two codes. The more the two disagree, the greater the length of time since transmission, and length of time since transmission multiplied by the speed of light equals distance. Thus by measuring phase shifts in the code, distance between satellite and receiver can be computed. For example, let's say that the closest the two are synchronized is .07 seconds, then by multiplying by the speed of light (3X100000km/s) the distance is 21000km.

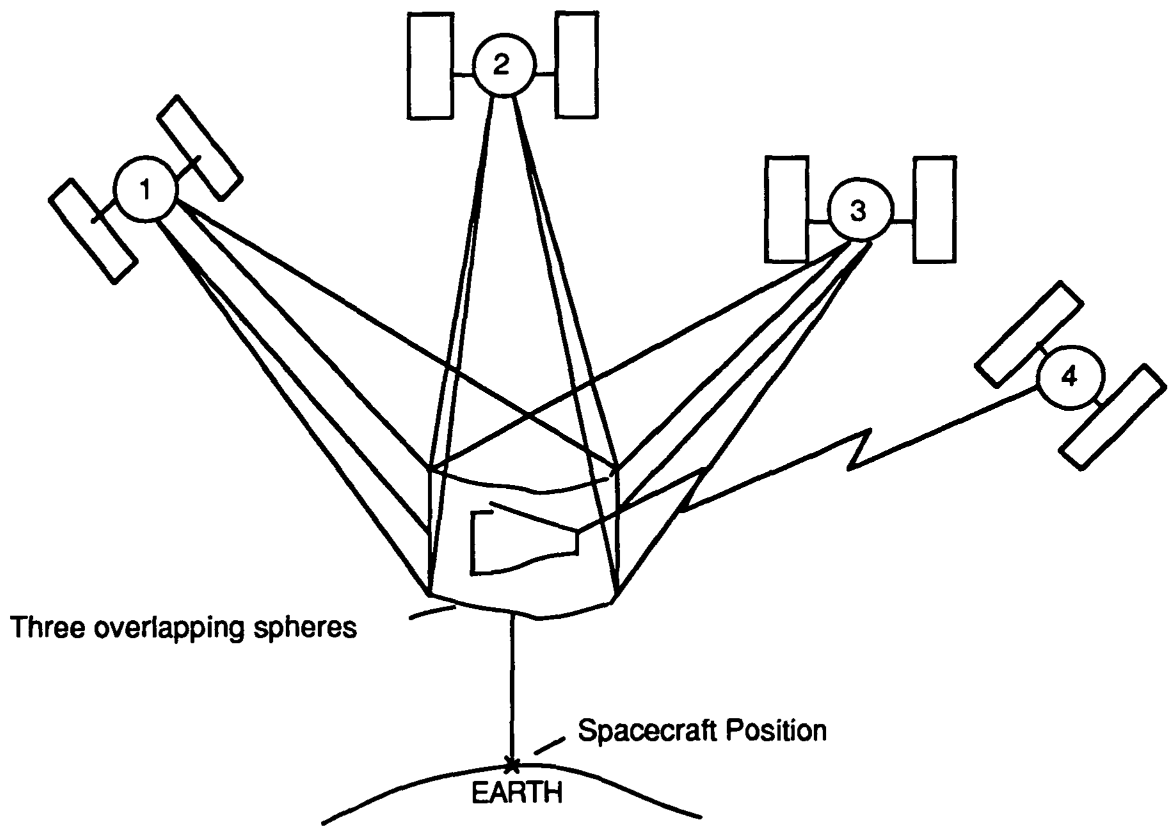

Number of satellites by 1992			21
Altitude of satellites			20,187km
Period of orbit			12h
Passive or Active			Passive
Chip code	C/A sent at 1.023Mbits/s		P Code sent at 10.23Mbits/s
Lock on			less than five minutes
Frequency	L1 = 1575.42Mhz		L2 = 1227.60Mhz
Positional accuracy	C/A code: 20-30m	P code: 1-10m	Differential: 10cm

Figure 5.1c. The Global Positioning System (Ref.2)

If we know the distance from a satellite, then it follows that we must be located somewhere on the surface of a sphere with a radius of that distance, centered on that point. Three satellites make three surfaces and intersect at one point . This is a point in space based on the distance. By knowing how far the spacecraft is from each satellite and the satellite's position, the on board computer can calculate its position (see figure 5.1c).

GPS Vs Others

GPS is the best choice for the navigational system to update the INS. With the accuracy of 1-10m and a 100% coverage, GPS is guaranteed to give good accuracy at any time. No signal is required from the spacecraft to receive the position data because GPS is a passive system, another advantage. One disadvantage of GPS is the fact that four satellites must be used for accuracy including the time bias, but with the number of satellites at their altitude, this should not be a problem.

The Tracking Data Relay Satellite System (TDRSS) is another major satellite system. It provides close to 85% continuous unified S-band coverage to as many as 24 satellites at once below 3700km altitude. The same dish used for communication (its primary use) can be used for navigation because they both work on the same band (Ku). A downfall for TDRSS is that all transmissions must pass through a ground terminal in White Sands, NM. This puts the dependency for information on one station. Also, as of 1983, numerous system outages have occurred, lasting from a few minutes to several hours or more. When this occurs, the spacecraft has to rely on ground stations for all communications. Single points of failure exist throughout the computer and communication systems and can cause system outages.

Another downfall is the 15% unavailable coverage. If TDRSS was to be used as the primary navigation system, there would always be the 15% where only the INS could give the spacecraft position, where accuracy decreases with time. Performing orbital maneuvers during the 15% unavailable coverage would not be very accurate.

NASA is in the process in constructing a second TDRSS ground terminal at White Sands because of concerns about the reliability of the first one. The second terminal will provide backup to the first and eliminate it as a single point of failure. When the second terminal is completed in 1993, the original terminal will be completely overhauled to be identical with the new terminal.

Another form of navigation is ground based. A ground system can use simple and inexpensive quartz oscillators to time the interval between the start of a signal and the receipt of the return pulse.

Ground based systems (active) require a signal from the user, but these can be intercepted, jammed, modified, and targeted by the opposition. Also, ground clutter and precipitation often mask return signals. A ground based station can only be used when the spacecraft is flying in the range of the station. This means many different stations would have to used to navigate a mission. Ground station navigation would be used only in conjunction with another form of a navigational system.

Sensors

The guidance system will, in general, consist of sensors and satellites for measuring various dynamic variables such as acceleration, velocity, position, and angular velocity. Transducers will process the sensor information, then the computer will interpret the transducer information. The computer will give commands to the actuators whose function it is to develop and apply forces and moments to the vehicle in the manner directed by the computer's outputs.

Trajectories influence the guidance and control of the vehicle. The resulting optimum trajectory dictates the path along which the guidance and control must direct the aerospace vehicle.

The gyro of the INS will be used for inertial censoring. The purpose of the gyro is to provide a physical element, arranged either to preserve angular fixes in inertial space about all axes, regardless of spacecraft motion, or to precisely measure angular motions of the craft relative to inertial space. The gyro will need to be as insensitive to vehicle motion as possible.

Accelerometers will be used to measure changes in vehicle speed. The orientation of the accelerometers will be established with help from the gyro system so gravity is taken into account as well as components of vehicle velocity changes, due to thrust, drag and other non-gravitational forces when determining velocity and displacement.

Rendezvous

There are three functions necessary for rendezvous: 1) Progressively improve the craft's estimate of position and velocity with respect to the target; 2) Determine maneuvers necessary to close in on the target; 3) Perform the necessary maneuvers.

The Delta spacecraft will be able to have guidance sensors to help in rendezvous. Three types of rendezvous sensors are rendezvous radar (RR), star trackers (ST), and The Crew Optical Alignment Sight (COAS) (see figure 5.1d).

Rendezvous radar operates on the Ku-Band system and it provides automatic target detection, tracking and acquisition. It helps to reduce target location uncertainties during rendezvous maneuvers. The radar provides range rate, range, pitch, and roll relative to the spacecraft. It can detect both active (those with transponders) and passive targets (those without). The range of the radar for an active target is 555km and for a passive target it is 22.2-27.75km with a target having a 1 square meter radar cross-section. The accuracy in range is about 23.8m and a range rate accuracy of about .3m/s.

A star tracker is used to track orbiting targets from spacecraft during rendezvous. It is a image dissector electro-optical tracking device that operates at visual wavelengths.

The Crewman Optical Alignment Sight is an optical sighting device. The crew uses it during rendezvous to view the target.

The Space Shuttle uses all three sensors for rendezvous. After comparing the RR and the ST, it was determined that the DART would not need a ST. A ST is very good in measuring the target angle because it is designed to track stars. A ST doesn't use too much volume, has relatively low mass (compared to a RR), and it doesn't need much power to operate. A ST, however, doesn't measure angle rate, range, and range rate.

A RR will measure the target angle not as accurate as the ST, needs more volume, more required mass, and more required power for operation. The RR is also able to measure the angle rate, range, and range rate. By having these other features that the ST doesn't have, the ST can be eliminated from rendezvous operations. A star tracker would be a waste of money, power, and mass. The excess mass could be used for payload or other operations.

Ground stations can uplink the position of the target to the DART and uplink burns to place the DART into RR range. Once in RR range, the information from the radar can be used to determine when to burn. Once in the range of the COAS, it can be used for closer burns. The astronauts could look through the COAS to see how the target is moving relative to the spacecraft. The COAS has an advantage of looking through it rather than a window because a window doesn't have any way of letting you know how much the target is moving left, right, up, or down relative to the ship. The COAS has marks which will let you know which way the target is moving.

Because Rendezvous Radar is a sensor, more RR accuracies are given in the sensor section.

	Data Types			Range Limits (km)	
Sensor	Angle	Range	Rge Rate	Maximum	Minimum
Star Tracker	Yes	No	NO	407.44	7.41
Rendez-vous Radar	Yes	Yes	Yes	22.2 passive 555 active	.019
Crew Opt. Align. Sight	Yes	No	No	185.2	0.19

	Rendezvous Radar	Star Tracker
Angle	.46 degrees	.02 degrees
Volume	.09 cubic meters	.03 cubic meters
Mass	75.30kg	13.70kg
Power	2W	460W
Angle Rate	.008deg./s	NO
Range	.0244km R<2.4km 1% of R, 2.4<R<9.07km 91m, 9.07<R<22.2km (Passive Target)	NO
Range Rate	.3m/s, R<18.52km	NO

Figure 5.1d. Rendezvous equipment (Ref.3)

Section 5.2 Attitude Determination and Control

Introduction

As mentioned in section 5.1, the inertial navigation system requires updating periodically to correct the inherent errors which accumulate over time. These correction updates are provided by additional sensors on the capsule. This section discusses different types of attitude determination sensors used on spacecrafts and provides their advantages and disadvantages. Additionally, attitude control techniques will be discussed.

Requirements

The attitude requirements for the Delta DART capsule are set forth by the missions it will perform. From their intended missions, the rendezvous and reentry requirements are the most stringent in terms of attitude. From these requirements, an accuracy of better than one-quarter degree will be needed for both attitude determination and control. Hence, the sensors therefore must provide an accuracy of better than 0.20 degrees to ensure accuracy between the periodic updates. These requirements, as well as mass and volume constraints, set the guidelines to determine which techniques to implement.

Attitude Determination

Overview

Various techniques to determine a spacecraft's attitude were studied. These studies involved analog and digital sun sensors, horizon sensors, magnetometers, star sensors, and various types of gyroscopes. Each technique was evaluated on its accuracy, its typical mass, volume and power requirements, and its costs and complexity.

Sun Sensors

Sun sensors are the most widely used sensor in space applications today. This is due to its many advantages. Since the angular radius of the sun is fairly constant for an orbit around the earth, and appears small enough at this distant, the simplification of the sun as a point source can be made without loss of accuracy. This, in turn, simplifies the sensor itself and the algorithm associated with the attitude determination. Also, due to the brightness of the sun, it is easily distinguishable from other bodies in space. Hence, the sensor does not require additional distinguishing mechanisms, and will require less power. Another factor for this type of sensor is that other equipment such as solar panels need to face the sun, so no special orientations are needed just for the sensor.

Sun sensors come in single-axis and two-axis configurations. The single-axis system provides the angle of the sun in reference to the spacecraft. Meanwhile, the two-axis system provides the vector to the sun from the spacecraft.

There are two types of sun sensors that were examined - analog and digital. Analog sensors use a photocell whose output current indicates the angle of incidence of the solar radiation. Analog systems require no input power or control electronics, but have only a fair accuracy rating. Digital sun sensors, however, can have very good accuracies (better than 0.1°), with the costs of power required and additional electronics. The digital sensors use a number of photocells, which represent the specific bit used to generate a digital output signal representing the angle of the sun to the spacecraft. Although digital sun sensors require slightly more power, mass and volume, their improved accuracy outweighs these disadvantages. Therefore, the DART capsule will use the two-axis digital sun sensors system to obtain the given sun vector.

Horizon Sensors

Horizon sensors are the most common method of determining the orientation of the spacecraft with respect to the earth. Present-day sensors make use of the infrared spectra band to limit errors associated with visible light sensors, allow night determination, and reduced the effects of reflected sunlight off the spacecraft. But these infrared sensors are not without disadvantages such as higher costs, slower response times (on the order of milliseconds instead of microseconds) and lower signal-to-noise ratios in comparison to the visible light sensors.

Horizon sensors require some type of scanning mechanism to search across space. For a spinning spacecraft, simply mounting the sensor on the body is sufficient. But since the DART capsule will not be spinning while in orbit, some type of mechanical device must be used. Methods such as attaching the sensor to a momentum wheel are inadequate on the DART because of the extra mass required. Therefore, a system similar to the panoramic attitude sensor (manufactured by Ball Brothers Research Corporation) is desirable. This type of system can be used on a rotating spacecraft or can use internal scanning when the spacecraft is not rotating.

Horizon scanners provide good accuracy (in the 0.05° range) during both day and night. Some limitations on these sensors are that they are orbit dependent (but since the DART will maintain a somewhat constant orbit, this is not a major concern) as well as being poor in yaw. Also they are somewhat heavier in comparison to sun sensors and magnetometers (to be discuss next) and require more complicated mechanisms for spanning. But as with sun sensors, this improved accuracy outweighs these disadvantages and therefore will be used on the DART capsule.

Magnetometers

Magnetometers are also widely used in spacecraft today because of their many advantages. Magnetometers are typically lightweight, cheap, reliable (mainly because of the need for few moving parts), have low power requirements, and supply continuous coverage. Also, they are vector sensors, determining the direction and magnitude of the magnetic field of the earth. However, since they depend on the little known magnetic field and the models used to predict the field's strength and direction, which are subject to significant errors, their accuracy is poor (in the 1.0° range). Hence, this poor accuracy prevents their use on the DART capsule.

Star Sensors

Star sensors provide vectors to stars with respect to the spacecraft. Using known star positions the attitude of the spacecraft can be determined. Star sensors are the most accurate attitude sensor (in the 0.005° range). But for the DART capsule, this excellent accuracy is outweighed by the costs associated with this sensor. Star sensors are expensive, heavy, sensitive to light, and require more power than any other previously described sensor. Also the computer processing requirements are much more extensive. For these reasons, star sensors are presently not part of the capsule design.

Gyroscopes

Gyroscopes are the primary attitude determinate technique when there exists gaps in which other sensors can not obtain readings. Gyroscopes provide updated attitude angular displacements and/or rates. When the attitude system is designed with gyroscopes, the spacecraft is essentially using the gyros for its attitude reference and these gyros are updated periodically by the other sensors to insure accuracy and correct for integration errors. The accuracy of gyroscopes is in the range of 0.01° per hour drift.

There are two types of attitude determination gyroscopes, rate gyros and rate-integrating gyros. Rate gyros measure the angular rates of the spacecraft while the rate-integrating gyros measure the spacecraft's angular displacements directly. Both types may be used for spin rate control and attitude stabilization. For these functions, rate-integrating gyros are usually more accurate than rate gyros, but usually cost more as a result.

As mentioned in section 5.1, gyroscopes are utilized in the INS. The use of laser fiber-optic gyroscopes provide many advantages such as having few moving parts, high levels of reliability and are able to withstand harsher conditions. Fiber-optic gyros also have the ability to be very compact and light.

Table 5.2a provides a summary of the characteristics of these previously discussed attitude determination sensors. (Ref. 4)

Table 5.2a Sensor Characteristics

Sensor	Accuracy	Mass(kg)	Vol.(m^3)	Power(W)
Digital Sun Two-Axis Sys	.01°-.05°	.4 - 1.7	.001 - .01	~1.8
Analog Sun Two-Axis Sys.	.03°-2°	.05 - .1	< .001	none
Horizon Scanwheel	.02° - .05	3. - 6	~ .02	~ 5.5 (incl. wheel)
Panoramic	.02° - .05°	~ 1.0	< .01	
Magnetometers	.25° - 1.°	.1 - 1.	.001 - .005	< 1.0
Star Sensors	.001° - .02°	13.0	~ .03	~ 2.0
Gyroscopes	.01° / hr	< .3	< .001	< 1.0

Attitude Control

Five different systems where studied for the attitude control system. These five systems include reaction wheels, momentum wheels, reaction jets (thrusters), control moment gyros, and magnetic torquers. From these, reaction jets were chosen as the technique to be used for attitude control. This is due mainly to their quick, high force response ability and good accuracy. Although reaction and momentum wheels, as well as control moment gyros, provide a quick and accurate response, the mass required for these systems to be effective control techniques is well beyond the limits set for the DART spacecraft. (This conclusion comes from a design study to determine the needed sizes of reactions and momentum wheels for effective torque on the DART capsule.) As for magnetic torquers, they are lightweight, but provide only a slow response with poor accuracy.(Ref 5) Hence thrusters are the focus of the control model. See section 4.3 on propulsion for complete details on the design of the reaction control system.

Section 5.3 Data Processing

Introduction

The primary function of the data processing system is to monitor all equipment on the Delta DART capsule. Through the use of sensors (discussed in section 5.4) and output devices, this system will keep the astronauts informed about the present condition of all aspects of the spacecraft.

Another function of the data processing system is to perform necessary navigation, guidance and attitude and flight control computations. The goal of this system is to allow for as many on-board processing capabilities as possible and thereby relying lass on ground-based computations. Also, with recent technologies, the goal is to obtain much faster computation speeds, much larger memory capability, and better display units, thus reducing the need of the astronauts for maintenance and computer administration functions.

Requirements

The basic requirements for the data processing system is to be able to handle all sensor inputs and present this information to the astronaut in a concise form. The processing of this data involves reading in the sensor data and comparing the value with the limits set for that sensor. If the value is not within the specified range, a warning is sent to the astronaut and action is taken to try to correct the problem while auxiliary equipment is used in replace of the malfunctioning object. (Note that additional sampling from the sensor will be performed to insure that the data is correct and was not corrupted.) Along with reading the sensor data, the processor must update certain sensors with information from other sensors. For example, the INS is updated by the attitude sensors and the GPS (as discussed in sections 5.1 and 5.2).

Another requirement of the data processing system is to make the necessary computations for the guidance and navigation system (OMS) and the attitude and flight control systems (RCS). These computations involve determining the directional vector to the target position, number and duration of OMS engine burns and the required thruster firings for attitude control. Also, these computations must be adaptive to possible failures of any system at any time.

The data processing system is also required to interact with other external systems on the spacecraft. For example, the communication system must be linked to the processors to allow for data uplink and downlink. (New code may be uplinked in the case of changes to the predefined mission.) Also, the astronauts must be able to enter commands and perform any necessary changes.

The final requirement of the data processing system in to provide a 95% mission success rate. For the DART spacecraft, reliability of the processing system is essential to ensure a successful completion of the missions. But, in the event that the system fails, manual control capabilities must be available to provide a safe return of the astronauts. In other words, this system must be designed to control all systems of the spacecraft in case the astronaut is unable to perform his duties, allow for dual control when both the computer and astronaut are functioning, and allow for manual control if the computer malfunctions.

System Description

System Architecture

Three major types of architecture were studied for DART capsule design: centralized, federated, and distributed. A distributed system has multiple processors throughout the spacecraft performing specific tasks. This type of system allows for short, quicker buses, and faster program execution. However, this design allows for different processors and requires more software development . It also restricts the amount of shared information, which is a primary requirement for the spacecraft. The federated system has each major system sharing input and sensor data over common data buses. This system allows for independence of the major systems while insuring a common data base. One disadvantage of the type of system is partitioning (limiting the spread and effects of a subsystem's failure) is difficult. The centralized system has all processors together, making design and software development simpler. But this design leads to long buses for data and command communications.

For the DART design, a centralized system will be used. As can be seen in figure 5.3a (layout similar to Rockwell's block diagram for the shuttle's data processing system) , this design will consist of four general purpose processors for guidance, navigation, and control. From these central processors will be links to main memory, the sensors, display controls, engine interfaces, and other external interfaces. These four processors will perform synchronized computations, processing the information simultaneously. Intercomputer comparisons will be done to check for computation errors. In the event of a disagreement, the outvoted processor removes itself from the loop and attempts self correction.

The choice of using four processors was determined after looking at different systems consisting of from one to five processors. The primary decision-making factors were the reliability and mass of the systems. Because of reliability requirements, using only one or two processors is not a viable option. For systems using three to five processors, estimates of 5 kg and 20 W of power required for each processor and its associated RAM (Ref. 6) were used. For a three processor system, a single failure would result in a possible standoff between the two remaining processors. Therefore, a single failure would force the mission to be aborted. Using four processors allows for fail safe operations, i.e. continued operations after one failure. (Ref. 7) Therefore, four processors provide the required reliability for the system. Hence, adding a fifth processor is excessive and would just add more mass without a significant increase in reliability.

As previously mentioned, each processor will have its own RAM associated with it. The size of the RAM will be 16 Mbtye. This size allows for an estimated 1 Mbyte of software, 8 Mbytes reserved for runtime memory and 7 Mbyte for temporary data storage and space for uplinked code if needed. In the case this memory gets corrupted, the capability to reload the software from the mass memory will exist. The decision to go with individual RAM was made to allow for quicker and more independent execution.

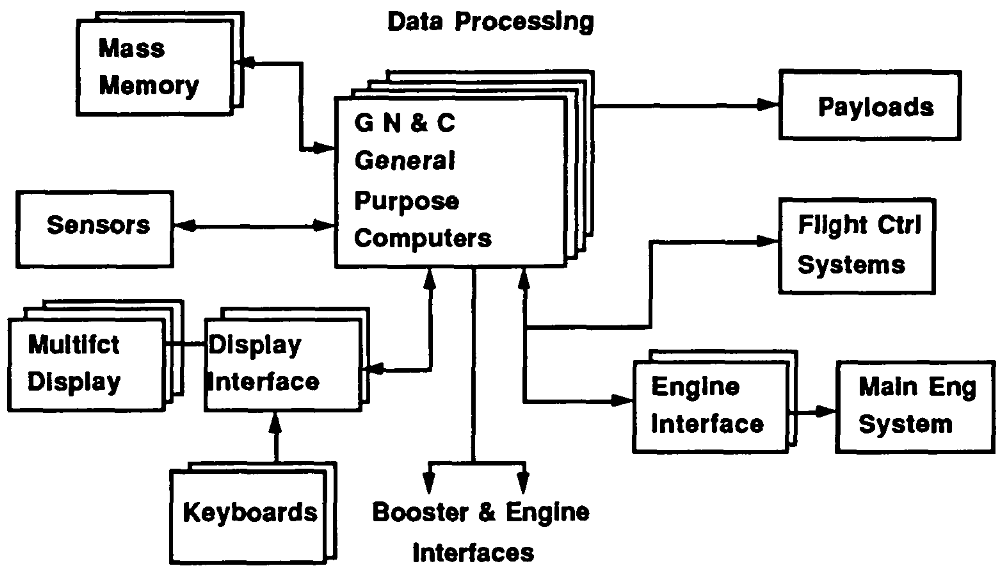

Figure 5.3a Avionics System Design

Associated with each processor will also be an I/O processor to handle all the required sensor input. After looking at the amount of sensor data to be handled (discussed in section 5.3.3.4) and the amount of computations for other systems, a processor with at least a 1 MHz capability is required.

Data Bus Design

The design of the data bus consists of a two-way linear bus configuration. The linear configuration is used due to its ease and simplification for design and modifications. Although the bus controller is a single point of failure, having dual redundancy and well partitioned buses will increase reliability. Fifteen busses will be used on the DART capsule, four between the four processors, two for sensors, two for mass memory, two for displays and keyboards, two for engine interfaces, and two for external interfaces and communications.

Displays

The choice of the type of display equipment for our system involves three types: CRT's, liquid crystal displays (LCD) and luminous flat panels. For CRTs, reliability and versatility are its main advantages, but its size is a significant disadvantage. It's depth requirement is up to ten times more than that of the other two types (approximately 10 to 75 cm). LCDs, on the other hand, require little depth space (approx. 2.0 cm), low power and are digitally compatible. But they do require some type of external backlight. Both of these types have good resolution (approx. 80 lines/cm) and full color capability. Luminous flat panels have the advantage of being very rugged and having uniform resolution and brightness. They are also compact in depth and like LCDs, are digitally compatible. But these displays have been limited in resolution (only 25 lines/cm) and size in the past (approx. 8.0 cm depth). (Ref. 8) For these reasons, the DART capsule will use LCDs for their three displays. One of these displays will be used for the video camera, which is needed for rendezvous and inspection.

Mass Memory

Mass memory is required to store a backup copy of all software needed by the processors in the case of memory error on the RAM. It is also needed to store data while communications downlink is not available. The amount of this data storage is dependent on the input cycle rates of the sensors and the downlink rate of the communication system (8 Kbyte/sec). Table 5.3a provides a breakdown of the input cycle rates for the different sensors. These rates were determined based on the importance of the system and on possible fluxuations with the sensor values. (These rates are for the time when the OMS or RCS engines are firing and main life support is functioning.) From this data, it can be seen that 288 sensors are processed 12.5 times per second, 145 sensors at 25 times per second and 36 at 100 times per second. This gives a total of 10825 inputs per second. With an average of 2 bytes per sensor input, the total is 21.7 Kbytes per second. For the worst case of 30 minutes without the capability of downlink, and if every other data value was saved, the mass memory would be required to have at least 19.5 Mbytes of space free for data. Therefore, to allow for software, data storage and auxiliary space, the mass memory needs to be at least 40 Mbytes.

Table 5.3a Sensor Cycle Rates (at time of engine firing)

System	Sensor Type	# Sensors	Cycle Rate (input/sec)
Propulsion	Temperature	20	12.5
	Pressure	40	25
	Flow	20	100
	Valve	92	12.5

Table 5.3a Sensor Cycle Rates (at time of engine firing)

System	Sensor Type	# Sensors	Cycle Rate (input/sec)	
Main Life Supp	Temperature	11	25	
	Pressure	19	25	
	Flow	16	100	
	Valve	28	12.5	
	Level	15	25	
	Filter	6	12.5	
Secondary Life	Temperature	8	12.5	
	Pressure	16	12.5	(Main Life
	Flow	16	12.5	Support
	Valve	38	12.5	Functional)
	Level	6	12.5	
RCS	Temperature	12	12.5	
	Pressure	56	25	
	Valve	30	12.5	
Abort	Electro/Static	2	25	
	Pressure	2	25	
	Control	6	12.5	
Miscellaneous		10	12.5	

Summary

Table 5.3a lists estimated characteristics of the data processing system's components. (Ref. 6)

Table 5.3b Component Characteristics

Component	Mass (kg)	Volume(m^3)	Power (W)
(4) Processors	20	0.025	80
(3) Displays	10	0.015	90
(2) Mass Memory	16	0.016	40
(2) Keyboard	6	0.020	5
(4) Display & Engine Interfaces	14	0.020	40
(15) Bus Controllers	30	0.035	120
Totals:	96 kg	0.132 m^3	375 W

Wake Up Check

TOP TEN 412 LINES

10.) A little bitter over there?..........J. Travisano
9.) **No ! NOOOO! NNNOOOOOO!**......Wait a minute, wait a minute!!!...F. Carreon
8.) **Reeettttccchhhhh!!!!!**....... D. Stud Loveless
7.) This is going to be the funnest class of your undergrad. career....... M. Lewis.
6.) I Hate This **F'N CLASS** ....You name him/her.
5.) Well......actually, I pulled 10 gs in a Cessna........ it was by accident.......... E. Vandersall.
4.) **EEHH**! Oww Do Jew Work Dees Tings!!!! ....O. Bello
3.) Hey Dave, isn't it time for the confidential faculty meeting...... M. Lewis.
2.) Huh? .... D. Akin
1.) We have a PDR in 3 hours....**I NEED THAT COMPUTER NOW**......B. Rivers Hey, there's a herd running around the computer room! Bill just had a cow.....a lot of them......M. Gates

Section 5.4 Sensors

Introduction

In order for the Delta Manned Capsule to operate through computer and/or manual control, sensors are required. The sensors return information concerning all operational systems on the Delta Capsule to the astronauts for updates, as well as corrections. For this reason, sensors will be applied to the following systems: propulsions, main life support, secondary life support, reaction control, and abort.

Since the Delta Capsule will be performing rendezvous and docking, a Radar system will be required. This system will assist in the searching and tracking of satellites and the space station for extra vehicular activity, repairs and resupply.

Radar

In order for successful rendezvous and docking of the Delta Capsule, a Radar system had to be chosen. Restrictions of the system included power consumption, mass, antenna size and component volume. Of all radar systems researched, the Integrated Radar and Communications Subsystem (IRACS) proved to fit the requirements best.

The IRACS radar, developed by Hughes Aircraft Company, was initially tested on the space shuttle orbiter, Challenger, during its February 1984 Space Transportation System-11 (STS-11) mission. Its tracking capability and communication subsystem proved successful during these tests.

The major benefit of the IRACS radar system is that it not only operates as rendezvous radar, but can operate as a communications system which provides a two-way link between orbiter and ground tracking stations. The system is compatible with the Tracking and Data Relay Satellite System (TDRSS) and can be used as a backup in case of navigation malfunction.

For rendezvous, the IRACS system can operate in either passive or active mode. In passive mode, the radar has a range of twelve nautical miles with a 1m^2 noncooperative target. In active mode, the radar can track a target out to three hundred nautical miles which contains a transponder emitting a +14 dBm signal (See Table 1).

Specific differences in the physical system from the other radar systems researched can be found in the antenna and transmitter types. The radar signal

M. G. Kaczmarek

is transmitted on a center-fed parabola antenna, type I SBR, using linear polarization with a gain of 38.3 dB at 13.8 GHz. The transmitter employs a Traveling Wave Tube (TWT) with an peak power output of 50 Watts at approximately 44 dB (See Table 1).

Overall physical characteristics include a 75 kilogram total weight with a prime power requirement of 460 Watts (See Table 1). (Ref. 9)

Table 1: IRACS Radar Characteristics (Ref. 9)

Detection Performance	
Pd	99%
Target	1 m^2; Swerling I
Range	12 nmi
False-Alarm Rate	1/hr
Search Scan	+- 30 Degree Cone
Track Performance	
Angle Accuracy	8 mrad
Angle Rate	0.14 mrad/angle Accuracy 80 ft, R < 1.3 < R < 4.9 nmi; 1% of R, 1.3 < R < 4.9 nmi 300 ft, 4.9 < R < 12 nmi
Range Rate Accuracy	1 ft/s, R < 10 nmi
System Parameters	
RF	13.75-14.02 GHz
PRF	0.3, 3, 7 kHz
Pulsewidth	0.122,2.075,4.15,8.3, 16.6, 33.2, 66.4 micro sec
System Noise Temperature	Approx. 1585 K
Antenna	
Type	Parabola; prime-focus feed
Diameter	36in
Depth	12.5in, overall
Gain	38.4 dB at 13.8 GHz
Beamwidth	1.68 Degrees
Polarization	Linear
Transmitter	
Type	TWT
Peak Power	50 Watts
Gain	Approx. 44 dB
Receiver	
Type	Single-Channel Monopulse
Noise Figure	< 5 dB; GaAs FET LNA
System (Physical)	
Deployed Assemblies Weight	61.2 kgs
Radar Processor Weight	14.1 kgs
Electronics Volume	Approx. 3 ft^2
Prime Power	460 Watts

Trade studies were done on Lunar Sounder radar, SEASAT Synthetic Aperture radar, and OMV rendezvous radar systems.

Lunar Sounder radar was used on the Apollo 17 mission to map the surface of the moon, which can be adapted for use as a rendezvous radar system. Lunar Sounder radar is based on Synthetic Aperture Radar (SAR) tracking and mapping.

The hardware of Lunar Sounder radar consists of two separate radar subsystems; one operating on HF radiated signals, and another operating on VHF transmitted signals. The HF signals are sent and received by way of two center-fed dipole antennas extended on either side of the module. The VHF signals are transmitted via a Yagi antenna. Each subsystem can operate *simultaneously with data being sent to a ground station and/or on board CRT* located in the command module. Each antenna can be retracted, extended and controlled by the astronaut. (Ref. 10)

The major drawbacks of the system are found in the satisfactory resolution as compared to other radar systems researched (See Table 2).

Table 2: Lunar Sounder Radar System (Ref. 10)

	HF1	HF2	VHF
Wavelength (m)	60	20	2
Estimated Depth (m)	1300	800	260
Center Frequency (MHz)	5.266	15.8	158
RF Bandwidth (MHz)	0.5333	1.6	16.0
Pulsewidth (micro seconds)	240	80	8.0
Range Resolution, free source (m)	300	100	10
Transmitter Average Power (W)	12.4	3.7	1.5
Transmitter Peak Power (W)	130	118	95
Effective Antenna Gain (dB)	-0.8	-0.7	+7.3
Noise Figure (dB)	11.4	11.4	10.0
PRF $(s)^{-1}$	397	397	1984
AGC Gain Range (dB)	12.1	12.1	13.9
Recorder			
Duration (micro seconds)	600	600	70
Type	Optical		
Film Capacity	10 hr		
Weight	55 kg		
Prime Power	100 Watts dc, 17 VA, 400 Hz		
Radar System Weight	49 kg		
Radar Prime Power	103 Watts		

SEASAT-SAR was initially designed to study the earth's oceans for mapping and wave patterns, but it has found its way into the design of high-resolution spaceborne radar systems. SAR systems are designed to achieve satisfactory along-track azimuth resolution from 1 to 2 meters. Their carrier signal can be either transmitted via an extending antenna or deployable dish. (Ref. 9)

Compared to the other radar systems researched, the SEASAT-SAR system requires much more mass and volume then is available on the Delta Space Capsule (See Table 3).

Table 3: SEASAT Synthetic Aperture Radar (Ref. 9)

Antenna	
Type	Planar phased array (10.74m x 2.16m)
Beamwidth	1.1 AZ, 6 EL (1 dB points)
Look Angle	20 Degrees depression, 90 Degrees with respect to velocity vector
Gain	34.7 dB
Polarization	Horizontal
Weight	113 kg
Transmitter	
Type	Solid-State Transistor
Efficiency	38%
RF Carrier	1275 MHz
Peak Power	800W (nom), 1125W (max)
PRF	1463, 1540, 1645 pulses/s
Duty Cycle	0.056 (max)
Average Power	44.5W (nom), 62.6W (max)
Waveform	Pulse, LFM, 19-MHz bandwidth
Receiver	
Noise Temperature	550 K
Bandwidth	22 MHz
System Input Noise	-127.42 dBW
AGC Time Constant	5 s
STC Gain Variation	9 dB
STALO Stability	$3x10^{-10}$ in 5 ms
Recorder	25 kbs digital
System Weight	110 kg (excluding antenna)
Total Prime Power	624 W (max)
Resolution	25 m
Swath Width	1000 km
Swath Length	2000 km per pass
Swath Orientation	Right side of orbit path
Signal-to-Noise Ratio	9 dB (nom)

Orbital Maneuvering Vehicle (OMV) Rendezvous Radar, under development by the Motrola Corporation, is designed as an autonomous system with low volume, mass and power requirements (See Table 4).

Major benefits of the system are found in its Rendezvous Radar Set (RRS) and antenna type. The RRS contains parallel redundant electronics hardware on both the outboard assembly and inboard electronics requiring a prime power under 60 Watts. The antenna is a Type I SBR planar slotted array antenna with a gain of 30.5 dB at 9.65 GHz. (Ref. 9)

Although the OMV system requires under 60 Watts of power and takes up approximately thirty-five kilograms in weight, its development will not be completed until late 1995 making it unavailable for use on the Delta Space Capsule.

Table 4: OMV Radar Characteristics (Ref. 9)

Detection Performance	
Pd	99%
Target	1 m^2; Swerling I
Range	4.5 nmi
False-Alarm Rate	1/hr
Search Scan	+- 20 Degrees cone
Scan Time	5 min
Track Performance	
Angle Accuracy	20 mrad
Range Accuracy	Greater of 20ft or 2% of range
Range-Rate Accuracy	Greater of 0.1 ft/s or 2% range rate
System Parameters	
RF	9.5-9.8 GHz
PRF	6.67 kHz
Pulsewidth	0.005, 0.2, 1.5, 15 micro sec
System Noise Temperature	Approx. 900 K
Antenna	
Type	Planar Slotted Array
Size	0.3556 m x 0.381 m
Depth	25.4 mm overall
Gain	30.5 dB at 9.65 GHz
Beamwidth	5.0 Degrees
Polarization	Linear
Transmitter	
Type	GaAs FET
Peak Power	2 Watts
Gain	Approx. 30 dB
Receiver	
Type	3-channel monopulse
Noise Figure	< 4 dB; GaAs FET LNA
System Physical	
Deployed Assembly Weight	11.8 kgs
Inboard Assembly Weight	22.7 kgs (redundant total)
Electronics Volume	Approx 2 ft^3 (redundant total)
Prime Power	< 60 Watts

Propulsion

For the propulsion system, It will be necessary to measure the conditions of the pressurant, oxidizer and propellant tank as well as the conditions of the plumbing and rocket combustion chamber. Conditions which will be measured are temperature, pressure, flow rate, and valve openings.

Temperature measurements will consist of tank temperatures of the pressurant, oxidizer and propellant as well as the temperature of the rocket combustion chamber. The tank temperature measurements will determine the necessity of abort based on an increase of the temperatures based on a maximum set by design. The measurements of the temperature of the rocket combustion chamber will determine the necessity for adjustments in the plumbing or tank system for its proper operation. A total of twenty temperature sensors ranging from 20 to 3000 Kelvin will be required in the system (See Table 5).

Pressure measurements consist of transducers installed inside of each tank as well as calibration gauges outside of each tank. There will also be pressure transducers installed at the pressurant filter and regulator as well as at the pressurant bleeder valve. Pressure measurements will also be taken inside of the combustion chamber of the rocket to determine the necessity to increase flow of either the propellant and oxidizer. A total of forty pressure sensors ranging from 1 to 30 MPa will be required for proper operation of the system (See Table 5).

The rate of flow from the propellant tank and the oxidizer tank will also be measured. These sensors will determine if the flow rate from the tanks remains consistent with the flow/propellant ratio set by design. For the plumbing and tanks, a total of approximately twenty flow rate sensors ranging from 300 to 800 cm^3/sec will be required in the system (See Table 5).

Valve sensors throughout the plumbing system as well as on the tank fill and bleeder lines will determine proper operation of the valves. The amount of valve sensors will approximately be ninety-two on the plumbing and tanks of the propulsion system (See Table 5).

The total amount of propulsion sensors required on the Delta Space Capsule will be one hundred seventy-two (See Table 5).

Table 5: Propulsion Sensors

Type	Range	Quantity
Temperature Sensors		
Pressurant Tank (2 Tanks)	20-100 Kelvin	4
Oxidizer Tank (2 Tanks)	100-400 Kelvin	4
Propellant Tank (2 Tanks)	100-400 Kelvin	4
Rocket Cmbstn. Chamber (4 Rockets)	1000-3000 Kelvin	8
Total Temperature Sensors		20
Pressure Sensors		
Pressurant Transducer (2 Tanks)	10-30 MPa	4
Oxidizer Transducer (2 Tanks)	1-4 MPa	4
Propellant Transducer (2 Tanks)	1-3 MPa	4
Pressurant Calibration Gauge (2 Tanks)	10-30 MPa	4
Oxidizer Calibration Gauge (2 Tanks)	1-4 MPa	4
Propellant Calibration Gauge (2 Tanks)	1-3 MPa	4
Pressurant Bleeder Valve Gauge (2 Lines)	10-30 MPa	4
Pressurant Filter & Regulator Gauge (2 Tanks)	10-30 MPa	4
Rocket Cmbstn. Chamber (4 Rockets)	1-3 MPa	8
Total Pressure Sensors		40
Flow Rate Sensors		
Propellant Flow	500-800 cm^3/sec	10
Oxidizer Flow	300-600 cm^3/sec	10
Total Flow Rate Sensors		20
Valve Sensors		
Tank Pressure Relief Valve (6 Tanks)	open/close	12
Tank Vent Valve (6 Tanks)	open/close	12
Tank Fill Valve (6 Tanks)	open/close	12
Tank Pressure Regulation Switch (6 Tanks)	open/close	12
Tank Supply Valve (6 Tanks)	open/close	12
Gas Filter Valve (2 Lines)	open/close	4
Pressurant Bleeder Valve (2 Lines)	open/close	4
High Pressure Gas Valve (2 Lines)	open/close	4
Pressurant Isolation Valve (2 Lines)	open/close	4
Check Valve (2 Lines)	open/close	8
Rocket Ignition Switch (4 Rockets)	on/off	8
Total Valve Sensors		92
Total Propulsion Sensors		172

Human Factors - Main Life Support System

For the main life support system of the Delta Capsule it will be necessary to measure the conditions of the nitrogen and oxygen tanks as well as cabin conditions.

Temperature measurements will be made in each of the tanks and also in the cabin. Temperature measurements on the nitrogen and oxygen tanks were not available for the final draft. Heater Freon temperature measurements will be made for proper cooling of the cabin, nitrogen and oxygen tanks ranging from 150 to 350 Kelvin. Cabin temperature measurements will range from 280-300 Kelvin. Eleven temperature sensors will be require in the system (See Table 6).

Pressure sensors are similar to those in the propulsion system where it will be necessary to measure the pressure in each tank: nitrogen, and oxygen. It will also be necessary to measure the pressure in the crew cabin as well. The total number of pressure sensors required in the system is nineteen (See Table 6).

Flow rates of the nitrogen/oxygen pump will also be measured in order to determine the amount left in each tank during the flight. Heater flow rates will be measured in the system as well as the rate of nitrogen and oxygen flowing through the plumbing (See Table 6).

Valve sensors will be placed in all the tanks as well as the pump, heater, and solid amine filter operation. These sensors will determine if each element is operation or not (See Table 6). The total number of valve sensors required is twenty-eight.

It is also necessary to measure the levels of nitrogen, oxygen and carbon dioxide in the cabin. Measurements of humidity and cabin radiation will also be taken into account (See Table 6).

The total number of main life support system sensors is ninety-five.

Table 6: Human Factors - Main Life Support System

Type	Range	Quantity
Temperature Sensors		
Oxygen Tank (1 Tank)	????	2
Nitrogen Tank (1 Tank)	????	2
Heater Freon	150-350 Kelvin	4
Cabin	280-300 Kelvin	3
Total Temperature Sensors		11

Table 6: Human Factors - Main Life Support System (Continued)

Type	Range	Quantity
Pressure Sensors		
Oxygen Transducer (1 Tank)	5-6 MPa	2
Nitrogen Transducer (1 Tank)	5-6 MPa	2
Oxygen Tank Calibration Gauge (1 Tank)	5-6 MPa	2
Nitrogen Tank Calibration Gauge (1 Tank)	5-6 MPa	2
Heater Gauge	????	6
Heater Pressure Change Gauge	????	2
Cabin	0-0.2 MPa	3
Total Pressure Sensors		19
Flow Rate Sensors		
Heater	450-910 kg/hr	2
Oxygen/Nitrogen Pump	????	2
Oxygen Plumbing	????	6
Nitrogen Plumbing	????	6
Total Flow Rate Sensors		16
Filter Level Sensors		
Carbon Dioxide Filter	????	2
Solid Amine Filter	????	2
Smoke/Dust Filter	0.5 micro meters up to 10^3 parts/mill.	2
Total Filter Sensors		6
Valve Sensors		
Oxygen Tank		
Relief Valve (1 Tank)	open/close	2
Tank Vent Valve (1 Tank)	open/close	2
Fill Valve (1 Tank)	open/close	2
Regulation Switch (1 Tank)	open/close	2
Supply Valve (1 Tank)	open/close	2
Nitrogen Tank		
Relief Valve (1 Tank)	open/close	2
Tank Vent Valve (1 Tank)	open/close	2
Fill Valve (1 Tank)	open/close	2
Regulation Switch (1 Tank)	open/close	2
Supply Valve (1 Tank)	open/close	2
Pump Operation	on/off	2
Separator Operation	on/off	2
Solid Amine Filter Operation	on/off	2
Heater Operation	on/off	2
Total Valve Sensors		28

Table 6: Human Factors - Main Life Support System (Continued)

Type	Range	Quantity
Level Sensors		
Cabin Nitrogen	75-85%	3
Cabin Oxygen	15-25%	3
Carbon Dioxide	Amount Extracted	3
Radiation	17-140 mrems	3
Humidity	40-60%	3
Total Level Sensors		15
Total Main Life Support Sensors		95

Human Factors - Secondary Life Support System

The sensors for the secondary life support system are similar to those in the main life support system due to their similar design. The only difference occurs in the addition of astronaut suit connection sensors. Once the secondary life support system is initiated, it will no longer be necessary to measure the conditions in the cabin. The total number of sensors required is eighty-four (See Table 7).

Table 7: Human Factors - Secondary Life Support System

Type	Range	Quantity
Temperature Sensors		
Oxygen Tank (1 Tank)	????	2
Nitrogen Tank (1 Tank)	????	2
Heater Freon	150-350 Kelvin	4
Total Temperature Sensors		8
Pressure Sensors		
Oxygen Transducer (1 Tank)	5-6 MPa	2
Nitrogen Transducer (1 Tank)	5-6 MPa	2
Oxygen Tank Calibration Gauge (1 Tank)	5-6 MPa	2
Nitrogen Tank Calibration Gauge (1 Tank)	5-6 MPa	2
Heater Gauge	????	6
Heater Pressure Change Gauge	????	2
Total Pressure Sensors		16
Flow Rate Sensors		
Heater	450-910 kg/hr	2
Oxygen/Nitrogen Pump	????	2
Oxygen Plumbing	????	6

Table 7: Human Factors - Secondary Life Support System

Type	Range	Quantity
Nitrogen Plumbing	????	6
Total Flow Rate Sensors		16
Filter Level Sensors		
Carbon Dioxide Filter	????	2
Solid Amine Filter	????	2
Smoke/Dust Filter	0.5 micro meters up to 10^3 parts/mill.	2
Total Filter Level Sensors		6
Valve Sensors		
Oxygen Tank		
Relief Valve (1 Tank)	open/close	2
Tank Vent Valve (1 Tank)	open/close	2
Fill Valve (1 Tank)	open/close	2
Regulation Switch (1 Tank)	open/close	2
Supply Valve (1 Tank)	open/close	2
Nitrogen Tank		
Relief Valve (1 Tank)	open/close	2
Tank Vent Valve (1 Tank)	open/close	2
Fill Valve (1 Tank)	open/close	2
Regulation Switch (1 Tank)	open/close	2
Supply Valve (1 Tank)	open/close	2
Pump Operation	on/off	2
Separator Operation	on/off	2
Solid Amine Filter Operation	on/off	2
Heater Operation	on/off	2
Suit Connection (5 Astronauts)	yes/no	10
Total Valve Sensors		38
Total Secondary Life Support Sensors		84

Reaction Control System

The reaction control system consists of 2 sets of tanks located at the upper and lower sections of the Delta capsule. The pressures and temperatures of each of these tanks will be measured in the system. The pressure of each thruster in the reaction control system will be taken into account in order to allow the computer to re-route required thrust and compensate for any malfunctions in the system. The total number of sensors required in the reaction control system equals ninety-eight (See Table 8).

Table 8: Reaction Control System

Type	Range	Quantity
Temperature Sensors		
Pressurant Tank (2 Tanks)	200-280 Kelvin	4
Oxidizer Tank (2 Tanks)	250-300 Kelvin	4
Propellant Tank (2 Tanks)	250-300 Kelvin	4
Total Temperature Sensors		12
Pressure Sensors		
Chamber Pressure (32 Rockets)	0-0.6 MPa	32
Pressurant Transducer (2 Tanks)	8-12 MPa	4
Oxidizer Transducer (2 Tanks)	1-1.5 MPa	4
Propellant Transducer (2 Tanks)	1-1.5 MPa	4
Pressurant Calibration Gauge (2 Tanks)	8-12 MPa	4
Oxidizer Calibration Gauge (2 Tanks)	1-1.5 MPa	4
Propellant Calibration Gauge (2 Tanks)	1-1.5 MPa	4
Total Pressure Sensors		56
Valve Sensors		
Tank Pressure Relief Valve (3 Tanks)	open/close	6
Tank Vent Valve (3 Tanks)	open/close	6
Tank Fill Valve (3 Tanks)	open/close	6
Tank Pressure Regulation Switch (3 Tanks)	open/close	6
Tank Supply Valve (3 Tanks)	open/close	6
Total Valve Sensors		30
Total Reaction Control System Sensors		98

Abort Systems

The abort system is made up of the abort tower and solid fuel rocket booster located on top of the Delta command module. This system consists of a solid fuel rocket booster which will ignite in case of any malfunctions occur prior to launch. Measurements throughout the system include electro/static buildup, chamber pressure of the rocket, and ignition controls. The abort control sensors will be placed on the system to guarantee that the tower has been deployed after launch and prior to re-entry (See Table 9). The total number of sensors used to operate this system is ten.

Table 9: Abort System

Type	Range	Quantity
Solid Fuel Rocket		
Electro/Static Buildup	????	2
Chamber Pressure	1-5 MPa	2
Ignition Control	on/off	2
Ejection Control	on/off	2
Abort Control	on/off	2
Total Sold Fuel Rocket Sensors		10

Miscellaneous Sensors

Extra sensors added to the Delta system include hatch and ejection determinations. It is necessary to guarantee that the astronaut entry hatch and the parachute deployment hatch are secure prior to launch and open when needed. Docking confirmation will be checked prior to astronaut exit from the command module. The determination of the abort tower ejection as well as the service module ejection will also be checked after launch and prior to re-entry. The total number of Miscellaneous sensors is ten (See Table 10).

Table 10: Miscellaneous Sensors

Type	Range	Quantity
Astronaut Entry Hatch	open/close	2
Parachute Deployment Hatch	open/close	2
Docking Confirmation	yes/no	2
Service Module Ejection	on/off	2
Abort Tower Ejection	on/off	2
Total Miscellaneous Sensors		10

Conclusion

Many different types of radar systems have been looked into to place on the Delta spacecraft since it is not greatly restricted to power, weight, and volume requirements. Based on all the types of systems researched, the Integrated Radar and Communications Subsystem proved to be the most reasonable choice in power and mass requirements as well as resolution and range.

Contained on the Delta orbital vehicle will be four hundred sixty-nine sensors making checks on all systems to guarantee proper functioning and allowing for necessary changes if malfunction occur.

Only those sensors necessary for the proper operation have been taken into account on the Delta sensors system. Any other extraneous sensor (example: reaction control system flow rate sensors placed along all plumbing lines) have been removed. This brings the total weight of the sensors to approximately thirty kilograms. The use of optical fiber wiring in the Delta system contains the very minimum amount of heat and radiation shielding. Approximately one hundred twenty kilograms have been set aside for wiring and digital/analog converters. The entire mass of the sensors system on the Delta service module is approximately one hundred fifty kilograms.

All sensors have been made double redundant and are 99.999% reliable.

Section 5.5 Communications

Introduction

Communications are needed for video and voice contact, data transmissions for rendezvous and navigation and in conducting experiments. It is also needed if there are any changes in the mission plan due to failures in equipment or on ground procedures. Communications adds safety to the situation of being a long way from the natural environment of earth. Other systems under communications are radar and EVA communications and telemetry.

On the Delta D.A.R.T. spacecraft the avionics was initially given a mass budget of 400 Kg. This budget allowed for any communicational needs that the missions may require. The possibilities include full video, audio, data, EVA, radar and navigational transmissions. All of which have been implemented on the Delta D.A.R.T. spacecraft. The following is the composition of the communications package on board the Delta D.A.R.T. spacecraft.

Receiving Stations

In order to insure communications are reliable two modes of communication have been chosen. One communication path through TDRSS and one directly to earth stations.

The primary receiving station will be the Telemetry Data Relay Satellite System better known as TDRSS. It consists of two satellites that enable communications for 80 minutes of the 95 minute orbit. This is how the system exists now, however by the year 1995 there should be at least three or up to five total satellites in the system. Having more satellites would enable constant communication capability. In order to communicate through TDRSS frequencies must be chosen from the S, C or Ku bands. These bands are chosen for their few atmospheric losses in transmission to earth. The range of 1 to 10 GHz is the only range with these few losses.

If communications cannot be made through TDRSS for what ever the reason the second choice for a receiving station will be direct transmission to earth. The number of earth stations is limited, however there exists enough to say there could be at least three used per orbit which would account for about 30 minutes of transmission time per 95 minute orbit.

The capsule will also receive transmissions from the Global Positioning System (GPS). These communications are used navigation as discussed in section 5.1. The capsule is passive in its communications with GPS. For its communicational requirements, they are as follows: They system is an off-the-self item consisting of an antenna and a receiver. The system operates on two frequencies, one at 1.575 GHz and one at 1.228 GHz. The systems mass, volume and power are as discussed in section 5.1. The antenna is placed on the capsule surface facing outwards to GPS, which can be seen in the exterior layout in earlier chapters.

These are the modes of communications for the capsule. Others for the capsule consist of EVA communications and telemetry which will be accomplished on the UHF band for compatibility with previous systems on other capsule systems.

Frequency Assignments

The frequency assignments are based in the S and Ku bands and are spaced so that not more than 500 MHz will be assigned for any one transponder as suggested by Morgan and Gordon in the Communications Satellite Handbook. (Ref. 11) The base frequencies were chosen to model the system and to calculate the quality of system. The frequencies may change slightly for exact system compatibility later in production, but will not change the calculations significantly.

The bandwidth for these base frequencies are determined from the amount of data that must be transmitted each second and the clarity that the data must have in order to receivable. For this reason data requires a larger bandwidth than voice for approximately the same data rate. The bandwidth is limited by the systems power and gain. For the systems frequency assignments see Table 5.5A.

Component	Frequency	Data Rate	Bandwidth
Voice Uplink	2.1 GHz	56 Kbit/s	4 KHz
Voice Downlink	2.2 GHz	56 Kbit/s	4 KHz
Command Uplink	2.15 GHz	64 Kbit/s	36 KHz
Data Downlink	2.25 GHz	64 Kbit/s	36 KHz
Video Uplink	12.1 GHz	1 Mbit/s	56 MHz
Video Downlink	12.2 GHz	1 Mbit/s	56 MHz
EVA	0.9 GHz	-	-
Rendezvous Radar	12.4 GHz	-	-
GPS Link L1	1.575 GHz	-	-
GPS Link L2	1.228 GHz	-	-

Table 5.5A Frequency Assignments

Link Budgets

The link budgets are used to determine whether or not a signal will be receivable. The method used in this analysis was taken from Communications Satellite Handbook. This process looks at the transmitters qualities and the losses in going to the receiver and then the receiver's ability to clearly interpret the signal.

A3.1

Appendix A3.1.1

Calculation of pressure cabin thickness

With the dimensions of the outer wall given (see Figure A3.1.1) the thickness of the pressure cabin wall can be calculated assuming the internal pressure remain constant as altitude increases. Note this is not the thickness of the outer shell. For the ideal situation the necessary internal pressure is assumed to be 15 psi greater than the outside pressure.

P= 15 psi = 103421.36 Pa
with a Factor of safety of 1.4 imposed (an assumed value)
P= 15 psi * 1.4 = 144789.90 Pa

Using the Pressure Handbook for formulas in terms of outside dimension for a conical section :

$$t = \frac{P \times D}{2 \times \cos \alpha \times (SE \times + .4 \times P)}$$

P= design pressure (psi)
D= outside bottom diameter (in.)
$\alpha = \frac{1}{2}$ of the included (apex) angle (degrees)
S= Tensile stress of material (psi)
E = Joint efficiency =1

Using Aluminum 2024-T4 where the tensile stress = 427.48 MPa (See Table 3.1.1). Aluminum 2024-T4 was used due to the low internal pressure.

S = 427.48 MPa= 62000.732 psi

$$t = \frac{15\ \text{psi} \times 1.4 \times 3.5\text{m} \times 39.37 \frac{\text{in}}{\text{m}}}{2 \times \cos {}^\circ 15 \times (62000.732 \times (1) + .4 \times 15\text{psi} \times 1.4)}$$

t = .0241 in. = .614 mm

F.Carreon

Appendix A3.1.2

Calculation of center of gravity

(See figure 3.1.2 for material placement along with Table 3.1.3 for coordinate location)

$$m_{total} \times r_{center} = \Sigma\, m_i \times r_i$$

$$r_{center} = \frac{\Sigma\, m_i \times r_i}{m_{toal}}$$

$$\begin{gathered} r_{center} = [[33\text{ kg}\times -.334j] + [2.9\text{ kg}\times -.125j] + [(2\times 15.338\text{ kg}) + 20] \\ 70\text{ kg}\times .18j + 3\times 247\text{ kg}\times 8.135\,j + 38.5\text{ kg}\times 5.225j \\ +500\text{ kg}\times -.205j + 3\times 119.9\text{ kg}\times .28j + 2\times 119.9\text{kg}\times 1.725j \\ +12.62\text{ kg}\times 3.925\,j + 15.44\text{ kg}\times(1.085\,i + 2.475j) \\ +15\text{kg}\times(-1.614i + .2j) + 200\text{kg}\times 3.975j + 662.45\text{kg}\times .2j]/3708.79\text{ kg} \end{gathered}$$

$r_{center} =$ 2.08 j m from bottom

F.Carreon

	Point loadings (kilogram)	Coordinate location with respect to the bottom center of the spacecraft (m)
Main propulsion tanks	2 (8.753 kg.+6.585 kg.) 20 kg for plumbing	(-.205 j)
Main engines	33 kg.	.1065 i -.334 j + .1065 k
	33 kg.	(-.1065 i -.334 j + .1065 k)
	33 kg.	.1065 i -.334 j - .1065 k
	33 kg.	(-.1065 i -.334 j - .1065 k)
Propulsion truss	2.9 kg	(-.125j)
Solar array	2 (35 kg.)	.18 j
Abort engines	3 (247 kg.)	8.135 j
Abort tower	38.5 kg.	5.225 j
Main fuel	500 kg.	(-0.205 j)
Heat shielding	293 kg	0
Crew with suits	119.9 kg	.623 i + .28j -.36 k
rear	119.9 kg	.28j +.72 k
	119.9 kg	(-.623 i + .28 j - .36 k)
crew with suits	119.9 kg	1.0 i + 1.725 j
front	119.9 kg	(-1.0 i +1.725 j)
Structures not accounted		
docking ring	12.62 kg	3.925j
Docking arm	15.44 kg	1.085i+2.475j
Deployable Dish Antenna	15 kg	(-1.614i+.2j)
Parachute	200 kg	3.975j
Impact ittentuation	129 kg	0
avionics package	662.45 kg	concentrated @ .2j
Total mass	3708.79 kg.	

F.Carreon

Center of gravity is

2.08 j meter from bottom

(-.244i) meter

F.Carreon

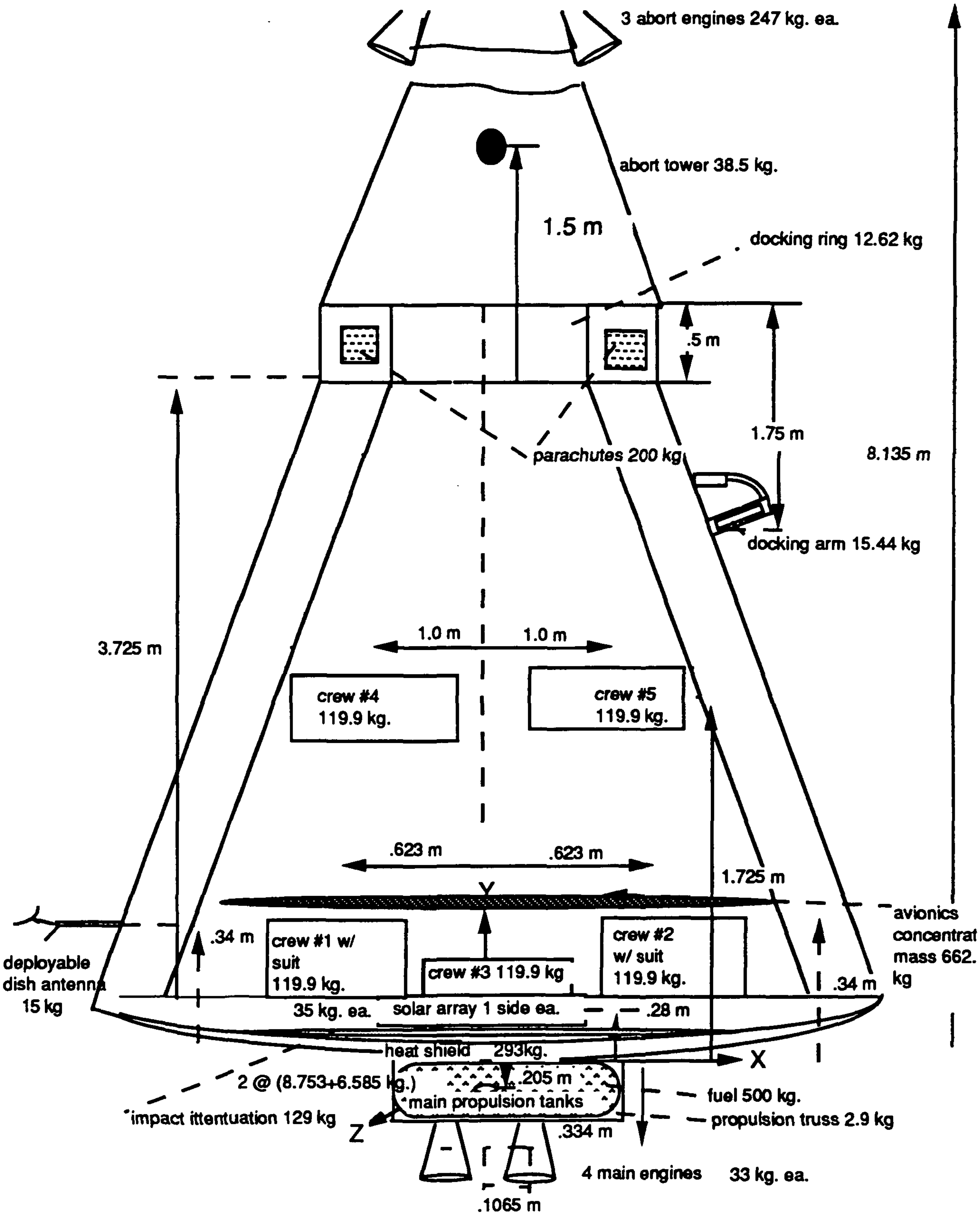

Figure 3.1 - Component layout for center of gravity

F.Carreon

Appendix A3.1.3 A.

Anlges	Stringers	Effective Area	STATION O	Station P
location of	number	avg of area of	Diameter= 1.5 m	diameter=2.035
stringers	(Graphite epoxy)	station S and O	height w.r.t central	height w. r.t central
		m^2	line (neutral Axis)	line (neutral axis)
			hi= rsin 0i	hi= rsin 0i
0	1	0.000208613	0	0
20	2	0.000371506	0.25679757	0.348151406
40	3	0.000489592	0.482551117	0.654312537
60	4	0.000489592	0.649969501	0.881557532
80	5	0.000549	0.738813668	1.002478546
80	6	0.000549	0.738813668	1.002478546
60	7	0.000489592	0.649969501	0.881557532
40	8	0.000489592	0.482551117	0.654312537
20	9	0.000371506	0.25679757	0.348151406
0	10	0.000208613	0	0
20	11	0.000371506	-0.25679757	-0.348151406
40	12	0.000489592	-0.482551117	-0.654312537
60	13	0.000489592	-0.649969501	-0.881557532
80	14	0.000549	-0.738813668	-1.002478546
80	15	0.000549	-0.738813668	-1.002478546
60	16	0.000489592	-0.649969501	-0.881557532
40	17	0.000489592	-0.482551117	-0.654312537
20	18	0.000371506	-0.25679757	-0.348151406
Axial force	A *		Iy of station O	Iy of station P
(maximum is	total stringer		with effective	with effective
due to abort=	area	SUM OF effective	stringer area	stringer area
10g's	0.008015986	cross-areas	0.002580023	0.004747379
4512600	m^2	80.15986166	0.002580023	0.004747379
N		Cm^2	m^4	m^4
		Mass of stringers	k2 at station O	K2 at station P
		45.38651367	387.5935058	210.6425589
			m^-4	m^-4
			My=Mz at station O	My= Mz at station Q
			978918.318	663036.318
			Nm	Nm

Appendix A3.1.3 B.

Station Q	Station R	Station S	station O	Station P
diameter =2.5717	diameter =3.10769	Diameter= 3.5m	D=1.5	D=2.305
height w. r.t centra	height w. r.t central	height w. r.t central	STATION O	
line (neutral axis)	line (neutral axis)	line (neutral axis)		
hi= rsin 0i	hi= rsin 0i	hi= rsin 0i	Yi=rcos0i	Yi=rcos Oi
0	0	0	0.75	1.017949
0.439793395	0.531435384	0.598521976	0.704771536	0.956561974
0.826543645	0.998774752	1.124856673	0.574541116	0.779804739
1.113605096	1.34565266	1.515523266	0.37501573	0.50899585
1.266355488	1.530232428	1.723403754	0.130259983	0.176797359
1.266355488	1.530232428	1.723403754	0.130259983	0.176797359
1.113605096	1.34565266	1.515523266	0.37501573	0.50899585
0.826543645	0.998774752	1.124856673	0.574541116	0.779804739
0.439793395	0.531435384	0.598521976	0.704771536	0.956561974
0	0	0	-0.75	-1.017949
-0.439793395	-0.531435384	-0.598521976	-0.70477154	-0.95656197
-0.826543645	-0.998774752	-1.124856673	-0.57454112	-0.77980474
-1.113605096	-1.34565266	-1.515523266	-0.37501573	-0.50899585
-1.266355488	-1.530232428	-1.723403754	-0.13025998	-0.17679736
-1.266355488	-1.530232428	-1.723403754	-0.13025998	-0.17679736
-1.113605096	-1.34565266	-1.515523266	-0.37501573	-0.50899585
-0.826543645	-0.998774752	-1.124856673	-0.57454112	-0.77980474
-0.439793395	-0.531435384	-0.598521976	-0.70477154	-0.95656197
ly of station Q	ly of station R	ly of station S	lz of station O	lz station P
with effective	with effective	with effective		
stringer area	stringer area	stringer area		
0.007575564	0.011061614	0.014030649	0.001931934	0.00355895
0.007575564	0.011061614	0.014030649	0.001931934	0.00355895
m^4	m^4	m^4	m^4	m^4
K2 AT STATION Q	K2 AT STATION R	K2 at station S	k3 at station O	K3 Station P
132.0033712	90.40271931	71.27253842	517.615983	280.9817834
m^-4	m^-4	m^-4	m^-4	m^-4
My= Mz at station Q	My= Mz at station Q	My=Mz at station P		
347154.318	31272.318	197742.132		
Nm	Nm	Nm		

Appendix A3.1.3 C.

Station Q	Station R	station S	dz/dx (P to O)	dz/dx (Q to P)	dz/dx (r to Q)
d=2.5717	d=3.10769	d=3.5			
		STATION P			
Yi=rcos Oi	Yi=rcos Oi	Yi=rcos0i			
1.285898385	1.553847575	1.75	0	0	0
1.208352774	1.46014339	1.64446692	0.09135384	0.09164199	0.09164199
0.985068657	1.190332426	1.34059594	0.17176142	0.17223111	0.17223111
0.642976162	0.776956377	0.8750367	0.23158803	0.23204756	0.23204756
0.223334803	0.269872212	0.30393996	0.26366488	0.26387694	0.26387694
0.223334803	0.269872212	0.30393996	0.26366488	0.26387694	0.26387694
0.642976162	0.776956377	0.8750367	0.23158803	0.23204756	0.23204756
0.985068657	1.190332426	1.34059594	0.17176142	0.17223111	0.17223111
1.208352774	1.46014339	1.64446692	0.09135384	0.09164199	0.09164199
-1.28589839	-1.55384758	-1.75	0	0	0
-1.20835277	-1.46014339	-1.6444669	-0.0913538	-0.091642	-0.091642
-0.98506866	-1.19033243	-1.3405959	-0.1717614	-0.1722311	-0.1722311
-0.64297616	-0.77695638	-0.8750367	-0.231588	-0.2320476	-0.2320476
-0.2233348	-0.26987221	-0.30394	-0.2636649	-0.2638769	-0.2638769
-0.2233348	-0.26987221	-0.30394	-0.2636649	-0.2638769	-0.2638769
-0.64297616	-0.77695638	-0.8750367	-0.231588	-0.2320476	-0.2320476
-0.98506866	-1.19033243	-1.3405959	-0.1717614	-0.1722311	-0.1722311
-1.20835277	-1.46014339	-1.6444669	-0.0913538	-0.091642	-0.091642
Iz station Q	Iz station R	Iz at station S			
0.005679147	0.008292522	0.01051831			
0.005679147	0.008292522	0.01051831			
m^4	m^4	m^4			
K3 Station Q	K3 Station R	k3 at station S			
176.0827868	120.5905778	95.0723234			
m^-4	m^-4				

dz/dx (S to R)	dz/dx entire lenght (O to S)	dy/dx entire lenght (O to S)	Stress(sigma b at station O Pa (N/m^2)	Stress at station P Pa (N/m^2)	Stress at station Q Pa (N/m^2)
0	0	0.26845638	942977899	842945308	784601234
0.06708659	0.0917381	0.25226722	1017495212	897849770	828064976
0.12608192	0.17243102	0.2056523	1037162916	912362234	839553411
0.16987061	0.23236343	0.13423382	999584933.5	884732365	817680930
0.19317133	0.26431949	0.0466255	909275740.1	818292580	765085554
0.19317133	0.26431949	0.0466255	909275740.1	818292580	765085554
0.16987061	0.23236343	0.13423382	999584933.5	884732365	817680930
0.12608192	0.17243102	0.2056523	1037162916	912362234	839553411
0.06708659	0.0917381	0.25226722	1017495212	897849770	828064976
0	0	-0.2684564	182922247.8	282954839	341298913
-0.0670866	-0.0917381	-0.2522672	108404934.8	228050377	297835171
-0.1260819	-0.172431	-0.2056523	88737230.84	213537912	286346735
-0.1698706	-0.2323634	-0.1342338	126315213.2	241167781	308219217
-0.1931713	-0.2643195	-0.0466255	216624406.6	307607567	360814593
-0.1931713	-0.2643195	-0.0466255	216624406.6	307607567	360814593
-0.1698706	-0.2323634	-0.1342338	126315213.2	241167781	308219217
-0.1260819	-0.172431	-0.2056523	88737230.84	213537912	286346735
-0.0670866	-0.0917381	-0.2522672	108404934.8	228050377	297835171

Appendix A3.1.3

Stress at station R Pa (N/m^2)	Stress (sigma b at station S Pa (N/m^2)	Margin of Safety Station O	Margin of Safety Station P	Margin of Safety Station Q	Margin of Safety Station R
746379178	725819141.5	0.3161072	0.47229006	0.58177167	0.66277415
782347928	757756258.8	0.21972073	0.38225797	0.49874712	0.58632746
791855270	766197950.9	0.19659118	0.36027112	0.47823829	0.56728135
773754532	750126071.6	0.24157534	0.40275189	0.51778029	0.60394537
730228828	711479038.1	0.3648885	0.51664579	0.62211924	0.69954944
730228828	711479038.1	0.3648885	0.51664579	0.62211924	0.69954944
773754532	750126071.6	0.24157534	0.40275189	0.51778029	0.60394537
791855270	766197950.9	0.19659118	0.36027112	0.47823829	0.56728135
782347928	757756258.8	0.21972073	0.38225797	0.49874712	0.58632746
379520969	400081005.2	5.78463126	3.38607096	2.63628466	2.27006965
343552219	368143887.9	10.4483718	4.44204318	3.16693568	2.61243483
334044876	359702195.9	12.9857869	4.81189535	3.33411612	2.71524932
352145615	375774075.1	8.82510316	4.14604394	3.02654972	2.52428072
395671318	414421108.6	4.72908667	3.03455615	2.4396059	2.13659329
395671318	414421108.6	4.72908667	3.03455615	2.4396059	2.13659329
352145615	375774075.1	8.82510316	4.14604394	3.02654972	2.52428072
334044876	359702195.9	12.9857869	4.81189535	3.33411612	2.71524932
343552219	368143887.9	10.4483718	4.44204318	3.16693568	2.61243483

Margin of Safety Station S	Fx * (dy/dx) station S	Fx * (dz/dx) station O	Fx * (dz/dx) station P	Fx * (dz/dx) station Q	Fx * (dz/dx) station R
0.70987499	-4.064841609	0	0	0	0
0.63780897	-7.101600564	-3.46775166	-3.04716771	-2.81919306	-2.663546823
0.61976419	-7.714519126	-8.75581713	-7.67232908	-7.07936375	-6.677158814
0.65446856	-4.929813673	-11.3716052	-10.0314179	-9.28956088	-8.790519037
0.74433811	-1.821201212	-13.1946274	-11.8449502	-11.0836751	-10.57871112
0.74433811	-1.821201212	-13.1946274	-11.8449502	-11.0836751	-10.57871112
0.65446856	-4.929813673	-11.3716052	-10.0314179	-9.28956088	-8.790519037
0.61976419	-7.714519126	-8.75581713	-7.67232908	-7.07936375	-6.677158814
0.63780897	-7.101599557	-3.46775116	-3.04716728	-2.81919266	-2.663546445
2.1020218	2.240593867	0	0	0	0
2.37112754	3.450200261	0.369457652	0.773968841	1.013996332	1.169642544
2.45024305	3.621687407	0.749127214	1.795704679	2.41456073	2.816765605
2.30267595	2.469579773	1.437003191	2.734448183	3.501636242	4.000677998
1.99468336	1.060810207	3.143467046	4.452681604	5.227064749	5.732028662
1.99468336	1.060810207	3.143467046	4.452681604	5.227064749	5.732028662
2.30267595	2.469579773	1.437003191	2.734448183	3.501636242	4.000677998
2.45024305	3.621687407	0.749127214	1.795704679	2.41456073	2.816765605
2.37112754	3.450200261	0.369457652	0.773968841	1.013996332	1.169642544
	sum (shear taken)	sum shear	sum shear	sum shear	sum shear
	-23.75396059				
		-62.1814921	-45.6781228	-36.2290691	-29.98164159
	N	N	N	N	N
	thickness of outer skin	Vweb station O	Vweb station P	Vweb station Q	Vweb station R
		442172.6185	442189.1219	442198.5709	442204.8184
		N			
		flexural shear flow station O	flexural shear flow station P	flexural shear flow station Q	flexural shear flow station R
		0	0	0	0
		16350.27798	12047.25834	9537.113566	7892.622398
		56840.10892	41885.53379	33158.34036	27440.82452
		111377.658	82086.74496	64983.30049	53778.1845
		180892.19	133349.4605	105565.0101	87362.3615
		250406.722	184612.1759	146146.7197	120946.5385
		304944.2711	224813.3871	177971.6798	147283.8985
		345434.102	254651.6626	201592.9066	166832.1006
		361784.3777	266698.9192	211130.0188	174724.7219
		361784.3777	266698.9192	211130.0188	174724.7219
		345434.0997	254651.6609	201592.9052	166832.0995
		304944.2688	224813.3854	177971.6784	147283.8974
		250406.7197	184612.1742	146146.7183	120946.5374

Appendix A3.1.3

		180892.1877	133349.4587	105565.0087	87362.36038
		111377.6557	82086.74325	64983.29914	53778.18338
		56840.1066	41885.53208	33158.33901	27440.8234
		16350.27566	12047.25663	9537.112213	7892.621278
		-0.00231937	-0.00170896	-0.00135289	-0.001119608
		max shear	max shear	max shear	max shear
		flow station O	flow station P	flow station Q	flow station R
		361784.3777	266698.9192	211130.0188	174724.7219
		N/m	N/m	N/m	N/m

Fx * (dz/dx)	Fx * (dy/dx)
station S	station O
0	-5.2810068
-2.58252864	-9.5358428
-6.46830796	-10.442749
-8.53367961	-6.5692524
-10.3243718	-2.3275093
-10.3243718	-2.3275093
-8.53367961	-6.5692524
-6.46830796	-10.442749
-2.58252827	-9.5358415
0	1.02442871
1.254680673	1.01595802
3.036636386	0.89345719
4.274928819	0.83014108
6.013722639	0.55450212
6.013722639	0.55450212
4.274928819	0.83014108
3.036636386	0.89345719
1.254680673	1.01595802
sum (shear	sum (shear)
stringer	
-26.6578386	-55.419168
N	N
Vweb station S	
442208.1422	
N	
flexural	
shear flow S	
0	
7008.013927	
24365.24525	
47750.70274	
77570.75091	
107390.7991	
130776.2566	
148133.4879	
155141.5008	
155141.5008	
148133.4869	
130776.2556	
107390.7981	

Appendix A3.1.3

77570.74992	
47750.70174	
24365.24426	
7008.012933	
155141.5008	
Max shear	
flow station S	
155141.5008	
N/m	

Appendix 3.1.3

Station	Coordinates	Stress area 1	Margin of	Stress area 2	Margin of
	of centroid	N/m^2	Safety	N/m^2	safety
		b= 2.54 cm		b=2.54 cm	
		t=3.0 cm	Area=2.09 cm^2	t=2.8 cm	Area =3.72 cm^2
1	(-b-2t,.5t)	3.95E+09	1.31	3.79E+09	1.33
2	(-b/2+t/2,b/2)	1.51E+09	0.18	2.61E+09	0.52
3	(b-t/2,0)	1.47E+09	0.16	1.02E+09	0.22
4	(b/2-t/2,b/2)	1.25E+09	0.01	2.48E+09	0.50
5	(b-2t,.5t)	2.13E+09	0.42	2.98E+09	0.58
		Izz		Izz	
		area 1		area 2	
		4.43E-07		3.72E-07	
		m^4		m^4	
		Iyy		Iyy	
		area 1		area 2	
		2.07E-06		1.66E-06	
		m^4		m^4	

Appendix 3.1.3

Stress area 3	MARGIN OF	Stress area 4	MARGIN OF
N/m^2	of safety	N/m^2	Safety
b=2.54 cm		b=2.54 cm	
t=2.7 cm	Area=4.90 cm^	t= 2.65 cm	Area=5.49 cm^2
3.46E+09	1.36	3.85E+10	1.03
2.69E+09	0.54	3.05E+09	0.59
9.78E+08	0.27	6.54E+09	0.81
2.61E+09	0.52	6.25E+08	0.99
1.65E+09	0.25	-1.13E+10	0.89
Izz		Izz	
area 3		area 4	
3.23E-07		3.00E-07	
m^4		m^4	
Iyy		Iyy	
area 3		area 4	
1.37E-06		1.08E-07	
m^4		m^4	

A3.2

Appendix 3.2.1

Mass breakdown for the first system

Parts	Mass (kg)
Main docking ring	11.12
Crawl Tube	1.5
Actuators	4.8
Inert fingers	5.6
Drone	3.05
Bolts and Nuts	2.3
Adapter	22.7
Total	51.07

Ola Bello

Appendix 3.2.2

Mass breakdown for the second system

Parts	Mass(kg)
Main docking ring	11.12
Crawl tube	1.5
Actuators	6.44
Fluid	2.3
Shock Absorbers	5.3
Folding actuator	2.0
Bolts and Nuts	1.2
Total	29.86

Ola Bello

Appendix 3.2.3

Typical Sample Calculation of forces, mass, and stress analysis

Damping force on the shock absorber

Damping Force = - c dx/dt (1.2)

where : c = damping coefficient = 1.4x10^7 g/s=1.4x10^4 kg/s

dx/dt = vertical velocity = 2m/s

Damping Force = 2.8x10^4 kgxm/s^2

Stress analysis on the steel cable

Sigma = Exdw/D

Where : E = Modulus of elaciticity = 12 Mpsi

dw= diameter of the wire cable = .01m

D = sheave diameter, di/22.

Sigma = 22.23Mpsi

Mass for a cylindrical shapes was calculated using these form

M = Pi x L xRo/4xg{do^2-di^2}

Where : L = height of the cylinder

Ro = density of the material

do = outside diameter

di= inside diameter

g= accelleration of gravity

O. Bello

A4.1

Appendix A4.1.1

This is a list of the pros and cons that went into the decision between the two propulsion systems. In very decisive group meeting the strap-on propulsion package was chosen over the bolt-on system. These are most of the pros and cons that were decided upon in that meeting. Included is a sketch of the bolt-on system (figure A4.1a).

Bolt-on Pros
- Propellant tanks and plumbing are reusable

Bolt-on Cons
- Engines are located about 1.5 m off of centerline
- Could possibly interfere with an explosive egress hatch
- Less volume for the pressure vessel
- Would interfere with a para-shield
- Explosive bolt scars near re-entry surface
- Relatively new technology

Strap-on Pros
- Provides more room for the pressure vessel
- Located about 10 cm off of centerline
- Less weight for re-entry
- Relatively old and proven technology

Strap-on Cons
- Cost to replace tanks, plumbing and housing structure
- Could possibly cause problems with the avionics monitoring equipment
- Raises the center of gravity

A4.1.1

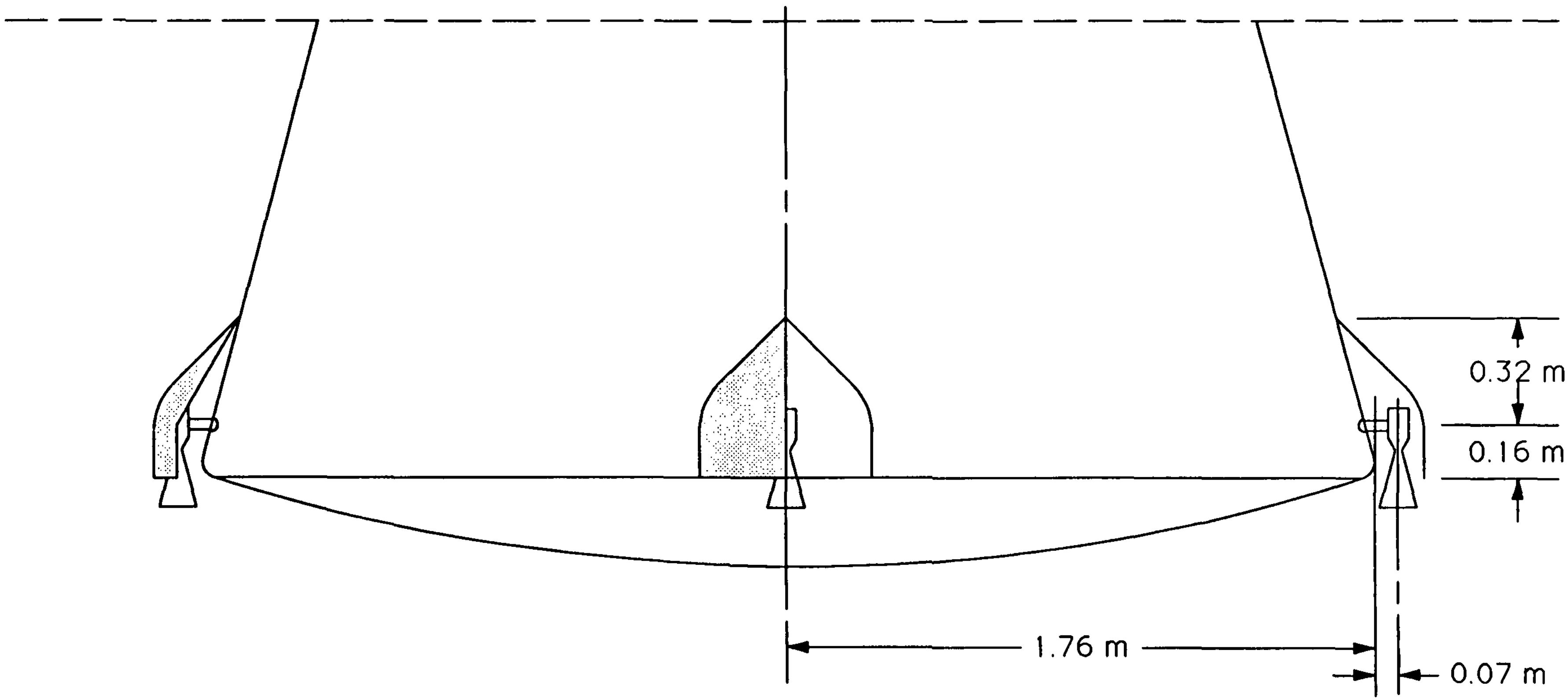

Figure A4.1a : "Bolt-on" Engine System

Appendix A4.1.2

This program is used to vary the thrust and exit diameter to determine the variation in some parameters such as chamber pressure and propellant mass flow. The equations that are used in this program are from reference 4.1. The assumptions used in this program are that the flow is isentropic and that thenozzle is one-dimensional.

```
      REAL AE,DE,FTE,FTM,T1E,T1M,M,R,K,PEE,PEM,P1M,P1E,E1
      REAL MDOT,VOL1,ARAT,AT,VOLT,VOLE,UT,U1,EPC,VC,VCDUM
      REAL LCY,GEE,ISP,BET,MC,ME,MASSC,UMT,UME,MASSN
      REAL WGT,MASS,THK,E2,U2,ETA,A1,BETA
      EXTERNAL WGT,MASS,THK
      PARAMETER (GEE=9.8066,U1=91.0)
C FUEL: HYDRAZINE AND NITROGEN TETRAOXIDE
      PARAMETER (M=19.0,K=1.26,T1M=2857.0)
C EXIT PRESSURE IS SET FOR SPACE (1 psi)
      PARAMETER (PEE=1.0)
C ***** NEED EXIT DIAMETER, DE, CHAMBER LENGTH, LCY, CHAM
ANGLE,BET
      PI=2*ASIN(1.0)
      E1=(K-1.0)/K
      E2=1.0/K
      WRITE (5,*) ' Thrust(lbs) Exit D(m) Flow rate(kg/s) Area Ratio
   *ChamPres(psi) Exit Vel(m/s)'
C ***** LOOP VARYING THRUST
      DO 200 FTE=100.0,500.0,50.0
C ***** LOOP VARYING EXIT DIAMETER
      DO 100 DE=0.05,0.15,0.01
C CALCULATION OF EXIT AREA (m2)
            AE=(PI)*(DE/2.0)**2.0
C CONVERSION TO METRIC UNITS (N,K,Pa)
            FTM=FTE*4.4482
            PEM=PEE*6.8948E3
C CALCULATION OF GAS CONSTANT (J/K*kg)
            R=8.31434E3/M
C CALCULATION OF CHAMBER PRESSURE P1(FT,K,Ae,Pe) (Pa)
            P1M=((FTM*(K-1.0)/(2*K*AE*PEM**E2))+PEM**E1)**(1/E1)
            P1E=P1M/6.8948E3
            ETA=1-(PEM/P1M)**E1
C CALCULATION OF EXIT AND THROAT VELOCITIES (m/s)
            U2=0.98*((2.0*K*R*T1M*ETA/(K-1.0))**(0.5))
            UT=(2.0*K*R*T1M/(K+1.0))**(0.5)
C CALCULATION OF SPECIFIC VOLUME (m3/kg)
            VOL1=R*T1M/P1M
            VOLT=VOL1*((K+1.0)/2.0)**(1.0/(K-1.0))
            VOLE=VOL1*(P1M/PEM)**E2
```

```
C CALCULATION OF PROPELLANT FLOW RATE (kg/s)
            MDOT=(FTM-PEM*AE)/U2
C CALCULATION OF THROAT AREA AND EXIT/THROAT (m2)
            AT=MDOT*VOLT/UT
            ARAT=AE/AT
C CALCULATION OF CHAMBER AREA AND CHAMBER/THROAT (m2)
            A1=MDOT*VOL1/U1
            EPC=A1/AT
C CALCULATION OF SPECIFIC IMPULSE
            ISP=(U2+PEM*AE/MDOT)/GEE
            IF (P1E.LT.500.0.AND.P1E.GT.250) THEN
             WRITE (5,5) FTE,DE,MDOT,ARAT,P1E,U2
5            FORMAT (1X,2X,F6.1,5X,F4.2,7X,F9.4,6X,F9.4,6X,F9.2,2X,
     *          F8.2)
            ENDIF
100   CONTINUE
200   CONTINUE
      STOP
      END
```

Appendix A4.1.3

This program calculates performance characteristics from propellant combination parameters. The equations that are used to calculate the characteristics are from reference 4.1. Some the performance characteristics that are calculated are chamber pressure, specific impulse and propellant flow rate. The assumptions that are made in the calculations are that the flow is isentropic and for the nozzle that the flow is one-dimensional. The only correction that is made is for conical nozzle flow. The input parameters that are required for this program are thrust, exit diameter, exit pressure and fuel characteristics. The fuel characteristics that are required are molecular weight, ratio of specific heats and chamber temperature.

```
      IMPLICIT REAL (A-Z)
      EXTERNAL WGT
      PARAMETER (GEE=9.8066,U1=91.0,ALPHA=15.0,LSTAR=1.0)
      WRITE (*,*) ' Enter thrust(lb), exit dia.(m), M, k, Pe(psi)'
      READ (*,*) FTE,DE,M,K,PEE
      WRITE (*,*) ' Enter chamber:temp.(K)'
      READ (*,*) T1M
      PI=2*ASIN(1.0)
      E1=(K-1.0)/K
      E2=1.0/K
C CALCULATION OF EXIT AREA (m2)
      AE=(PI)*(DE/2.0)**2.0
C CONVERSION TO METRIC UNITS (N,K,Pa)
      FTM=FTE*4.4482
      PEM=PEE*6.8948E3
C CALCULATION OF GAS CONSTANT (J/K*kg)
      R=8.31434E3/M
C CALCULATION OF CHAMBER PRESSURE P1(FT,K,Ae,Pe) (Pa)
      P1M=((FTM*(K-1.0)/(2*K*AE*PEM**E2))+PEM**E1)**(1/E1)
      P1E=P1M/6.8948E3
      ETA=1-(PEM/P1M)**E1
C CORRECTION FACTOR FOR CONICAL NOZZLE
      LAMBDA=0.5*(1+COS(ALPHA*PI/180.0))
C CALCULATION OF EXIT AND THROAT VELOCITIES (m/s)
      U2=LAMBDA*((2.0*K*R*T1M*ETA/(K-1.0))**(0.5))
      UT=(2.0*K*R*T1M/(K+1.0))**(0.5)
C CALCULATION OF SPECIFIC VOLUME (m3/kg)
      VOL1=R*T1M/P1M
      VOLT=VOL1*((K+1.0)/2.0)**(1.0/(K-1.0))
      VOLE=VOL1*(P1M/PEM)**E2
C CALCULATION OF PROPELLANT FLOW RATE (kg/s)
      MDOT=(FTM-PEM*AE)/U2
C CALCULATION OF THROAT AREA AND EXIT/THROAT (m2)
      AT=MDOT*VOLT/UT
      ARAT=AE/AT
```

```
C CALCULATION OF CHAMBER AREA AND CHAMBER/THROAT (m2)
      A1=MDOT*VOL1/U1
      EPC=A1/AT
C CALCULATION OF CHAMBER VOLUME VC(Lcy,EPc,At,Beta) (m3)
C     BETA=BET*PI/180.0
C     VCDUM=(1/(TAN(BETA))*(EPC**1.5-1.0)))
C     VC=AT*(LCY*EPC+(1.0/3.0*(AT/PI)**0.5*(VCDUM)))
      VC=LSTAR*AT
      LCY=VC/A1
C CALCULATION OF SPECIFIC IMPULSE
      ISP=(U2+PEM*AE/MDOT)/GEE
      WRITE (5,*) ' Mol Wt(kg/kmol)  Cp/Cv    Comb Temp(K)'
      WRITE (5,5) M,K,T1M
      WRITE (5,*) ' Exit Area(m2) Exit vel(m/s)  Isp(sec)'
      WRITE (5,10) AE,U2,ISP
      WRITE (5,*) ' Cham Len(m) Cham Area(m2) Cham Vol(m3)'
      WRITE (5,15) LCY,A1,VC
      WRITE (5,*) ' Exit/Throat  Cham/Throat Cham Pres(psi)'
      WRITE (5,20) ARAT,EPC,P1E
      WRITE (5,*) ' Cham m(kg)  Flow rate(kg/s)  Thrust(lbs)'
      WRITE (5,25) MASSC,MDOT,FTE
      WRITE (5,*) ' Throat Area(m2)  Cham Thk(m)'
      WRITE (5,30) AT,THC
5     FORMAT (1X,4X,F5.2,8X,F5.2,6X,F8.2)
10    FORMAT (1X,3X,F6.4,8X,F7.2,7X,F6.2)
15    FORMAT (1X,3X,F6.4,5X,F7.5,6X,F8.6)
20    FORMAT (1X,4X,F6.2,5X,F6.2,5X,F8.2)
25    FORMAT (1X,2X,F6.2,7X,F6.4,10X,F6.1)
30    FORMAT (1X,3X,F9.7,6X,F9.7)
      STOP
      END
```

Appendix A4.1.4

This program uses the heat conduction equations from reference 4.2 to calculate the thickness of the walls assuming that they are to be heat sinks.

```
      IMPLICIT REAL (A-Z)
      REAL B(5),C(5),THR(5),THE(5)
      INTEGER N,I
      PARAMETER (HF=2600,TO=2600,TM=1800,PW=8900,KW=40,CW=700)
      DO 1500 W=0.03,0.1,0.001
      AL=KW/(PW*CW)
      NU=HF*W/KW
      THETA=(TO-TM)/(TO-300)
      DO 50 N=1,5
       IF (N.EQ.1) DUM=0.0
       DO 100 DUMMY=DUM,15,0.001
        TEST=NU-DUMMY*TAN(DUMMY)
        IF (ABS(TEST).LE.0.01) GOTO 70
100    CONTINUE
70     DUM=DUMMY+0.1
       B(N)=DUMMY
       C(N)=4*SIN(B(N))/(2*B(N)+SIN(2*B(N)))
       THR(N)=C(N)*COS(B(N))
       THE(N)=-B(N)**2*AL/W**2
50    CONTINUE
      TIME=83.3
      TH1=THR(1)*EXP(THE(1)*TIME)
      TH2=THR(2)*EXP(THE(2)*TIME)
      TH3=THR(3)*EXP(THE(3)*TIME)
      TH4=THR(4)*EXP(THE(4)*TIME)
      TH5=THR(5)*EXP(THE(5)*TIME)
      TESTER=THETA-TH1-TH2-TH3-TH4-TH5
      WRITE (*,*) TESTER,W
      IF (ABS(TESTER).LE.0.04) GOTO 700
1500  CONTINUE
700   WRITE (*,*) ' WIDTH=',W
      STOP
      END
```

Appendix A4.1.5

This program calculates the mass of a cylinder and conic section given a known value of thickness.

```
      IMPLICIT REAL (A-Z)
      PARAMETER (RHO=8900,AL=15,RE=0.095,RT=0.018,BE=45,RC=0.052)
      PARAMETER (LC=0.089,T2=0.037)
      EXTERNAL VCS
      PI=2.0*ASIN(1.0)
C MASS OF NOZZLE
      T1=0.01
      GA=(180/PI)*ATAN((RE+T1-(RT+T2))/((RE-RT)/TAN(AL*PI/180)))
      VN=VCS(RE,RT,T1,T2,AL,GA)
      MN=VN*RHO
C MASS OF CHAMBER
C     CONVERGING SECTION
      VCHC=VCS(RC,RT,T2,T2,BE,BE)
C     TUBULAR SECTION
      VCHT=PI*LC*((RC+T)**2-(RC)**2)
      VCH=VCHC+VCHT
      MC=VCH*RHO
      WRITE (*,*) ' MASS OF CHAMBER=',MC
      WRITE (*,*) ' MASS OF NOZZLE=',MN
      STOP
      END

C*************************************************
C VOLUME OF A CONICAL SECTION
C*************************************************
C 1 IS THE BIG END AND 2 IS THE SMALL END
      REAL FUNCTION VCS(R1,R2,T1,T2,AN1,AN2)
      IMPLICIT REAL (A-Z)
      PI=2.0*ASIN(1.0)
      AN=AN*PI/180
      H1=(R1+T1)/TAN(AN2)
      H1P=R1/TAN(AN1)
      H2=(R2+T2)/TAN(AN2)
      H2P=R2/TAN(AN1)
      VCP=(1.0/3.0)*PI*((R1+T1)**2*H1-(R2+T2)**2*H2)
      VCPP=(1.0/3.0)*PI*(R1**2*H1P-(R2**2*H2P))
      VCS=VCP-VCPP
      RETURN
      STOP
      END
```

Appendix A4.1.6

This program calculates the mass ratio, R, and the propellant mass. It also breaks the fuel down into its components, fuel and oxidizer. An addition was added to the program for the structures design team. This addition calculated several possible tank configurations and masses. This was done using equations from reference 4.6.

```
      REAL GEE,MASS,RHOF,RHOX,MRW,PI,ISP,R,DV,MF,MFF,MOX
      REAL MFT,RADOX,MOXT,N,HGT,TKF,TKO,RADF,P1E
      EXTERNAL INFO,PRTSET
      PARAMETER (GEE=9.8066,MASS=4600.0)
C Fuel and oxidizer densities and their mass mixture ratio
      PARAMETER (RHOF=1008.0,RHOX=1447.0,MRW=1.08)
      PI=2*ASIN(1.0)
      WRITE (*,*) ' WHAT IS ISP AND CHAMBER PRES'
      READ (*,*) ISP,P1E
      WRITE (5,*) '   R      FUEL MASS'
C The value of delta V
      DV=340.0
C The number of tanks per propellant (i.e. 2 tanks for fuel & 2 tanks for oxidizer)
      N=2.0
C The calculation of the mass ratio and propellant mass
      R=EXP(DV/(ISP*GEE))
      MF=MASS*(1.0-(1.0/R))
      WRITE (5,5) R,MF
5     FORMAT (1X,F6.3,5X,F9.4)
      WRITE (5,*) ' DELTA V=',DV
C Calculation of fuel and oxidizer mass
      MFF=MF/(1.0+MRW)
      MOX=MF-MFF
C Calculation of mass per tank
      MFF=MFF/N
      MOX=MOX/N
      DO 100 HGT=0,0.8,0.1
C Calls a subroutine to solve for tank radius and thickness for both cylindrical
C and spherical. The subroutine also calculates the mass of each tank
      CALL INFO(MFF,RADF,P1E,RHOF,MFT,HGT,TKF)
      CALL INFO(MOX,RADOX,P1E,RHOX,MOXT,HGT,TKO)
      CALL PRTSET(HGT)
      WRITE (5,*) ' TYPE  MASS(kg)  RAD(m)  MsTnk(kg) #TANK  HGT(m)
     * Thk(mm)'
      WRITE (5,10) N*MFF,RADF,MFT,N,HGT,TKF*1000
10    FORMAT (1X,6X,F6.1,4X,F6.4,2X,F8.3,5X,F3.1,3X,F3.2,2X,F6.3)
      WRITE (5,15) N*MOX,RADOX,MOXT,N,HGT,TKO*1000
15    FORMAT (1X,6X,F6.1,4X,F6.4,2X,F8.3,5X,F3.1,3X,F3.2,2X,F6.3)
100   CONTINUE
      STOP
      END
```


R Scott Bennett

```
C ******************************************
C     SUBROUTINES
C ******************************************
      SUBROUTINE INFO(M,RAD,P,D,MS,H,T)
      REAL M,RAD,P,D,MS,H,PI,VOL,T,THK,SPHERE,CYLIN,MSSP,MSCY
      EXTERNAL THK,SPHERE,CYLIN,MSSP,MSCY
      PI=2*ASIN(1.0)
      VOL=M/D
      IF (H.EQ.0) THEN
            RAD=SPHERE(VOL)
      ELSE
            RAD=CYLIN(VOL,H)
      ENDIF
      T=THK(P,RAD)
      IF (H.EQ.0) THEN
            MS=MSSP(RAD,T)
      ELSE
            MS=MSCY(RAD,T,H)
      ENDIF
      RETURN
      END

C ******************************************

      SUBROUTINE PRTSET(H)
      REAL H
      IF (H.EQ.0) THEN
            WRITE (5,*) ' SPHERE'
      ELSE
            WRITE (5,*) ' CYLINDER'
      ENDIF
      RETURN
      END
C ******************************************
C     FUNCTIONS
C ******************************************
C Fuction finds the thickness of the tank under radial pressure
      REAL FUNCTION THK(P,R)
      REAL P,R,STR
      PARAMETER (STR=2.06844E8)
      THK=6.8948E3*(P*R/(2.0*STR))
      RETURN
      END
C The following functons calculate the radius and mass of the tanks for both
C sperical and cylindrical
C ***** FOR A SPHERE *********************

      REAL FUNCTION SPHERE(V)
```

```
      REAL V,PI
      PI=2*ASIN(1.0)
      SPHERE=(3.0*V/(4.0*PI))**(1.0/3.0)
      RETURN
      END

      REAL FUNCTION MSSP(R,T)
      REAL R,T,RHOAL
      PARAMETER (RHOAL=2.7E3)
      PI=2.0*ASIN(1.0)
      MSSP=RHOAL*(4.0*PI/3.0*((R+T)**3.0-R**3.0))
      RETURN
      END

C ***** FOR A CYLINDER ********************

      REAL FUNCTION CYLIN(V,H)
      REAL V,H,PI,DUM
      PI=2.0*ASIN(1.0)
      DUM=(V/(PI*H))**(0.5)
      CYLIN=DUM
      RETURN
      END

      REAL FUNCTION MSCY(R,T,H)
      REAL R,T,H,PI,RHOAL
      PARAMETER (RHOAL=2.7E3)
      PI=2.0*ASIN(1.0)
      MSCY=RHOAL*PI*H*((R+T)**2.0-R**2.0)
      RETURN
      END
```

Appendix 4.1.7

ORIGINAL PAGE IS
OF POOR QUALITY

Delta Dart Abort System Hardware

This chapter section starts with the driving requirements for the abort system hardware on the Delta booster, and then describes the initial trade studies for the optiumization of the system placement, and finally follows the step-by-step rocket motor engine development and description. Interfacing with the capsule structure, and electronic controls will be briefly overviewed, since these will be or have been covered in other chapters of this report.

Specific Requirements

The abort system is required to insure crew survival in case of a critical failure of the Delta booster system. A critical failure denotes an explosive detonation of the booster fuel and/or a malfunction which would make the rocket system uncontrollable. Both would result in the destruction of the rocket system, and there would be a minimal chance of crew survival with out an adequate abort system.

Starting with the assumption of a five second detection time before the fuel in the booster detonates, the abort system would have to place the Delta Dart crew capsule at a distance of half a mile or 805 meters from the launch site or moving booster, and place the capsule at a minimum of 500 meters in altitude for parachute recovery deployment. References for these abort criteria were established by space systems specialist Dr. David Akin, at the University of Maryland, and the Air Force space launch facility at Vandenberg AFB, California. Five seconds corresponds to the average detection time of a critical failure by electronic sensing devices. The 805m radial distance represents the typical danger radius of a detonating booster rocket system.

With a constant thrust (neutral burning) from the abort system, the constant acceleration equation states:

•Distance = initial velocity*time +(.05)* acceleration * time^2

With time and distance known, and the worst case occurring during the booster ignition with an initial velocity equal to zero, the constant acceleration required from the abort system was calculated to be 64.4 m/sec^2. Looking at the worst case of accelerating in the pure vertical direction fighting gravity, the final required acceleration came to be 74.21 m/sec^2 or 7.56 g.

James Clegern

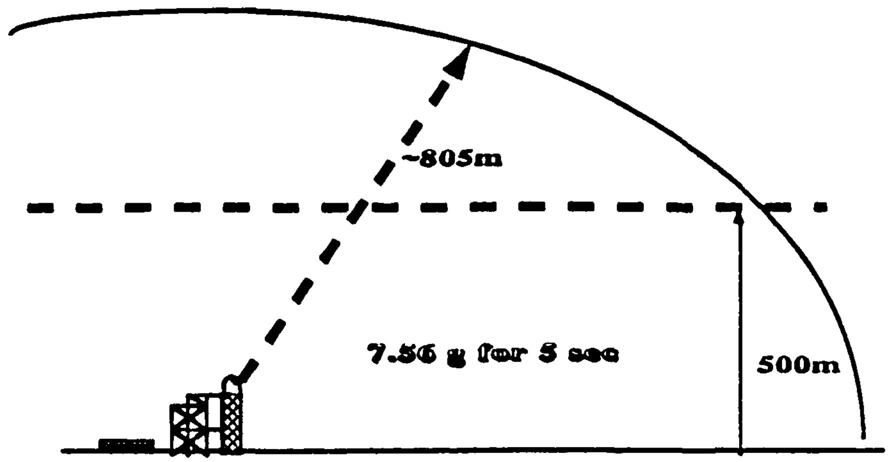

FIGURE 4.4.a: Requirements for the Delta Dart Abort system.

After examining the specifics of the Delta booster system, it was noted that the booster produces a peak acceleration of ~ 5g. If the critical failure was to occur at this time, the required abort would have to overcome the Delta booster's acceleration as well as accelerating away from the booster. The combination of these accelerations would be over the eleven g sustained forces limit which was deemed hazardous to the capsule crew by the human factors division.

Three solutions became apparent, first was accept the danger of not being able to abort from the accelerating booster while it was in the high thrust/acceleration region. Second, was to increase the thrust of the abort rocket motors to give the required acceleration. The third solution was modify the Delta booster with thrust termination ports. The first solution was unacceptable for the 99.9% crew survival rate since the booster has only a reliability of 95% and with no capability for abort during the high thrust range, the danger to crew safety was too high. The second solution was also unacceptable since the increased acceleration would black out and possibly injure the crew, the deployment of the parachute and the landing of the aborted capsule would have to be on auto-pilot, and the mass of the abort system fuel would be very high. The third solution was picked for incorporation into the abort system since thrust termination ports have been widely used on solid rocket systems, like the Minuteman ICBM, and the technology is well developed. [1] The thrust termination device or "blow out " ports would almost instantaneously vent the pressure and extinguish the flame within the thrust chamber, thereby dropping the acceleration of the solid Delta booster to zero. With the trust termination ports activated, the acceleration of the Delta booster would be negated, and the abort system could function well within the required limits.

[1] Hill,P.G, C.R. Peterson, *Mechanics and Thermodynamics of Propulsion.* Reading, Mass:Addison-Wesley ,1970, page 462

James Clegern

Appendix 4.4.4 Delta Abort Motor Data

SOLID ROCKET CALCULATIONS
WEIGHT ESTIMATE
Composite case mass
modeled as a cylinder
w/ two spherical ends (kg)
10.76960555
Liner Mass (kg)
5.61225574
Nozzle mass (kg)
5.851833291
Igniter Mass (kg) [eq 12-1]
0.052280098
Propellant (effective) (kg)
221.4791639
Unusable Propellant [2%] (kg)
4.429583279
TOTAL Motor MASS (kg)
248.1947219
TOTAL ABORT SYSTEM MASS (kg)
744.5841656
Tower attachment angle (radians)
0.17453

2

CLEGBRN

Appendix 4.4.4 Delta Abort Motor Data

SOLID ROCKET CALCULATIONS	SOLID ROCKET CALCULATIONS
GRAIN CONFIGURATION	***NOZZLE DESIGN***
The grain will be solvent cast into	Pressure Ratio, Pc/Pa
the case and isolated by an	126.3261781
elastomeric liner w/ av thickness	
of 0.00254m inside the case, but	Thrust Coefficient, Cf (fig 3-7)
~1cm at the nozzle.	1.64
Density (kg/m^2)	
1107	Throat Area, At (m^2)
	0.005420573
Outside grain diameter, D (m)	
0.28712282	Throat Diameter, (m)
	0.117487761
Inside grain diameter, d (m)	
0.064584641	Opt. exp. ratio, Ae/At (fig 3-7)
	12
Effective Length, L (m)	
2.042799981	Exit Area, Ae (m^2)
	0.065046875
Case free Volume (m^3)	
0.039727829	Exit Diameter, (m)
	0.406989544
Web Fraction	
0.775062666	Nozzle cone half angle (radians)
	0.17453
L/D	
7.114725274	Nozzle length (m)
	0.82093714
Average Burn Area (m^2)	
10.52687711	

Appendix 4.4.4 Delta Abort Motor Data

SOLID ROCKET CALCULATIONS	SOLID ROCKET CALCULATIONS
BASIC DESIGN	***CASE DIMENSIONS***
Propellant mass (kg)	Average Diameter, D (m)
664.4374918	0.3
Silver Loss, 2% Prop.mass(kg)	Rocket motor Casing Material:
13.28874984	Organic Filament Composite
	Tensile strength (n/m^2)
Total Propellant Mass (kg)	1.724E+09
677.7262416	Density (kg/m^2)
	1384
Number of Engines used	Safety Factor (suggested)
3	3.5
Thrust per engine (n)	Wall Thickness,t (m)
113788.6667	0.00389859
Engine Prop. Mass (kg)	
225.9087472	
Engine Prop. Volume (m^3)	Spherical head & nozzle end assumed
0.125574623	
Web Thickness, b (m)	
0.111269089	

CLEBBRN

Appendix 4.4.4 Delta Abort Motor Data

ABORT DATA (REQUIREMEMTS)	SOLID FUEL DATA
	[DB/AP-HMX/AL]
Abort Radial Distance Required (m)	
805	Specific Impulse, Isp (sec)
	270
Abort Time, max (seconds)	
5	Burn Rate, r (m/sec)
	0.022253818
Abort acceleration, vert. (m/s^2)	
74.21	Specific wt. of Grain, Sw (kg/m^3)
	1799
Abort Acceleration, G	
7.564729867	Specific Heat Ratio, k
	1.24
Mass of the Capsule (kg)	
4600	Chamber pressure,Pc (n/m^2)
	12800000
Av. Thrust required, T (n)	
341366	Flame Temperature, Tf ('C)
	3700
Abort Rocket Burn Time, tb (sec)	
5	
Total Impulse, It (sec)	
1706830	
Ambient S.L. Pressure, Pa (n/m^2)	
101325	

CLUBERN

Appendix 4.4.3 Chamber Pressure TRADE-STUDY

Chamber Pressures (n/m^2)	Burn Rates (m/sec)	Motor Mass (kg)
4000000	0.011113573	762.67
5000000	0.01202599	752.78
6200000	0.013220303	745.51
6894800	0.013965299	742.21
7000000	0.014081701	739.18
8400000	0.015726393	738.12
9000000	0.016488813	736.99
10600000	0.018707546	735.24
11000000	0.019307395	734.34
11500000	0.020084325	733.11
11700000	0.020403782	733.89
12800000	0.022253818	733.56
13500000	0.02351752	733.63
15000000	0.026472334	735.41

CLEBORN

Appendix 4.4.3 Tower Height Angle TRADE-STUDY

Angle,deg°	Angle, Radians	Motor Mass(kg)	Tower Height (m)	Tower mass (kg)	Total Mass (kg)
2	0.034906	734	24.13216228	132.7268925	866.7268925
4	0.069812	735.3	10.79984325	59.39913789	794.6991379
6	0.104718	737.5	6.348508335	34.91679584	772.4167958
8	0.139624	740.6	4.117406205	22.64573413	763.2457341
10	0.17453	744.6	2.774382313	15.25910272	764.7591027
12	0.209436	749.5	1.875381523	10.31459838	765.7145984
14	0.244342	755.4	1.230091345	6.765502395	769.1655024
16	0.279248	762.4	0.743352724	4.088439983	774.38844
18	0.314154	770.3	0.36229697	1.992633336	781.3926333
20	0.34906	779.4	0.055200513	0.303602821	789.9736028
22	0.383966	789.67	-0.198126577	-1.089696171	800.1103038
24	0.418872	801.2	-0.411146334	-2.261304835	811.8386952
26	0.453778	814.1	-0.59318062	-3.26249341	-3.26249341

CLEGERN

Engine Casing Material

--- Engine Casing Material selection is in progress. Looking for highest stress load handling while at the lowest mass for a safe casing. Tentative: Organic Filament Composite because of its high strength and low density---

	D6aC Steel	Maraging Steel	Titanium (6% Al - 4%V)	Glass Filament Composite	Organic Filament Composite
Tensile Strength (MPa)	1585.8	1379 to 2068.4	965.3	1172	1723.7
Density (kg/m^3)	7833.4	7999.5	4622.5	1993.0	1384.0
Modulus (MPa)	199,950	189,607	110,317	31,716	75,843

Table 4.4.b Possible casing materials for the abort motors [4]

Final Abort Motor Masses and Dimensions

----Work in progress First Approximation = 795.58 kg (including tower)----

Directional Control During Abort

The method used to place the Delta capsule a horizontal distance from the Delta booster during an emergency abort would be to angle one of the abort motors to provide a horizontal acceleration. The extent of the horizontal distance would be dependent on the angle the abort motor would be place before launch or having a variable angle nozzle on one or more of the abort motors.

-----Further work is in progress-----

Attachment Hardware and Interfacing

--- Work in progress with structures ----

[4] Sutton, G.P. *Rocket Propulsion Elements.* New York: John Wiley & Sons, 1986, Page 327

James Clegern

The following is a list of the final performance characteristics of the DB/AP-HMX/AL solid fuel determined so far:

•Specific impulse (Isp)	= 270 sec
•Burn rate (r)	= 0.02208 m/sec
•Specific weight of the grain (Sw)	= 1799 kg/m^3
•Specific heat ratio (k)	= 1.24
•Chamber pressure (Pc)	= 12800000 n/m^2
•Flame temperature (Tf)	= 3704°C
•Total fuel mass (Mf)	= (790 kg approximate)

Internal Motor Design

--- Final Internal Motor Design is in progress. Looking for grain combination, burn area, web thickness, and other variables. Currently in use: George P. Sutton's text, Rocket Propulsion Elements as a basis for design, Appendix 4.4.section4 gives the first cut values.---

Ignition System

--- Ignition System selection is in progress. Looking for high ignition rates with as small as possible time lags before propellant ignition. Tentative: Pyrotechnic Igniter which will be surface bonded or grain mounted ---

James Clegern

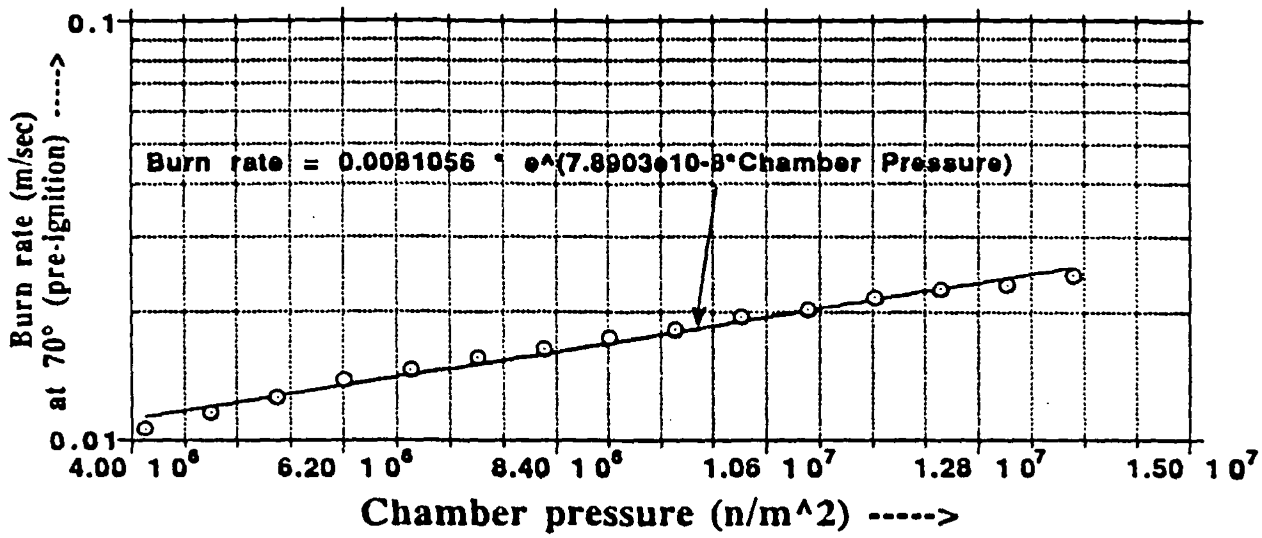

Figure 4.4.e Graph of burn rate vs. Chamber pressure

The final chamber pressure and burn rate came from a trade study which varied the chamber pressure in the abort motor spreadsheet program to find the optimum lowest final mass of the abort motors. As denoted in figure 4.4.f, the optimum chamber pressure for the abort motors was **1.28e8 n/m^2** which yielded a basic motor mass of **773.58**kg. The spreadsheet and data for this chamber pressure trade study is available in Appendix 4.4.section2 and 4.4.section3.

Optimization trade-study on the nozzle cone angle (Appendix 4.4.section 3) yielded that the best conic half angle of the nozzle was 10°.

James Clegern

Preliminary Performance Calculations and Fuel Selection

Entering into the design stage of the abort motor system, the total mass of the aborting capsule was estimated to be 4600 kg. This value includes the crew capsule and the mass of the attached abort system. A trade study, shown in Appendix 4.4.section1 was done to determine the best abort time length required to reach the 805m abort radius. The trade study showed that the longer the time, the lower the fuel mass would be. Since 5 sec was the upper limiting factor, it was taken as the abort burn time which yielded the lowest fuel mass.

To reach 805 meters in 5 seconds, the solid motors must be able to produce 7.56g of acceleration on the 4600 kg Delta capsule, which is equal to an average thrusting force of 341,366 newtons. The total impulse of the system is Force*time = 1,706,830 n-sec. The mass of the solid fuel required is equal to the total impulse divided by the specific impulse of the engine and by acceleration of gravity. To reduce the mass of the system, an high energy, solid double base fuel was selected based on the need for a solid propellant with the highest specific impulse possible. The DB/AP-HMX/AL double base fuel was chosen with its Isp of 270 sec. [2]

Abort Motor Performance

Specific impulse was directly tied to the characteristics of the double base fuel, so very little could be done to increase the specific impulse and decrease the mass through that means. Therefore, a spreadsheet (Appendix 4.4.section2) was developed to calculate the various design aspects of the abort solid motors, and to do trade studies on chamber pressure, cylindrical motor diameter, cone nozzle angle, engine number, and tower attachment angle to reduce the overall motor mass. The data on the trade studies is available in Appendix 4.4.section3.

First , the chamber pressure and the burn rate were varied to find the best combination which gave the lowest abort motor mass. As denoted on figure 4.4.e, the solid fuel burn rate and chamber pressure are linked exponentially for this type of solid double base fuel.[3]

[2] Sutton, G.P. *Rocket Propulsion Elements.* New York: John Wiley & Sons, 1986, page 293

[3] Sutton, G.P. *Rocket Propulsion Elements.* New York: John Wiley & Sons, 1986, Page 267

James Clegern

Abort Motor Selection

A trade study of solid verses liquid engines resulted in the following trade-study table being generated with examples of the relative engine sizes shown below:

	SOLID	LIQUID
PROS	- High Thrust to Weight - Simple in design - Very Reliable - Few, if any moving parts - Lower volume requirements - Easy to store	- Controllable Thrust duration - Multiple starts - Higher Specific Impulse - Longer thrust duration times - Requires less fuel mass per unit thrust
CONS	- One Shot Operation - Thrust not controllable after motor ignition - Lower Specific Impulse - Toxic exhausts (HCl gas) - Fuels can be highly explosive	- Lower Thrust to Weight - Complex system with multiple parts - Less reliable, requires redundancies - Separate oxidizer and fuel with pressurent (He) - Liquid propellants require higher volumes - Requires special storage facilities - Fuels & Oxidizer often highly toxic - Fuel/Oxidizer mixtures explosive

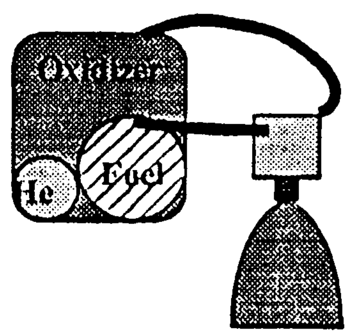

Table 4.4.a & Figures 4.4.b, 4.4.c

The selection of solid abort motors can come without any big surprises. Solid rockets meet the criteria of the abort system with the largest thrust per mass, simple design, and having a complete rocket motor in a storable, movable container. Solid abort motors also have a historic trend of use from the earlier Apollo and Gemini space programs, which shows their use by many similar type abort operations.

James Clegern

A6.1

A.6.1.1

A computer program written in c that calculates the re-entry analysis is included in the following:

```
/*************************************************************************
**     Re-entry Dynamics Program Using Chapman's Z-function          **
**     Written by Makiko Kosha              March 1991               **
**     Mission Analysis              Delta - Dart                    **
*************************************************************************/
#include <stdio.h>
#include <math.h>

double Inclination();
double Altitude();
double Velocity();
double Deceleration();
double flighttime();
double Range();

main()
{
 /* Declaration of variables */
 double rho, Cd, r, m, A, M, u, initialh, h, du, Z, dZ, ddZ;
 double calc1ddZ, calc2ddZ, calc3ddZ, cofphi, phi, LD, dV, V, dec;
 double betah, betar, roverbeta, muoverr;
 double Z1, dZ1, ddZ1, subsonic, supersonic;
 double s, t;
 int i, foo;
 char dataalt[] = "dataalt.dat";
 char datavel[] = "datavel.dat";
 char dataphi[] = "dataphi.dat";
 char datatime[] = "datatime.dat";
 char datafile[] = "datafile.dat";
 FILE *fp1;
```

```
FILE *fp2;
FILE *fp3;
FILE *fp4;
FILE *fp5;
s = 0.0;
t = 0.0;
i = 0;
Cd = 1.0;
foo = 0;

fp1 = fopen(dataalt, "w");
fp2 = fopen(datavel, "w");
fp3 = fopen(dataphi, "w");
fp4 = fopen(datatime, "w");
fp5 = fopen(datafile, "w");

/* Enter the initial values */

printf ("Enter the value of altitude.   ");
scanf ("%lf", &h);
printf ("Enter the value of mass.   ");
scanf ("%lf", &m);
printf ("Enter the value of reference area.   ");
scanf ("%lf", &A);
printf ("Enter the value of velocity.   ");
scanf ("%lf", &V);
printf ("Enter the value of inclination angle.   ");
scanf ("%lf", &phi);
printf ("Enter the value of lift to drag ratio.   ");
scanf ("%lf", &LD);
printf ("Enter the value of du.   ");
scanf ("%lf", &du);

/* Calculations of the initial values */

du = -1*du;
```

```
initialh = h;
r = h+6378000.0;
muoverr = 398532500000000.0/r;
betah = h/7000.0;
betar = r/7000.0;
roverbeta = r*7000.0;

rho = 1.2*exp(-1*betah);
M = V/297.0;            /* at T = 220K */
cofphi = cos(phi);
u = (V*cofphi)/(sqrt(9.81*r));

Z = ((rho*Cd*A)/(2.0*m))*(sqrt(roverbeta))*u;
dZ = (-1)*sqrt(betar)*sin(phi)+(Z/u);
calc1ddZ = (1.0-pow(u,2))/(u*Z);
calc2ddZ = calc1ddZ*(pow(cofphi,4));
calc3ddZ = sqrt(betar)*LD*(pow(cofphi,3));
ddZ = (1/u)*(calc2ddZ-calc3ddZ+dZ-(Z/u));

printf("\n  ALTITUDE  VELOCITY   PHI   DECEL.  TIME   RANGE  Z   dZ
ddZ\n");
fprintf (fp1, "\n ALTITUDE  \n");
fprintf (fp2, "\n VELOCITY  \n");
fprint  (fp3, "\n PHI  \n");
fprintf (fp4, "\n TIME  \n");
fprintf (fp5, "\nALTITUDE  VELOCITY   PHI  DECEL   TIME   RANGE\n");

/* Calculation of Z using Taylor series */
while (h > 1000)
{
  h = Altitude (initialh,Z,Cd,A,m,u);
  r = h+6378000.0;
  phi = Inclination (Z,dZ,betar,u);
  V = Velocity (u,phi,r);
  M = V/297.0;
  r = h+6378000.0;
```

```
    dec = Deceleration (betar,u,Z,phi,LD);
    rho = 1.2*exp (-1*h/7000.0);
    t = flighttime (t,u,du,r,m,rho,Cd,phi,A);
    s = Range (u,s,phi,m,r,rho,Cd,A,du);
    i++;
    if (i%40 == 0.0)
    {
      printf ("%lf %lf  %lf  %lf  %lf  %lf  %lf %lf  %lf\n",h,V,phi,dec,t,s,Z,dZ,ddZ);
      fprintf (fp1, "%lf  \n",h);
      fprintf (fp2, "%lf  \n",V);
      fprintf (fp3, "%lf  \n",phi);
      fprintf (fp5, "%lf   %lf   %lf  %lf  %lf  %lf\n",h,V,phi,dec,t,s);
      fprintf (fp4, "%lf   \n",t);
    }

    u = u+du;
    Z1 = Z+(dZ*du)+(0.5*ddZ*pow(du,2));
    dZ1 = dZ+ddZ*du;
    cofphi = cos(phi);
    betar = r/7000.0;
    calc1ddZ = (1.0-pow(u,2))/(u*Z);
    calc2ddZ = calc1ddZ*(pow(cofphi,4));
    calc3ddZ = sqrt(betar)*LD*(pow(cofphi,3));
    ddZ1 = (1/u)*(calc2ddZ-calc3ddZ+dZ1-(Z1/u));
    Z = Z1;
    dZ = dZ1;
    ddZ = ddZ1;
   }
 }

/*Calculation of inclination angle */
double Inclination (Z,dZ,betar,u)
double Z;
double dZ;
double u;
double betar;
```

```
{
  double sofphi, phi;
  sofphi = (-1)*(dZ-(Z/u))/(sqrt(betar));
  phi = asin(sofphi);
  return (phi);
}

/*Calculation of altitude */

double Altitude (initialh,Z,Cd,A,m,u)
double initialh;
double Cd;
double Z;
double A;
double m;
double u;

{
  int count;
  double altfnc, h, betaoverr,fnc, y, y2, y1, y0, num1, n, diff;
  fnc = 1.6666667*(m/(Cd*A))*(Z/u);
  altfnc = (pow(fnc,2))/7000.0;
  y = initialh;
  y2 = y;
  y1 = y/2;
  y0 = 0;
  num1 = (y1+6378000)*exp((-2.0*y1)/7000.0);
  n = altfnc-num1;
  diff = fabs(n);
  count =0;
  while (count++ < 15)
  {
   if (altfnc<num1)
   {
     y0 = y1;
     y1 = y2-((y2-y1)/2);
```

```
        num1 = (y1+6378000)*exp((-2.0*y1)/7000.0);
    }
    if (altfnc > num1)
   {
       y2 = y1;
       y1 = y0;
        num1 = (y1+6378000)*exp((-2.0*y1)/7000.0);
    }
    n = altfnc-num1;
    diff = fabs(n);
  }
  if( diff > 5){
       printf( "\nWhile loop failed to converge, diff = %f\n", diff);
       }
  h = y1;
  return(h);
}

/*Calculation of Velocity */
double Velocity (u,phi,r)
double r;
double phi;
double u;
{
  double V;
  V = (u/cos(phi))*sqrt(9.81*r);
  return (V);
}

/*Calculation of deceleration in g's */
double Deceleration (betar,u,Z,phi,LD)
double u;
double betar;
double Z;
double phi;
double LD;
```

```
{
   double calc, term, dec;
   term = tan(phi)-LD;
   calc = 1.0+pow(term,2);
   dec = (((sqrt(betar)*u*Z)/cos(phi))*sqrt(calc))/9.81;
   return (dec);
}

/*Calculation of flighttime */
double flighttime (t,u,du,r,m,rho,Cd,phi,A)
double t;
double u;
double du;
double r;
double m;
double rho;
double Cd;
double phi;
double A;
{
   double t1,u1,u2,dt,a;
   t1 = t;
   u1 = u;
   u2 = u1+du;
   a = r*9.81;
   dt = (1.0/(sqrt(a)))*((2.0*m)/(rho*Cd*A))*cos(phi)*(log(u1)-log(u2));
   t = t1 +dt;
   return (t);
}

/*Calculation of range */
double Range(u,s,phi,m,r,rho,Cd,A,du)
double r;
double rho;
double Cd;
double u;
```

```
double s;
double phi;
double m;
double A;
double du;
{
  double s1, u1, u2, ds;
  s1 = s;
  u1 = u;
  u2 = u1+du;
  ds = ((cos(phi)*2.0*m)/(rho*Cd*A))*(log(u1)-log(u2));
  s = s1+ds;
  return(s);
}
```

A6.2

Appendix A6.2.1

```
C  FORCE COEFFICIENTS AND L/D AT MACH 22.9 FOR GIVEN HEAT
C  SHIELD RADIUS OF CURVATURE AND VARIABLE ANGLE OF ATTACK
C  USING MODIFIED NEWTONIAN THEORY  by A. J. Harrison
C
      IMPLICIT REAL (A-Z)
C  DEFINE DIMENSIONS OF HEAT SHIELD
      WRITE(*,*) 'RHO?'
      WRITE(5,*) 'RADIUS OF CURVATURE(M)'
      READ(*,*) RHO
      WRITE(5,*) RHO
        RMAX=1.75
        PHIMAX=ASIN(RMAX/RHO)
C  INPUT ANGLE OF ATTACK
 1    WRITE(*,*) 'ALPHA?'
      WRITE(5,*) 'ANGLE OF ATTACK(DEGREES)'
      READ(*,*) ALPHA
      WRITE(5,*) ALPHA
        PI=ACOS(-1.0)
        A=ALPHA*PI/180
C  COMPUTE STAGNATION POINT PRESSURE COEFFICIENT
       MACH=22.9
       GAMMA=1.4
    CP1=2/(GAMMA*MACH**2)
    CP2=(((GAMMA+1)**2)*MACH**2)/((4*GAMMA*MACH**2)-
    2*(GAMMA-1))
    CP2=CP2**(GAMMA/(GAMMA-1))
    CP3=(1-GAMMA+2*GAMMA*MACH**2)/(GAMMA+1)
    CPMAX=CP1*(CP2*CP3-1)
C  COMPUTE COEFFICIENTS OF DRAG AND LIFT, AND L/D
       SA=SIN(A)
       CA=COS(A)
       SP=SIN(PHIMAX)
       CP=COS(PHIMAX)
       SREF=PI*RMAX**2
      CD1=(3.0*PI/4.0)*(SA**2)*CA*(SP**4)
      CD2=(PI/2.0)*(CA**3)*((SP**2)*(CP**2)+(SP**2))
      CDRAG=((RHO**2)*CPMAX/SREF)*(CD1+CD2)
       WRITE(*,*) 'CD=',CDRAG
       WRITE(5,*) 'DRAG COEFFICIENT=',CDRAG
      CL1=(PI/4.0)*((SA**3)-2*SA*(CA**2))*(SP**4)
      CL2=(PI/2.0)*SA*(CA**2)*((SP**2)*(CP**2)+(SP**2))
      CLIFT=((RHO**2)*CPMAX/SREF)*(CL1+CL2)
       WRITE(5,*) 'LIFT COEFFICIENT=',CLIFT
       WRITE(*,*) 'CL=',CLIFT
```

```
LIFTTODRAG=CLIFT/CDRAG
 WRITE(5,*) 'L/D=',LIFTTODRAG
 WRITE(*,*) 'L/D=',LIFTTODRAG
GOTO 1
END
```

Appendix A6.2.2

```
C  PRESSURE DISTRIBUTION ON HEAT SHIELD
C  USING MODIFIED NEWTONIAN FLOW  by A. J. Harrison
C
      IMPLICIT REAL (A-Z)
C  INPUT PARAMETERS OF CALCULATION
      WRITE(*,*) 'TRIM ALPHA?'
      WRITE(5,*) 'TRIM ANGLE OF ATTACK(DEGREES)'
      READ(*,*) ALPHA
      WRITE(5,*) ALPHA
      WRITE(*,*) 'RHO?'
      WRITE(5,*) 'RADIUS OF CURVATURE OF HEAT SHIELD(M)'
      READ(*,*) RHO
      WRITE(5,*) RHO
      WRITE(*,*) 'ALT?'
      WRITE(5,*) 'INSTANTANEOUS ALTITUDE(M)'
      READ(*,*) H
      WRITE(5,*) H
      WRITE(*,*) 'VELOCITY?'
      WRITE(5,*) 'VELOCITY(M/S)'
      READ(*,*) VELOCITY
      WRITE(5,*) VELOCITY
C  INPUT THE HEAT SHIELD LOCATION OF INTEREST
 1    WRITE(*,*) 'THETA?'
      WRITE(5,*) 'THETA(DEG)'
      READ(*,*) THETA
      WRITE(5,*) THETA
      WRITE(*,*) 'PHI?'
      WRITE(5,*) 'PHI(DEG)'
      READ(*,*) PHI
      WRITE(5,*) PHI
       PI=ACOS(-1.0)
       A=ALPHA*PI/180
       T=THETA*PI/180
       P=PHI*PI/180
C  CALCULATE THE AMBIENT PRESSURE
       REARTH=6356766.0
       G=9.80665*(REARTH/(REARTH+H))**2
     TAMB=288.66
       SGC=287.0
       RATIO=EXP(-G*H/(SGC*TAMB))
       PAMB=101325*RATIO
C  CALCULATE THE STAGNATION POINT COEFFICIENT OF PRESSURE
     GAMMA=1.4
       MACH=VELOCITY/(GAMMA*SGC*TAMB)**0.5
```

```
      CP1=2/(GAMMA*MACH**2)
       CP2=(((GAMMA+1)**2)*MACH**2)/((4*GAMMA*MACH**2)-
      2*(GAMMA-1))
      CP2=CP2**(GAMMA/(GAMMA-1))
      CP3=(1-GAMMA+2*GAMMA*MACH**2)/(GAMMA+1)
      CPMAX=CP1*(CP2*CP3-1)
C  CALCULATE THE PRESSURE RATIO AND PRESSURE ON THE HEAT
SHIELD
              SA=SIN(A)
              CA=COS(A)
              SP=SIN(P)
              CP=COS(P)
              CT=COS(T)
        PRATIO=(0.5)*(MACH**2)*GAMMA*CPMAX*(SA*SP*CT+CA*CP)
      **2+1
        PSHIELD=PRATIO*PAMB
         WRITE(*,*) 'PRESSURE RATIO = ', PRATIO
         WRITE(5,*) 'PRESSURE RATIO = ', PRATIO
         WRITE(*,*) 'PRESSURE =', PSHIELD
         WRITE(5,*) 'PRESSURE =', PSHIELD
        GOTO 1
        END
```

```
TRIM ANGLE OF ATTACK(DEGREES)
    +15.0000000
RADIUS OF CURVATURE OF HEAT SHIELD(M)
     +5.5999999
INSTANTANEOUS ALTITUDE(M)
  +46755.0000000
VELOCITY(M/S)
   +6720.0000000
THETA(DEG)
 +0.000000E-01
PHI(DEG)
    +18.0000000
PRESSURE RATIO =      +500.4024048
PRESSURE =  +216967.5000000
THETA(DEG)
 +0.000000E-01
PHI(DEG)
    +16.0000000
PRESSURE RATIO =      +501.6214600
PRESSURE =  +217496.0781250
```

THETA(DEG)
+0.000000E-01
PHI(DEG)
+14.0000000
PRESSURE RATIO = +501.6213989
PRESSURE = +217496.0468750
THETA(DEG)
+0.000000E-01
PHI(DEG)
+12.0000000
PRESSURE RATIO = +500.4023438
PRESSURE = +216967.4843750
THETA(DEG)
+0.000000E-01
PHI(DEG)
+10.0000000
PRESSURE RATIO = +497.9700012
PRESSURE = +215912.8437500
THETA(DEG)
+0.000000E-01
PHI(DEG)
+8.0000000
PRESSURE RATIO = +494.3363342
PRESSURE = +214337.3437500
THETA(DEG)
+0.000000E-01
PHI(DEG)
+6.0000000
PRESSURE RATIO = +489.5191956
PRESSURE = +212248.7031250
THETA(DEG)
+0.000000E-01
PHI(DEG)
+4.0000000
PRESSURE RATIO = +483.5418091
PRESSURE = +209656.9843750
THETA(DEG)
+0.000000E-01
PHI(DEG)
+2.0000000
PRESSURE RATIO = +476.4333496
PRESSURE = +206574.8593750

THETA(DEG)
+0.000000E-01
PHI(DEG)
+0.000000E-01
PRESSURE RATIO = +468.2284851
PRESSURE = +203017.3437500
THETA(DEG)
+180.0000000
PHI(DEG)
+2.0000000
PRESSURE RATIO = +458.9671936
PRESSURE = +199001.7812500
THETA(DEG)
+180.0000000
PHI(DEG)
+4.0000000
PRESSURE RATIO = +448.6946716
PRESSURE = +194547.7500000
THETA(DEG)
+180.0000000
PHI(DEG)
+6.0000000
PRESSURE RATIO = +437.4608459
PRESSURE = +189676.9218750
THETA(DEG)
+180.0000000
PHI(DEG)
+8.0000000
PRESSURE RATIO = +425.3203735
PRESSURE = +184412.9843750
THETA(DEG)
+180.0000000
PHI(DEG)
+10.0000000
PRESSURE RATIO = +412.3326111
PRESSURE = +178781.6718750
THETA(DEG)
+180.0000000
PHI(DEG)
+12.0000000
PRESSURE RATIO = +398.5607605
PRESSURE = +172810.3906250

THETA(DEG)
+180.0000000
PHI(DEG)
+14.0000000
PRESSURE RATIO = +384.0718994
PRESSURE = +166528.2187500
THETA(DEG)
+180.0000000
PHI(DEG)
+16.0000000
PRESSURE RATIO = +368.9365845
PRESSURE = +159965.7656250
THETA(DEG)
+180.0000000
PHI(DEG)
+18.0000000
PRESSURE RATIO = +353.2285767
PRESSURE = +153154.9843750

Appendix 6.2.3

```
C  CENTER OF GRAVITY OFFSET FROM AXIS OF SYMMETRY
C  USING MODIFIED NEWTONIAN THEORY  by A. J. Harrison
C
      IMPLICIT REAL (A-Z)
C  DEFINE HEAT SHIELD GEOMETRY
 1    WRITE(*,*) 'RHO?'
      WRITE(5,*) 'RADIUS OF CURVATURE(M)'
      READ(*,*) RHO
      WRITE(5,*) RHO
       RMAX=1.75
       PHIMAX=ASIN(RMAX/RHO)
C  INPUT TRIM ANGLE OF ATTACK
      WRITE(*,*) 'ALPHA?'
      WRITE(5,*) 'ANGLE OF ATTACK(DEGREES)'
      READ(*,*) ALPHA
      WRITE(5,*) ALPHA
       PI=ACOS(-1.0)
       A=ALPHA*PI/180
C  CALCULATE STAGNATION POINT COEFFICIENT OF PRESSURE
       MACH=22.9
       GAMMA=1.4
   CP1=2/(GAMMA*MACH**2)
   CP2=(((GAMMA+1)**2)*MACH**2)/((4*GAMMA*MACH**2)-
   2*(GAMMA-1))
   CP2=CP2**(GAMMA/(GAMMA-1))
   CP3=(1-GAMMA+2*GAMMA*MACH**2)/(GAMMA+1)
   CPMAX=CP1*(CP2*CP3-1)
C  CALCULATE FORCE COEFFICIENTS ABOUT CENTER OF CURVATURE
       SA=SIN(A)
       CA=COS(A)
       SP=SIN(PHIMAX)
       CP=COS(PHIMAX)
       SREF=PI*RMAX**2
      CD1=(3.0*PI/4.0)*(SA**2)*CA*(SP**4)
      CD2=(PI/2.0)*(CA**3)*((SP**2)*(CP**2)+(SP**2))
      CDRAG=((RHO**2)*CPMAX/SREF)*(CD1+CD2)
      CL1=(PI/4.0)*((SA**3)-2*SA*(CA**2))*(SP**4)
      CL2=(PI/2.0)*SA*(CA**2)*((SP**2)*(CP**2)+(SP**2))
      CLIFT=((RHO**2)*CPMAX/SREF)*(CL1+CL2)
C  INPUT AXIAL CG LOCATION AS GIVEN BY STRUCTURES GROUP
      WRITE(*,*) 'DISTANCE FROM BOTTOM TO CG?'
      WRITE(5,*) 'DISTANCE FROM BOTTOM TO CG(M)'
      READ(*,*) B
      WRITE(5,*) B
```

```
      ZCG=RHO - B
C   CALCULATE REQUIRED DISTANCE FROM AXIS TO CG
      XCG=(-(CLIFT*CA-CDRAG*SA)/(CDRAG*CA+CLIFT*SA))*ZCG
       WRITE(*,*) 'XCG =',XCG
       WRITE(5,*) 'XCG =',XCG
      END
```

```
RADIUS OF CURVATURE(M)
    +5.5999999
ANGLE OF ATTACK(DEGREES)
    +15.0000000
DISTANCE FROM BOTTOM TO CG(M)
 +9.060000E-01
XCG =  +6.444772E-02
```

A6.3

Appendix A6.3.1

```
c     aftheat
c
c
c      This program calculates the convective stagnation heat
c      flux and the stagnation point equilibrium temperature
c      on the blunt nose of the DART capsule during re-entry.
c      The thermal equilibrium equation states that the
       convective heat flux transferred to the heat shield
c      from the boundary layer is balanced by the radiative
c      heat flux,the heat of ablation of the ablative material
c      and the heat of O2 dissociation emminating away
c      from the heat shield. Note that SI units (i.e., m, kg, s, K)
c      are used throughout.
c
        tol=0.001
c
c       DO 55 freevel=8000.0,7600.0,-100.0
c       DO 55 freerho=0.001,0.030,0.005
c       DO 55 emissivity=0.7,1.0,0.1
c       DO 55 radius=4.0,8.0,0.5
c
      freevel=7854.0
      freerho=1.29E-3
      emissivity=0.8
      radius=5.6

c      Use the Newton-Rhapson method of approximation.
c
        p0=500.0
        p1=1000.0
        q0=evalf(p0,freevel,freerho,emissivity,radius)
        q1=evalf(p1,freevel,freerho,emissivity,radius)
        p=p1-q1*(p1-p0)/(q1-q0)
        diff = abs(p-p1)
c
        DO WHILE(diff.gt.tol)
        p0=p1
        q0=q1
        p1=p
        q1=evalf(p,freevel,freerho,emissivity,radius)
        p=p1-q1*(p1-p0)/(q1-q0)
        diff = abs(p-p1)
c
        ENDDO
c
```

T. Lewerenz

```
      WRITE(*,100) p,freevel,freerho,emissivity,radius
      WRITE(5,100) p,freevel,freerho,emissivity,radius
c
c55   ENDDO
c
100   FORMAT(' equilibrium temperature: ',F10.5,/,
   &  ' freevel: ',F10.5,/,' freerho: ',F10.8,/,' emissivity: ',
   & F10.5,/,' radius: ',F10.5,/,/,
    & '_____________________________________________',/,/)
c
   STOP
   END


c     ************** functions*************************

      FUNCTION evalf(equiltemp,freevel,freerho,emissivity,radius)


      REAL m,n

      n=0.5
      m=3.0
      mach=freevel/340.3
      gamma=1.4
      statictemp=282.0
      totaltemp=statictemp*(1.0+((gamma-1.0)/2.0)*(mach**2))
      sbc=5.6703E-8
      htablat=14.0E+6
      ablatrho=320.368
      ablatvel=8.4667E-5
      heat_o2=4871.063

     chap1 = 1.83E-8/SQRT(radius)
     chap2 = 1.0-(equiltemp/totaltemp)
     chap=chap1*chap2
     check=(freerho**n)*(freevel**m)
      heat_conv=(freerho**n)*(freevel**m)*chap*(100.0**2)
     heat_rad=(emissivity)*(sbc)*(equiltemp**4.0)
     heat_ablat=htablat*ablatrho*ablatvel
     evalf=heat_conv - (heat_rad+heat_ablat+heat_o2)

c    WRITE(*,*) freevel,freerho,check
c    WRITE(5,*) freevel,freerho,check
     WRITE(*,*) heat_conv,heat_rad,heat_ablat,heat_o2
     WRITE(5,*) heat_conv,heat_rad,heat_ablat,heat_o2

      RETURN
      END
```

+1323287.5000000	+2835.1501465	+379744.3750000	+4871.0629883
+1300948.0000000	+45362.4023438	+379744.3750000	+4871.0629883
+1000993.4375000	+1.605867E+08	+379744.3750000	+4871.0629883
+1299323.7500000	+52327.3281250	+379744.3750000	+4871.0629883
+1297724.0000000	+59941.7460938	+379744.3750000	+4871.0629883
+1149609.0000000	+1.680595E+07	+379744.3750000	+4871.0629883
+1290244.1250000	+107098.2109375	+379744.3750000	+4871.0629883
+1283575.1250000	+168771.0781250	+379744.3750000	+4871.0629883
+1212321.8750000	+3594727.7500000	+379744.3750000	+4871.0629883
+1268698.0000000	+398692.6562500	+379744.3750000	+4871.0629883
+1260284.3750000	+603866.5625000	+379744.3750000	+4871.0629883
+1249577.7500000	+968847.8125000	+379744.3750000	+4871.0629883
+1252538.5000000	+854802.5000000	+379744.3750000	+4871.0629883
+1252206.3750000	+867062.3125000	+379744.3750000	+4871.0629883
+1252192.5000000	+867579.9375000	+379744.3750000	+4871.0629883
+1252192.5000000	+867577.0625000	+379744.3750000	+4871.0629883

equilibrium temperature: 2091.23584
freevel: 7854.00000
freerho: .00129000
emissivity: .80000
radius: 5.60000

Appendix A6.3.2

```
c       conicalheatdist
c
c       This program calculates the convective heat flux
c       distribution across the conical heat shield which is
c       modelled as a laminar flat plate.  Note that SI units
c       (i.e., m, kg, s, K) are used throughout.
c
c
        REAL mw,nw,machw,ml,nl,machl
c
c       windward side ***********************************************
c
        nw=0.5
        mw=3.2
        gammaw=1.4
         freerhow=2.365E-3
         freevelw=2972.602
        machw=freevelw/340.3
        phiw=-0.6108
        equiltempw=2091.236
        statictempw=3954.353
        totaltempw=statictempw*(1.0+((gammaw-1.0)/2.0)*(machw**2.0))
        distw=0.01
c
        DO WHILE (distw.lt.3.9)
        chap1w=((2.53E-9)*(COS(phiw)**0.5)*SIN(phiw))/(distw**0.5)
        chap2w=1.0-(equiltempw/totaltempw)
        chapw=chap1w*chap2w
        heat_convw=(freerhow**nw)*(freevelw**mw)*chapw*(100.0**2.0)
        WRITE(*,100) distw,heat_convw
        WRITE(5,100) distw,heat_convw
        distw=distw+0.55
c
        ENDDO
c
c       leeward side ***********************************************
c
c       nl=0.5
        ml=3.2
        gammal=1.4
        freerhol=2.238E-3
        freevell=1599.410
        machl=freevell/340.3
        phil=0.0873
        equiltempl=2091.236
```

```
      statictempl=3843.827
     totaltempl=statictempl*(1.0+((gammal-1.0)/2.0)*(machl**2.0))
      distl=0.01
c
      DO WHILE (distl.lt.3.9)
      chap1l=((2.53E-9)*(COS(phil)**0.5)*SIN(phil))/(distl**0.5)
      chap2l=1.0-(equiltempl/totaltempl)
      chapl=chap1l*chap2l
      heat_convl=(freerhol**nl)*(freevell**ml)*chapl*(100.0**2.0)
      WRITE(*,200) distl,heat_convl
      WRITE(5,200) distl,heat_convl
      distl=distl+0.55
c
      ENDDO
c
 100  FORMAT(/,' distancew: ',F6.3,'m',/,' convective heat fluxw: ',
  &   F11.3,'W/m^2',/,
   &  '___________________________________________________________')

 200  FORMAT(/,' distancel: ',F6.3,'m',/,' convective heat fluxl: ',
  &   F11.3,'W/m^2',/,
   &  '___________________________________________________________')
c
      STOP
      END
```

distancew: .010m
convective heat fluxw: -803447.063W/m^2

---

distancew: .560m
convective heat fluxw: -107365.148W/m^2

---

distancew: 1.110m
convective heat fluxw: -76259.844W/m^2

---

distancew: 1.660m
convective heat fluxw: -62359.594W/m^2

---

distancew: 2.210m
convective heat fluxw: -54045.715W/m^2

---

distancew: 2.760m
convective heat fluxw: -48361.840W/m^2

---

distancew: 3.310m
convective heat fluxw: -44161.457W/m^2

---

distancew: 3.860m
convective heat fluxw: -40894.391W/m^2

---

distancel: .010m
convective heat fluxl: 354379.031W/m^2

---

distancel: .560m
convective heat fluxl: 47355.898W/m^2

---

distancel: 1.110m
convective heat fluxl: 33636.176W/m^2

---

distancel: 1.660m
convective heat fluxl: 27505.152W/m^2

---

distancel: 2.210m
convective heat fluxl: 23838.117W/m^2

---

distancel: 2.760m
convective heat fluxl: 21331.117W/m^2

---

distancel: 3.310m
convective heat fluxl: 19478.438W/m^2

---

distancel: 3.860m
convective heat fluxl: 18037.424W/m^2

Appendix A6.3.3

```
c       shieldmass
c
c
c       This program estimates the total mass of the DART TPS.
c       The DART TPS consists of both phenolic epoxy resin and
c       silica fiber thermal blankets.  The ablative part of
c       the TPS is made up of two layers:(1) a char zone and
c       (2) a virgin zone,with the virgin zone being far denser
c        than the char zone.  The outer shell of the capsule
c       is divided into a number of sections for analytical
c       purposes.  First the surface area (S) will be
c       determined for each section, and then the volume (V)
c       will be determined by estimating the heat shield
c       thickness (T).  The densities of the two different TPS
c       materials are used to calculate the mass (M) of each
c       section.  The sum of all the masses will be the total
c       heat shield
c       mass.
c
c       variables
c
      REAL mc6,mc7,mc8,mv6,mv7,mv8,m1,m2,m3,m4,m5,m6,m7,m8,
     & l3,l4,l5,lc6,lv6
c
        INTEGER c1,c2,c3,c4,c5,c6,c7,c8
c
        pi=3.14159
c
c       density of char layer (kg/m^3)
        rho1=320.368
c
c       density of virgin layer (kg/m^3)
        rho2=512.588
c
c       density of the silica fiber thermal blanket (kg/m^3)
c
        rho3=144.165
c
c       Find the S (m^2) of each layer of each section.
c
c       Section 1 (top circle)
c
        r1=0.750
        s1=pi*r1**2
```

```
c
c       Section 2 (top cylinder)
c
        r2=0.750
        h2=0.500
        s2=2*pi*r2*h2
c
c       Section 3 (cone)
c
        r31=0.750
        r32=0.982
        l3=0.864
        s3=pi*(r31+r32)*l3
c
c       Section 4 (cone)
c
        r41=0.989
        r42=1.220
        l4=0.864
        s4=pi*(r41+r42)*l4
c
c       Section 5 (cone)
c
        r51=1.225
        r52=1.457
        l5=0.864
        s5=pi*(r51+r52)*l5
c
c       Section 6 (cone)
c
        rc61=1.459
        rc62=1.690
        lc6=0.864
        sc6=pi*(rc61+rc62)*lc6
        rv61=1.445
        rv62=1.676
        lv6=0.864
        sv6=pi*(rv61+rv62)*lv6
c
c       Section 7 (toroid)
c
        rc7=1.739
        xc7=0.134
        sc7=2*pi*rc7*xc7*2
        rv7=1.722
        xv7=0.134
        sv7=2*pi*rv7*xv7*2
c
c       Section 8 (slice of sphere)
```

```
c
      rc8=5.634
      xc8=5.354
      sc81=2*pi*rc8**2
      sc82=2*pi*rc8*xc8
      sc8=sc81-sc82
      rv8=5.600
      xv8=5.320
      sv81=2*pi*rv8**2
      sv82=2*pi*rv8*xv8
      sv8=sv81-sv82
c
c     Find the V (m^3) of each layer of each section.
c
c     thicknesses (m)
c
      t1=0.0130
      t2=0.0130
      t3=0.0167
      t4=0.0203
      t5=0.0240
      tc6=0.01848
      tc7=0.02112
      tc8=0.0330
      tv6=0.00924
      tv7=0.01056
      tv8=0.0165
c
      v1=s1*t1
      v2=s2*t2
      v3=s3*t3
      v4=s4*t4
      v5=s5*t5
      vc6=sc6*tc6
      vc7=sc7*tc7
      vc8=sc8*tc8*0.666
      vv6=sv6*tv6
      vv7=sv7*tv7
      vv8=sv8*tv8*0.666
c
c     Find the M (kg) of each layer of each section.
c
      m1=v1*rho3
      m2=v2*rho3
      m3=v3*rho3
      m4=v4*rho3
      m5=v5*rho3
      mc6=vc6*rho1
      mc7=vc7*rho1
```

```
      mc8=vc8*rho1
      mv6=vv6*rho2
      mv7=vv7*rho2
      mv8=vv8*rho2
c
c     Calculate the total S, V, and M of each section.
c
      s6=sc6+sv6
      s7=sc7+sv7
      s8=sc8+sv8
c
      v6=vc6+vv6
      v7=vc7+vv7
      v8=vc8+vv8
c
      m6=mc6+mv6
      m7=mc7+mv7
      m8=mc8+mv8
c
c     Calculate the total S, V, and M of the entire heat shield.
c
      st=s1+s2+s3+s4+s5+s6+s7+s8
      vt=v1+v2+v3+v4+v5+v6+v7+v8
      mt=m1+m2+m3+m4+m5+m6+m7+m8
c
c     Assign section numbers.
c
      c1=1
      c2=2
      c3=3
      c4=4
      c5=5
      c6=6
      c7=7
      c8=8
c
c
      WRITE(*,*) '                    Heat Shield Mass Data'
      WRITE(5,*) '                    Heat Shield Mass Data'
      WRITE(*,*)
      WRITE(5,*)
      WRITE(*,*) '        Sect.#','       ','S(m^2)','         ',
     &   'V(m^3)','           ','M(kg)'
      WRITE(5,*) '        Sect.#','       ','S(m^2)','         ',
     & 'V(m^3)','           ','M(kg)'
      WRITE(*,*)
      WRITE(5,*)
      WRITE(*,*) c1,s1,v1,m1
      WRITE(5,*) c1,s1,v1,m1
```

```
      WRITE(*,*) c2,s2,v2,m2
      WRITE(5,*) c2,s2,v2,m2
      WRITE(*,*) c3,s3,v3,m3
      WRITE(5,*) c3,s3,v3,m3
      WRITE(*,*) c4,s4,v4,m4
      WRITE(5,*) c4,s4,v4,m4
      WRITE(*,*) c5,s5,v5,m5
      WRITE(5,*) c5,s5,v5,m5
      WRITE(*,*) c6,s6,v6,m6
      WRITE(5,*) c6,s6,v6,m6
      WRITE(*,*) c7,s7,v7,m7
      WRITE(5,*) c7,s7,v7,m7
      WRITE(*,*) c8,s8,v8,m8
      WRITE(5,*) c8,s8,v8,m8
c
     WRITE(*,*)
     WRITE(5,*)
     WRITE(*,*) 0,st,vt,mt
     WRITE(5,*) 0,st,vt,mt
c
      STOP
      END
```

Heat Shield Mass Data

Sect.#	S(m^2)	V(m^3)	M(kg)
1	+1.7671444	+2.297288E-02	+3.3118849
2	+2.3561926	+3.063050E-02	+4.4158463
3	+4.7012262	+7.851048E-02	+11.3184624
4	+5.9959641	+1.217181E-01	+17.5474854
5	+7.2798438	+1.747162E-01	+25.1879673
6	+17.0188751	+2.362327E-01	+90.7276306
7	+5.8279514	+9.246589E-02	+35.5089760
8	+19.7638397	+3.261060E-01	+125.2843628
0	+64.7110367	+1.0833528	313

T. Lewerenz

Appendix A6.3.4

TPS Material Trade-Off Study: Aft Heat Shield

	Phenolic Epoxy Resin	Carbon Carbon
Temperature Limit	3033 K	2473 K
Mass of DART Aft Heat Shield	139 kg	355 kg
Material Cost	$ 175 per kg	$ 450 per kg
Advantages	• Light • Inexpensive • Can be applied to DART vehicle in the form of spray-on ablative foam • Can be stripped off DART vehicle during refurbish-ment using a water cannon	• Reusable - designed to last for DART vehicle's operational life • One-piece construction results in simple bolt-on attachment to DART vehicle
Disadvantages	• Nonreusable - aft heat shield must be completely replaced after each flight	• Heavy • Expensive • Difficult to manufacture

T. Lewerenz

Appendix A6.3.5

TPS Material Trade-Off Study: Conical Heat Shield

	RSI Tiles	**Ablative Cork**
Temperature Limit	1533 K	?
Mass of DART Conical Heat Shield	227 kg	121 kg
Material Cost	$ 175 per kg	$ 350 per kg
Advantages	• Reusable • Minimum refurbishment after each flight	• Damps vibrations • Low thermal conductivity • Char layers formed
Disadvantages	• Not designed for the impact that occurs during a water landing • Smallest tile thickness obtainable is 1 inch • Difficult to manufacture	• Nonreusable • When sheet becomes too thick (>1.6 cm) it is difficult to mold to vehicle • Cork is difficult to obtain

T. Lewerenz

Appendix A6.3.5 cont'd

TPS Material Trade-Off Study: Conical Heat Shield cont'd

	Phenolic Epoxy Resin	Thermal Blanket
Temperature Limit	3033 K	922 K
Mass of DART Conical Heat Shield	176 kg	116 kg
Material Cost	$ 175 per kg	?
Advantages	• Light • Inexpensive • Can be applied to DART vehicle in the form of spray-on ablative foam • Can be stripped off DART vehicle during refurbishment using a water cannon	• Reusable • Light • Durable • Low fabrication and installation costs • Glue on
Disadvantages	• Nonreusable - aft heat shield must be completely replaced after each flight	• Blankets only protect areas where temperatures are below 922 K

T. Lewerenz

A7.1

Appendix 7.1 Parashield Concept

The parashield is an umbrella-like structure that is deployed upon reentry, serving as large heat shield. It is made of a flexible insulating material, Quilite, which can withstand temperatures up to 1260K and a maximum heating rate of 117 kW/m^2, and is supported by 15 radial struts. The shield also serves as a parachute after rotation of the spacecraft during the transition from supersonic to subsonic speeds. The main advantage of the parashield is that it precludes the need for an angle on the spacecraft for reentry, since the shield extends far beyond the craft, providing a shadow zone and allowing a cylindrically shaped vehicle. A schematic is shown in Figure A7.1a.

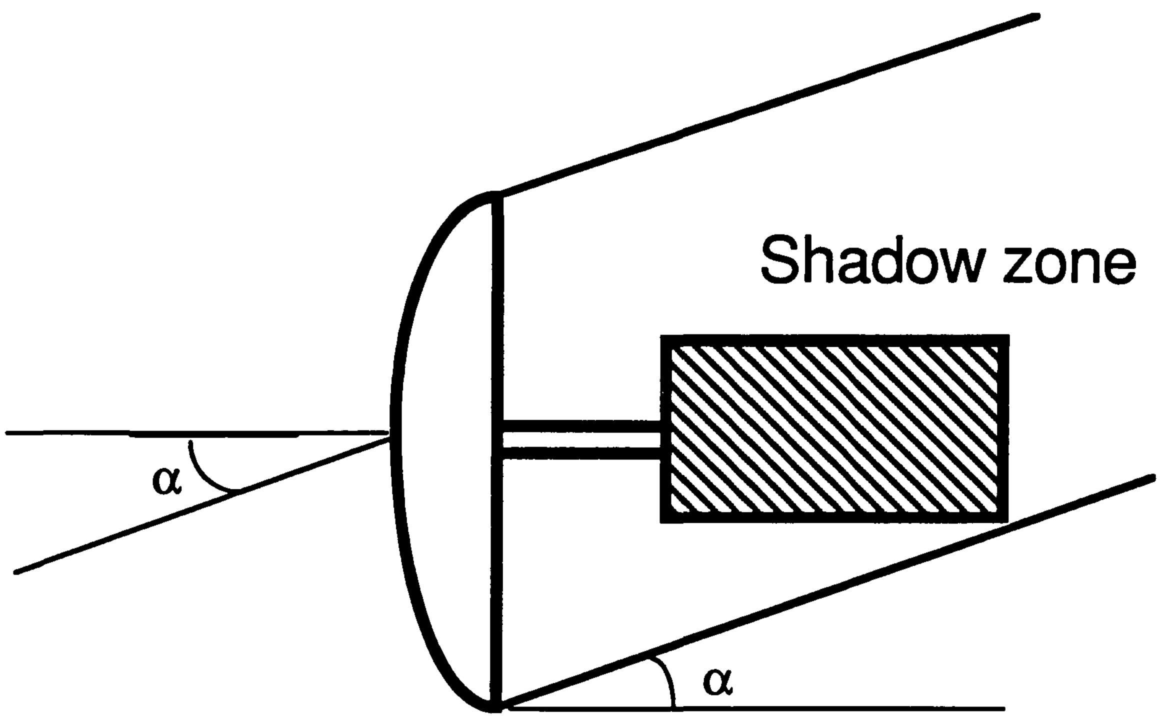

Figure A7.1a: Parashield Configuration during reentry[1].

The parashield was not chosen for use with the DART. The parashield and heat shield weights are approximately equal, while the parashield requires considerably more volume than the heat shield when stowed. In addition, though the parashield allows a cylindrical design, the DART's docking mechanism, capsule interface, and engine designs are all placed along the length of the capsule, leaving no additional room to stow the parashield lengthwise on the DART. Finally, the actuators for deployment of the shield are quite heavy, adding weight to the DART.

1. 16.86 Alternative Manned Spacecraft Draft Report, Dr. Dave Akin

M. Gates

MISSING
PRECEDING PAGE ~~BLANK~~ NOT FILMED

A7.3

Appendix A7.3.1

DDT&E and First Unit Cost Breakdown

System	Mass (kg)	DDT&E	First Unit
ECISS/crew Accomidations	634	$472.60	$60.53
Avionics	442	$844.21	$56.52
Sabilization and Contol*	0	$0.00	$0.00
Contol Moment Gyros*	0	$0.00	$0.00
Structures/TPS	1073	$160.78	$25.95
Electrical Power	131	$31.42	$6.87
Docking Module	28	$7.67	$0.91
RCS/Propulsion System	342	$68.24	$8.47
Cryo Tanks	80	$5.80	$0.93
Total	**2730.86**	**$1,590.72**	**$160.17**

System	Parameter		Cost
Software	600,000	program words	$1,155.00
Systems Engineering and Integration	$1,590.72	(DDT&E cost)	$1,336.20
Integration, Assembly, and Checkout	$160.17	(First Unit Cost)	$40.69
Subsystems Development Test	$17,121.02	(Total Direct Cost)	$1,249.83
Ground Support Equipment	$17,121.02	(Total Direct Cost)	$1,540.89
Project Management	$17,121.02	(Total Direct Cost)	$513.63

REUSABLE

ITEM		COST
Non-Reccuring Cost		$6,468.00
Recurring Cost	(200 FLIGHTS / 10 PER YEAR)	$10,653.02
Total		$20,425.37

-C.White

Appendix A7.3.2

RELIABILITY ANALYSYS

System	Subsystem	system part	reliability
Delta launch vehicle			**0.960000**
abort systems			**0.999574**
	structures		0.999990
	propulsion		0.999700
		engine 1	0.999900
		engine 2	0.999900
		engine 3	0.999900
	chutes		0.999884
		chute1	0.989250
		chute2	0.989250
stuctures			**0.999340**
	main structure		0.999990
	tps		0.999850
	docking		0.999500
propulsion			**0.999992**
	main engines		0.999996
		set 1	0.998000
		set 2	0.998000
	rcs		0.999996
		set 1	0.998000
		set2	0.998000
avionics			**0.999890**
	data prossesing		1.000000
	communication		0.991900
	sensors		0.999990
	guidence and nav		0.999950
	power		0.999950
		system 1	0.995000
		system2	0.990000
human factors	eclss		**0.999999**
		system1	0.999000
		system2	0.999000
crew survivability			**0.999235**
mission success			**0.959252**

-C.White

Appendix A7.3.3

Mass breakdown

System	Subsystem	Mass(kg)
Avionics		
	Data processing	96
	Altitude sensors	10
	Sensors	150
	Radar	75
	Guidance and navigation	29
	Communication	82
	Power generation	131
Human factors		
	ECLSS	634
	Food & water	574
	5 Astronauts	400
Systems Integration		
	Interface	0
	Propulsion	3
Structures		
	Main structure	237
	Docking module	28
	TPS	318
	Abort tower/motors	-22
	Impact attenuation system	129
	Chutes	200
Propulsion		
	Main engines	136
	Main propellant tanks&plumbing	80
	RCS	491
	Fuel	767
Total		**4548**

-C.White

For the purpose of calculating the capsule's system two models were made to qualify the communications onboard. The first model was for the earth station. It has a 10 meter diameter antenna with a gain of 316K times that of the isentropic reception and an amplification power of 1000 watts. The TDRSS model has a 4 meter diameter antenna with a gain of 4K to 141K times that of isentropic reception and an amplification power of 200 watts. These values as well as all others are converted to decibels for the link budget calculations.

The overall qualifying figure in the link budget determination is the carrier to noise ratio. In the Communications Satellite Handbook this ratio must be positive and be at least 10 to 12.5 dB in order for the signal to have good reception. For the results of the link budget calculations see Tables 5.5B,C,D,E.

Frequency Band, GHz	2.1	2.15	12.1
Satellite antenna dia., m	4	4	4
Satellite Station			
Transmitter power, dBw	23	23	23
Feed losses, dB	-2.1	-2.1	-2.1
Antenna gain, dBi	36.29	36.49	51.50
EIRP, dBw	57.19	57.39	72.40
Satellite to Capsule			
Path losses	191.76	191.97	206.97
Capsule			
Antenna gain, dBi	2.15	2.15	36.45
System noise temp.,dBK	0.15	0.15	21.45
G/Ts, dBw/K	2	2	15
Illumination level, dBw/m^2	-67.79	-67.59	-52.58
(C/T)u, dBw/K	-93.73	-93.73	-80.73
1/Boltzmann const., dBHz	228.6	228.6	228.6
C/kT, dBHz	134.87	134.87	147.87
1/ bandwidth, dBHz	-36.02	-45.56	-77.48
(C/N)u, dB	98.85	89.31	70.39

Table 5.5B Uplinks from TDRSS

Frequency Band, GHz	2.1	2.15	12.1
Earth station antenna dia., m	10	10	10
Earth Station			
Transmitter power, dBw	30	30	30
Feed losses, dB	-3.5	-3.5	-3.5
Antenna gain, dBi	55	55	55
EIRP, dBw	81.5	81.5	81.5
Earth to Capsule			
Path losses	153	153	168
Capsule			
Antenna gain, dBi	2.15	2.15	36.45
System noise temp.,dBK	0.15	0.15	21.45
G/Ts, dBw/K	2	2	15
Illumination level, dBw/m^2	-43.48	-43.48	-43.48
(C/T)u, dBw/K	-69.42	-69.63	-71.64
1/Boltzmann const., dBHz	228.6	228.6	228.6
C/kT, dBHz	159.18	158.97	156.96
1/ bandwidth, dBHz	-36.02	-45.56	-77.48
(C/N)u, dB	123.16	113.41	79.48

Table 5.5C Uplinks from Earth

Frequency Band, GHz	2.2	2.25	12.2
Capsule beam type	omni.	omni.	dish
Satellite antenna dia., m	-	-	0.5
Capsule			
Transmitter power, dBw	14.7	14.7	13.01
Feed losses, dB	-1.7	-1.7	-1.7
Antenna gain, dBi	2.15	2.15	36.45
EIRP, dBw	15.15	15.15	47.76
Capsule to Satellite			
Path losses	191.76	191.97	206.97
Illumination level, dBw/m^2	-148.72	-148.72	-116.11
Satellite			
Antenna gain, dBi	36.29	36.49	51.50
System noise temp.,dBK	-30	-30	-30
G/Ts, dBw/K	6.29	6.49	21.50
(C/T)d, dBw/K	-170.78	-170.77	-137.84
1/Boltzmann const., dBHz	228.6	228.6	228.6
C/kT, dBHz	57.82	57.83	90.76
1/ bandwidth, dBHz	-36.02	-45.56	-77.48
(C/N)d, dB	21.80	12.27	13.28

Table 5.5D Downlinks from TDRSS

Frequency Band, GHz	2.2	2.25	12.2
Capsule beam type	omni.	omni.	dish
Satellite antenna dia., m	-	-	0.5
Capsule			
Transmitter power, dBw	14.7	14.7	13.01
Feed losses, dB	-1.7	-1.7	-1.7
Antenna gain, dBi	2.15	2.15	36.45
EIRP, dBw	15.15	15.15	47.76
Capsule to Earth			
Path losses	-153	-153	-168
Illumination level, dBw/m^2	-109.83	-109.83	-75.52
Earth Station			
Antenna gain, dBi	50	50	50
System noise temp.,dBK	-21	-21	-21
G/Ts, dBw/K	29	29	29
(C/T)d, dBw/K	-109.18	-109.37	-89.75
1/Boltzmann const., dBHz	228.6	228.6	228.6
C/kT, dBHz	119.42	119.23	138.85
1/ bandwidth, dBHz	-36.02	-45.56	-77.48
(C/N)d, dB	83.40	73.67	61.37

Table 5.5E Downlinks to Earth

The link equations used are:

Gain for a parabolic antenna dBi

$$G = 10 \log \pi - 20 \log c + 20 \log d + 20 \log f + 10 \log \eta a$$

c - speed of light
d - diameter , m
f - frequency, GHz
ηa - efficiency

EIRP (equivalent isentropic radiated power) dBw

$$EIRP = 10 \log G + 10 \log W$$

W - amplification power, watts

Path loss dB

$$L = 92.45 + 20 \log S + 20 \log f$$

S - path length, Km
f - frequency, GHz

Gain to system noise ratio dBi/K

$$G/Ts = 10 \log G - 10 \log Ts$$

G - gain
Ts - system temperature, K

Illumination level dBw/m^2

$$W = EIRP - 20 \log S - 70$$

Carrier to noise ratio dB

$$C/T = W + G/Ts - 21.5 - 20 \log f \qquad (dBw/K)$$

$$C/kT = C/T - 10 \log k$$

k - Boltzmann constant

$$C/N = C/kT - 10 \log B$$

B - bandwidth, Hz

The weakest link is the downlink to TDRSS. In this link the carrier to noise ratio have been reduced to the minimum needed for good reception. This gave a parabolic antenna of 0.5 meters in diameter with 20 watts of amplification power and a dipole antenna with the standard gain of 1.64 and 30 watts of amplification power. For the parabolic an efficiency of 50 percent was used. The path length of transmission was used as a worst case of 3000 Km to earth and 50000 Km to TDRSS in order to calculate the path losses. The results will only vary slightly if fine tuning of the base frequencies needs to be done. All not calculated were estimated using the graphs given throughout the Communications Satellite Handbook for system modelling.

Antennas

In order to transmit and receive the desired frequencies different antennas are needed to cover the gaps in the bands used. Each band requires a different type of antenna based on the bandwidth necessary.

For the S - band a dipole antenna will be implemented and housed under a skin blemish to avoid the need for mechanical deployment. There will be two of these antennas, one facing earth and one 180 degrees around the spacecraft so that it is facing space. The two antennas supply a mode of redundancy and make serving earth stations and TDRSS efficient during orbit. Skin and whip antennas were also considered for this application, however due to deployment being necessary dipoles were chosen. The dipoles give higher gain and take up less space.

The UHF band will use a helical coil antenna because of its suitability to EVA communications application. It will be located on the egress face of the capsule, so as to face the astronauts as they perform EVA.

The Ku - band is for the high data rate requirements of the video link, this infers a very wide bandwidth. A deployable parabolic antenna will be used to fulfill these requirements. The antenna was calculated to be 0.5 meters in diameter, in order to overcome material and construction losses the diameter could be multiplied by a factor of 1.4 to give a diameter of 0.7 meters. The antenna will deploy out of a slot on either the pilots left or right side through the exterior skin of the capsule. Its location was chosen to be able to point to TDRSS and earth during orbit. It will open in an umbrella type fashion. This antenna can also be used rendezvous radar as discussed in section 5.4.

The L - band antenna will mounted on the skin in the same fashion as the S-band antennas but only on the surface facing GPS satellites.

Equipment

The equipment used onboard the capsule was based on the equipment outline presented for the British Multi-Role Capsule. This was done because of its similar mission capability and capsule size similarity. Using this outline the volumes and masses were also estimated. For the summary of equipment on board see Table 5.5F.

Unit	Equipment	Quantity	Total mass Kg	Volume mm x mm x mm	Power watts
Data	S-Band Tx/Rx	2	6	195 x 188 x 122	20
	Switch	1	0.5	-	
	RF Harness	1	1	-	
	Dipole antenna	2	1	300 x 175 x 80	
Audio	Intercoms	5	5	-	30
	Audiomixer	1	2	200 x 190 x 130	
	EMU Tele. / Extrac.	2	6	300 x 296 x 250	
	UHF TX/Rx	1	10	375 x 345 x 220	
	RF Harness	1	1	-	
	Helix coil antenna	1	0.5	140 x 140 x 80	
Video	Crew interface	1	5	-	20
	Antenna control	1	12	-	
	Ku- band Tx/Rx	1	10	375 x 345 x 220	
	Video duplexer	1	10	200 x 190 x 130	
	Parabolic antenna (closed)	1	12	500 x 300 x 80	
					50 % efficiency
			Total = 82 Kg		Total = 140 watts

Table 5.5F Equipment Summary

Redundancy / Reliability / Costing

The voice and data relay components (the S-band system) has two complete systems for redundancy. All other systems are singular and need to be made reliable enough for mission success. For the data and voice system the table on reliability in the Communications Satellite Handbook gave a value of 0.9919 and all the singular systems a value of 0.91.

The estimated DDT & E cost for the communications package based on 82 Kg was 318.31 $M91 and the first unit cost of 12.059 $M91.

Chapter 5 References

[1] *Jane's, All the World's Avionics*, IEEE, 1990

[2] Clausing, D.J., *The Aviator's Guide to Modern Navigation,* TAB Books Inc., 1987

[3] Kayton,M., *Navigation: Land, Sea, Air, and Space* ,IEEE Press, 1989

[4] Wertz, J. R., *Spacecraft Attitude Determination and Control*, Boston: D. Reidel Publishing Co., 1986

[5] Griffin, M. D. and J. R. French, *Space Vehicle Design*, New York: AIAA, 1991

[6] .*Jane's, All the World's Avionics*, IEEE, 1990

[7] Kent, A. and J. G. Williams, *Encyclopedia of Computer Science and Technology*, Marcel Dekker, Inc.

[8] Spitzer, C. R., *Digital Avionics Systems*, New Jersey: Prentice Hall Inc., 1987

[9] Cantafio, Leopold J. Ed. *Space-Based Radar Handbook.* Artech House Inc. Norwood, MA : 1989

[10] Kovaly, John J. *Synthetic Apeture Radar.* Consulting Engineer Raytheon Company Missile Systems Division Bedford : 1988

[11] . Morgan, Walter l. and Gordon, Gary D. *Communications Satellite Handbook*, John Wiley & Sons, New York, 1989

Chapter 5 Bibliography

Agrowal, B. N., *Design of Geosynchronous Spacecraft*, Prentice Hall Inc., 1986

Cantafio, Leopold J. Ed. *Space-Based Radar Handbook.* Artech House Inc. Norwood, MA : 1989

Ewell, George W. *Radar Transmitters.* McGraw-Hill Book Company New York, NY 1981

Fitch, J. Patrick. *Synthetic Apeture Radar.* Springer-Verlag New York, NY : 1988

Griffin, M. D. and J. R. French, *Space Vehicle Design*, New York: AIAA, 1991

Helfrick, Albert. *Modern Aviation Electronics.* Prentice-Hall, Inc. Englewood Cliffs, NJ 1984

Hempsell, C.M. *Multi-Role Capsule - An Introduction*, Journal of the British Interplanetary Society, 1989

Hempsell, C. M., *Multi-Role Capsule System Description*, Journal of the British Interplanetary Society, 1989

Hord, R. Michael. *Handbook of Space Technology: Status and Projections.* CRC Press Inc. Boca Raton, FL 1985

Human Factors in Long-Duration Spaceflight. National Academy of Sciences Washington, D.C. : 1972.

Jane's, All the World's Avionics, IEEE, 1990

Kayton,M., *Navigation: Land, Sea, Air, and Space* ,IEEE Press, 1989

Kendal, Brian. *Manual of Avionics: Second Edition.* BSP Professional Books Oxford: 1987

Kent, A. and J. G. Williams, *Encyclopedia of Computer Science and Technology*, Marcel Dekker, Inc.

Kovaly, John J. *Synthetic Apeture Radar.* Consulting Engineer Raytheon Company Missile Systems Division Bedford : 1988

Leondes, C.T., *Guidance and Control of Aerospace Vehicles*, McGraw-Hill Book Company, Inc., 1963

McLean, Ian S. *Electronic and Computer-Aided Astronomy: From Eyes to Electronic Sensors*. Ellis Horwood Limited New York, NY : 1989

Morgan, Walter l. and Gordon, Gary D. *Communications Satellite Handbook*, John Wiley & Sons, New York, 1989

NASA, *Satellite Acquisition: Global Positioning System Acquisition Changes After Challenger's Accident*, 1987

NASA, *Space Operations: NASA's Communications support for Earth Orbiting Spacecraft*, 1989

Norton, Harry N. *Biomedical Sensors: Fundamentals and Applications.* Noyes Publications Park Ridge, NJ : 1982

Principles of Radar. McGraw-Hill Book Company New York, NY : 1946

Sinclair, Ian R. *Sensors and Transducers.* BSP Professional Books Oxford : 1988

Smart Sensors. Technical Insights ,New York, NY : 1988

Space Tech: Conference Proceedings. Anaheim, CA : September 23-25, 1985

Spitzer, C. R., *Digital Avionics Systems*, New Jersey: Prentice Hall Inc., 1987

Taylor, Denis. *Introduction to RADAR and RADAR Techniques.* Philosophical Library, Inc. New York, NY : 1966

Van Wyck, Samuel M. and Carpenter, Max H. *The Radar Book.* Cornell Maritime Press Centerville, MD : 1984

Wertz, J. R., *Spacecraft Attitude Determination and Control*, Boston: D. Reidel Publishing Co., 1986

Chapter 6

Re-entry Studies

Section 6.1 Re-entry Trajectory

Introduction

The re-entry analysis conducted for the DART spacecraft is described in this section. DART's re-entry is modeled as a gliding re-entry with a small lift to drag ratio. The DART spacecraft has a lift to drag ratio of 0.25 and mass of 4414.0 kg at re-entry. The scenario for the re-entry of the DART vehicle firing an impulsive thrust manueuver at an altitude of 500 km. The delta-V from this thrust will allow a change in the altitude by changing the orbit of spacecraft to an elliptical orbit with apogee at 500 km altitude. The intermediate phase of the re-entry will begin at about 120 km altitude where deceleration of DART will become significant due to Earth atmosphere. The trajectory to this altitude is calculated by using Vis-Viva Equation for Keplerian ellipse geometry.

The re-entry equations of the intermediate and gas dynamics phases can be derived by summing the forces in two dimensions by making the lift vector normal to the capsule. These equations can be put into a second order differential equation; therefore, some assumptions are made to obtain solutions to entry parameters. Several solutions of the differential equation with various assumptions are available today; these equations were applied to the DART. The Z function method by Dr. Chapman is used to write a computer program for the re-entry analysis. A copy of the code is included in the appendix A.6.1.1.

Re-entry Equations

First Order Equations

Initially, the first order equations by Allen and Eggers for gliding entry were studied. These equations are stated to be valid for a lift to drag ratio of 0.25 to 1.0 and the initial inclination angles of 3 to 15 degrees. But the following equations were not used for the re-entry trajectory analysis due to the amount of error introduced by its primary assumption. The assumption is that the velocity is very close to the circular velocity. Obviously, this analysis will not work for all cases. The equations are listed as follows [26]:

$$\left(\frac{V^2}{gR_o}\right)=\left(\frac{V_f^2}{gR_o}\right)\exp\left[\frac{2}{\left(\frac{L}{D}\right)}(\theta_f-\theta)\right]$$

$$\cos\theta-\cos\theta_f=\frac{1}{2}\left(\frac{L}{D}\right)\left(\frac{C_dA}{m\beta}\right)(\rho-\rho_f)$$

M. Kosha

where V = velocity
g = gravitational constant
L/D = lift to drag ratio
Cd = coefficient of drag
A = reference area = $9.61 m^2$
β = atmospheric density decay parameter
ρ = density
m = mass
θ = flight inclination
R_o = radius of earth

The conditions at maximum deceleration were studied in these equations because the above assumption will not introduce significant errors to these calculations[26]. The initial inclination angle of 3^o was determined from this analysis to avoid deceleration that is too big for manned vehicle.

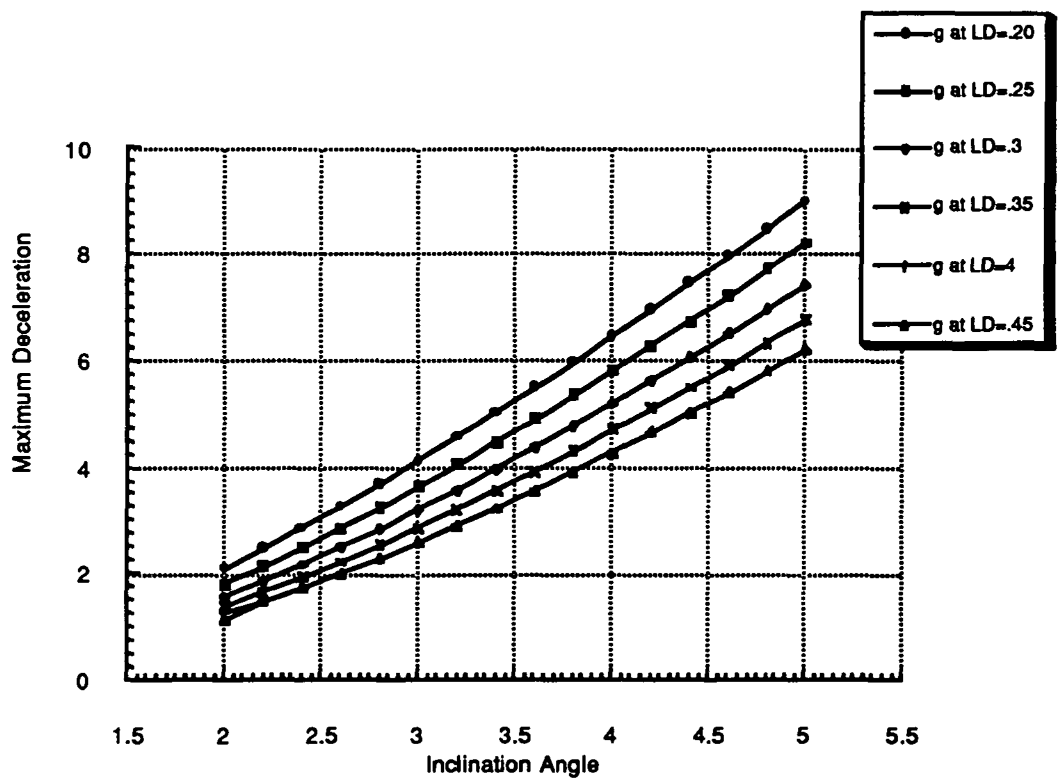

Figure 6.1a Maximum Deceleration vs Initial Inclination Angle

The equations used were as follows[26]:

$$\theta^* = \frac{\left(\frac{L}{D}\right)}{2}\left[-1 \pm \sqrt{1 + \left[\frac{2}{\left(\frac{L}{D}\right)}\theta_f\right]^2}\right]$$

$$\left(\frac{dV}{dt}\right)_{max} = -\frac{\beta}{\left(\frac{L}{D}\right)}(\cos\theta^* - \cos\theta_f)V_f^2 \exp\left[-\frac{2}{\left(\frac{L}{D}\right)}(\theta_f - \theta^*)\right]$$

The results were calculated by using Microsoft Excel. Figure 6.1a is plotted using the above equations with various lift to drag ratios. This was done to show the effect of lift to drag ratios and initial inclination angle that will cause a maximum deceleration. It shows that to minimize the deceleration, lift to drag ratio need to be maximized and the initial angle should be minimized. A larger initial inclination angle produces a smaller downrange for the landing of the spacecraft. This trend was taken into account when the lift to drag analysis was conducted by the Systems Integration.

Summation of Forces

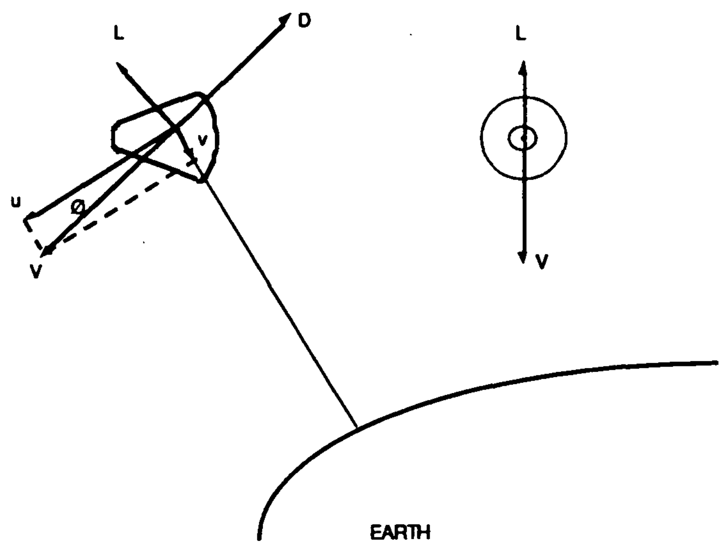

Figure 6.1b Forces on a Vehicle During Re-entry

The aerodynamic forces on the vehicle during re-entry is shown in Figure 6.1b. The equation of the vector forces is listed below:

$\vec{F} = (-mg+L\cos\theta+D\sin\theta)\vec{e_r} - (D\cos\theta-L\sin\theta)\vec{e_\psi}$

where $\vec{e_r}$ = *vector in the radial direction*

$\vec{e_\psi}$ = vector in circumferential direction.

The equation of the vector acceleration in polar coordinate is listed below:

$$\vec{a} = \left(\frac{dv}{dt} - \frac{u^2}{r}\right)\vec{e_r} + \left(\frac{du}{dt} + \frac{uv}{r}\right)\vec{e_\psi}$$

where u = circumferential velocity component
v = vertical velocity component
r = distance from the center of earth.

Because of assumption 4 , $\frac{uv}{r}$ term can be disregarded Therefore, if the forces are equated to mass × acceleration, two equations of motion can be derived:

$$\frac{du}{dt} = \frac{\rho_\infty \quad u^2}{2\left(\frac{m}{C_d A}\right)\cos\theta}$$

$$-\frac{1}{g}\frac{dv}{dt} = -\frac{1}{g}\frac{d^2y}{dt^2} = 1-\bar{u}^2 + \frac{\rho_\infty C_d A r \bar{u}^2}{2\ m\cos^2\theta}\left(\sin\theta - \frac{L}{D}\cos\theta\right)$$

Assumptions:

1. Atmosphere and planet are spherically symmetric
2. Variations in atmospheric temperature and molecular weight with altitude are negligible compared to the density variation.
   This leads to the exponential model for density variation:
   $\rho_\infty = 1.2 \times e^{-\beta y}$ where $\beta = \frac{1}{7000}$
3. Peripheral velocity of planet is negligible compared to the velocity of the entering vehicle.
4. $\left|\frac{dr}{r}\right| << \left|\frac{du}{u}\right|$ The change in altitude is much smaller than the change in circumferential velocity.
5. $\left|\frac{L}{D}\tan\theta\right| << 1$ θ = flight path angle

The information in this section is from reference 12.

Z - Function

The Z function method for the calculation of re-entry dynamics is applied to the analysis of the re-entry of the DART spacecraft. But the Z function method is inaccurate at the lower altitude where the flight angle becomes very large. At this point, the assumption number 5 produces large errors.

In this method, a dimensionless dependant variable Z is introduced and defined as

$$Z \equiv \frac{\rho\bar{u}}{2\left(\frac{m}{CdA}\right)}\sqrt{\frac{r}{\beta}}$$

where ρ = density
m = mass

Cd = coefficient of drag
A = reference area
r = radius
$\bar{u}$ = nondimensionalized radial velocity

β = atmospheric density decay parameter[12]

Using the above definition and applying the following assumptions, the calculations of various dynamic parameters such as inclination angle, velocity, deceleration, range, and time at each altitude become easier. The two equations of motion can be rewritten into one equation.

The equation of motion during re-entry which implemens Z-function analysis is given below:

$$\bar{u}Z'' - \left(Z' - \frac{Z}{\bar{u}}\right) = \frac{1-\bar{u}^2}{\bar{u}Z}\cos^4\theta - \sqrt{\beta r}\frac{L}{D}\cos^3\theta$$

Each terms represent different physical parameters as follows:

$\bar{u}Z''$ = vertical acceleration

$\left(Z' - \frac{Z}{\bar{u}}\right)$ = vertical component of drag force

$\frac{1-\bar{u}^2}{\bar{u}Z}\cos^4\theta$ = gravity minus centrifugal force

$\sqrt{\beta r}\frac{L}{D}\cos^3\theta$ = lift force[12]

A computer program in c was written to calculate the Z function at different point of the re-entry. The circumferential velocity ratio $\bar{u}$ which is a independent variable was decremented by $d\bar{u}$. At each point of $\bar{u}$, Z, Z', and Z" was calculated by using Taylor series; the flight path angle, altitude, velocity, deceleration, flight time, and range are calculated from Z. The initial conditions for altitude, velocity, and flight path angle along with mass, lift to drag ratio, and the reference area of the spacecraft and $d\bar{u}$ are the input values for this program. The local gravity value is approximated at constant value of 9.81 m/s^2. The input values used for the calculation of the trajectory is listed below:

altitude = 120 km	V = 7782 m/s
$d\bar{u}$ = 0.00005	m = 4414 kg
reference area = 9.6 m^2.	

The initial flight path angle is varied:
The initial flight path angle : 2^o, 3^o, and 4^o

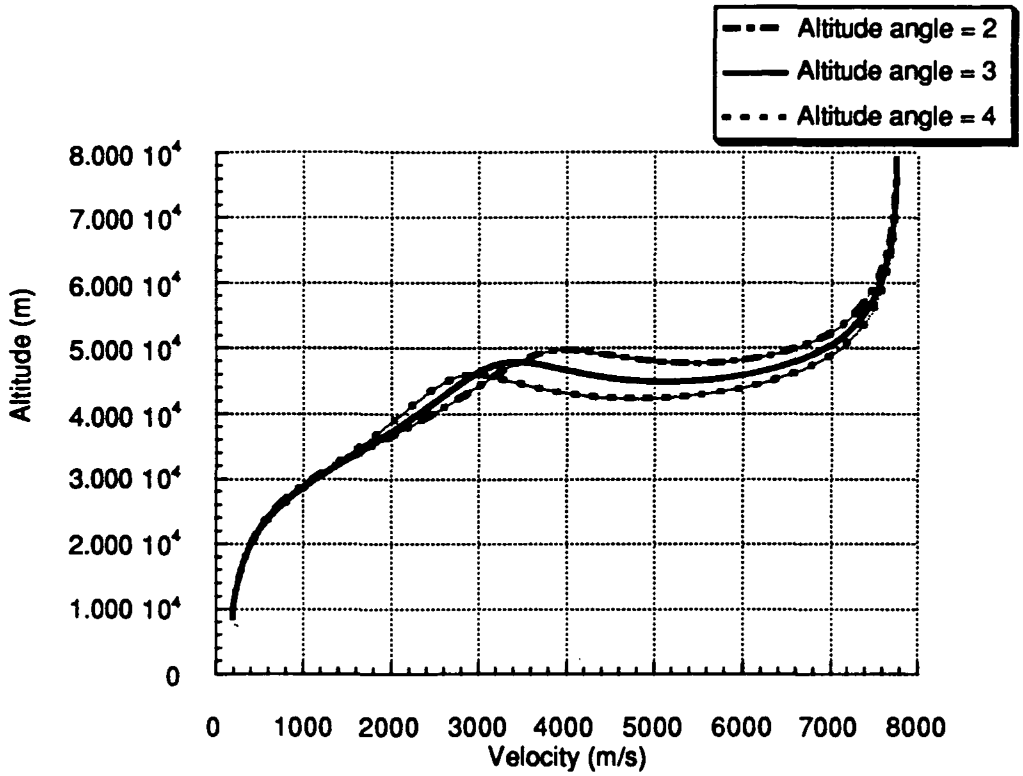

Figure 6.1.c Velocity at Various Initial Angles

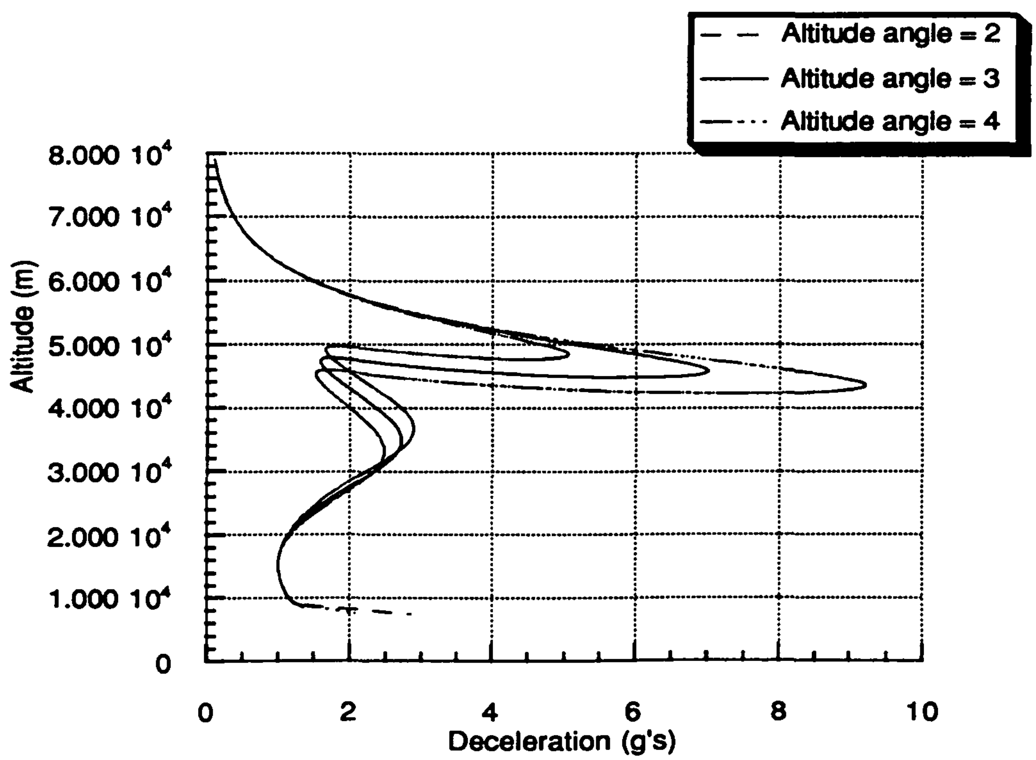

Figure 6.1d Deceleration at Various Initial Angles

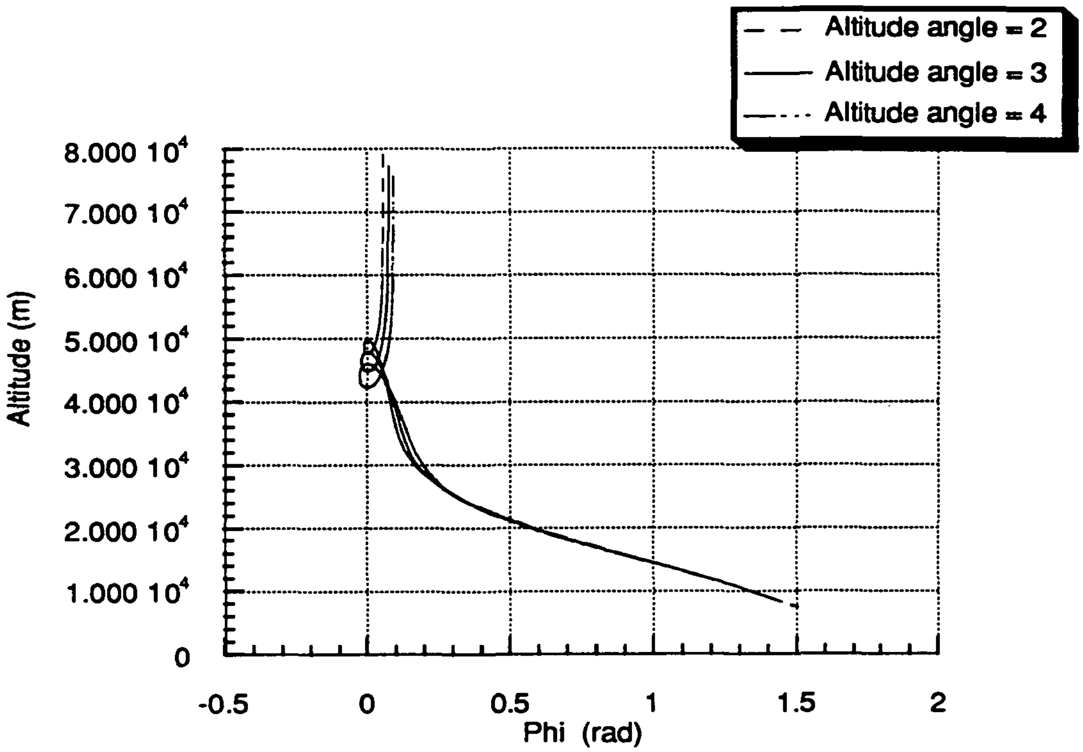

Figure 6.1e Flight Angle at Various Initial Angle

The results of Z function program is compared to the result from Dr. Russ Howard's re-entry simulation spreadsheet. As long as the initial condition starts around 120 km to 80 km the Z function gave good result. Because of assumption 4, a higher initial altitude resulted in a large error. The subject of altitude versus velocity is plotted in Figure 6.1f.

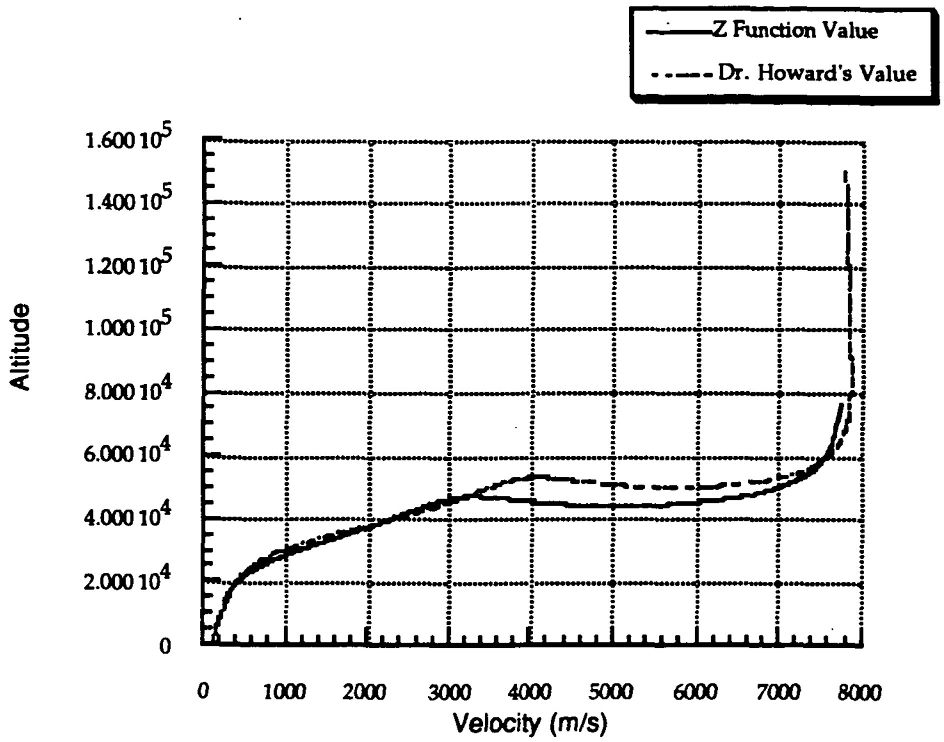

Figure 6.1f Velocity Comparison

From the plot of altitude versus flight angle, the altitude where some assumptions starts to fail can be observed. In fact, after about 10,000 km altitude the analysis will start to become unreliable.

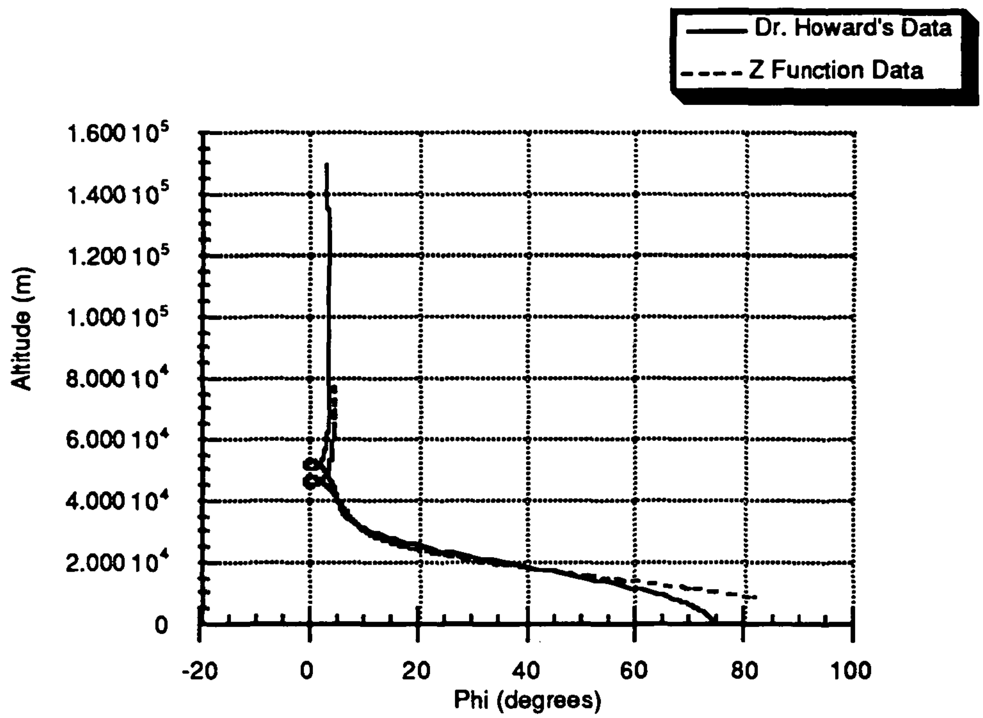

Figure 6.1g Flight Angle Comparison

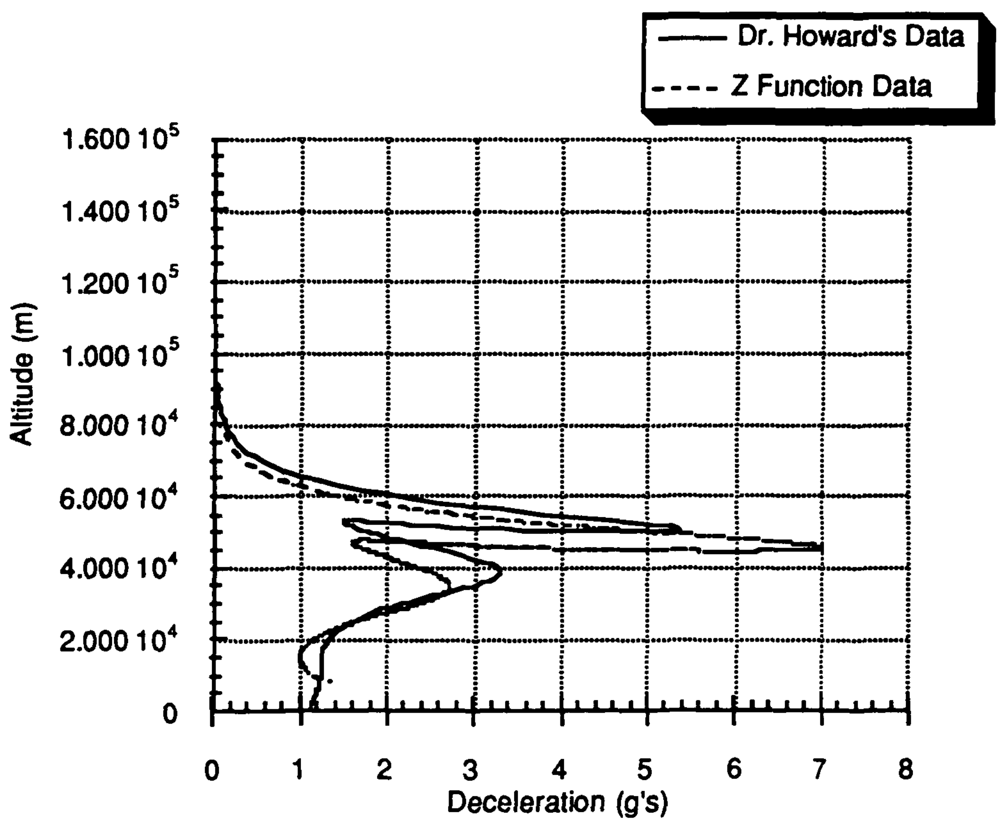

Figure 6.1h Deceleration Comparison

The Figure 6.1h shows that the conditions at the maximum deceleration occurs at the altitude that is not effected by the flight angle that is too large therefore it is in the good accuracy range. But Z function method gives the maximum deceleration that is larger than Dr. Howard's result. This is definitely of concern but the causes has not been investigated yet.

Dr. Russ Howard uses exponential atmosphere modeling with sea level density of 1.4 and the atmospheric decay of $\frac{1}{7140}$. The density data are compared in the following figure.

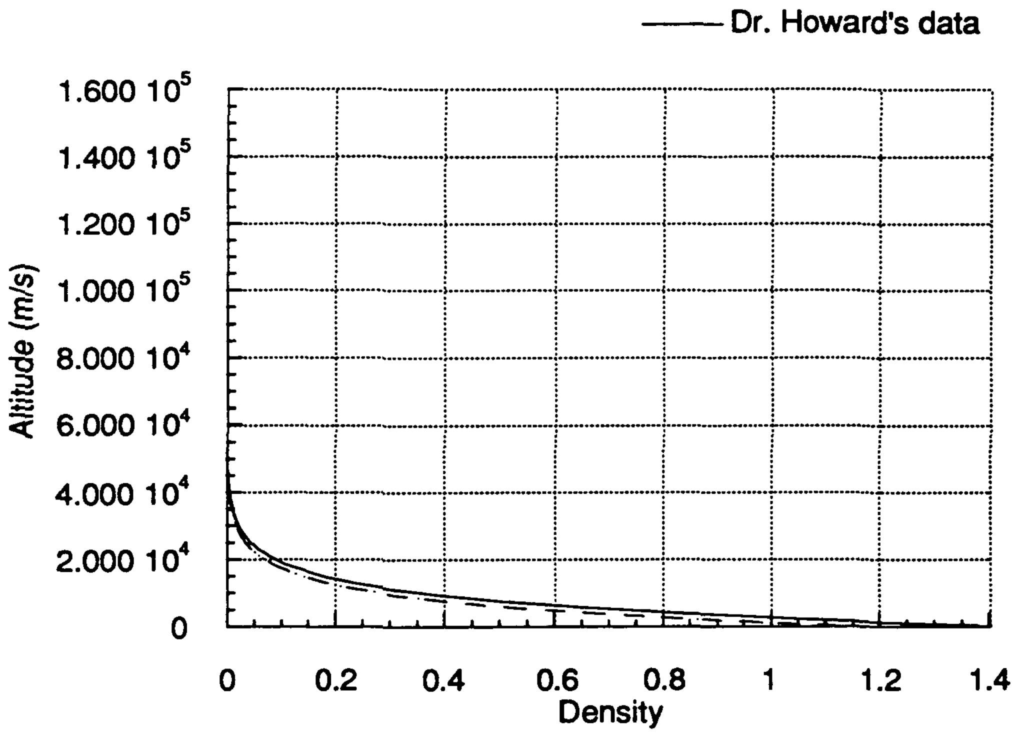

Figure 6.1i Density Model Comparison

Previously, the initial conditions were calculated using the restrictions on this method from the assumptions mentioned earlier, mainly assumption number 4.[12]

The approximation ratio was defined as

$$\widetilde{r_m} \equiv \frac{\frac{dr}{r}}{\frac{du}{u}} = \frac{\overline{u}\sin\theta_m}{\sqrt{\beta r} Z_m} \approx \frac{\overline{u_i}}{(\beta r)(\overline{u_i} - \overline{u_m})}.$$

in order of meet the assumption that $\widetilde{r_m} = 0.1$, set $\overline{u_m} = 0.99 * \overline{u_i}$. This condition allows the calculation of initial conditions using the Vis-Viva equation and the geometry of Keplerian ellipse. The following equations were used to calculate the initial parameters.[12]

$$\frac{\sqrt{\frac{r}{\beta}}\rho_m}{2\left(\frac{m}{CdA}\right)} = Z_m \approx \sqrt{\beta r}\,(\overline{u_i} - \overline{u_m})(-\sin\theta_o)$$

$$\rho_m = 2\left(\frac{m}{CdAr}\right)\frac{\overline{u_1}}{\tilde{r}_m}(-\sin\theta_o)$$

Unfortunately, this method does not work for our scenario. It is very clear from the plots of altitude versus velocity that the DART falls into the atmosphere very quickly and all of a sudden the curve flattens out about 60 km. Therefore if the above method was implemented to this analysis, it will begin around 60 km. A detailed analysis cannot be seen starting at this altitude because between 60 km and 40 km, velocity decreases rapidly and the altitude moves up and down. By implementing this method the initial condition may be chosen at an altitude that is too low. For this reason, the initial altitude of 120 km was used after analyzing the trajectory from Dr. Howard's method.

The foot print of DART is calculated. The sketch of the footprint is shown in Figure 6.1k. The footprint is calculated by the three dimensional analysis applied to the range at the touch down.

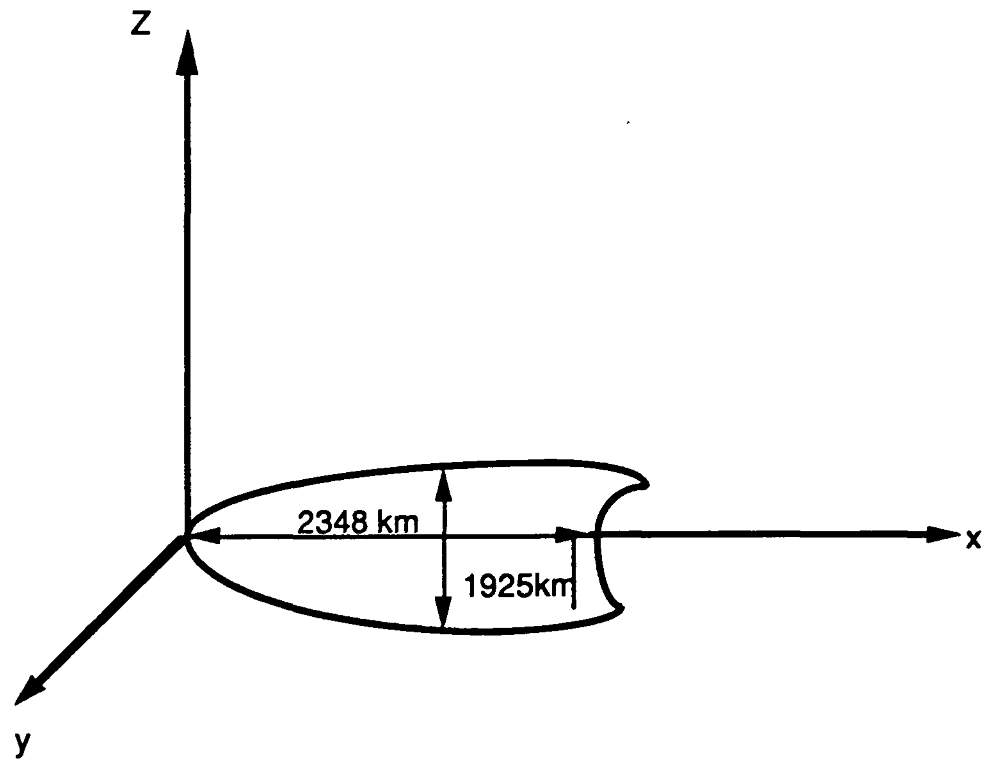

Figure 6.1j Footprint of DART

In the above figure, x is in the direction of flight, z is radial direction, and y is the direction of lift vector shift. The length of the footprint is 2348 km is the distance between where the spacecraft will land if the lift is normal to the spacecraft and the point of minimum range possible for maximum deceleration allowed. The width of the footprint which is 1925 km is calculated from the maximum deflection of lift in y direction.

Keplerian Phase

The conic perigee is the distance from the center of earth to the point in space where the perigee would be for the specific Keplerian ellipse trajectory. The conic perigee is defined by the distance at the initial orbit and the conditions at the initial point of atmospheric re-entry. The conic perigee is sketched in Figure 6.1k. The conic perigee of the trajectory with maximum allowable deceleration defines the undershoot boundary. The overshoot is not of concern for this spacecraft since it is already orbiting the planet, and no energy is added to the orbit. The conic perigee for our spacecraft entering atmosphere at 7782 m/s is calculated to be 64413 km.

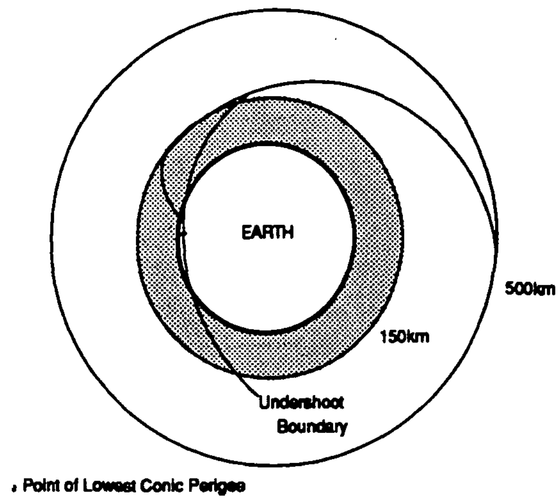

Figure 6.1k Sketch of Conic Perigee

The delta-V which is required to deorbit from the altitude of 500 km to the initial re-entry point is calculated using Vis-Viva equation. the delta-V at the apogee is calculated to be 239.86 kg. Vis-Viva equation is written below:

$$V^2 = GM\left(\frac{2}{r} - \frac{1}{\frac{1}{2}(r_{min} + r_{max})}\right)$$

where G = gravitational constant
M = mass of the Earth

The bar graph of Figure 6.1l shows the delta-V needed for getting different velocity ratio entering at flight path angle of 3^o. The velocity ratio of 0.996 at V = 7782 m/s is used for this analysis, therefore it is highlighted.

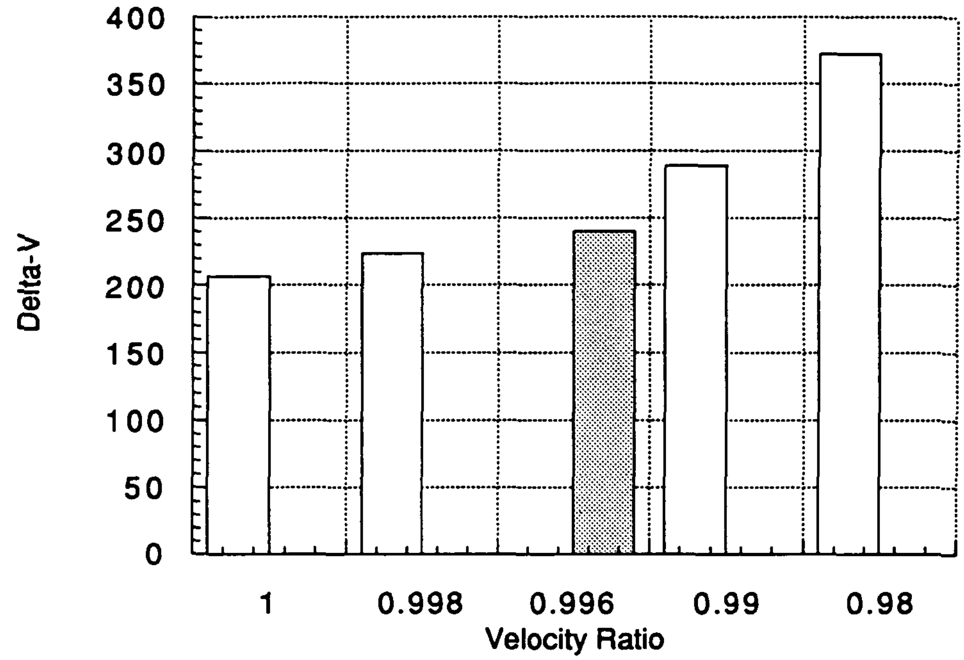

Figure 6.11 Delta-V versus Velocity Ratio

Conclusion

After the spacecraft slows down significantly the parachute is opened for landing. The details on recovery system are discussed in the section 6.4.

Section 6.2 Re-entry Aerodynamics

Introduction

The re-entry aerodynamic and thermodynamic properties of the DART vehicle are dependent upon the flight trajectory, the shape of the outer shell, and the orientation of the craft. A re-entry flight trajectory has been calculated by the Mission Analysis group and will be used in the analyses of this section. A blunt-body capsule design with a center of gravity offset has been chosen as the optimum vehicle shape. Blunt-body re-entry vehicles have high drag but relatively low heating input due to the strong shock wave diverting heat to the atmosphere. A semi-ballistic L / D can be achieved with a symmetric, spherical shield by changing the trim angle of attack. This is done by having the center of gravity in a location where no resulting moments occur.

Figure 6.2a illustrates the generic mathematical model for the DART used in the following analyses.

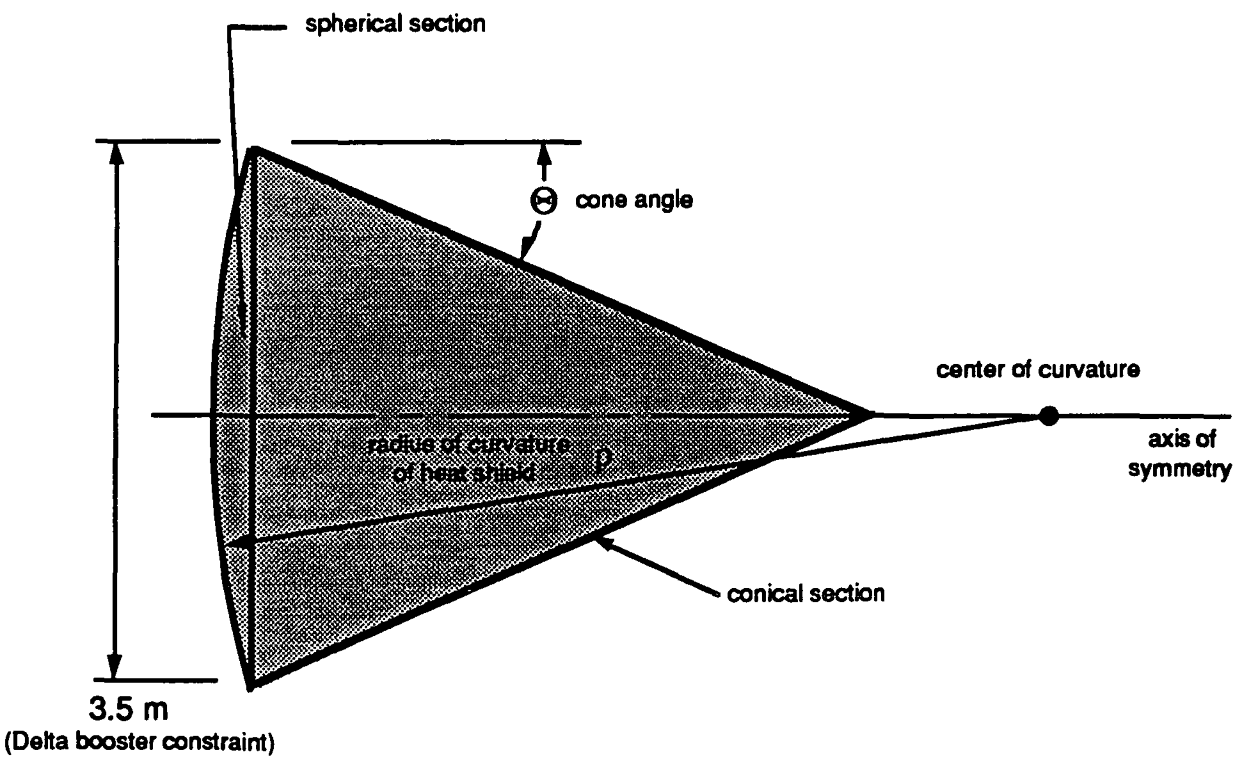

Figure 6.2a Geometric Simplification of DART Surface

The radius of curvature of the heat shield portion of the capsule is determined by optimizing the interior space and aerodynamic requirements. The cone angle of the leeward portion is constrained principally by the need to prevent the airflow from impinging on the surface. Such a condition would complicate the thermodynamic and aerodynamic calculations beyond the scope of the design group. It will be maximized for interior space requirements.

The pressure distribution across the vertical plane of the heat shield has been calculated. Peak values and a qualitative distribution has been found for the conditions of maximum re-enty heating. The values obtained here can be used by the Structures Group to design the heat shield and its supporting structure.

*Finally, the center of gravity offset required for static stability during re-*entry is found from the force coefficient results. The axial location of the CG has been found by the Structures Group.

Lift and Drag Calculations

The force coefficients of the spherical surface will be estimated fairly accurately by using Modified Newtonial Theory, where:

$$C_P = C_{P_{MAX}} \sin^2 \delta \qquad \text{(Eq. 6.2a)}$$

The coefficient of pressure at any given point on the surface is calculated in terms of the stagnation pressure coefficient behind a normal shock and the local surface deflection angle.

In order to translate the pressures into force components, the pressure distribution and the surface area must be defined. The diagram in Figure 6.2b illustrates the decomposition of the pressure into lift and drag. Equations 6.2b and c are integrated over $0 < \phi < \phi(\text{max})$ and $0 < \theta < 360°$ following substitution of Equations 6.2d into both. If the coefficient of pressure from Equation 6.2a is then substituted into the resultant lift and drag formulas, the lift, drag, and L/D values are found at the center of pressure (ie center of curvature) as functions of angle of attack, radius of curvature of the heat shield, and maximum Cp.

$$dL = (p - p_\infty)\,(\sin\alpha\cos\phi - \cos\alpha\sin\phi\cos\theta)\,dA \qquad \text{(Eq. 6.2b)}$$

$$dD = (p - p_\infty)\,(\sin\alpha\sin\phi\cos\theta + \cos\alpha\cos\phi)\,dA \qquad \text{(Eq. 6.2c)}$$

$$dA = \rho^2 \sin\phi\, d\phi\, d\theta \qquad \text{(Eq. 6.2d)}$$

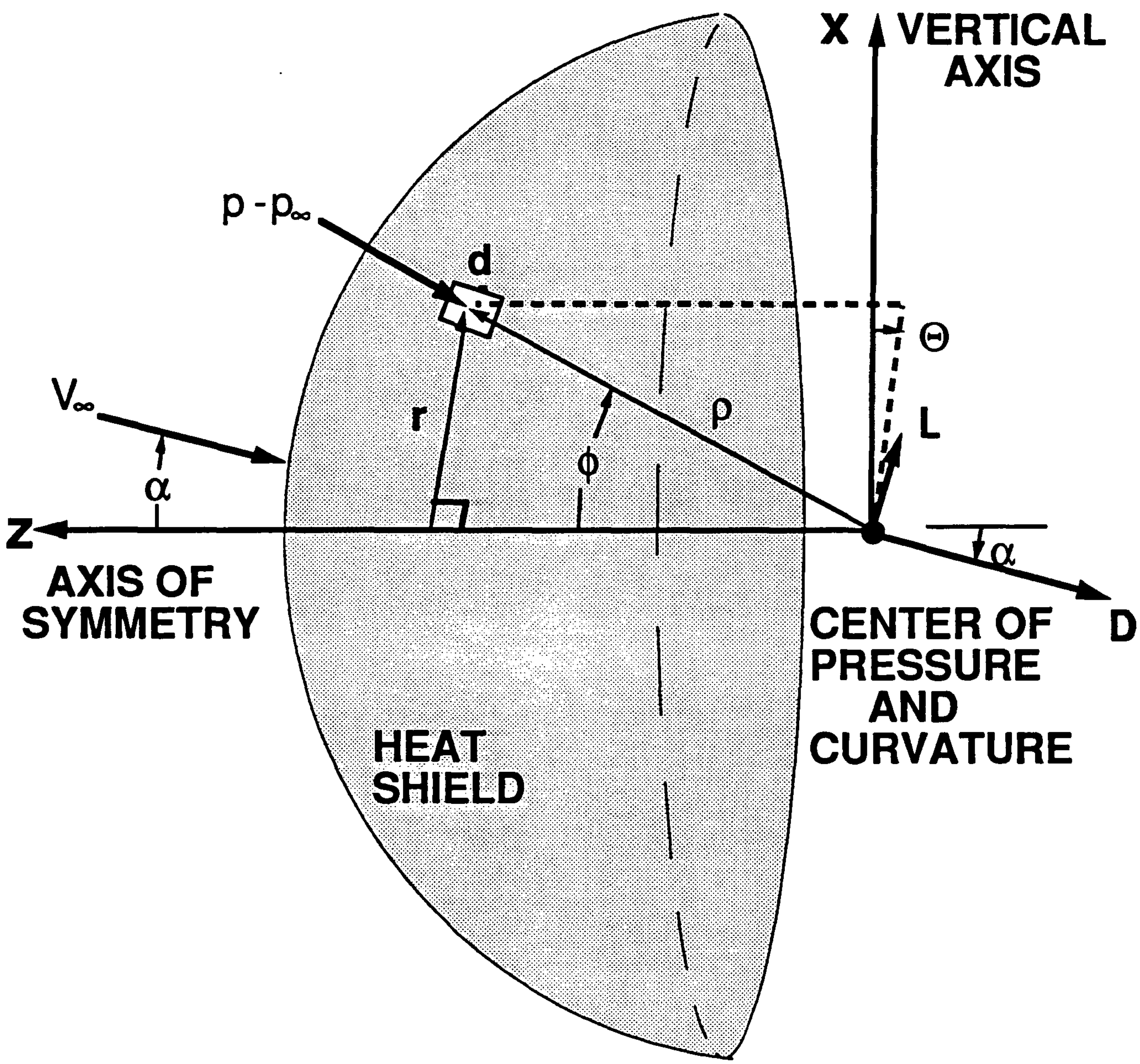

Figure 6.2b Heat Shield Coordinate System

The calculations were done by the computer program in Appendix 6.2.1. The values of the lift, drag, and L / D for given angle of attack and radius of curvature are graphed in Figs. 6.2c,d, and e. A 15 degree maximum angle of attack is required to keep the flow off of the rear of the capsule. An L / D of .25 can be achieved for a radius of curvature of 5.6 m, the initial design value. Keeping L / D greater than 0.2 requires the trim angle of attack to be over 11 degrees (flat plate extreme). A 5.6 m radius would give a volume addition of approximately 1.5 sq.m at the bottom of the capsule.

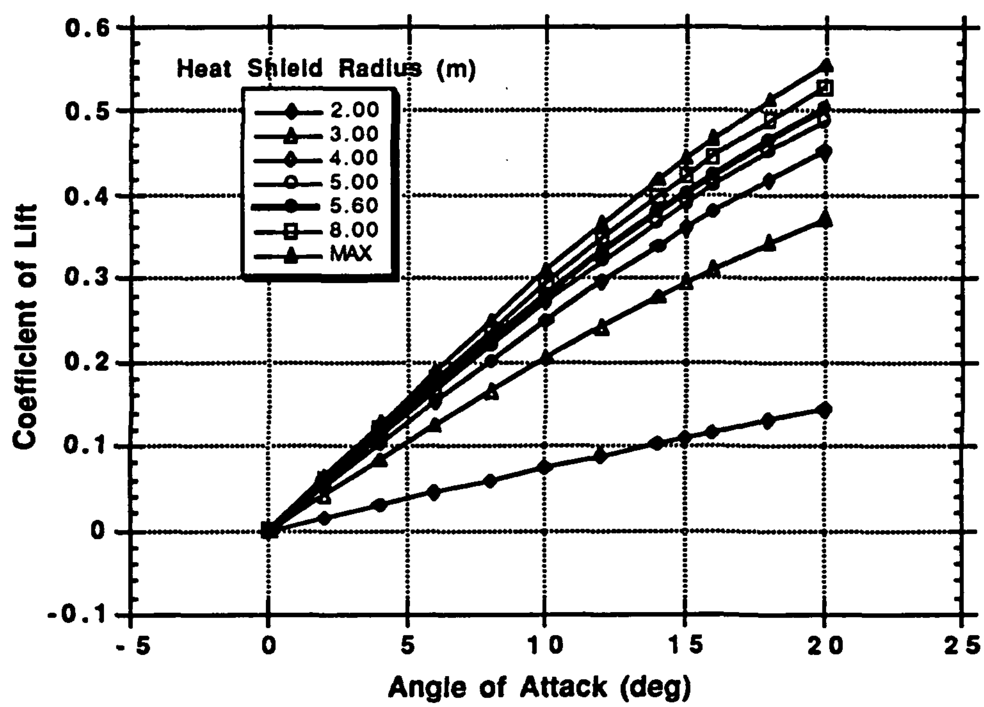

Figure 6.2c Coefficient of Lift vs Angle of Attack for Different Radii of Curvature

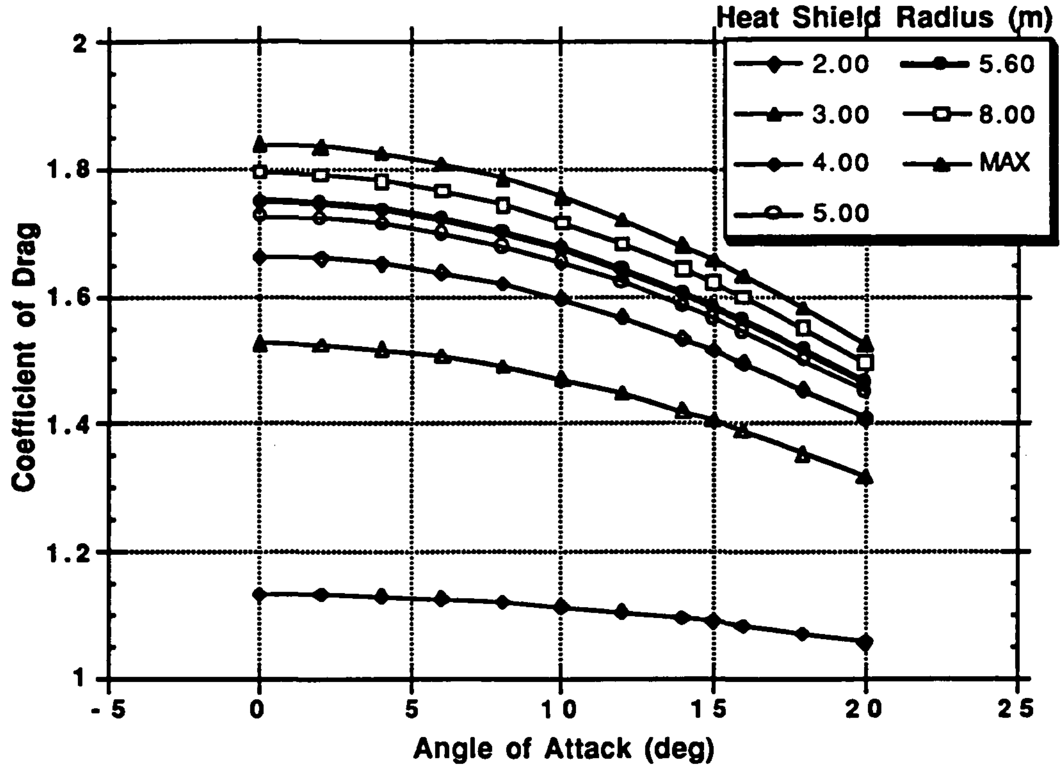

Figure 6.2d Coefficient of Drag vs Angle of Attack for Different Radii of Curvature

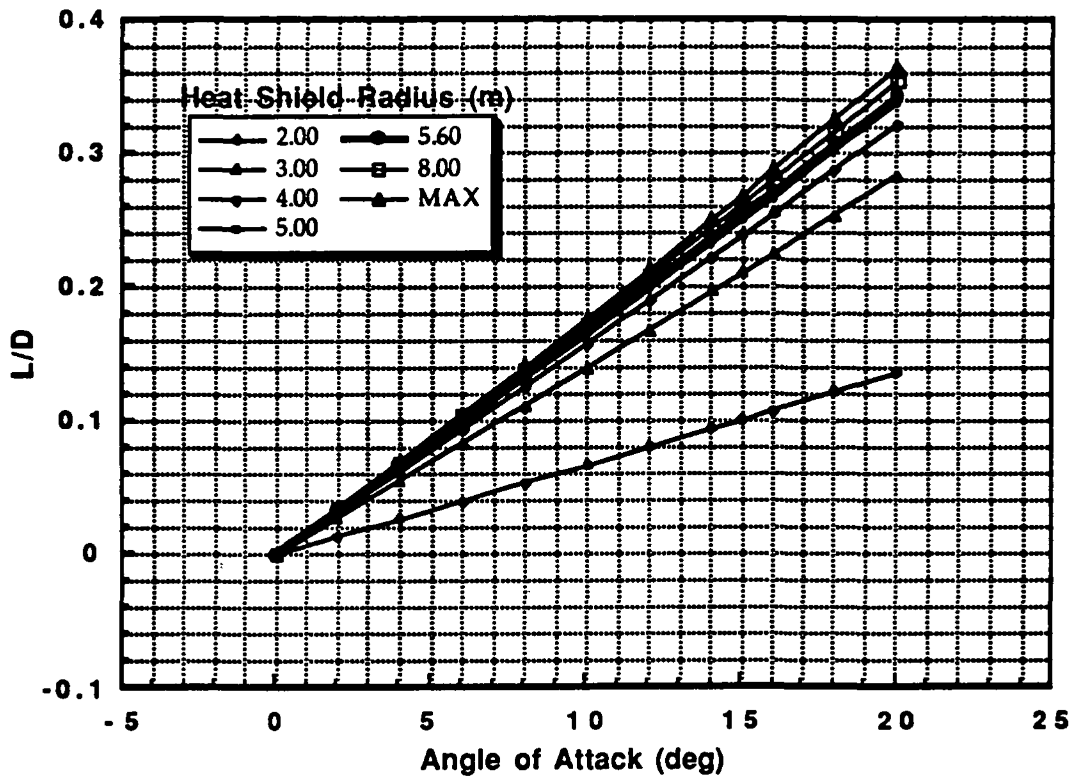

Figure 6.2e L/D vs Angle of Attack for Different Radii of Curvature

Assumptions were made in this local surface inclination technique.

1) The center of pressure is on the heat shield center of curvature.

2) The shock layer is under Newtonian flow conditions.

3) The pressure on the leeward face is negligible compared to the windward face.

Heat Shield Pressure Distribution

The pressure distribution is found using Modified Newtonian Flow in the program of Appendix 6.2.2. From the output received, the qualitative values of the pressures on the heat shield are shown on Figure 6.2f. At the maximum heating conditions, the pressure ratio is approximately 500 and the maximum pressure is 5 X 10^7 N/m^2.

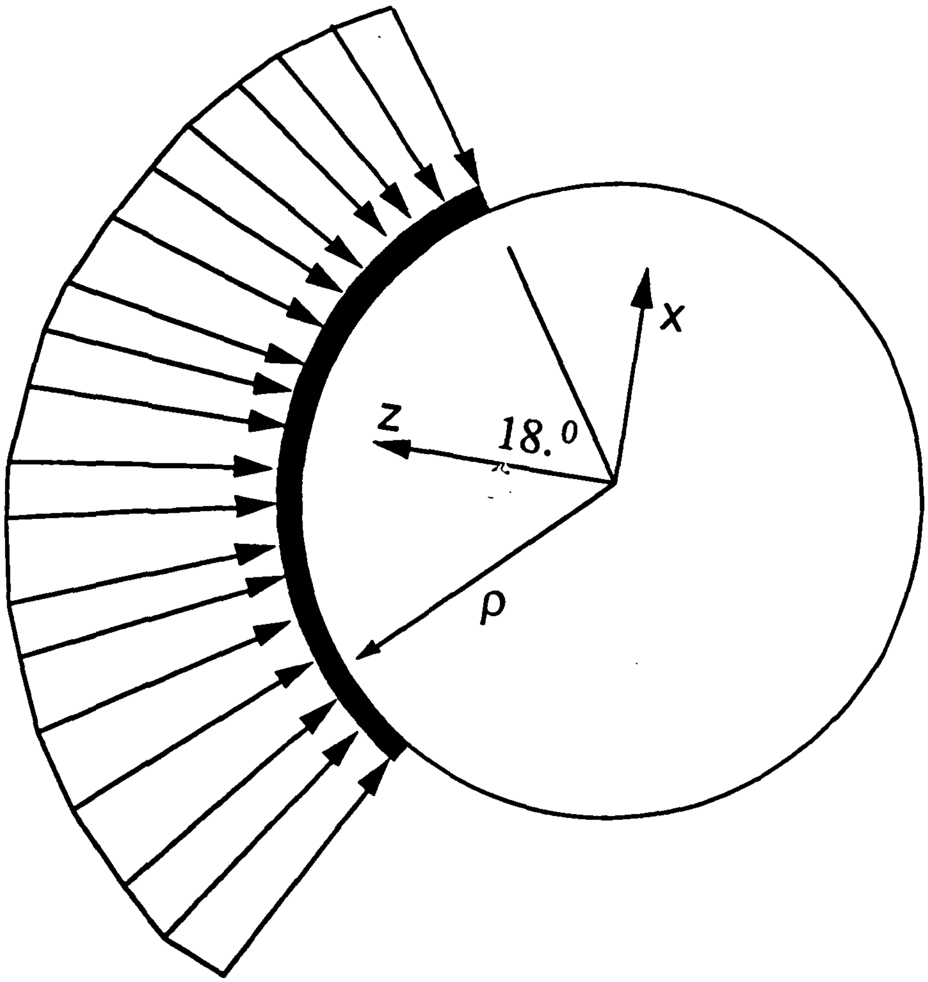

Figure 6.2f Pressure Distribution Across Vertical Plane Cross-Section of Heat Shield

Center of Gravity Offset

The center of gravity of the DART has to be offset from the axis of symmetry in order to achieve static stability during re-entry. Since DART is pitched (to create lift), moments are created about the CG. Only by shifting the CG can these moments be nullified, hence static stability is restored.

Utilizing the equation and diagram in Figure 6.2g, the computer program in Appendix 6.2.3 calculates the required CG offset. The force coefficients and the axial CG location, found by the Structures Group, are required to find the offset. The value found for a design radius of curvature of 5.6 m and angle of attack of 15 degrees prescribes a CG offset of .064 m from the axis of symmetry. (Eq. 6.2e)

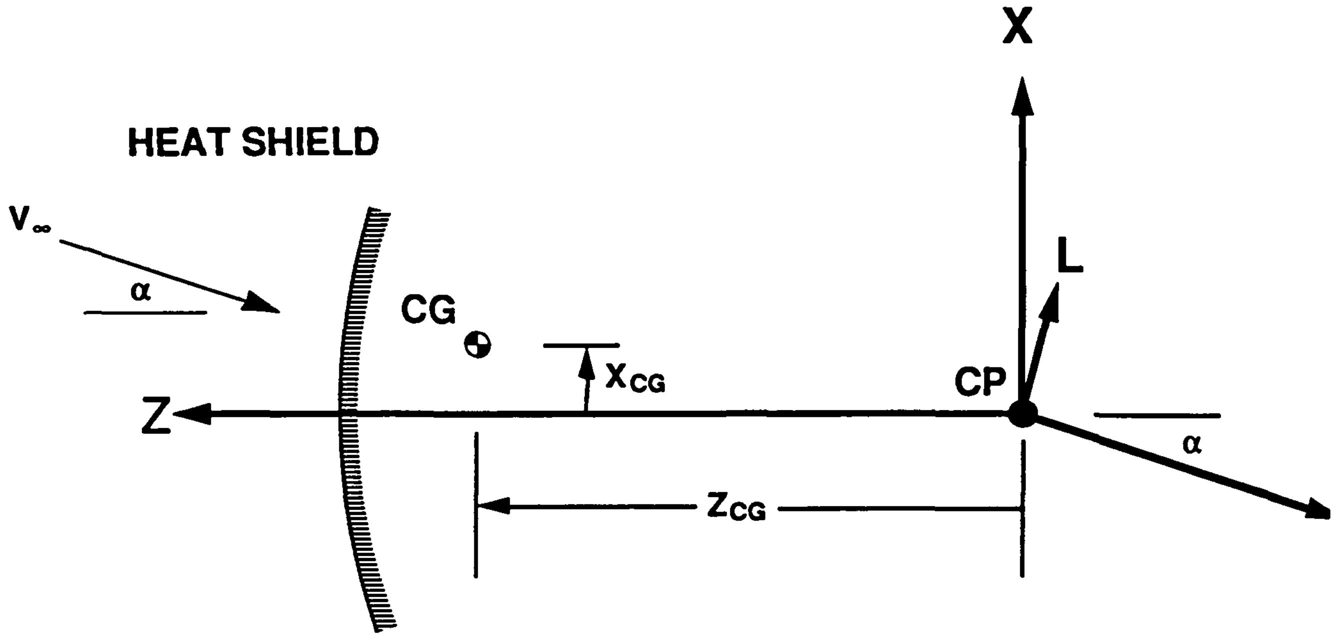

$$X_{CG} = \frac{C_L \cos\alpha - C_D \sin\alpha}{C_D \cos\alpha + C_L \sin\alpha} Z_{CG}$$

Figure 6.2g Center of Gravity Offset Coordinate System

Nomenclature

Symbol	Variable
A	Surface Area of Heat Shield
C_D	Coefficient of Drag
C_L	Coefficient of Lift
C_P	Coefficient of Pressure
D	Drag
g	Acceleration of Gravity
h	Altitude
L	Lift
p	Pressure at a Point
p_∞	Ambient Pressure
r	Radial Distance from Axis of Symmetry
R_o	Radius of Earth
S	Reference Area of Heat Shield
V_∞	Instantaneous Re-entry Velocity
α	Angle of Attack of Capsule
ϕ	Angular Distance Around Center of Curvature from Axis of Symmetry
Θ	Radial Angle About Axis of Symmetry
ρ_∞	Freestream Density
ρ	Radius of Curvature of Heat Shield
δ	Flow Deflection Angle on Surface

Section 6.3 Thermal Protection System

Introduction

The DART thermal protection system (TPS) consists of both ablative material (low-density phenolic epoxy resin) and thermal blankets (silica fiber) that are applied to the outer structural skin of the vehicle (figure 6.3a). The TPS serves to maintain the skin within acceptable temperatures during the launch and re-entry phases of the mission. Since the aerodynamic heating seen by the DART vehicle during launch is small in comparison to that seen during re-entry, only the re-entry heating is addressed. This aerodynamic heating is dissipated by two very different mechanisms, namely absorbtion and radiation. Heat is absorbed by the ablative material which chars and then melts, flying off the spacecraft and taking with it the aerodynamic friction heat which then does not penetrate the spacecraft interior. It is seen from figure 6.3a that the ablative material is located on the blunt face and the lower part of the capsule's conical section where the highest heating occurs. The thermal blankets, on the other hand, radiate heat away from the DART vehicle. Note that the blankets are located on the upper conical section of the capsule where aerodynamic heating is minimal. In addition to dissipating heat, the TPS also establishes the aerodynamics over the vehicle. This is of importance because the thicknesses of both the ablative material and the thermal blankets are determined by the aerodynamic heating load. Since TPS's have historically made up about 20% of the total vehicle re-entry weight, this heat shielding thickness is of great concern.

The first of the following sections reports on an analysis of the aerodynamic heating seen by the DART capsule during re-entry. More specifically, the stagnation temperature on the blunt face of the capsule as well as the temperature distribution along the conical section of the capsule were calculated. Next, DART's baseline TPS and its mode of attachment to the external structure of the vehicle are discussed in depth. This includes the determination of appropriate TPS materials for the DART vehicle and their required thicknesses. Finally, the last section briefly discusses thermal barriers which are used in the closeout areas between various components of the DART capsule and TPS.

Aerodynamic Heating Analysis

In order to select a practical TPS for the DART capsule, a detailed aerodynamic heating analysis was conducted to calculate the heat distribution on the vehicle during re-entry. For this analysis, the TPS was divided into two parts: (1) the aft heat shield and (2) the conical heat shield. It was determined from a DART trajectory analysis that the peak heating rate occurs at an altitude of 53,555 m. Therefore, standard atmospheric conditions at this altitude were used in the calculations, and the heating numbers represent the highest temperatures and convective heat fluxes that will be seen by the DART capsule during re-entry.

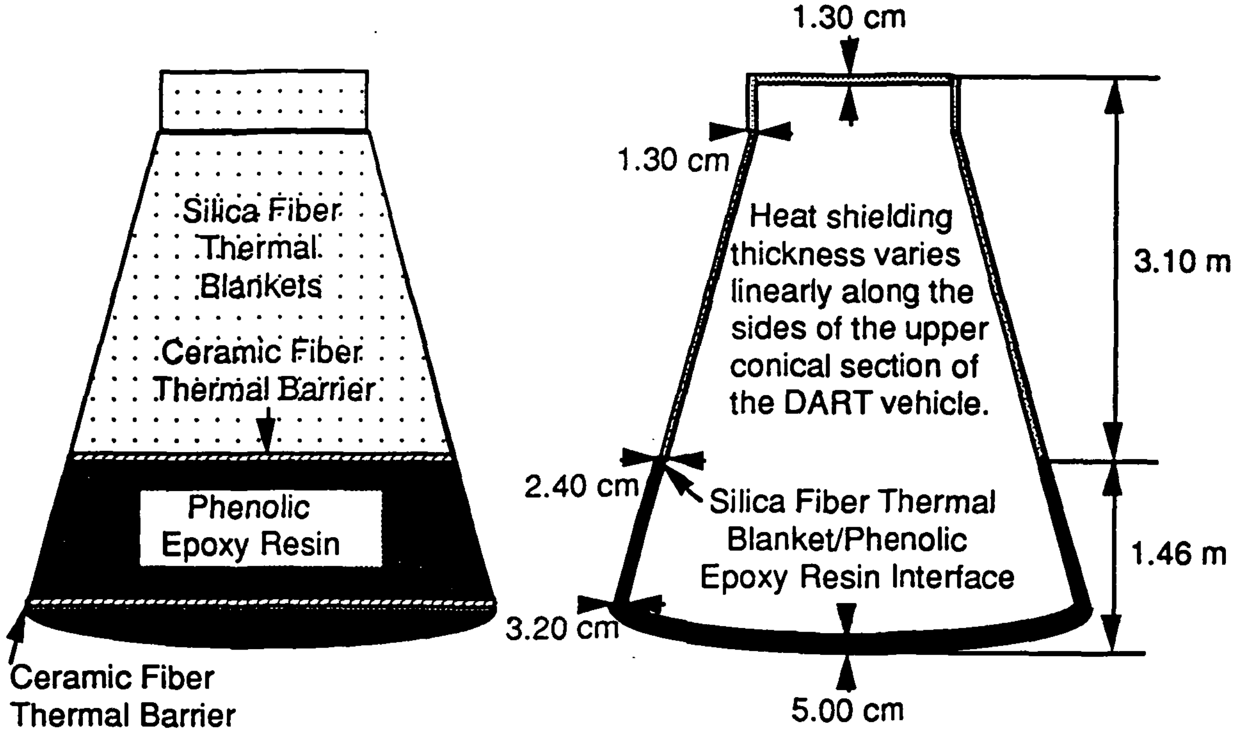

Figure 6.3a

First, the wall temperature (T_{wall}) and the convective heat flux ($q_{convective}$) at the stagnation point located on the aft heat shield were determined. Figure 6.3b depicts the local flowfield properties during re-entry. An approximate method found in reference 2 was used to determine the convective heat flux transferred from the hot boundary layer to the cooler surface of the DART aft heat shield. This simple method can be stated as:

$$q_{convective}=\rho_\infty^{0.5}V_\infty^{3.0}C, \text{ with } C=(1.83E\text{-}3)(R^{-0.5})(1-\frac{T_{wall}}{T_{total}}) \qquad (1)$$

where R is the nose radius and C is dependent upon R, T_{wall}, and T_{total}.

To balance this convective heat flux to the surface of the DART vehicle, it was assumed that the only means by which heat flux was transferred out of the surface was through radiation, ablation, and O2 dissociation. Thus, the energy balance can be stated as follows:

$$q_{convective}=q_{radiative}+q_{ablative}+q_{O2dissociation} \qquad (2)$$

where the standard formula for radiation flux was used. Ablation and dissociation heat fluxes were derived from the heat of ablation and the bond energy associated with O2 dissociation. These equations are stated in words below.

$q_{ablative}$=(heat of ablation)(density of material)(rate of ablation) (3)

$$q_{O2dissocation}=\frac{(\text{moles of O2})(\text{bond energy})(\text{rate of dissociation})}{(\text{volume of shock layer})} \quad (4)$$

Equation (2) was solved iteratively (appendix 6.3.1) to find T_{wall}. Then T_{wall} was used to solve for $q_{convective}$ at the stagnation point. It should be noted that this heating on the aft heat shield was calculated using phenolic epoxy resin as the baseline TPS material. Also, since the aft heat shield has a radius of curvature of 5.6 m, the laminar flat plate heating equation (reference 1) can't be used to determine the heat distribution across the aft heat shield.

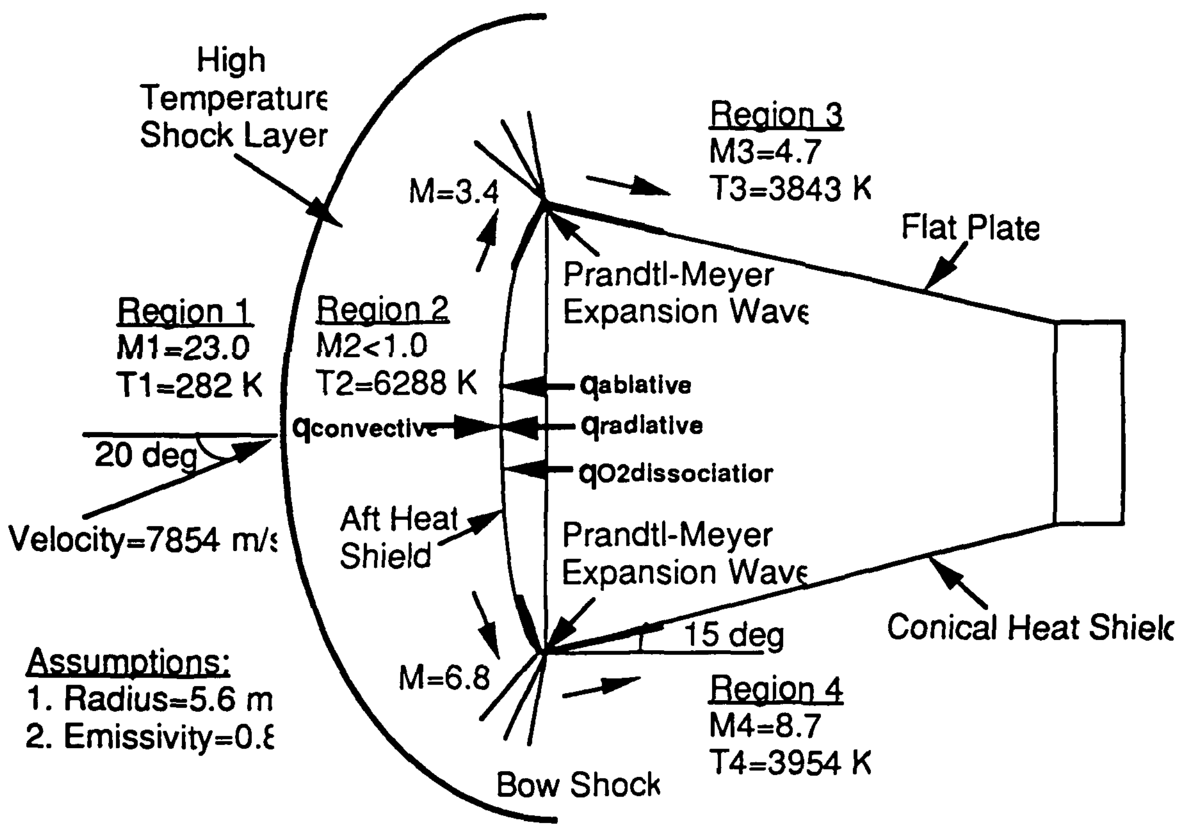

Figure 6.3b

The laminar flat plate heating equation, can, however, be used to calculate the convective heat flux at various stations along the conical heat shield (appendix 6.3.2). It is stated as follows:

$$q_{convective}=\rho_{\infty}^{0.5}V_{\infty}^{3.2}C, \text{ with } C=(2.53E\text{-}9)(\cos\varnothing)^{0.5}(\sin\varnothing)(x^{0.5})\left(1-\frac{T_{wall}}{T_{total}}\right) \quad (5)$$

where ø equals the local body angle with respect to the freestream velocity, x equals the distance along the plate, and where C is dependent on ø, x, Twall, and Ttotal. Referring again to figure 6.3b, it can be seen that the air first flows through a strong bow shock and then expands around the corners of the capsule. The velocity around the corners of the capsule was determined using the continuity equation. Since there is no general relationship between Twall and qconvective at a given point on the DART capsule's surface, temperatures along the conical heat shield were approximated by using the qconvective values from above and scaling them with Apollo flight data of wall temperature versus convective heat flux.

Figure 6.3c shows the results of this aerodynamic heating analysis. Because of the 20 degree angle of attack, the heating seen by the windward side of the capsule is naturally greater than that seen by the leeward side. Note that Twall varies from 2091 K at the stagnation point to 225 K at the top of the capsule on the leeward side. Also note that some of the Twall's on the leeward side of the DART capsule are below the ambient temperature of 282 K given for an altitude of 53,555 m. This is caused by a vacuum being formed on the leeward side of the capsule due to aerodynamics. TPS materials were selected bearing in mind that the external structure of the DART vehicle is made of 2024-T3 aluminum honeycomb which has a temperature limit of 422 K.

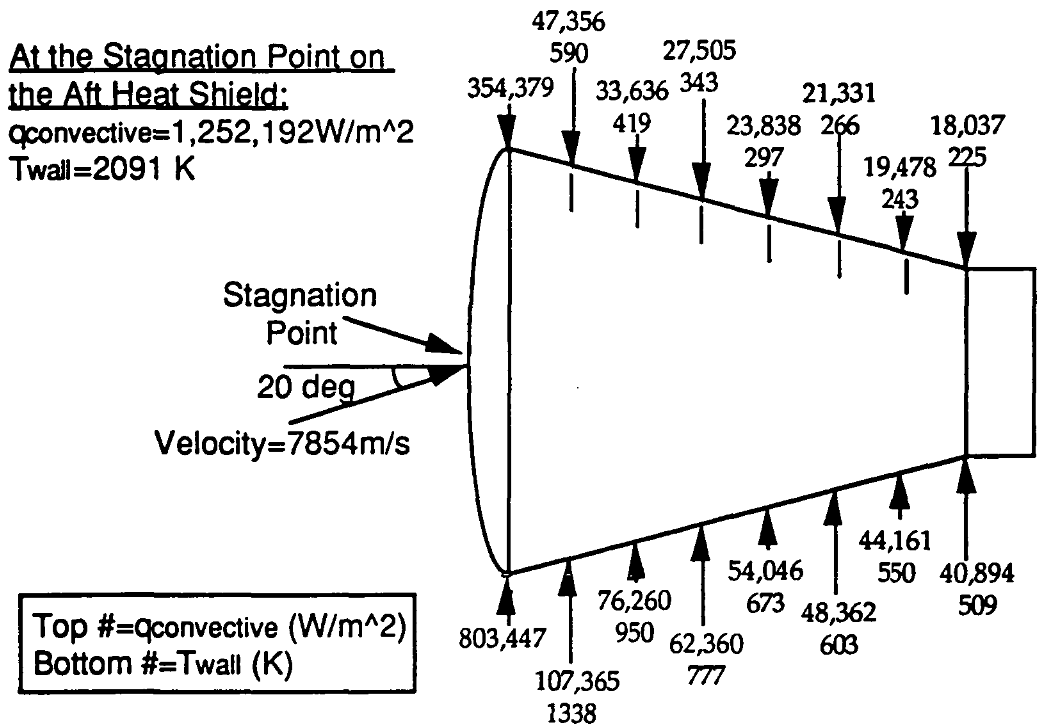

Figure 6.3c

Baseline TPS and Mode of Attachment

As stated in the introduction, the DART TPS consists of both ablative material and thermal blankets. As seen in figure 6.3a, ablative material covers the aft heat shield and the lower portion of the conical heat shield. Low-denstiy epoxy resin was chosen for its light weight, low material cost, and thermal characteristics (i.e., phenolic resins give the highest yield of carbon of any reinforced plastic during pyrolisis). The phenolic epoxy resin can be applied to the DART vehicle in the form of spray-on foam, and can be stripped during refurbishment using a water cannon (reference 1). Figure 6.3d is a closeup view of a typical cross section of ablative material. Note the different regions of the ablator and the processes that take place in each region. The evolution of gas from the char layer and reaction zones during re-entry is of special significance because it thickens the boundary layer and interferes with the convective transfer of heat to the surface of the vehicle. Such blocking action can reduce the net heating of the vehicle surface by more than 50%.

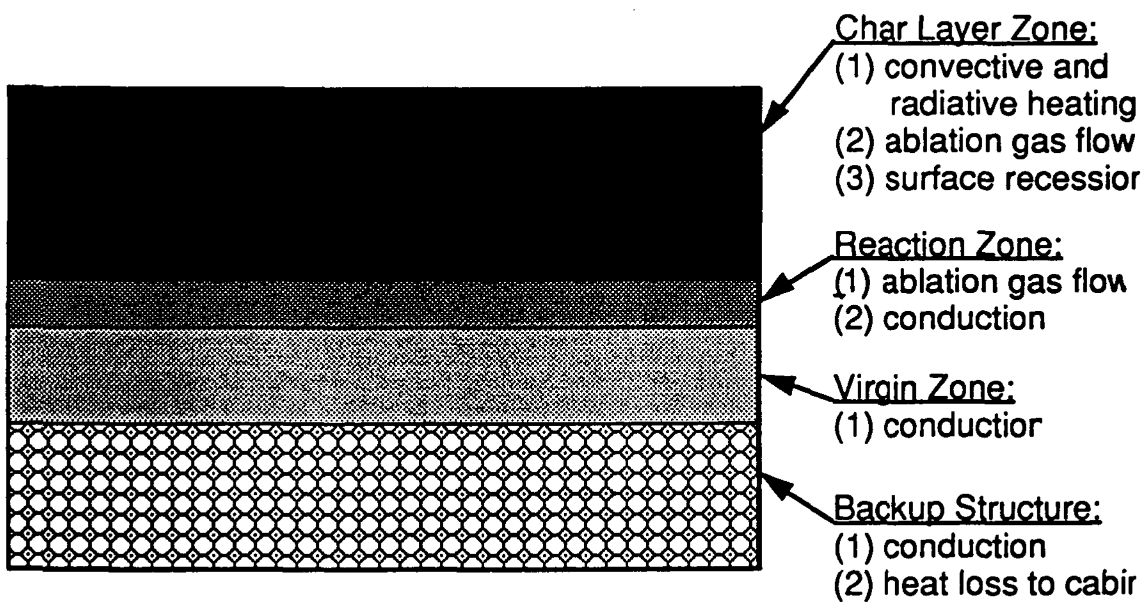

Figure 6.3d

From figure 6.3a it is also seen that thermal blankets are used to protect the upper conical section of the DART capsule during re-entry. The blankets dissipate heat by radiating it away from the capsule. The thermal blankets consist of low-density fibrous silica batting that is made up of high-purity silica and 99.8-percent amorphous silica fibers (1 to 2 mils thick). This batting is sandwiched between an outer woven silica high temperature fabric and an inner woven glass lower temperature fabric. After the composite is sewn with silica thread, it has a quilt-like appearance. The blankets are coated with a ceramic colloidial silica and high-purity silica fibers that improve endurance. The blankets are cut to the planform shape required and bonded directly to the external structure of the DART capsule by RTV silicon adhesive 0.20 inches thick. The very thin glue line reduces weight and minimizes the thermal expansion during temperature changes.

To obtain the mass of the DART TPS, the vehicle was divided into a number of sections. The sectional densities and the required thicknesses of the ablative material and thermal blankets were determined based on the aerodynamic heating calculations in the previous section. A computer program was written to calculate the surface area, volume, and mass of the heat shield based on sectional densities and thicknesses (appendix 6.3.3). The results of this mass analysis are listed below:

Mass of DART TPS

Silica Fiber Thermal Blankets	62 kg
Phenolic Epoxy Resin (Conical Heat Shield)	108 kg
Phenolic Epoxy Resion (Aft Heat Shield)	143 kg
Thermal Barriers	5 kg
	318 kg

The baseline method of ablator and thermal blanket attachment will be direct bond, as opposed to bonding the materials to a subpanel (plate or honeycomb) and mechanically attaching the subpanel to the DART capsule external structure. The direct bond method was chosen because it has the lowest possible mass penalty (i.e., no fasteners are required) of all heat shield attachment systems and also the lowest program cost.

A brief history on the decision to use a combination of ablative material and thermal blankets to protect the DART capsule during re-entry is appropriate here. A trade-off study was conducted to determine the most appropriate material(s) for the DART TPS. At first, just ablative materials and radiative materials (specifically reusable surface insulation (RSI) tiles like those on the Space Shuttle) were compared, but the trade-off study was later expanded to include carbon carbon, ablative cork, and thermal blankets. As was stated before, the DART TPS can be divided into two parts: (1) the aft heat shield and (2) the conical heat shield. From the aerodynamic heating analysis, it was determined that only two readily available and proven materials could withstand the kind of heating seen at the aft heat shield stagnation point (2091 K). These two materials are reinforced plastic ablators and carbon carbon. The ablative material, phenolic epoxy resin, was chosen over carbon carbon because it is light, inexpensive, and easy to apply in the form of spray-on foam. A full breakdown of the TPS materials considered in the aft heat shield trade-off study can be found in appendix 6.3.4.

Next, possible materials for the conical heat shield were examined. The materials in this trade-off study were phenolic epoxy resin, thermal blankets, RSI tiles, and ablative cork. A full breakdown of the conical heat shield trade-off study can be found in appendix 6.3.5. In short, a combination of phenolic epoxy resin and silica fiber thermal blankets was chosen to minimize the mass, material cost, installation difficulty, and refurbishment expenses of the conical heat shield. The advantages of the phenolic epoxy resin are stated above. The advantages of thermal blankets are that they are reusable, light, and have low fabrication and installation costs. The single concern with the thermal blankets is that they will only protect areas where temperatures are below 922 K. This is the main reason for using ablative material on the lower portion of the conical heat shield where temperatures reach over 1338 K. Another reason is that during a possible firing of the abort tower rockets, exhaust will impinge on the lower conical section of the capsule with a temperature of about 3000 K for 5 seconds.

Thermal Barriers

Thermal barriers are used in the closeout areas between various components of the DART capsule and TPS, such as the interface between the silica fiber thermal blankets and the phenolic epoxy resin. Another interface is located between the conical and aft heat shields. The reason for the conical and aft heat shields being separate is that during the water landing the aft heat shield blows off and an air bag comes out to help with impact and flotation. Thermal barriers are also needed around crew hatches and windows. The barriers will be similar in compostion to those currently used on the Space Shuttle-- namely some type of ceramic silica fibers braided around an inner tubular spring made from wire with additional silica fibers within the tube.

Section 6.4 Recovery System

Preliminary Investigation of a Paraglider Landing System Option for the DART Spacecraft

At present two recovery system options are being considered for the dart spacecraft. The first of these is the standard round parachute. A standard parachute is a single, symmetrical non-controllable drag device (figure 6.~~5~~4a). In addition to the parachute, a parallel study is being done on the possible use of a paraglider landing system. The purpose of this report is to provide a qualitative analysis of the paraglider concept.

A paraglider is essentially a two-lobed triangular wing consisting of three structural membranes-two leading-edge booms and a keel which are interconnected by a flexible, nonporous membrane. The DART spacecraft is suspended below the wing by cables (figure 6.~~5~~4b).

Two of the major advantages of such a paraglider recovery system over a conventional parachute are:

1.) A controlled descent and landing.
2.) Reduction of vertical velocity at touchdown.

The ability to bring down the spacecraft, safely, on land, to a *predetermined point is clearly preferred over a relatively arbitrary landing point* on water within a wide area. This control is achieved by adjusting the length of the various cables connected between the paraglider and the spacecraft's landing control system. Lateral maneuvering is accomplished by adjusting the lengths of the side shroud lines (figure 6.~~5~~4b). In addition, pitch control is achieved by changing the angle of attack of the wing so as to shift the position of the center of gravity of the spacecraft relative to the center of pressure of the wing(a method used by hang glider pilots).

Another very important concern is the vertical velocity of the spacecraft during touchdown. By using a flaring maneuver just prior to touchdown the vertical velocity of the spacecraft can be reduced to almost 0 m/sec. This is important in that it serves to attenuate the landing shock significantly. If using a conventional parachute for a land touchdown the impact forces could be as high as 75 g's (figure 6.~~5~~4c) requiring the use of some type of impact attenuation device. This case is considered as an abort option where a land touchdown may be required for a spacecraft using conventional parachute recovery.

VT= TERMINAL VELOCITY(7.62 M/S)
WT=VEHICLE WEIGHT(4200 Kg)
CD=DRAG COEFFICIENT(.65)
S=PARACHUTE AREA(1332 M^3 PER CHUTE)
ρ=AIR DENSITY

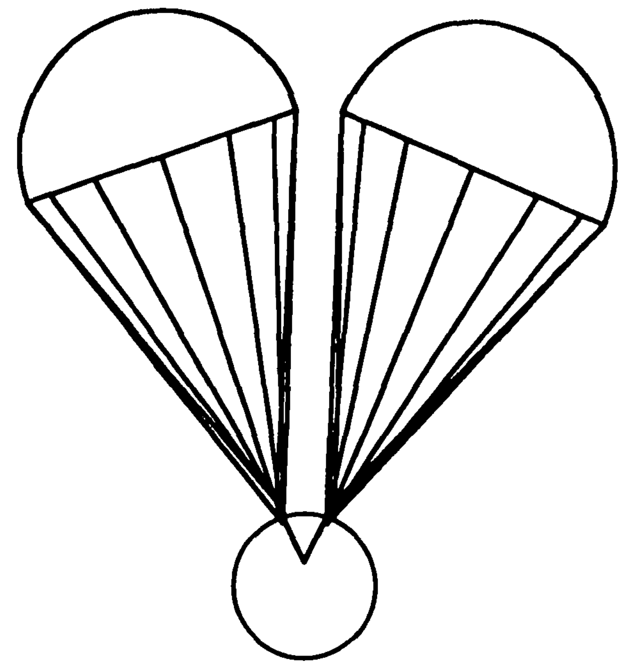

$$V_T=[2*W_T/S*C_D*\rho]^{.5}$$

CONTACT ANGLE IS EXPECTED TO BE BETWEEN 10 TO 15 DEGREES SO AS TO REDUCE IMPACT FORCE

IN THE EVENT OF A PARACHUTE FAILER A SINGLE PARACHUTE WOULD GIVE A DESCENT RATE OF 10.79 M/SEC

Figure 6.4a Parachute Recovery System

Z. KHAN

L/D=3

C_L=.5 AT ANGLE OF ATTACK OF 22°

CL=1.18 AT ANGLE OF ATTACK OF 43°

DURING FLARING MANEUVER

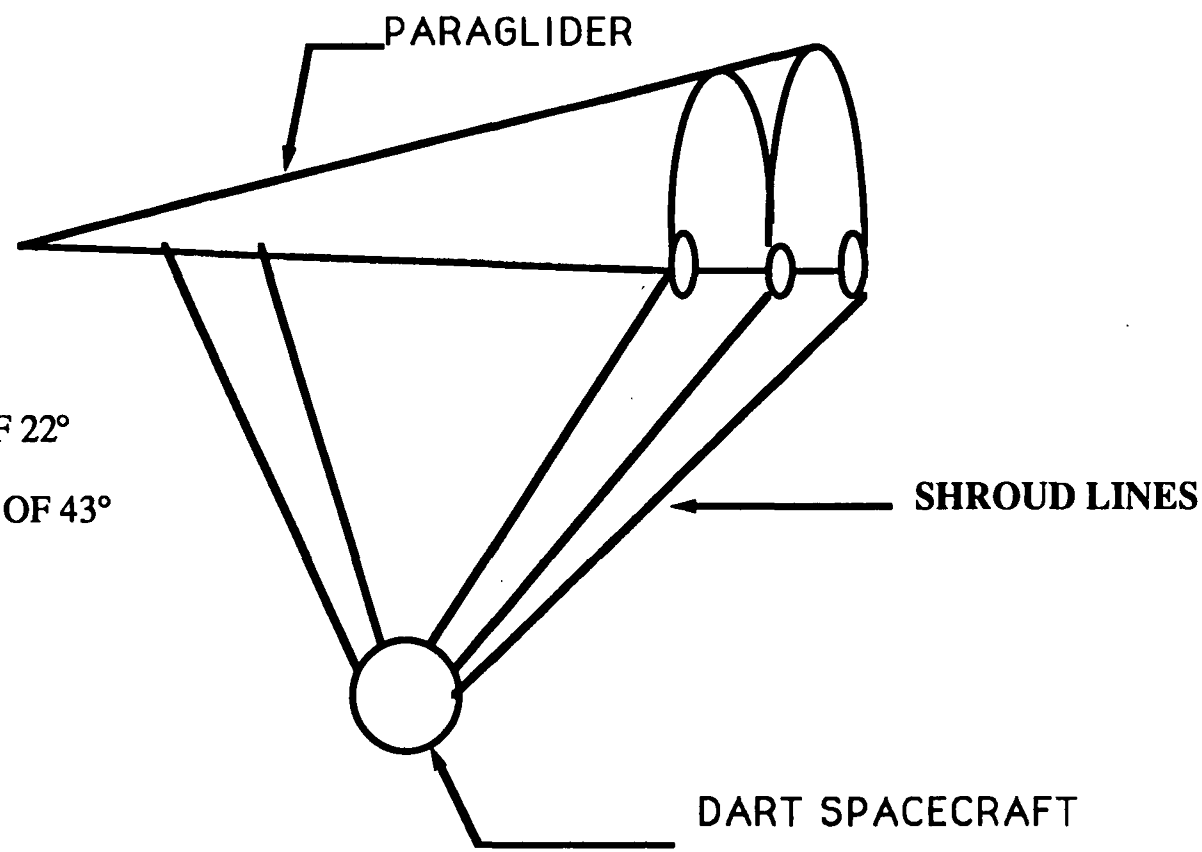

Figure 6.4b Paraglider system

Z. KHAN

3=HIGH IMPORTANCE
2=MEDIUM IMPORTANCE
1=LOW IMPORTANCE
0=NOT APPLICABLE

PERFORMANCE CHARACTERISTICS	IMPORTANCE TO LANDING SPACECRAFT	RELATIVE PERFORMANCE OF PARAGLIDER SYSTEM	PERFORMANCE OF ROUND PARACHUTE
* RELIABILITY OF OPERATION	3	NOT EXPECTED TO BE AS GOOD AS PARACHUTE	HIGHLY RELIABLE BASED ON EXPERIENCE
* REPEATIBILITY OF PERFORMANCE	2	EXPECTED TO BE GOOD	VERY GOOD
* REUSE	0	POSSIBLY CAN BE REUSED IF INITIAL RESULTS INDICATE LITTLE WEAR	NOT REUSABLE FOR DART MISSIONS
* WEIGHT AND VOLUME	3	LARGER VOLUME REQUIREMENTS WEIGHS 42% MORE THAN CHUTE	LOW VOLUME LOWER WEIGHT
* STABILITY	2	GOOD STABILITY EXCEPT DURING DEPLOYMENT	PITCHES FROM 5 TO 15 DEGREES
* HIGH DRAG	2	VARIABLE WITH ANGLE OF ATTACK	HIGH DRAG BY DESIGN
* LOW OPENING FORCES	1	UNABLE TO FIND ANY DATA	UNKNOWN,BUT EXCEPTABLE
* LOW MAINTENANCE	1	WILL REQUIRE MORE THAN PARACHUTE	RELATIVELY LOW
* COST	1	EXPECTED TO BE HIGHER THAN CHUTE IF NOT REUSED	CHEAPER THAN PARAGLIDER

FIGURE 6.4C: COMPARISON OF PERFORMANCE BETWEEN A PARAGLIDER AND A STANDARD PARACHUTE

Z. KHAN

Paraglider versus Parachute: A Parallel Study

The purpose of this section is to compare the relative merits of using one recovery system over another. In particular, a comparison between the parachute and paraglider recovery systems will be made to determine which is more suited for the DART spacecraft. This analysis will show that the standard parachute is the best option for recovering the spacecraft.

As was discussed previously the paraglider landing system offered the advantages of a controlled descent and landing aswell as reducing the impact forces through a reduction of vertical velocity. However, the disadvantages to using such a system as related to the DART spacecraft outweigh these advantages. But, in order to choose one recovery system over another the design criteria for a good recovery system must first be defined. These performance characteristics and their relative importance to a landing spacecraft(assigned a numerical value ranging from 0 to 3) are shown in figure 6.4a. Also shown are qualitative assesements of the performance of the paraglider and parachute recovery systems. The more important characteristics such as reliability,weight and volume, and stability characteristics are discussed further, below.

Ofcourse, reliability is a prime concern in the design of any recovery system. Although research has been done on the paraglider, there is no operational experience on such a recovery device on which to base an assesment of reliability. On the otherhand, the standard parachute has been used extensively on manned missions and out of 31 parachute recoveries all have been successful. Hence it is a known that the parachute offers the most reliable recovery option available whereas the reliability of the paraglider is expected to be good but not approach that of a parachute due to it's relative complexity (see reference 44).

Another critical design concern is the weight and volume requirement of the recovery system. The parachute recovery system for DART would require in total a volume of .056 m^3 based on a nominal packed density of about 3.6E3 Kg/m^3 (see reference 44) and a parachute weight of 200 Kg. This would take up approximately 6% of the space in the nose of the spacecraft. The paraglider system volume requirements would be about .090 m^3 based on a packed density of 5.34E3 Kg/m^3 (see reference 44) requiring about 10% of nose space. Another more telling disparity between the parachute and the paraglider options is the weight of each system. The parachute weighs about 5% (200 Kg) of the capsule reentry weight whereas the paraglider system will weigh about 12%(480 Kg) of the capsule weight (see reference 44). Once again the analysis shows that in terms of weight and volume constraints, the parachute system is a better option for DART.

Next we consider the stability aspects of the parachute versus the paraglider system. Results obtained by Rogallo (see reference 36) indicate that the paraglider is very stable between 20° to 90° angle of attack. However deployment of the paraglider system remains a major problem. It was found that inorder to deploy a paraglider without introducing instabilities, elaborate deployment methods were required which added weight and volume requirements to this option. Parachutes on the other hand are not as complicated to deploy but they do have a tendency to sway between 5°-15° (see reference 44). Nevertheless the parachute is a better option from the standpoint that there is considerable experience in the use of such a system.

The above analysis and figure 6.4c clearly indicate that the standard parachute recovery system is the best option for the DART spacecraft. However, it is suggested that an unmanned version of either the DART or the TAURUS vehicle could be used to obtain additional and more representative data on the paraglider system.

Parachute Design and Deployment

Having decided on the use of a parachute recovery system for DART the design of the parachute follows. The forces acting on the DART vehicle after the chute has fully deployed are as shown in figure 6.4d. To simplify the analysis the assumption is made that the drag of the capsule is negligible compared to that of the parachute. Note that each parachute would have to have a diameter of 41m based on the use of two chutes inorder to give the capsule a descent rate of 7.62 m/s (25 ft/s).

Two parachutes are used instead of one large parachute due to the fact that the larger chutes are difficult to manufacture and take longer to deploy. Also, even if a large single chute is used, a reserve would be required in the event of a parachute failure. In using two parachutes, effectively both the main and the reserve are deployed. In the event one parachute fails, the other will safely recover the DART with a descent rate of 10.79 m/s. Although this descent rate results in a higher impact shock it is still below 20 g's (see reference 44) since an airbag is used to cushion the impact shock.

Before proceeding to the discussion of the parachute deployment sequence, the placement of the parachute system in the nose of the spacecraft will be discussed (figure 6.4f). As mentioned previously the total volume requirement for the parachute system is .056 m^3 which is to say .028 m^3 for each parachute. This can easily be accomodated in the region shown in figure 6.4f along with the associated pilot chute, mortar, and SOFAR bomb used to help in locating the capsule on water. The parachute deployment sequence (figure 6.4e) begins at an altitude of 4000m (point where terminal velocity has been established) with the extraction of the pilot parachutes by mortars. The pilot parachutes in turn deploy the main parachutes which will fully inflate in about 6 seconds (see reference 44). After the chutes have fully deployed and stabilized a simple release mechanism will let go the heatshield, which is connected to the airbag, thus pulling the airbag down in preperation of impact. The need for such an airbag system is discussed in the next section. However,

$D_p+D_c=W_p+W_c=W_T$

Assume $D_c<<D_p$

$D_c=.5*\rho*(VT\text{^}2)*C_d*S=W_T$

$S=W_T/((V_T\text{^}2)*C_d*\rho$

W_T=4200 Kg

V_T=7.62 m/s

C_d=.65

ρ=.0835 Kg*S^2/m^4

R=21 meters

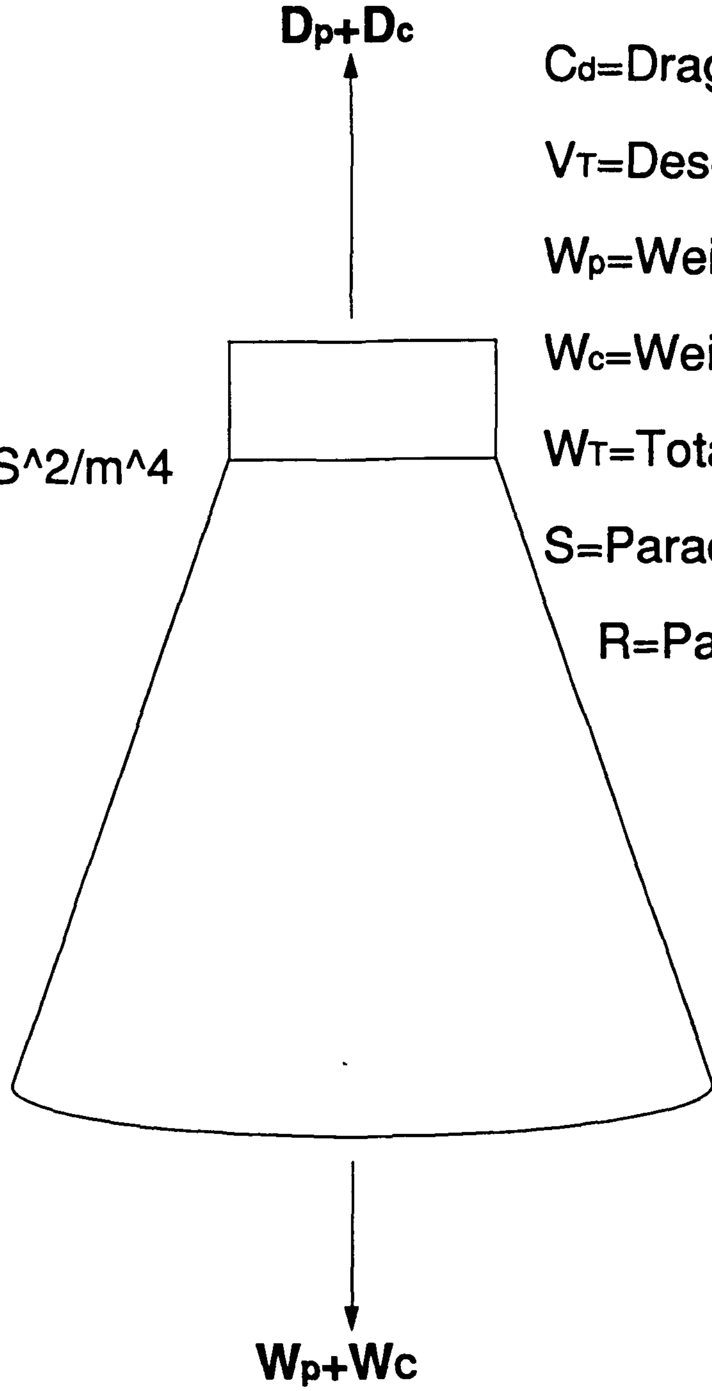

<u>Variable Definitions:</u>

D_p=Drag force on parachute

D_c=Drag force on capsule

ρ= Air density at 4000 m

C_d=Drag coefficient of chute

V_T=Descent rate

W_p=Weight of chutes

W_c=Weight of capsule

W_T=Total weight

S=Parachute area per chute

R=Parachute radius

Figure 6.4d Calculation of parachute radius

Z. KHAN

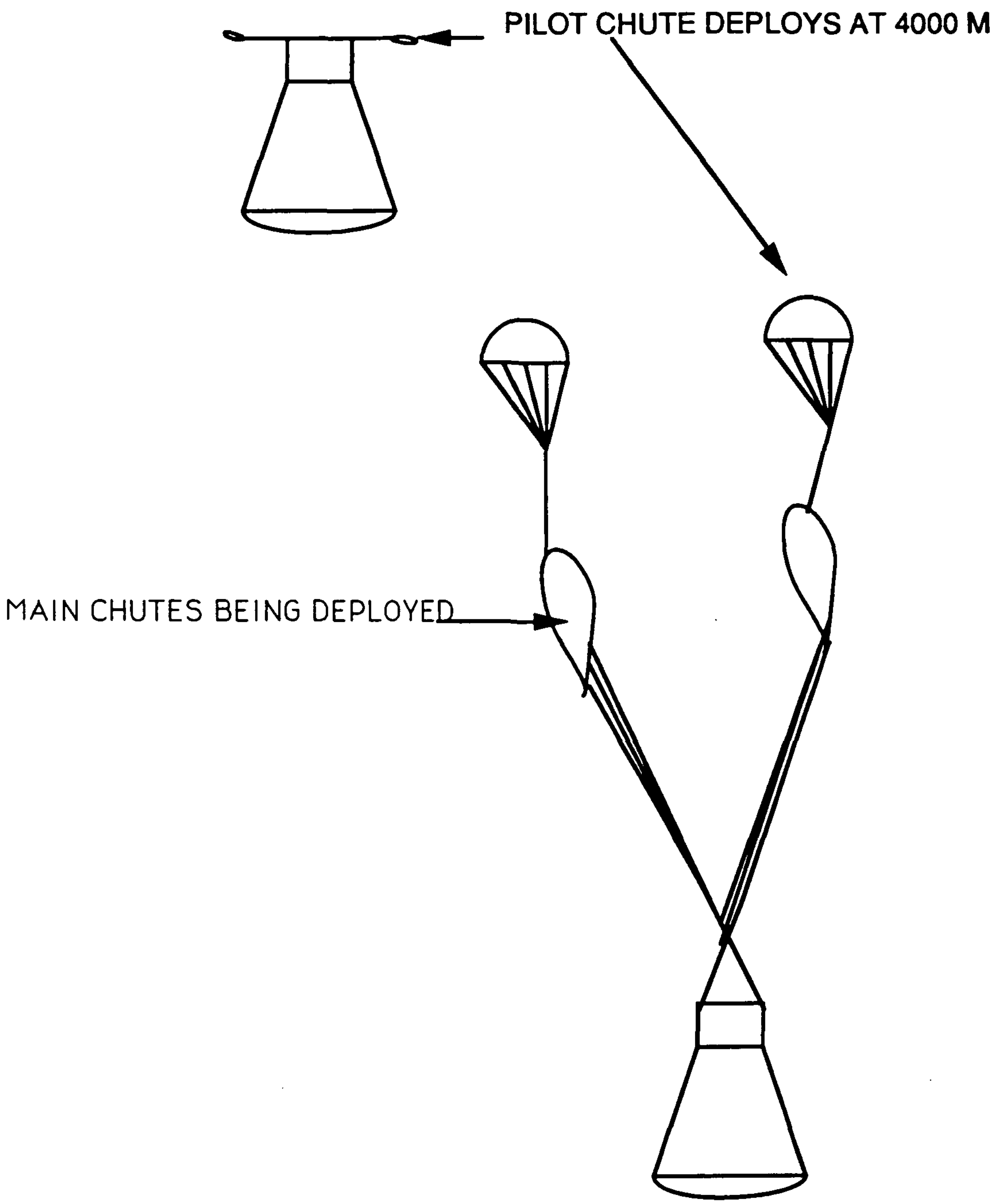

Figure 6.4e Parachute deployment sequence

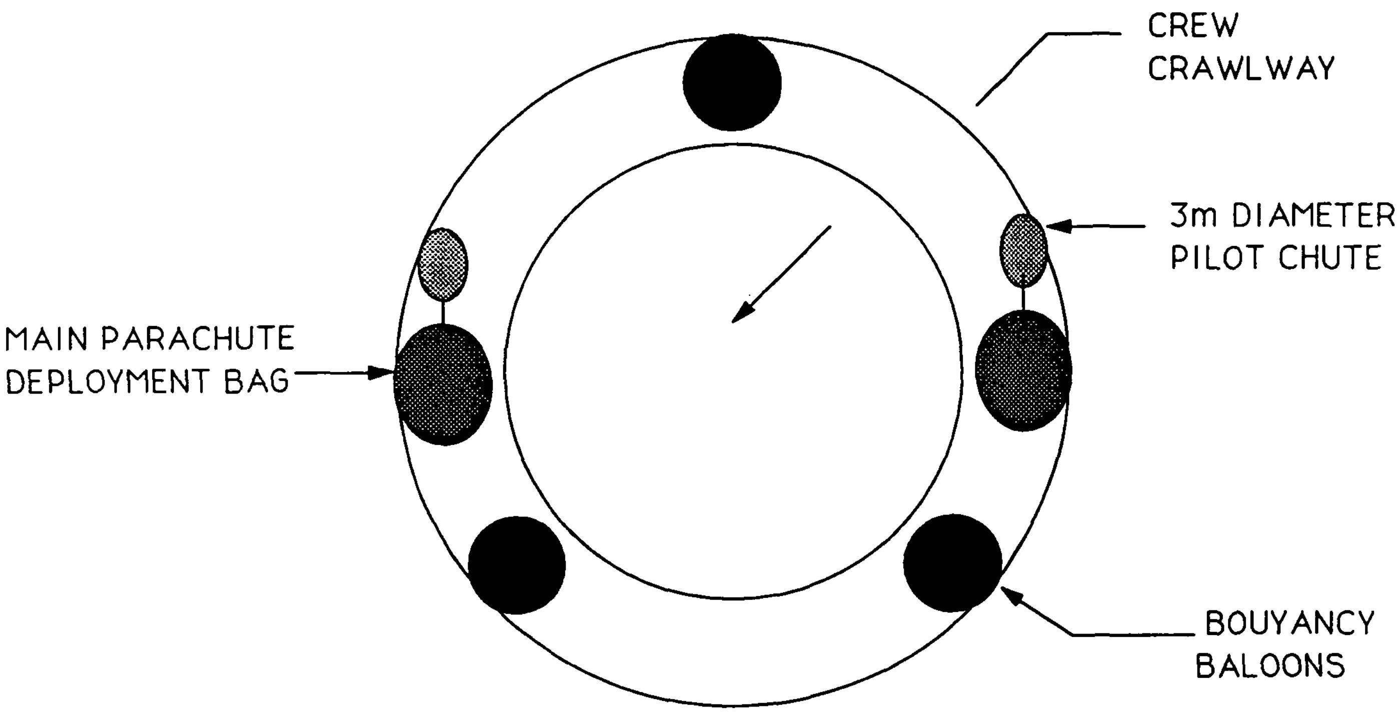

Figure 6.4f Top veiw of DART docking hatch showing placement
ofparachute

before proceeding it is important to note that once the craft landed the parachutes are released to prevent them from dragging the vehicle.

Section 6.5 Impact Attenuation and Egress

Impact Attenuation

Once the mission of any manned spacecraft is completed, it is of course required to return to a safe landing on Earth. However,landing poses several problems. Among the more important ones is the need for impact attenuation. Another area of concern is providing for egress. This then is the objective of this section. Here we will describe in approximate terms the expected impact forces and propose a method for reducing them. This will be followed by a description of the proposed crew egress procedures for the DART spacecraft. The forces encountered on impact of course depend on the composition of the surface of impact. The ideal case is landing in water where a larger portion of the impact energy is absorbed by the water than is on land. Using a descent rate of 7.62 m/s (25 ft/s) and assuming the worst case land impact and no attenuation system, the peak deceleration of around 75 g's is expected(figure 6.5a). Clearly, in this worst case scenario, there would be a need for some type of attenuation system. If however the landing was to be on water the maximum acceleration would be between 65 t0 70 g's which is outside tolerance levels (see reference 44) thus requiring an attenuation system.

If now we look at the accelerations with an attenuation system, in particular a pneumatic bag, there is a significant drop in the acceleration impacts (figure 6.5a). For the land impact case this value would drop to about 10 g's and for the water landing case the acceleration would be between 7-10 g's. Both values are within the human tolerance ranges but it is clear that the water impact case is the preferred landing mode.

The decision to use the pneumatic bag (figure 6.5b) was based primarily on the limited space available between the heatshield and the pressure bulkhead (this is still being worked on). There are options that would be liter and in fact more efficient, however the pneumatic bag has the overriding advantage of storability. This system would be activated shortly before impact. The bag would have holes that surround the circumference of the airbag that would

Figure 6.5a Impact Accelerations for the DART Spacecraft

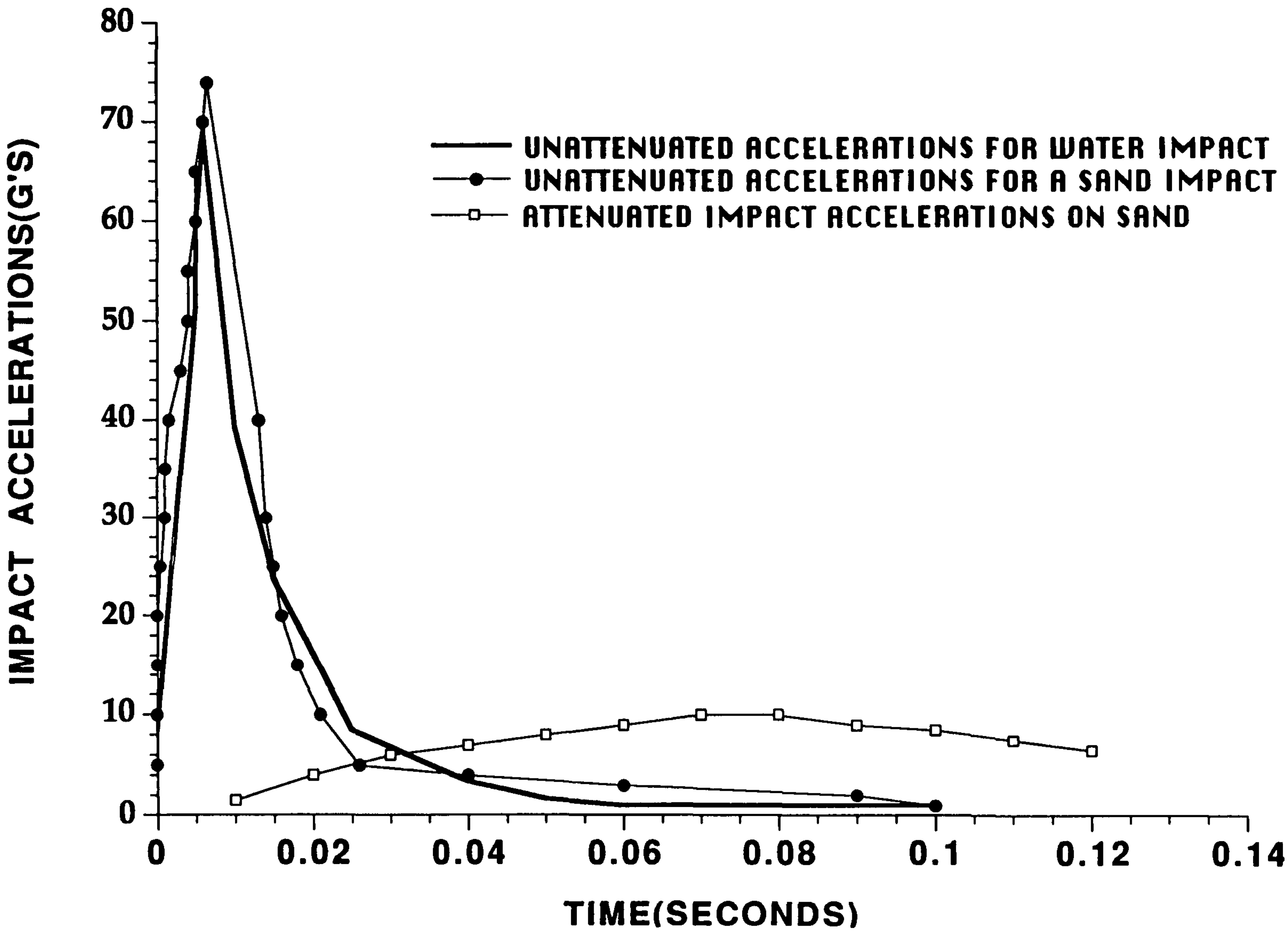

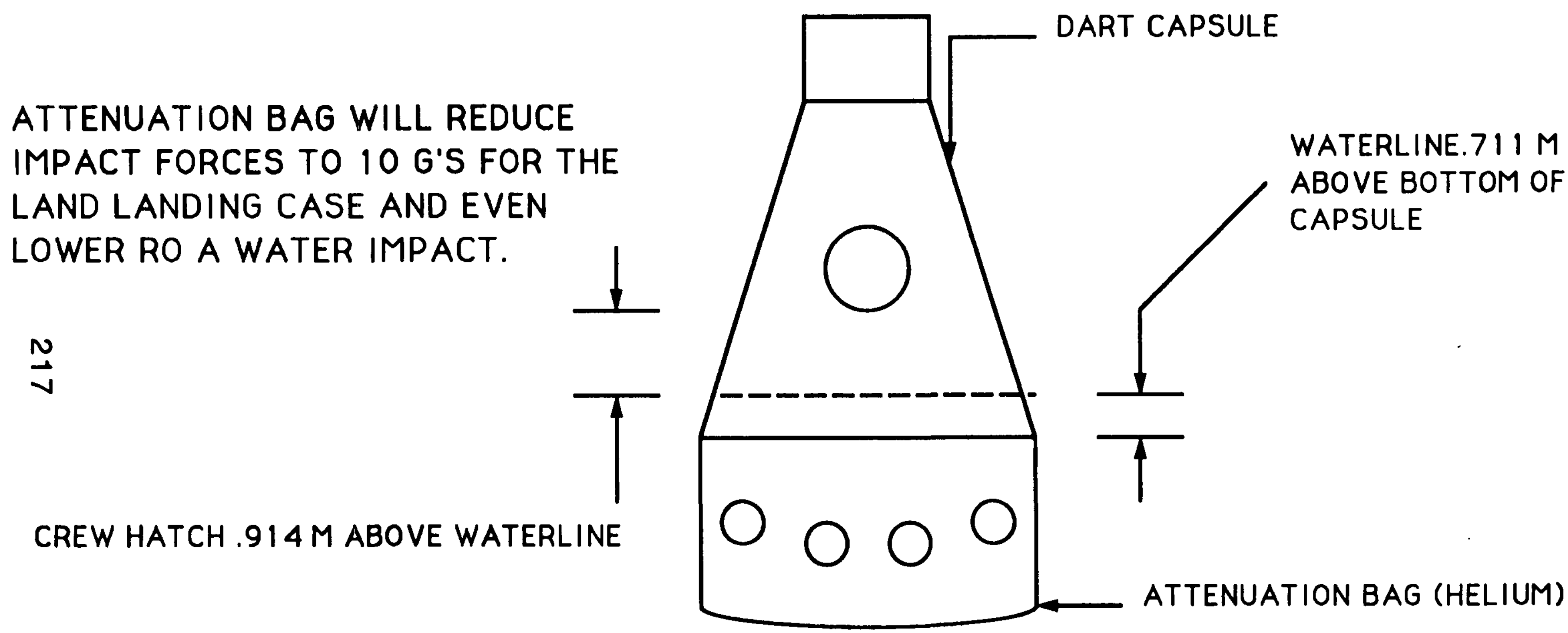

Figure 6.5b Impact attenuation airbag

Z. KHAN

exhaust air through them during impact, thus softening the shock. The bag is to be constructed of a thin nylon cloth covered with a thin coating of rubber. In addition, to add strength to the bag, the outside surface of the bag is reinforced with 24-36 cables(looking at composites for this reinforcement). Also to prevent wave action from ripping away the bag 24-36 cables (same material) would be connected from the top to the bottom of the bag. Note that the heat shield is attached to the bottom of bag and serves to stabilize the craft in rough waters as that this lowers the center of gravity of the system.

Finally we consider matters concerning crew egress. The First area of concern is the location of the crew access hatch. The objective is to determine a location that places the hatch above the waterline and make allowances for a conservative 3 ft estimate of wave heights in the Atlantic. Using a simple weight of capsule equals weight of water displaced and using a volume integral to evaluate the volume of the capsule that is equal to the volume of the displaced water, it was found that the water line was .711m from the bottom of the capsule. Then adding an additional 3 ft for waves placed the crew hatch at 1.63m from the bottom of the craft(figure 6.5b).

Another concern is the stability of the spacecraft in the water. The c.g. of the capsule was located at .96m above the bottom. If the capsule is disturbed slightly, the metacenter of the DART remained above its c.g. thus tending to right the vehicle. In the event the capsule was subjected to waves that tipped it on its sides, buoyancy balloons located at the top of the craft would right the vehicle. In addition the air bag filling with water tended to lower the c.g. of the system thus making it more stable.

Chapter 6 References

1. Akin, D., Conversation Concerning Installation and Refurbishment of Ablative Material Heat Shields

2. Anderson, J., *Hypersonics and High Temperature Gas Dynamics.* New York: McGraw-Hill, Inc., 1989.

3. Anderson, J., *Introduction to Flight.* New York: McGraw-Hill, Inc., 1985.

4. Anderson, J., *Modern Compressible Flow.* New York: McGraw-Hill, Inc., 1990.

5. *Apollo Program Summary Report.* JSC-09423, 1975.

6. Bacon, D., *Basic Heat Transfer,* Great Britain: Butterworth & Co., 1989.

7. Bauer, P., and H. Collicott, *Entry Vehicle Heating and Thermal Protection Systems: Space Shuttle, Solar Starprobe, Jupiter Galileo Probe.* New York: AIAA Inc., 1980.

8. Burden, R., *Numerical Analysis.* Boston: PWS Publishers, 1985.

9. Canberos, J., and L. Roberts, "Analysis of Internal Ablation for the Thermal Control of Aerospace Vehicles." *NASA CR-185919,* 1989.

10. Cecka, A., and W. Schofield, "Low-Cost Fabrication of Ablative Heat Shields." *NASA CR-1112124,* 1972.

11. Chapman, D., "An Analysis of the Corridor and Guidance Requirements for Supercircular Entry into Planetary Atmospheres." *NASA TR R-55,* 1960.

12. Chapman, D., "An Approximate Analytical Method for Studying Entry into Planetary Atmospheres." *NASA TR-11,* 1959.

13. Cleland, J., and F. Iannetti, "Thermal Protection System of the Space Shuttle." *NASA CR-4227,* 1989.

14. Curry, D., and E. Stephens, "Apollo Ablator Thermal Performance at Superorbital Entry Velocities." *NASA TN D-5969,* 1970.

15. Ede, A., *An Introduction to Heat Transfer Principles and Calculations.* Great Britain: Pergammon Press, 1967.

16. Ellis, R. and D. Gulick, *Calculus With Analytic Geometry.* New York: Harcourt Brace Jovanovich Inc., 1982.

17. Engelke, W., C. Pyron, and C. Pears, "Thermophysical Properties of a Low-Density Phenolic-Nylon Ablation Material." *NASA CR-809,* 1967.

18. Gosse, J., *Technical Guide to Thermal Processes.* Great Britain: Cambridge University Press, 1981.

19. Grayson, M., *Encyclopedia of Composite Materials and Components.* New York: John Wiley & Sons Inc., 1983.

20. Hall, J., *Fundamental Phenomena in Hypersonic Flow.* New York: Cornell University Press, 1966.

21. Hallion, R., *Apollo: Ten Years Since Tranquility Base.* National Air and Space Museum, 1979.

22. *Handbook of Composites Volume 1: Strong Fibers.* Netherlands: Elsevier Sciences Publishers, 1985.

23. Hempsell, C., and R. Hannigan, "Multi-Role Capsule System Description." *Journal of the British Interplanetary Society,* volume 42, 1989.

24. Holtzclaw, H., W. Robinson, and W. Nebergall, *General Chemistry.* D. Heath and Co., 1984.

25. Jones, E., *Viscous Fluid Flow and Thermal Control of Aerospace Vehicles.* 1988.

26. Loh, W., *Re-entry and Planetary Entry Physics and Technology.* New York: Springer-Verlag, 1968.

27. LTV Missiles and Electronics Group Brochure on Carbon Carbon

28. Lynch, C., *Practical Handbook of Materials Science.* Florida: CRC Press Inc., 1989.

29. Malik, P., and G. Souris, "Project Gemini: A Technical Summary." *Contract No. NAS 9-170,* 1966.

30. Matting, F., "Analysis of Charring Ablation with Descriptions of Associated Computing Programs." *NASA TN D-6085,* 1970.

31. McLain, A., and K. Sutton, "Experimental and Theoretical Investigation of the Ablative Performance of Five Phenolic-Nylon-Based Materials." *NASA TN D-4374,* 1968.

32. "Moldable Cork Ablation Material." *Dodge Cork Co. Inc.,* 1977.

33. *National Space Transportation Reference.* Volume 1, Systems and Facilities, 1988.

34. Olstad, W., *Entry Heating and Thermal Protection.* New York: AIAA Inc., 1980.

35. Purser, P., M. Faget, and N. Smith, "Manned Spacecraft: Engineering Design and Operation." New York: Fairchild Publications, 1964.

36. Rogallo, F., J. Lowry, T. Groom, and R. Taylor, "Preliminary Investigation of a Paraglider." *NASA TN D-443,* 1960.

37. Salakhutdinov, G., "Thermal Protection in Space Technology." *NASA TM-77145,* 1982.

38. Seiferth, R., "Ablative Heat Shield Design for Space Shuttle." *NASA CR-25779,* 1975.

39. Schniewind, *Concise Encyclopedia of Wood and Wood-Based Materials.* Great Britain: Pergammon Press, 1989.

40. Suris, A., *Handbook of Thermodynamic High Temperature Process Data.* Washington: Hemisphere Publishing Corp., 1987.

41. Vaughn, V., "Water-land Impact Accelerations for Three Models of Reentry Capsules." *NASA TN D-145,* 1959.

42. Waters, I., and C. Hempsell, "The Re-entry Environment of the Multi-role Capsule." *Journal of the British Interplanetary Society,* volume 42, 1989.

43. Wong, H., *Heat Transfer for Engineers.* New York: Longman Inc., 1977.

44. Wood, K., *Aerospace Vehicle Design Volume II: Spacecraft Design.* Colorado: Johnson Publishing Co., 1964.

Chapter 7

Viability and Growth

Section 7.1 Expanded Missions to Alternate Vehicles

Orbit Analysis

The Dart spacecraft was designed for use on the Delta II launch vehicle with a maximum altitude of 500 km, making the maximum weight 4600 kg. In order to complete other missions, alternative launch vehicles were considered. Larger launch vehicles give the DART a greater ΔV with which to reach other orbits. These orbits were analyzed using the assumptions given in Figure 7.1a.

Assumptions

- Earth is a sphere.
- Equator rotates at 1 rev/24 hours.
- Use average Isp.
- Launch is approximated as a Hohmann transfer.
- Used 9200 m/s for LEO at 300 km 28.5° from Kennedy to determine ΔV for drag.

Figure 7.1a: Assumptions used in the ΔV analysis.

Assuming launch trajectories are approximately Hohmann transfers, the vis-viva equation, given below, is used to calculate the ΔV for launches, excluding drag and the Earth's rotation.

$$V^2 = \mu\left(\frac{2}{r} - \frac{1}{a}\right)$$

where μ is the gravitational constant for Earth, r is the distance from the center of mass of the gravitating body, and a is the semi-major axis of the orbit.

Using the vis-viva equation, the ΔV for a Hohmann transfer to 300 km, 28.5° from Kennedy is 7691 m/s. Using 9200 m/s as a nominal value to 300 km, 28.5° from Kennedy, the ΔV due to drag and the Earth's rotation was found to be 1509 m/s. This value is constant for all launches from Kennedy Space Center (KSC).

The Hohmann transfer assumption was used to calculate velocities for many altitudes at 28.5° launching from KSC. The ΔV for drag and rotation of the Earth, 1509 m/s, was added to the Hohmann transfer ΔV. Figure 7.1b shows these results.

Altitude (km)	ΔV (m/s)
1000	9577
1500	9812
1900	9985
2000	10443

Figure 7.1b: ΔV's for different orbits at 28.5°inclination.

Changes in inclination were treated using the difference in components of the Earth's rotation from launch to final inclination angle. The component of the Earth's rotation aiding a launch from Kennedy Space Center, where the latitude is about 28.5° to an orbit with an inclination of ø°, is:

$$V = 463.8 \text{ m/s } \{\cos(28.5°) - \cos(ø°)\}$$

where 463.8 m/s is the rate of rotation of the equator.

To include launches from Vandenberg, the component of the Earth's rotation at Vandenberg is subtracted from that at Kennedy. Since Kennedy is at a latitude of about 28.5° and Vandenberg is at about 34.5°, the difference in components of the Earth's rotation is simply:

$$V = 463.8 \text{ m/s } \{\cos(28.5°) - \cos(34.5°)\}$$

$$V = 25.36 \text{ m/s.}$$

The Earth Observing System (EOS) or Mission to Planet Earth will be in a sun-synchronous orbit at 705 km, 98.2° inclination. The ΔV for launch from Vandenberg to the EOS orbit was calculated as follows:

$$\Delta V = \Delta V_{Hohmann} + \Delta V_{drag + rotation\ (KSC)} - \Delta V_{rotation}$$

where the $\Delta V_{drag+ rotation}$ is the value for drag and the Earth's rotation for a launch from Kennedy and $\Delta V_{rotation}$ is the component of the Earth's rotation lost by launching from Vandenberg instead of Kennedy and the component lost by launching to a 98.2° inclination.

The total ΔV for a launch to the EOS orbit from Vandenberg was calculated to be 9870 m/s.

Launch Vehicles

The Delta II is the baseline launch vehicle for the DART spacecraft and provides a ΔV of 9314 m/s with the DART as payload[1]. For future growth analyses, the Titan III and Atlas IIA launch vehicles were considered.

The Titan III can carry 13,000 kg to 300 km, 28.5° from KSC[2]. The initial mass of the Titan III is 693,000 kg and the average specific impulse is 294.5 seconds[2]. The Rocket equation is given below:

$$\Delta V = g I_{sp} \ln(\frac{M_i}{M_f})$$

where g is the acceleration of Earth's gravity, Isp is the specific impulse, Mi is the initial mass, and Mf is the final mass.

Using the rocket equation and 9200 m/s ΔV for a 300 km, 28.5° orbit, the final mass of the Titan III with a 13,000 kg payload was found to be 28,700 kg. Subtracting the difference between the masses of the 13,000 kg payload and the 4600 kg DART from both the initial and final masses, and applying the rocket equation, the ΔV capability of the Titan III with the 4600 kg DART is 10164.3 m/s.

The Altas IIA can carry 6600 kg to a 300 km, 28.5° orbit[3]. Following the same procedure as shown above, the ΔV capability of the Atlas IIA with the 4600 kg DART was found to be 9558 m/s.

DART Capabilities

With the larger ΔV's of the Atlas IIA and Titan III, higher orbits were analyzed. Larger DART payloads were also considered using the rocket equation with different payload weights.

Analysis of the Altas IIA yielded that the maximum payload weight it can take to the Space Station's 500 km, 28.5° inclination is 5600 kg, which is the DART and 1000 kg additional payload. The Atlas IIA can launch the existing DART to 1000 km, which is twice the altitude of the Delta II. The Atlas IIA does not provide enough ΔV to get to the EOS orbit with the existing DART.

With the largest ΔV, the greatest mission possibilities are found using the Titan III launch vehicle. The 4600 kg DART can be carried to a maximum of 1900 km at 28.5° inclination, which is almost four times that of the Delta II. The Titan can launch 11,000 kg to the Space Station (500 km, 28.5°), which would allow for a large amount of supplies to be transported with the five person crew, but would also require a great deal of structural reinforcement, according to the structures group.

The Titan III also provides a means to service the Earth Observing System. In fact, 6600 kg of payload can be taken to the EOS' sun-synchronous orbit at 700 km. This allows for 2000 kg of additional payload on the DART capsule. Although the radiation environment in high inclination orbits is quite severe, it is possible to fly during times of low exposure, such as during a solar minimum. Since there is currently no means to service EOS, it would be a nice capability if the DART were modified for safe manned travel in the polar radiation environment. This usually involves the addition of a heavier shield, which is feasible given the extra payload capability with the Titan III.

The ΔV's and maximum altitudes of the launch vehicles with the 4600 kg DART are shown below in Figure 7.1c.

Launch Vehicle	ΔV with 4600 kg DART	Max Alt with 4600 kg DART
Delta II	9314 m/s	500 km
Atlas IIA	9558 m/s	1000 km
Titan III	10164 m/s	1900 km

Figure 7.1c: Capabilities of launch vehicles with existing DART capsule.

The maximum payloads that the launch vehicles can take to the Space Station and EOS orbit are shown below in Figure 7.1d.

Launch Vehicle	Payload to Station	Payload to EOS
Delta II	4600 kg	no
Atlas IIA	5600 kg	no
Titan III	11000 kg	6600 kg

Figure 7.1d: Capabilities of launch vehicles with larger DART capsules.

Concluding Remarks

The Titan III launch vehicle was found to hold the most possibilities for the DART. The large ΔV allows for missions to very high inclinations and altitudes of almost four times that attained with the Delta II.

The Altas IIA was found to have more capability than the Delta II, providing twice the altitude or 1000 kg extra payload to the Space Station.

Launch vehicles capable of attaining geosychronous orbit were not considered for this analysis, because of the extremely hard radiation environment. Though the radiaiton environment in the EOS orbit is quite severe, it is less severe than that in geosynchronous orbit, making modifications to the DART more viable for polar orbits.

Section 7.2: Refurbishment Fraction Study

Background and Model

The refurbishment fraction (f) is a percent of the initial unit cost used to project the reuse and refurbishment costs for a system over its mission model. Historically, the fraction ranges between 0.03 for the X-15 project to 0.10 for the Shuttle Transport System. The DART system will fall between these two figures; it lacks the complexity of the shuttle but is much more advanced than the X-15. As opposed to basing the fraction solely on historical data, the Delta Design Team has conducted a costing survey over the mission model of the system to solve for the fraction.

The maximum mission model for the DART capsule is 10 flights per year over 20 years. This gives the program a 200 flight launch life-span. The refurbishment fraction outlined herein will use two parts; the refitting of the capsule per year of the model-with new systems-based on the original unit costs, and the refurbishment of the system per year over the model. A mathematical model will augment this data. It is based on the estimation of the life-span of DART components, and a power law used to increase the percentage of systems needing refitting per year.

The power law is based on data from project Gemini. Harvard Business School did a survey of the costing and technology transfer through time into the system over the entire life-span. Their results suggested that the amount of new technology needed to refurbish and refit the system to keep it functional increased by a power from zero to 30 percent of the initial cost of the program, also over twenty years. From this study the Delta Design Team has formulated a similar study.

Refurbishment Aspects

Refurbishing DART occurs after each mission (10 times per year). It is the evaluation procedures and man hours needed to retrieve the craft after each missions reentry.

Aspects of DART Refurbishment

1.) Cleansing and Dry-out of the Capsule from the Atlantic Splash-down
2.) Inspection and Testing of Computers and Avionics Systems
3.) Testing of the Sensors and Power Generation Systems
4.) Stringent Testing of the Structural Integrity
5.) Transportation Costs
6.) Clearing and Cleaning of all Fuel and Circulatory Plumbing

The refurbishment analysis comes directly from historical data. Barring the refitting with new systems and technology we will assume the portion of the refurbishment fraction for refurbishment solely is 0.02 (2% of the initial unit cost).

H. Magazu

Refitting Study

The Delta Mathematical Model for the refitting of the DART over the mission Model contains four terms: refit costs of the system per year, the upgrading of human technology (especially in the Human Factors Equipment), life span projections of the cost of the systems, and the power model outlined earlier.

The refit costs per year has been calculated from the known expendable DART systems and has been scaled for the incursion of interest over the 20 years in question.

Refit Needs Per Flight

1. New Propulsion Package	
Engines 4 at $50,000.00	200,000
Tanks/Plumbing	536,000
Truss System	192,000
2. Thermal Protective System	
Ablative Portion refit with Robotic System	100,000
3. In-Flight Abort System	
Tower	300,000
Solid Booster	1,300,000
4. Food and Incidental Costs	500,000
5. Solar Panels	2,240,000
6. Parachute System	1,000,000
7. Transportation and Storage Systems	500,000

RF= $6,872,000

This refit cost (RF) was multiplied by a factor of ten, representing the ten flights per year. It was then multiplied by a interest factor defined as:

$$(RF*10)(1 + r)^y$$

RF = Refit Cost   r = interest rate (10%)   y = Years from initial launch

The upgrading of human technology was taken as a \$61,290,000(IHF) term constantly upgraded and refurbished over the twenty year period by the above power term.

$$HF = IHF(1 + r)^y$$

To make the study as responsive to real life as possible the life-span of each component was factored in the equation and inflated by the years from the initial launch. This factor becomes noticeable, in Figure 7.2a, from the seventh to the twelfth year, before the power term takes over the function. During this time the Reaction Control System and Power Generation System will fail, based on the life-span solely.

The final term, as explained, is a power law increasing the percent of refit needs based on the history of the Gemini Program and a study by the Harvard Business School.

$$1.1^{1.2} * (\text{ Initial Unit Cost}/100)$$

Results

This equation has been calculated and plotted over the 20 year mission model. By graphically integrating the plot of this model and averaging the function over the years, the refitting portion of the refurbishment fraction has been found to be 0.05 (5 percent of the initial unit cost). Figure 7.2 shows this plot. You can see the irregularity in the eighth through the twelfth years from the life-span analysis, and the domination of the power term as the years go on. This represents the higher likely hood of failure after repetitive loading.

The final result is the combination of these two terms:

$$\mathbf{h} = 0.02 + 0.05 = 0.07$$

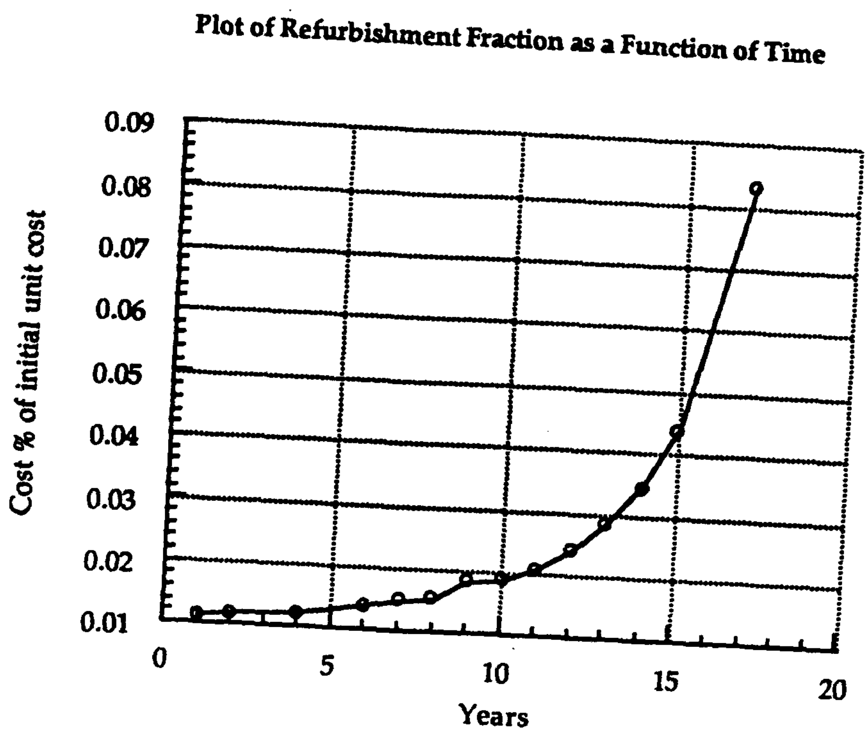

Figure 7.2a: Plot of Math Model

Section 7.3 Costing and Reliability

Costing

Introduction

This section will explain how an estimate of the cost of this project was derived. There were two main reasons for having an accurate and detailed cost analysis. The first reason was to show that the design groups choice of building a reusable craft was in fact the most economical. This will be discussed in detail in a later in this section under the heading *Reusable vs. Expendable Craft.* The second reason for this analysis was to show that the craft presented in this document could be a viable addition to our space program.

The main costs have been broken down into two categories, non–recurring and recurring. Both of these categories will be outlined in the subsections immediately following. From the addition of these two categories and the addition of a Management fee, the total cost and average cost per flight will be determined.

Non–Recurring

The non–recurring cost have been broken down into two parts, the cost of preparing to produce the craft and the cost of adapting the existing infrastructure to accommodate operation of the craft.

The main preparations for production would be design, development, testing, and engineering. A an estimate for the cost incurred in these areas was derived from a cost model (appendix A7.3.1)(reference 3) based on the mass budget (appendix A7.3.3). The masses used are non–redundant system masses (mass of entire system – mass of redundant components). These costs come to a total of $1.591 billion (FY91).

Because our craft uses an existing launch vehicle that has dedicated facilities (at Kennedy Space Center) the cost of adapting these facilities to manned flight would be very low in comparison to establishing new facilities. However, because of the flight model predicted (10 flights per year) significant improvements might need to be made. The estimate for man–rating and improving these facilities for constant use was set at $25million (FY91).

With the addition of systems engineering and and integration cost the total

–C.White

non–recurring cost estimates then comes out to be $4.181 billion (FY91). Because the non–recurring cost of a reusable craft would inherently be much higher, a factor of three was assumed for the reusable vs. expendable analysis. That is the total non–recurring cost for a reusable craft would be two and a half times that for a non-reusable one. However; the cost of the software should not follow this trend and remain the same for both reusable and expendable craft alike. As before systems engineering and integration cost are added and for a reusable craft the total non-recurring cost come to a total of $6.468 billion (FY91).

Recurring

Recurring cost are dependent almost solely on the mission model. The following items are considered under recurring cost:

The cost of the craft itself
Transportation cost
Launch vehicle cost
Launch preparations
Ground support
Recovery cost
Refurbishment and refit cost (for a reusable craft only)

The cost of the craft was also estimated by use of the cost model (appendix A7.3.1). When estimated the cost of producing many craft a learning curve serves as a good model (see reference5). Historically an 80% learning curve best estimates these cost. This means that the cost of producing a second craft should only be 80% of the cost of producing the first. The cost of the n^{th} unit can be found by the following power law:

$$C_n=C_o n^p$$

Where C_n is the cost of the n^{th} unit, C_o is the cost of the first unit, and p is the learning curve coefficient (p=-.324 for 80%). Inflation was also considered in the cost of the craft. Because the program could run over quite a number of years the cost of building a craft a few years from now could actually be much higher than the first unit. For this consideration an annual percentage rate of 10% was used. The cost of building an a number of expendable craft can be evaluated by the following formula:

$$C_t = \sum_{i=1}^{n} C_o i^p + \sum_{j=1}^{y} \sum_{i=1}^{n} C_o i^p (1+r)^j$$

Where C_t is the total cost of building the capsules, n is the number of capsules produced in a year, y is the number of years in the future, C_o is the cost of the first unit, p is the learning curve coefficient, and r is the annual percentage rate.

The transportation were assumed to be small for this case. For our craft, if it

–C.White

were not produced or assembled near KSC a C-5A could be utilized. A C-5A is one of the few aircraft that could accommodate a fully assembled DART capsule (3.5 meter diameter base before packaging for transit). Because of size limitations transportation by 747, train, and flatbed (for long distances) would not be possible. Cargo ship or barge transportation would be possible and reliable but very slow.

Launch vehicle cost have been neglected at this point for simplicity but it should be noted that for a reusable vs. expendable study this cost would be exactly the same for either craft. The reason for neglecting this cost is that the cost of a Delta booster at this point would not reflect the actual cost they could be produced if the DART program were enacted and an appropriate production schedule established. A secondary reason for not including this cost is that the development of a different launch vehicle is inevitable and there is no accurate way of estimating the cost of such a system.

Launch operations cost have been included in the categories of ground support equipment and project management. For a reusable vs. expendable analysis these values should vary with the number of missions only and therefore not be a factor for this study.

The cost of recovering the craft and astronauts will only vary slightly on whether or not the craft is reusable or expendable. A reusable craft will require more care in recovering and storage, but because the safety of the astronauts is the first concern this will exert little influence. This cost has also been neglected because it will most probably be incurred by the military and therefore possibly not in our budget at all.

Refurbishment and refit cost are so important to this study that the section 7.2 has been dedicated to validating this value. This cost has been set at about 5% of the original cost of the craft. This cost would only be incurred for a reusable craft. The total cost of refurbishing the capsule after each flight is as follows:

$$C_t = \sum_{i=1}^{x} C_o F_r$$

where C_t is the total cost of refurbishment over the project, C_o is the first unit cost, F_r is the refurbishment fraction, x is the number of times a craft is refurbished. For an expendable craft a new craft is built for every flight and after it could be donated to a museum or university (maybe even an amusement park).

Total Program Cost

The total program cost is found by simply adding together the non-recurring and the reccuring cost, and then adding the cost of ground support equipment, subsystem development test, and project management. For a flight model of 150 flights (ten per year for fifteen years) and a refurbishment factor of 5% the cost model shows that the total project cost would be $20.425billion in FY91 dollars or an average of $102 million per flight in FY91 dollars.

--C.White

Reusable vs. Expendable Craft

The following trade-off study was done to show that the choice of designing a reusable craft was correct. This study compares the total program cost of a reusable craft to that of an expendable one over constant mission model. This model set the number of missions at ten a year for twenty years starting in 1995. This was estimated to be a median value of what could be expected. The number of flights per craft (reusable craft) was set at ten, although a higher value such as twenty might be expected. In this model inflation was purposely not accounted for so that the total program cost could be seen as an initial investment in 1991 dollars with interest yield the same as the inflation rate.

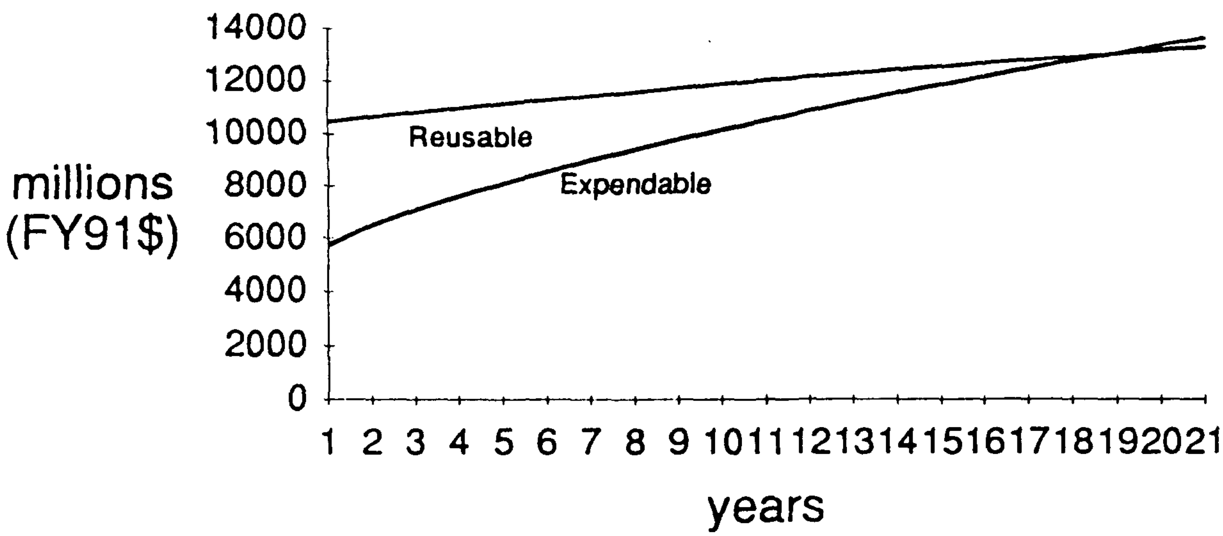

Figure7.3.1

The results of this study (figure 7.3.1) demonstrate if more than 18 flights are expected a reusable craft becomes more economical. Because our mission model is expected to go for at least 200 flights (ten flights a year for twenty years) it can be seen that our decision to go with a reusable craft was justifiable.

–C.White

Reliability

One of the established design criteria of this project was to assure that there would be a 99.9% chance of the crew surviving, and a mission success rate of 95%. This section will show how a value for the chance of the crew surviving was derived from a breakdown of the capsules systems reliability. The reliability for each system was determined by the member of the design team in charge of that system (appendix A7.3.2). For systems with redundant subsystems the value for its reliability was based on the probability that both or all of the redundant systems fail. This can be seen as follows:

$$R_s=1-C_{f1}xC_{f2}$$

where R_s is the reliability of the system, C_{f1} is the chance of failure of subsystem 1, and C_{f2} is the chance of failure of subsystem 2. For any system or subsystem the chance of failure is one minus the reliability ($C_{fx}=1-R_x$).

The chance of crew survivability was taken as the chance of the booster failing times the chance of the abort system working plus the chance of the booster not failing times the chance of all systems operating without failure. This allows for failure of parts of certain systems as long as there are redundancies. The estimated crew survivability of our capsule is 99.92%

The mission success rate was determined by the probability of a successful launch times the probability of no system errors. This gave us a value of 95.93%

Both of these values fit our design goals even though they may be lower than actually experienced because of possible corrective action taken in flight.

–C.White

References

1. Delta II Commercial Spacecraft Users Manual, McDonnell Douglas Astronautics Company, 1989.

2. Titan III Commercial Launch Services Customer Handbook, Martin Marietta Commercial Titan, Inc., December 1987.

3. Mission Planner's Guide for the Atlas Launch Vehicle Family, General Dynamics Commercial Launch Services, Inc., March 1989.

4. Dr. Akin, Class Presentation, University of Maryland College Park, 1991.

5. The Management of Aerospace Programs, AAS Science and Technology Series, 1967.

CONCLUSION

This report has outlined the definite need and the advantages of the DART, alternate manned vehicle. This system will provide both an augmentative and an alternative launch system to the United States manned space program. The DART craft uses the Delta II, 7920 commercial booster. This gives the system a 96 percent reliable launch system, with existing ground support facilities at Cape Canaveral, Florida.

The Delta Design Team has refit with current technology a capsule based manned space vehicle. The DART capsule has a maximum launch weight of 4600 kg, a base diameter of 3.5 m, a height of 4.055 m, and a cone side angle of 15 degrees. The program is designed for a mission model of 10 flights per year over 20 years.

DART uses an ablative thermal protection system and semi-ballistic re-entry with a parachute guided, Atlantic splashdown. In orbit propulsion is generated using a hypergolic, expendable propulsion package. The craft utilizes the Tracking Data Relay Satellite System as-well-as the Global Positioning System for communications and positioning.

The system maintains a refurbishment fraction of 0.07 and an initial cost $160,170,000. When integrated into U.S. manned space program the DART will add flexible, reliable, and cost-effective launch of crew and cargo to specific space destinations. This added capability will further microgravity experimentation and aide in the effort for a permanent manned access to space.

Appendices